Analysis of Polar Organic Compounds in Environmental Samples

by Mass Spectrometric Techniques

by

Curtis James Hedman

A dissertation submitted in partial fulfillment of

the requirements for the degree of

Doctor of Philosophy

(Environmental Science and Technology)

at the

UNIVERSITY OF WISCONSIN-MADISON

2012

Date of final oral examination: 05/29/12

The dissertation is approved by the following members of the Final Oral Committee:
William C. Sonzogni, Professor Emeritus, Environmental Chemistry and Technology
James J. Schauer, Professor, Environmental Chemistry and Technology
David E. Armstrong, Professor Emeritus, Environmental Chemistry and Technology
Joel A. Pedersen, Professor, Soil Science & Environmental Chemistry and Technology
Sharon C. Long, Professor, Soil Science
James P. Hurley, Professor, Environmental Chemistry and Technology

Table of Contents

Acknowledgements

First and foremost, I am deeply grateful to my advisor and mentor, Dr. William Sonzogni, for encouraging my continued pursuit of graduate studies in the Environmental Chemistry and Technology Program at UW-Madison after the completion of my Master's Degree from this department in 2006. This experience has undoubtedly improved my abilities as a research scientist. I am appreciative of the support and advice of the additional members of my thesis committee: Dr. James Schauer, Dr. David Armstrong, Dr. Joel Pedersen, Dr. Sharon Long, and Dr. James Hurley.

I am also thankful to the current and former members of management of the Wisconsin State Laboratory of Hygiene (WSLH) who were so supportive of my academic efforts over the past several years, including: Steven Geis, Dr. James Hurley, Dr. William Sonzogni, Dr. Charles Brokopp, and Dr. Ronald Laessig. Key WSLH colleagues also assisted with some of the laboratory work that is presented within. Many thanks to Archie Degnan, William Krick, Mark Mieritz, Dr. Tan Guo, Dr. Jocelyn Hemming, and Dr. Martin Shafer for this support.

I would like to extend thanks and best wishes to the many UW-Madison students (too many to name within) with whom I have shared this experience - many which were collaborators on various research projects during this time.

Finally, I would not have been able to complete these degree requirements without the unwavering love and support of my wife, Lori, and my daughters, Kaitlyn and Rachel. It is for this reason that I dedicate this thesis to them.

Summary of Tables and Figures

TABLES:

FIGURES:

Analysis of Polar Organic Compounds in Environmental Samples

by Mass Spectrometric Techniques

Curtis James Hedman

Under the supervision of Professor William C. Sonzogni

at the University of Wisconsin-Madison

Abstract: Mass spectrometry (MS) has been used for close to a century to help solve chemical identification and quantification problems in environmental science. Mass spectrometric instrumentation and techniques have evolved over this time period to become an increasingly valuable tool in environmental analyses. In this work, the utility of an array of modern MS techniques is highlighted in three separate studies in which a wide variety of organic compounds are analyzed in complex environmental matrices. First, a battery of mass spectrometric techniques is used to identify and quantify over 180 different compounds in air and bulk crumb rubber samples collected to assess the health effects of athletes breathing air over crumb rubber amended synthetic turf. Quality control data from this study demonstrate the efficacy of these MS techniques for the purpose intended. Second, high performance liquid chromatography coupled with tandem mass spectrometry (HPLC-MS/MS) in multiple reaction monitoring mode is used to measure very low levels of estrogenic and androgenic compounds in samples from confined animal farming operations (CAFOs). A fractionation technique is used to isolate hormonal activity and to determine whether the toxicological potency, as

measured by bioassay, can be accounted for by the types and concentrations of hormones identified. Third, HPLC-MS/MS was used with a variety of scan modes along with isotope labeling to propose abiotic breakdown pathways for the sulfonamide antimicrobial compound sulfamethazine. In the first study of crumb rubber amended turf air monitoring, the battery of MS tests were able to analyze most of the volatile, semi-volatile, and rubber related target compounds at the low ng/sample level with good accuracy and precision. However, common laboratory solvents and other compounds in laboratory air presented interference problems for a number of analytes, notably carbon disulfide, 2-methyl butane, acetone, benzene, methylene chloride, methyl alcohol, and pentane. HPLC-MS/MS was successfully used in a new adaptation of established gas chromatographic methods to measure N-Nitrosamines, benzothiazole, 2-mercaptobenzothiazole, 4-tert-octylphenol, butylated hydroxytoluene, and butylated hydroxyanisole at low levels. In the CAFO hormone study much of the hormonal bioactivity in the samples could be accounted for by the hormones measured by targeted HPLC-MS/MS analysis. In addition to 17-beta-estradiol (an estrogen often found in environmental samples), 4-androstene-3,17-dione, progesterone, 17,20-dihydroxyprogesterone, nandrolone, and zearalenone, were detected and quantified. The use of isotope dilution techniques allowed high confidence in these results. However, not all of the hormonal bioactivity could be accounted for by the measured hormones. Further work on the bioactive fractions by GC/MS identified compounds potentially responsible for the observed endocrine disrupting bioactivity, including a triazine herbicide compound and a phthalate compound. However, the exact identity of these compounds will require additional effort. Finally, HPLC-MS/MS analysis showed that

the sulfonamide antimicrobial sulfamethazine is transformed under oxic conditions in an azo-dimer self-coupling product and SO2 extrusion products. Overall, these three studies demonstrate how a battery of MS techniques can be a practicable approach in determining a wide array of polar and non-polar organic compounds in difficult environmental matrices. In particular, using HPLC-MS/MS in versatile ways has allowed polar compounds, such as polar rubber related compounds, the rarely reported hormones nandrolone and zearalenone, and the antimicrobial sulfamethazine (and its breakdown products), to be measured in complex environmental samples.

Approved

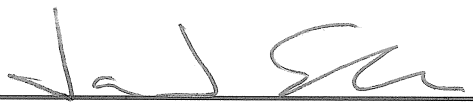

James J. Schauer, Professor

Environmental Chemistry and Technology Program

Chapter 1

Introduction and Background:

Analysis of Organic Compounds by Mass Spectrometry in Environmental Science

Analysis of Organic Compounds by Mass Spectrometry in Environmental Science

Historical Perspective

Mass spectrometry has been available as a chemical analysis technique since the early twentieth century. Beginning in 1907, J.J. Thompson studied the passage of positive rays, termed canal rays, by passing neon through a magnetic and electric field and measuring its trajectory by exposing a photographic plate, providing evidence for different atomic masses (Ne^{20} and Ne^{22}) being present within the canal rays [1]. A student in Thompson's laboratory, Francis Aston, continued this research, building a mass spectrograph in 1919 that he used to identify a large number of the naturally occurring elemental isotopes, including Cl^{35}/Cl^{37} and Br^{79}/Br^{81} [2].

The first modern mass spectrometer was developed in 1918 by Arthur Dempster. His instrument was more than 100 times more accurate than previous versions, and his research into the basic theory and design of mass spectrometers continues to be used today [3]. In 1935, Dempster discovered U^{235} during his mass spectrometric research [4]. An industrial scale sector mass spectrometer, called a Calutron, was developed by Ernest Lawrence during the Manhattan Project, to provide the enriched uranium used for early nuclear weapons [5].

The development of the electron impact ionization source in the 1950s was an important advance in mass spectrometry research, as it allowed the coupling of gas chromatography (GC) as a compound mixture separation tool prior to the mass analyzer [6]. It wasn't until the late 1950s, when gas chromatography-mass spectrometry (GC/MS) was commercialized by Dow

Chemical Company, that mixtures of organic molecules could begin to be analyzed in environmental matrices [7]. Also during this time, the discovery that electron ionization (EI) was an extremely robust ionization technique allowed commercial compound databases to be developed for the identification of unknown organic compounds, and these databases have evolved over time [8]. Even then, the compounds best suited for analysis by this technique were more non-polar in nature, such as petroleum products. With the creation of the US EPA and its environmental monitoring program in the early 1970s, GC/MS was becoming commercialized, and was relied upon heavily for the analysis of priority persistent organic pollutants (POPs) such as PCBs, dioxins, and DDT [9]. In order to extend the polarity range of compounds amenable to GC/MS, a great deal of research occurred in derivatization chemistry in the 1960s and 1970s [10].

A major innovation in mass spectrometry instrument design occurred in the mid 1980s, when Fenn published on research relating to the electrospray MS interface [11]. With this technique, large compounds, like proteins and nucleic acids, delivered in a charged, nebulized liquid could be introduced into a mass analyzer. Fenn received the Nobel Prize in Chemistry for this work in 2002 [12]. With the electrospray interface, researchers could reliably utilize high performance liquid chromatography (HPLC) as a separation technique and couple it to mass spectrometry as a detection system. This dramatically extended the range of polarity and size of analytes that could be analyzed by mass spectrometry, and a great deal of research occurred using this technique through the 1970s through the 1990s, while commercialization of LC/MS ion source design and instrumentation matured. Other source designs for LC eluent introduction to MS were developed during this timeframe, such as particle beam and thermospray interfaces

[13], but these techniques proved less robust and difficult to commercialize and were therefore left by the wayside. One alternative interface that emerged around the same time that proved to be as useful as electrospray was the atmospheric pressure chemical ionization interface (APCI) [14]. Although this ionization technique is less susceptible to matrix interferences and can ionize less polar analytes, the necessity to run at high temperatures precluded APCI use for more thermally labile compounds. Rapid proliferation of LC/MS research involving more polar analytes has occurred from the advent of ESI and APCI to the present. Yet another alternative MS interface, called Matrix Assisted Laser Desorption Ionization (MALDI), allows for the direct introduction of organic compounds into the mass analyzer by laser ablation [15]. A more thorough discussion of these MS interfaces is treated in a later section of this chapter.

The Key Concepts of Mass to Charge Ratio and Mass Resolution

The primary output of a mass spectrometer is the mass spectrum. This is essentially a graph where the y-axis shows signal intensity and the x-axis presents the mass to charge ratio (*m/z*) of detected components in the sample. If the charge state is one, as it is for most small molecules under approximately 600 u, the *m/z* value is the same as its mass in Daltons (Da). For larger compounds, such as peptides and proteins, their multiple charged molecular ions reduce the *m/z* value that they respond at. For example, a triply charged peptide of a mass of 2,100 Da is detected in a mass spectrum at *m/z* 700. If compound fragmentation occurs prior to the mass analyzer, these fragments give multiple peaks in the mass spectrum according to their *m/z* values, and can be used to deduce molecular structures or record and/or compare mass spectra from compound identification database records.

Before discussing the various mass spectrometer designs and their utility for different experimental goals, it is also important to define mass resolution (R). This is the ability of a mass analyzer to distinguish one *m/z* peak from an adjacent mass. The equation for mass resolution is:

$$\mathbf{R_m = m/\Delta m}$$

Where $\mathbf{R_m}$ is mass resolution in *m/z*, **m** is the measured mass, and **Δm** is the difference between two adjacent peaks (or alternatively, the full width at half maximum (FWHM) of a non-centroided mass spectral peak). **Table 1** lists mass resolution values possible for various types of mass analyzers that are discussed in more detail in the following sections. A unit mass resolution MS (R=1000) is sufficient for quantitative MS experiments, while a higher mass resolution instrument (R= 10,000 to 40,000 or higher) is required for removal of background contaminants with the same nominal mass, or for the determination of fewer possible molecular formulas from accurate mass tables. **Figure 1** shows examples of MS peak widths at different mass resolutions.

General Instrumental Configuration

A diagram showing the general instrumental configuration for the mass spectrometric analysis of polar organic compounds is shown in **Figure 2**. Two key components for mass spectrometry analysis are the ionization source and mass analyzer. The ionization source creates charged analytes that can be drawn into the mass analyzer by voltage gradient. The mass

analyzer then detects compounds by their mass to charge (*m/z*) ratio. Several varieties exist for each of these components, and they are discussed in the following sections.

Different Mass Analyzers Available for Environmental Analysis

Quadrupole Systems (**Figure 3**) – Over the course of the last century, mass spectrometry research has produced a number of different types of mass spectrometric analyzers. The most commonly used mass analyzer is the quadrupole system. In this analyzer, two pairs of opposing stainless steel rods are oriented in a high vacuum chamber. By rapidly alternating direct current (DC) and radio frequency (RF) current to these rods, charged molecules will pass through the quadrupole in a predictable fashion. Quadrupole mass analyzers can operate in two main modes – scan and single ion monitoring (SIM). In scan mode, the voltages are applied in a way that allows all charged molecules within a programmed mass to charge (*m/z*) range to pass through. All other *m/z* values take a trajectory that moves them away from the quadrupole and out of the MS system via vacuum waste lines. In SIM mode, the DC and RF voltages are manipulated in a way that only a single m/z value is allowed to pass through the quadrupole, causing all other *m/z* values to pass through to waste. The mass resolution of this analyzer is unit mass, or approximately +/-0.7amu [15].

Ion Trap Mass Analyzer (**Figure 4**) – In an ion trap mass analyzer, ions introduced by the source are pulsed, or ion injected, into a chamber between two plates called end caps. The middle of this chamber is surrounded by a ring shaped electrode that contains RF voltage [15]. When the ions encounter the RF only voltage, they are confined and moved into the center of the

trap by helium buffer gas. During the process of trapping, ions move into an oscillating frequency that is related to their m/z ratios. In scan mode, the ring RF voltage is ramped while a small RF voltage is also applied to the end caps in order to eject the ions to the detector over a time period of 50 to 100 milliseconds. In SIM mode, a single m/z can be trapped while all other m/z values are ejected during the pulse and ion accumulation period. The selected ion is then ejected from the trap. While triple quadrupole instruments are capable of MS/MS (or MS^2) fragmentation analysis, the ion trap analyzer can theoretically perform unlimited fragmentation, termed MS^n. In MS^n, all ions are ejected except the selected m/z, and a resonating RF frequency is applied that causes this ion to oscillate and collide with the helium buffer gas in the trap. This effect causes fragmentation, and the resulting fragment ions are moved to the center of the trap again by the buffer gas, and one of the fragment ions is selected for the next fragmentation. This type of fragmentation analysis can be extremely useful for deducing chemical structures in unknown compound ID studies. It should be noted that there is a low mass cutoff for this analyzer, similar to that observed with fragmentation analysis using a triple quadrupole mass analyzer. Therefore, low mass fragments may not always be detected using the ion trap mass analyzer. Recently, linear ion trap (LIT) technology has been developed and commercialized [16,17]. The LIT can perform like a quadrupole, but can also trap and eject ions without the low mass cutoff issues observed in orbital trap and quadrupole instruments. This allows enhanced detection of all fragments and makes database identification work with HPLC-MS/MS more feasible. The LIT is capable of only MS^3 fragmentation, however, instead of the MS^n fragmentation capabilities of the orbital ion trap mass analyzer. The resolution of ion trap mass analyzers are generally similar to quadrupole mass analyzers (unit mass resolution, or R=1000) [15].

Time of Flight Mass Analyzer (**Figure 5**) – The time of flight (TOF) mass analyzer consists of an ionization source, a flight tube, and a detector. TOF mass analyzers essentially scan all of the time, since they determine mass by arrival time without mass filtering effect. Therefore, SIM is not practical for this type of instrument [15]. Another effect of this continuous scanning operation is that temporal, spatial, and kinetic variation in compound ionization cause a simple time of flight mass spectrometer to have unit mass resolution (R=1,000). To compensate for these variable ionization effects, a series of electronic lenses called a reflectron are used to redirect ions so they hit the detector at the same time. The reflectron creates a constant electrostatic field in which ions with higher kinetic energy travel further into the reflectron than ions with lower kinetic energy. As a result, TOF instruments that use reflectrons can achieve much higher resolution (i.e. - R=5,000 or better) [18].

Magnetic Sector Mass Analyzer (**Figure 6**) – In this mass analyzer, a continuous beam of ions are accelerated out of the ionization source by an accelerating voltage through a source slit. Ions that pass through the slit then traverse a strong magnetic field. The motion of the ion toward the detector depends on its angular momentum and the centrifugal force caused by the magnetic field [19]. Ions of different m/z ratios are separated by the magnetic field by varying either the magnetic field strength or the accelerating voltage, and are resolved from each other by dispersing them in space. The resolution of the magnetic sector mass analyzer is determined by changing the widths of the source and detector slits to transmit a narrow band of ions to the detector, and can reach R values between 10,000 and 40,000 with ease [15].

Fourier Transform Ion Cyclotron Resonance Mass Analyzer (FT-ICR) – This mass analyzer is capable of the highest mass resolution measurements currently obtainable with mass spectrometric instrumentation (100,000+) (15). For this reason, it is used mainly for proteomics and metabolomics applications, but shows great promise in being able to provide unambiguous molecular formula designations for environmental unknown compounds. The FT-ICR/MS instrument is like an ion trap mass mass spectrometer in that a pulse of sampled ions are moved into a cubic cell consisting of trapping, transmitter, and receiving plates (**Figure 7**). It differs, however, in how the trapped ions are analyzed. A strong magnet is used to trap and keep the ions in a circular orbit. Radio frequency is then applied to excite the trapped ions into larger circular orbits, causing a frequency change detected as an image current. Because this frequency is inversely related to the ion's mass, a Fourier transform algorithm is applied to the data. FT-ICR analysis is also unique among MS instrument platforms in that it is the only non-destructive MS analyzer. Once ions are detected, a quenching radio frequency is applied to eject the ions from the cell prior to the next sampling of ions. This process of detection is capable of being performed in about 10 milliseconds (15).

Ion Mobility Analyzer (IMS) – The addition of this analyzer adds a different dimension of separation for compounds that have the same nominal mass to charge ratio (i.e. - isobaric compounds) [20]. A commonly applied version of IMS, called a differential mobility analyzer (**Figure 8**), uses a stream of gas perpendicular to an applied electric field. This analyzer is able to separate compounds by shape and charge state. In addition to the ability of IMS to separate isomers, IMS-MS can resolve nuisance background signals, and assist in the detection of compound charge states [20,21].

Hybrid Mass Analyzer Systems – Mass Spectrometry research in the 1970s showed that great gains in selectivity could be achieved by placing two or more mass analyzers in sequence within the instrument flow path that were separated by a collision chamber. The triple quadrupole (QQQ) mass analyzer allowed for several advances in the types of mass spectrometric analysis that could be performed on complex samples (**Figure 9**). The most common operating mode for the triple quadrupole system is termed multiple reaction monitoring (MRM). In MRM, the first quadrupole acts as a mass filter, allowing only the *m/z* of the compound of interest to pass. The second quadrupole (Q2) acts as a collision chamber. An inert gas (nitrogen or argon) is passed through this quadrupole, and when molecules pass through and collide with the gas molecules, they break into fragments called daughter ions. The *m/z* values for one or more of these daughter ion fragments are selected for in the third quadrupole (Q3), causing all other fragments to pass to waste. This double mass filtering with fragmentation creates a high amount of selectivity in detection, and the almost total reduction in matrix noise by this mass filtering effect causes an extreme reduction in background detector noise (background signal in the 10s to 100s of counts per second (cps) versus 10,000 or more cps observed in scan mode) (**Figure 10**). As a result, it is common to achieve instrumental lower limits of detection of high pcg/mL to low ng/mL range using MRM detection mode [15].

By using one or both Q1 and Q3 in scan mode with a triple quadrupole instrument, other interesting modes of operation become available for the analysis of complex mixtures or classes of compounds that share a given functional group. Three examples of this are precursor ion scan mode, neutral loss mode, and product ion scan mode [15]. In precursor ion scan mode, Q1 is

scanned over a predetermined range, and Q3 is held at a constant m/z relative to a common daughter ion for a compound class of interest. In neutral loss mode, both Q1 and Q3 sweep a m/z range that is a fixed mass apart. A signal is observed if the ion chosen by Q1 fragments by losing or gaining the mass difference of the neutral loss value specified. In product ion scan mode, Q1 is held at a fixed m/z value and Q3 sweeps a m/z range, allowing for all fragments from Q2 available from a given compound to be detected. These advanced MS/MS scan functions are very useful in the determination and characterization of non-targeted compounds present in a sample.

In recent years the concept of the hybrid mass spectrometry system has been expanded with the addition of quadrupole-ion trap (QTrap) [16,17,22] and quadrupole-time of flight (QTOF) [23] instrumentation. The advantages of QTrap over QQQ instruments is that the ion trap can be used to enhance sensitivity, give better mass resolution, provide better signal for low mass (<100amu) daughter fragments, and can be used in some cases to trap and fragment daughter ions (creating ms^3 (granddaughter) ions or ms^n ions, depending on the ion trap design) – all enhancing unknown compound identification. The QTOF instrument has the distinct advantage of much higher mass accuracy over the other hybrid systems mentioned.

All of the mass analyzer configurations listed above have been commercialized and are available in formats that will accept either LC or GC as a separation system front end. The key to their being able to do this is in the MS source design.

Important MS Source Designs Available for Polar Organic Compound Analysis

Mass spectrometers used for polar organic compound analysis in the environmental laboratory are usually interfaced with a chromatographic instrument, mainly GC and HPLC. In some cases, however, direct sample introduction techniques are also used. It is important to note that polar organic compounds require derivatization prior to GC/MS analysis in order to make them amenable to GC separation [10].

For GC/MS, two types of ionization dominate in environmental analysis – electron ionization and chemical ionization [24]. An overview of these two techniques follows:

Electron Ionization (EI) Interface – Earlier literature refers to this as 'electron impact' ionization, but this term has evolved to electron ionization over time. In EI, electrons emitted from a metal filament are accelerated (normally to 70eV) and concentrated to a beam moving toward a trap electrode (**Figure 11**). Molecules emerging from the GC column outlet pass through this beam, and the exposure to this electron energy causes fluctuations in the molecule's electron orbitals leading to extraction of molecular electrons and subsequent ionization and fragmentation [25]. The radical cations produced are directed toward the mass analyzer by a repeller voltage. Because EI creates a highly reproducible fragmentation pattern for organic compounds, commercially available compound identification libraries, such as the NIST Spectral Library [8], are routinely used for unknown GC/MS peak ID.

Chemical Ionization (CI) Interface – This type of GC/MS ionization provides different, and complimentary, mass spectral information when compared to EI derived mass spectra, and is

often used to determine the molecular ion of an unknown compound. In CI, a reagent gas (usually methane) is introduced into the ionization chamber with the compounds eluting from the GC column outlet [26]. This reagent gas is used to transfer charge initiated by an electron emission source to sample molecules by a variety of reactions, such as proton transfer, hydride abstraction, and ion attachment [24]. Because the electron energy required to create these CI reactions is much less than that required for EI technique, the resulting CI mass spectra do not contain the large amount of fragmentation normally observed with EI mass spectra.

For HPLC/MS analysis, two ionization techniques dominate the market; electrospray ionization and atmospheric pressure chemical ionization. A third more recently developed technique called atmospheric pressure photoionization is also worthy of discussion, as it extends the type of molecules that may be analyzed by HPLC/MS.

Electrospray Ionization (ESI) Interface – In electrospray (**Figure 12**), the HPLC eluent flowing out of a stainless steel capillary is nebulized with gas and is charged by application of a high voltage applied to the capillary tip (approximately three to five kV). The imparted charge exists on the outer surface of the nebulized droplets. By application of heated drying gases within the source, these droplets are rapidly desolvated to the point where charge repulsion exceeds a threshold termed the Reighleigh Coefficient. This causes a coulomb explosion, creating charged microdroplets containing analyte molecules. Upon further desolvation, the charge is transferred to (or from) the analyte molecule and a molecular ion is formed ($[M+H]^+$ or $[M-H]^-$, depending upon whether positive or negative electrospay mode is used). The fully desolvated molecular ions are then brought into the mass analyzer by voltage gradient. The

gentle nature of electrospray ionization makes it ideal for the MS analysis of delicate molecules, like peptides, proteins, and other thermally labile species [15,26]

Atmospheric Pressure Chemical Ionization (APCI) Interface – Instead of the room temperature spray created in electrospray, APCI uses a pneumatic nebulizer to create a fine spray that emitted into a chamber held at approximately 500°C (**Figure 13**). This causes rapid and full desolvation of the nebulized spray and vapor phase neutral analyte molecules to pass out of the heated chamber and into the ionization source. Within the APCI source, a corona discharge needle (usually Ni^{63}), emits electrons that ionizes surrounding gases creating ions such as N_2^+, O_2^+, H_2O^+, and NO^+ [15,28]. These charged gas ions interact with the neutral analyte molecules in the vapor phase, and the major reagent ion that transfers charge to the vapor phase neutral analytes is $H_3O^+(H_2O)_n$. APCI is more efficient than electrospray for analytes containing OH groups as their primary functional group, and extends the range of lower polarity substances that can be analyzed by HPLC/MS [15]. The high temperature desolvation can degrade thermally labile compounds in the source, however. This can create loss of water pseudo-molecular ions, such as $[M\text{-}H_2O+H]^+$ in positive APCI mode. These pseudo-molecular ions may be used for quantitative MS analysis, as long as this form of ionization is reproducible from sample to sample. As with electrospray, the molecular ions (or pseudo-molecular ions) are brought into the mass analyzer by voltage gradient.

Atmospheric Pressure Photoionization (APPI) Interface (**Figure 14**) – This type of ionization is an evolution of the APCI technique, with UV radiation initiating the ionization process instead of corona electron discharge [29]. A UV absorbing dopant, such as toluene, is

infused into the source area. The UV irradiated dopant molecules become ionized, initiating a cascade of reactions among the solvent molecules within the source. Pneumatically nebulized and desolvated HPLC eluent containing analyte molecules enter this area of the ionization source, where ion-molecule interactions lead to the formation of the ionized analytes by proton addition (positive mode $[M+H]^+$), charge exchange (positive mode $[M]^+$), or proton abstraction (negative mode $[M-H]^-$). A key benefit to APPI over ESI and APCI is the ability, using the charge exchange mechanism, to ionize compounds lacking functional groups and not amenable to ionization by these other methods. A prime example of this is the APPI analysis of polycyclic aromatic hydrocarbons (PAHs) – a group of compounds not amenable to HPLC-MS/MS analysis by other means [30]. APPI works for this analyte group because charge exchange can be applied to the *pi* bonds in the PAH ring structures.

Direct ionization interfaces allow compounds to be sampled into the mass analyzer without prior separation by HPLC or GC. This can be advantageous, depending upon the application. Two examples of this are the direct probe and matrix assisted laser desorption ionization.

Direct Probe (DP) Interface – The DP interface is essentially a chamber that allows a compound or mixture of compounds to be sampled directly into the mass analyzer. Some DP chambers are capable of running temperature gradients to move analytes into a gaseous state for introduction into the mass analyzer. One variation of DP, termed Direct Analysis in Real Time (DART), allows a series of samples to be analyzed by MS in very rapid succession, making it

appealing for applications such as product quality control assays and homeland security applications [31].

Matrix Assisted Laser Desorption Ionization (MALDI) Interface – Used for the analysis of large proteins such as bacterial toxins in the environment [15], MALDI-MS analysis is also performed without a separation component. In MALDI, the anlayte is intercolated into a UV absorbing solid crystal lattice, such as sinapinic acid, nicotinic acid, or amino benzoic acid, and introduced through a vacuum interlock into the path of a pulsed laser beam (i.e. - nitrogen laser at 337nm) [15]. A mass spectrum is generated from each laser pulse, and mass spectra from multiple pulses are often averaged to improve MS data quality.

Mass Spectrometric Techniques Used for This Thesis

In Chapter 2, the analysis of target compounds by both GC/MS and HPLC-MS/MS are employed to monitor semi-volatile organic compounds emitted from crumb rubber infill on outdoor and indoor artificial turf fields in analytical support of a human health risk assessment study. This chapter also highlights the need for specialized controls to assess and correct for sampling efficiency and matrix effect issues in MS analysis techniques. Chapter 3 describes the use of HPLC-MS/MS in target compound mode and GC/MS in unknown identification mode in a bioassay directed fractionation study of endocrine disrupting compounds arising from liquid and solid environmental sample extracts. Chapter 4 describes the use of HPLC-MS/MS in product ion scan mode with and without mass labeling to assist in the determination of unknown reaction byproducts in the transformation of sulfamethazine by birnessite (δMnO2).

Previously published articles are referenced in Chapter 5 for other MS analysis techniques performed recently by the author that are relevant to this dissertation. Derivatization and high resolution GC/MS are used to elucidate the fragmentation pattern for Beta-methyl aminoalanine (BMAA), a potential cyanobacterial derived neurotoxin [32]. Product ion scan MS data is generated along with orthogonal techniques, such as UV/DAD, and NMR spectroscopy to assist in the determination of unknown organic compound identification in environmental samples [33-35]. Advanced MS/MS scans are used to assist in the characterization of humic-like substances in atmospheric aerosol samples [36].

The overarching goal for this thesis is to add to the body of evidence supporting the following statements with the work presented in Chapters 2 through 4, as well as previous publications by the author:

1) The use of HPLC-MS/MS and GC/MS is practicable for multi-residue analysis of trace organic compound contaminants in complex environmental extracts.
2) HPLC-MS/MS and GC/MS can be successfully employed for unknown organic compound determinations in environmental samples.
3) Advanced MS/MS scans, such as precursor ion scan and neutral loss scan, can be used to generate useful data for the characterization of complex environmental extracts.
4) High resolution MS data can outperform unit resolution MS generated data for the elucidation of organic compound structure and fragmentation pathway analysis.
5) Derivatization and mass labeling are important aids when using mass spectrometry to study chemical transformation pathways.

In addition, the following hypotheses are postulated for the work presented in Chapters 2 through 4 of this dissertation:

1. Chapter 2
    a) By the evaluation of quality control results, HPLC-MS/MS is a viable alternative to GC with thermal energy analyzer (TEA) detection for the analysis of N-nitrosamine compounds in air samples as referenced in NIOSH Method 2522 [37].
    b) By the evaluation of quality control results, HPLC-MS/MS can effectively be used in place of GC with sulfur chemiluminescence detection for the analysis of benzothiazole compounds in air samples as referenced in NIOSH Method 2550 [38].
2. Chapter 3
    a) Using HPLC-MS/MS with isotope dilution targeted analysis and bioassays with potency factors for targeted analysis compounds, it is possible to quantitatively account for the bioactivity observed in fractionated environmental extracts.
3. Chapter 4
    a) The influence of oxygen in organic compound transformation product reactions can be determined by the use of 18O2 and H218O in reactions along with the analysis of reaction products by HPLC-UV-MS/MS.

References

[1] Thomson, J. J. 1913. Rays of positive electricity. *Proceedings of the Royal Society* A89:1-20.

[2] Squires, G. 1998. Francis Aston and the mass spectrograph. *Dalton Transactions* 23:3893-3900.

[3] Dempster, A. J. 1918. A new method of positive ray analysis. *Physical Review* 11:316-325.

[4] EncyclopædiaBritannica. 2011. Arthur Jeffrey Dempster. In *Encyclopædia Britannica Online*. Encyclopædia Britannica, Inc.

[5] Parkins, W. E. 2005. The uranium bomb, the Calutron, and the space-charge problem. *Physics Today* 58:45-51.

[6] Gohlke, R. S. 1959. Time-of-flight mass spectrometry and gas-liquid partition chromatography. *Analytical Chemistry* 31:535-541.

[7] Gohlke, R. S., McLafferty, F.W. 1993. Early gas chromatography/mass spectrometry. *Journal of the American Society for Mass Spectrometry* 4:367-371.

[8] NIST/EPA/NIH. 2011. Mass Spectral Library with Search Program (Data Version: NIST 11, Software Version 2.0g.

[9] Gudzinowicz, B. J.; Gudzinowicz, M. J.; Martin, H. F. 1976. *Fundamentals of Integrated GC-MS*. Marcel Dekker, Inc.: New York, NY, Vol. 7, 382pg.

[10] Knapp, D. R. 1979. *Handbook of analytical derivatization reactions*. John Wiley & Sons, Inc.: New York, NY, 741pg.

[11] Yamashita, M.; Fenn, J. B. 1984. Electrospray ion source. Another variation on the free-jet theme. *Journal of Physical Chemistry* 88:4451-4459.

[12] Grayson, M.A. 2011. John Bennett Fenn: A Curious Road to the Prize. *Journal of the American Society for Mass Spectrometry* 22:1301-1308.

[13] Niessen, W.M.A. 1999. *Liquid Chromatography-Mass Spectrometry, Second Edition, Revised and Expanded*. Chromatographic Science Series, Volume 79. CRC Press, 634pg.

[14] Thomson, B. A.; Iribarne, J. V. 1979. Field-induced ion evaporation from liquid surfaces at atmospheric pressure. *Journal of Chemistry and Physics* 71:4451-4463.

[15] Willoughby, R.; Sheehan, E.; Mitrovich, S. 2002. *A Global View of LC/MS*. 2nd ed.; Global View Publishing: Pittsburgh, PA, 518pg.

[16] Hopfgartner, G., Varesio, E., Tschappat, V., Grivet, C., Bourgogne, E., Leuthold, L.A. 2004. Triple quadrupole linear ion trap mass spectrometer for the analysis of small molecules and macromolecules. *Journal of Mass Spectrometry* 39:845-855.

[17] Douglas, D.J, Frank, A.J, Mao, D. 2005. Linear ion traps in mass spectrometry. *Mass Spectrometry Reviews.* 24:1-29.

[18] Mamyrin, B.A. 2001. Time-of-flight mass spectrometry (concepts, achievements, and prospects). *International Journal of Mass Spectrometry*. 206:251-266.

[19] Chapman, J. R. 1995. *Practical Organic Mass Spectrometry: A Guide for Chemical and Biochemical Analysis, 2nd Edition*. John Wiley: Chichester, 1985.

[20] Kanu, A. B.; Dwivedi, P.; Tam, M.; Matz, L.; Hill, H. H. 2008. Ion mobility-mass spectrometry. *Journal of Mass Spectrometry.* 43:1-22.

[21] Fenn, L. S.; McLean, J. A. 2008. Biomolecular structural separations by ion mobility-mass spectrometry. *Analytical and Bioanalytical Chemistry.* 391:905-909.

[22] March, R. 1997. An introduction to Quadrupole Ion Trap Mass Spectrometry. *Journal of Mass Spectrometry.* 32:351-369.

[23] Ferrer, I., Thurman, E.M. 2009. *Liquid Chromatography-Time of Flight Mass Spectrometry: Principles, Tools and Applications for Accurate Mass Analysis*. Wiley, New York, NY, 304pg.

[24] Budde W.L., Eichelberger, J.W. *Organics Analysis Using Gas Chromatography Mass Spectrometry: A Techniques & Procedures Manual*. Ann Arbor Science Publishers, Inc., Ann Arbor, MI. 242pg.

[25] Märk, T.D., Dunn, G.H. 1985. *Electron Impact Ionization.* Springer Verlag, New York, NY, 383pg.

[26] Munson, M. S. B., Field, F. H. 2006. Chemical ionization mass spectrometry. I. General introduction. *Journal of the American Chemical Society.* 88:2621-2630.

[27] McMaster, M. C. 2005. *LC/MS: a practical user's guide*. 1st edition. John Wiley & Sons, Inc.: Hoboken, NJ. 165pg.

[28] AB/SCIEX. 2002. API 4000 LC/MS/MS System Hardware Manual. AB/SCIEX Document Number D1000013652C. 114pg.

[29] Robb, D.B., Covey, T.R., Bruins, A.P. 2000. Atmospheric pressure photoionization: An ionization method for liquid chromatography-mass spectrometry. *Analytical Chemistry.* 72:3653-3659.

[30] Hutzler, C., Luch, A., Filser, J.G. 2011. Analysis of carcinogenic polycyclic aromatic hydrocarbons in complex environmental mixtures by LC-APPI-MS/MS. *Analytica Chimica Acta.* 702:218-224.

[31] Cody, R.B., Laramée, J.A., Durst, H.D. 2005. Versatile new ion source for the analysis of materials in open air under ambient conditions. *Analytical Chemistry.* 77:2297-2302.

[32] Guo, T., Geis, S., Hedman, C., Arndt, M., Krick, W., Sonzogni, W. 2007. Characterization of ethyl chloroformate derivative of beta-methylamino-L-alanine. *Journal of the American Society of Mass Spectrometry*. 18:817-825.

[33] Bialk, H., Hedman, C., Castillo, A., Pederrsen, J. 2007. Laccase-mediated Michael addition of 15Nsulfapyridine to a model humic constituent. *Environmental Science and Technology*. 41:3593-3600.

[34] Rubert, K.F., IV, Hedman, C.J., Pedersen, J.A. 2009. Influence of MnO2 on the transformation of oxy- and chlortetracycline in pond water. In: Veterinary Pharmaceuticals in the Environment, ACS Symposium Series No. 1018. Coats, J.R., Henderson, K.L. (eds.). Oxford University Press, New York, pp. 45-65.

[35] Hedman, C., Krick, W., Karner, D., Harrahy, E., Sonzogni, W. 2008. New measurements of cyanobacterial toxins in Wisconsin waters. *Journal of Environmental Quality*. 37:1817-1824.

[36] Stone, E.A., Hedman, C.J., Zhow, J., Mieritz, M., Schauer, J.J. 2010. Insights into the nature of secondary organic aerosol in Mexico City during the MILAGRO experiment 2006. *Atmospheric Environment*. 44:312-319.

[37] National Institute of Occupational Safety and Health (NIOSH). 1994. Method 2522 Nitrosamines. In: Eller PM, Cassinelli ME. Eds. NIOSH Manual of Analytical Methods, 4th ed., Cincinnati, OH: NIOSH. Accessed April 2, 2012 at http://www.cdc.gov/niosh/docs/2003%2D154/pdfs/2522.pdf.

[38] National Institute of Occupational Safety and Health (NIOSH). 1998. Method 2550 Benzothiazole in Asphalt Fume. In: Eller PM, Cassinelli ME. Eds. NIOSH Manual of Analytical Methods, 4th ed., Cincinnati, OH: NIOSH. Accessed April 2, 2012 at http://www.cdc.gov/niosh/docs/2003-154/pdfs/2550.pdf.

Table 1: Mass Resolution (R) ranges for various mass analyzers.

Mass Analyzer	**Resolution (R) Range**	**Mass Accuracy**
Quadrupole	1,000 to 2,000	0.1 Da
Ion Trap	1,000 to 2,000	0.1 Da
Time of Flight	1,000 to 40,000	0.1 Da to 0.005 Da
Magnetic Sector	5,000 to 100,000	0.1 Da to 0.001 Da
FT-ICR / Orbitrap	5,000 to 1,000,000	0.001 to 0.0001 Da

Figure 1: Examples of MS peak widths at different mass resolutions.

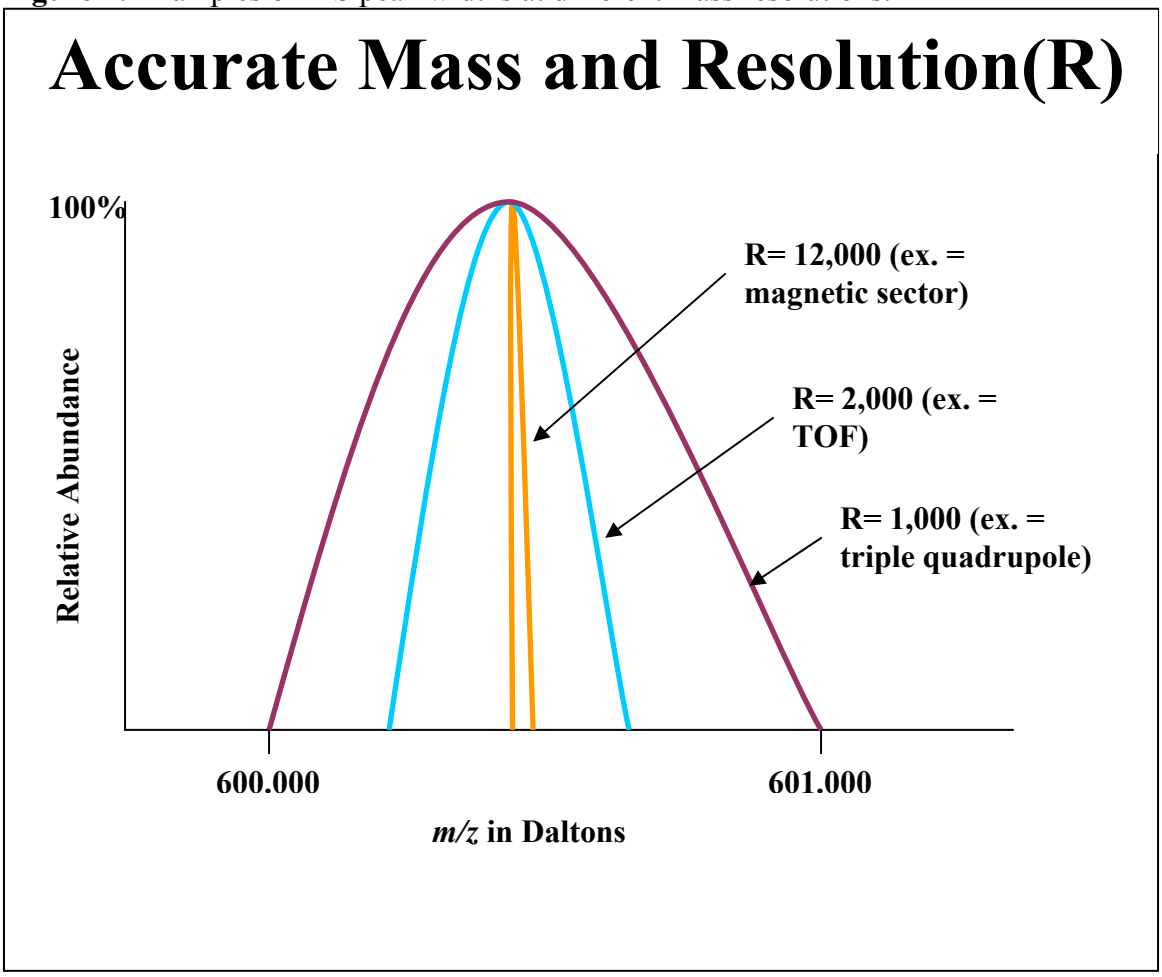

Figure 2: General diagram of instrumentation used for MS analysis of polar organic compounds.

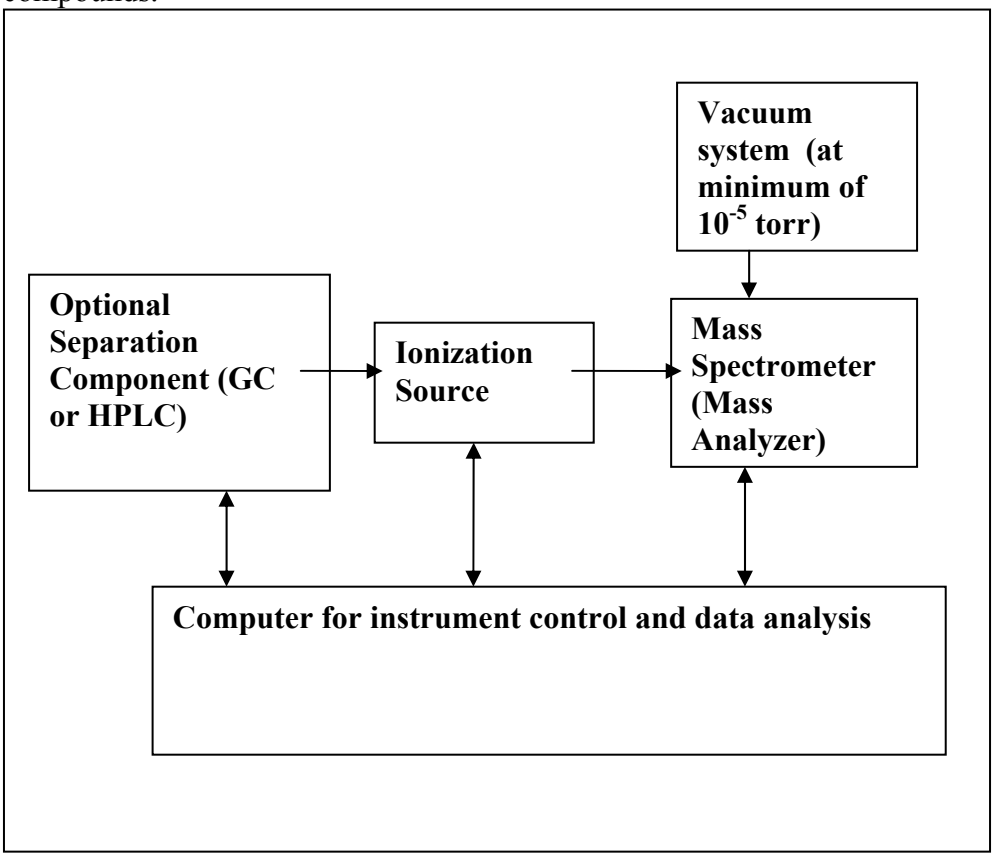

Figure 3: Schematic of a quadrupole mass analyzer.

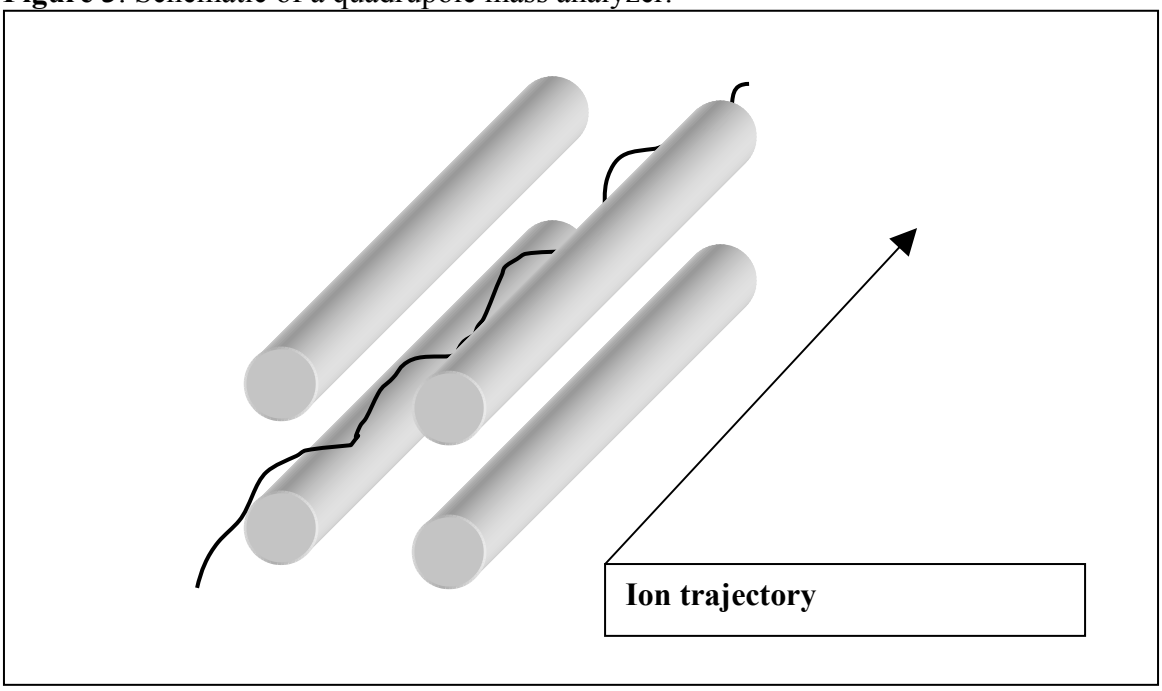

Figure 4: Schematic of an ion trap mass analyzer.

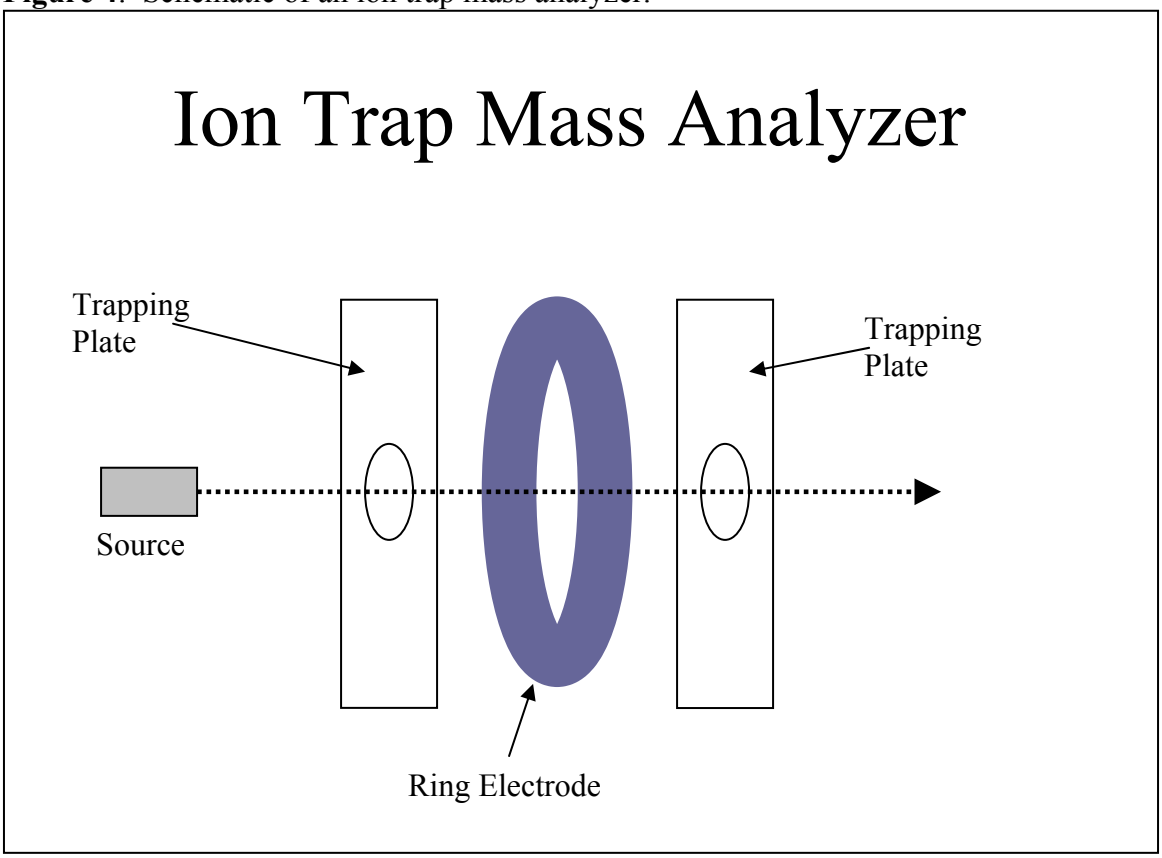

Figure 5: Schematic of a time of flight mass analyzer.

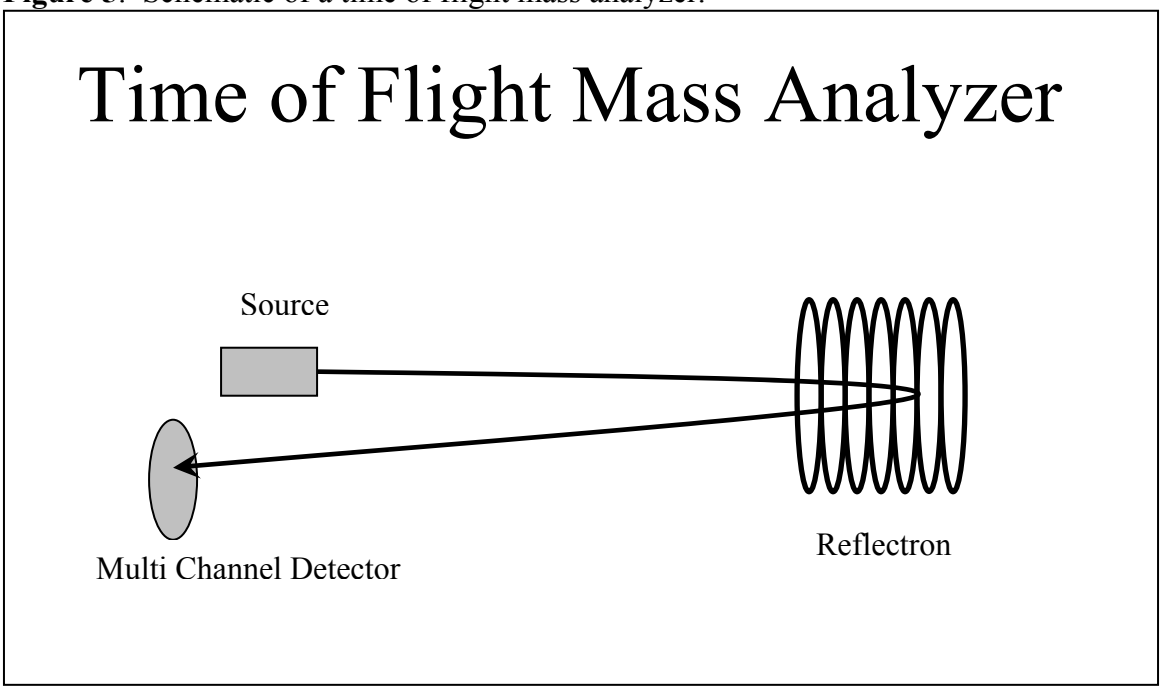

Figure 6: Schematic of a magnetic sector mass analyzer.

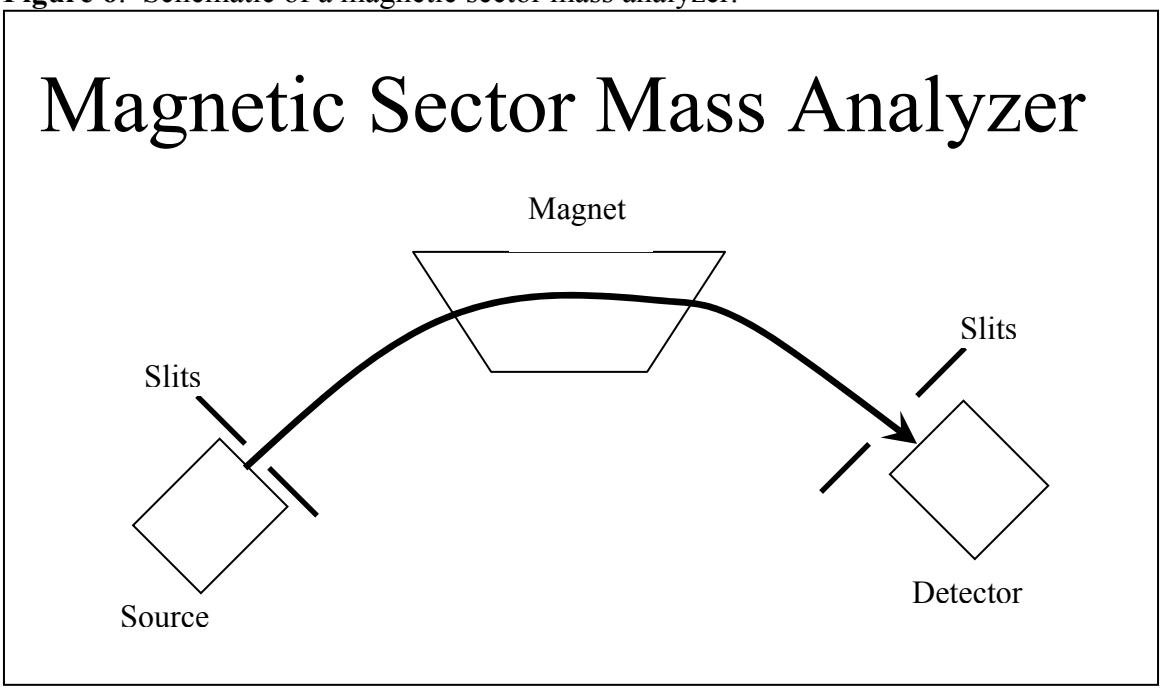

Figure 7: Schematic of a Fourier Transform Ion Cyclotron Resonance Mass Analyzer

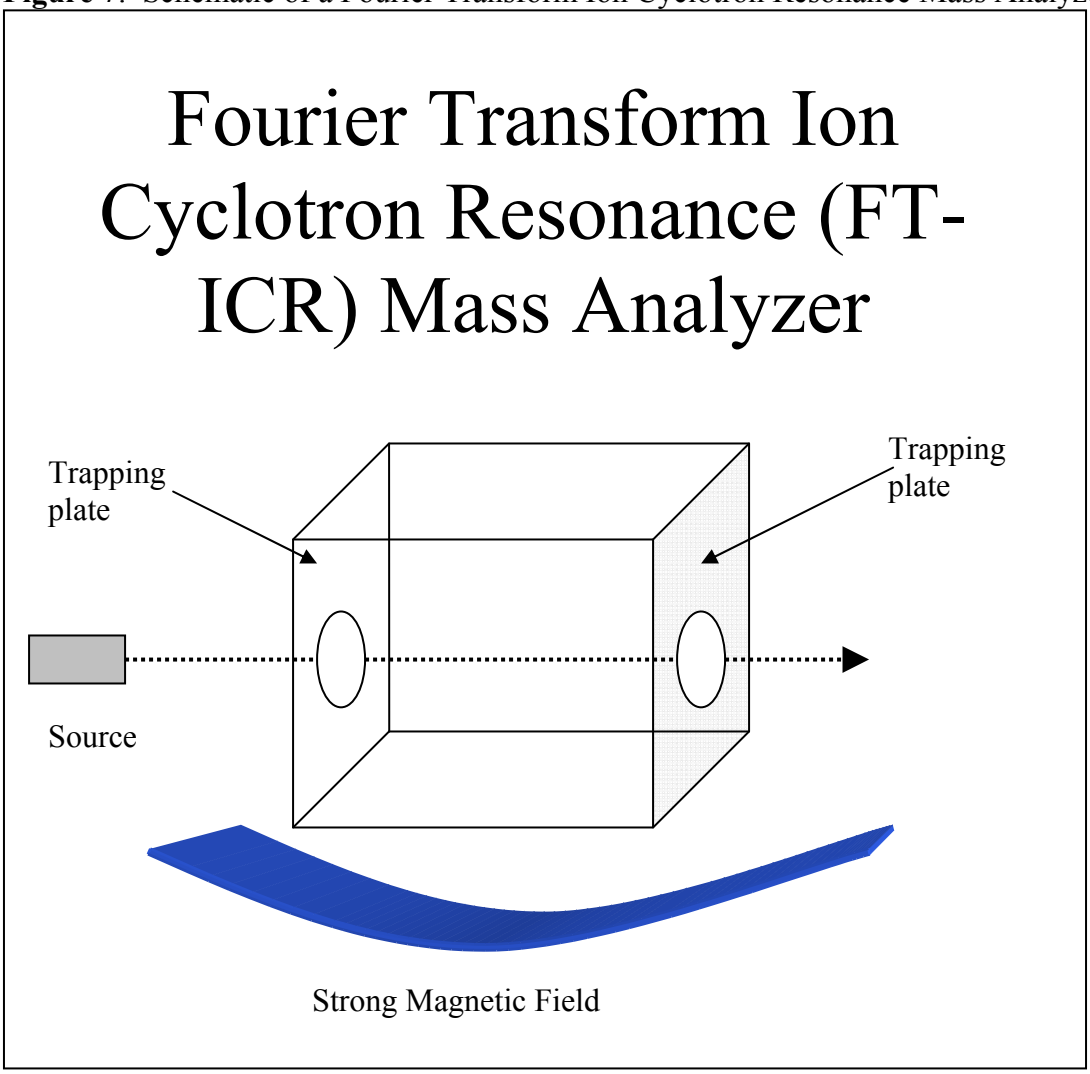

Figure 8: Schematic of a differential mobility analyzer. The symbols represent molecules with differing shapes and charge states.

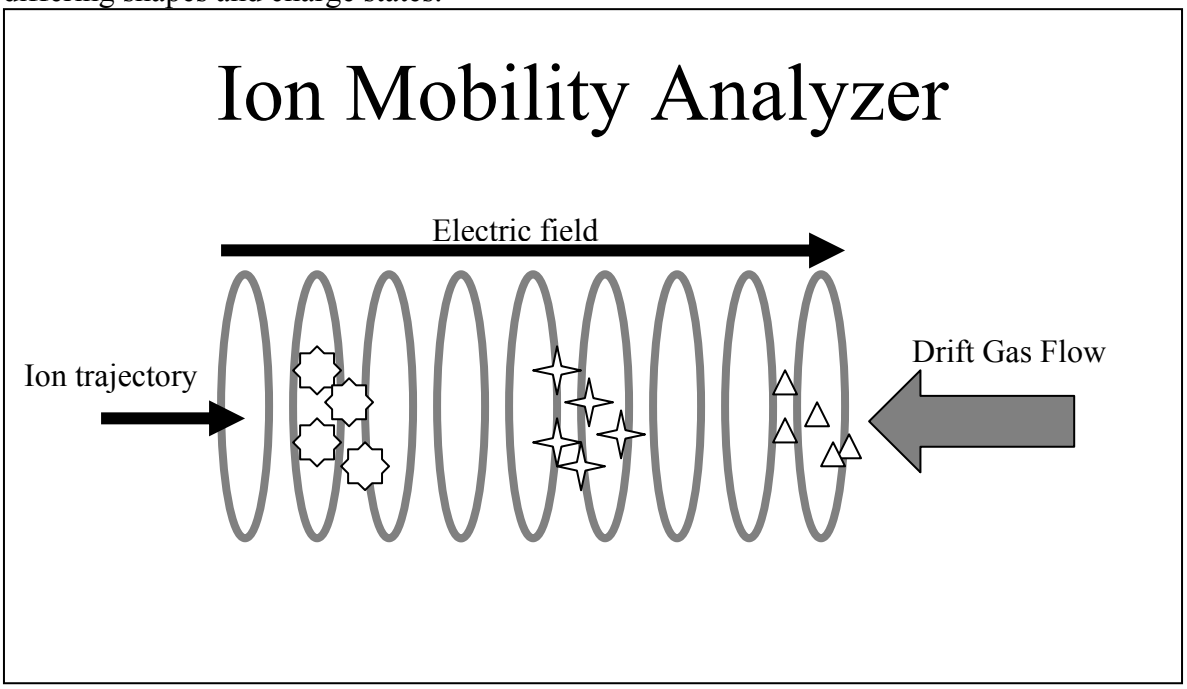

Figure 9: Schematic of a triple quadrupole (QQQ) mass analyzer. CAD = collisionally activated dissociation.

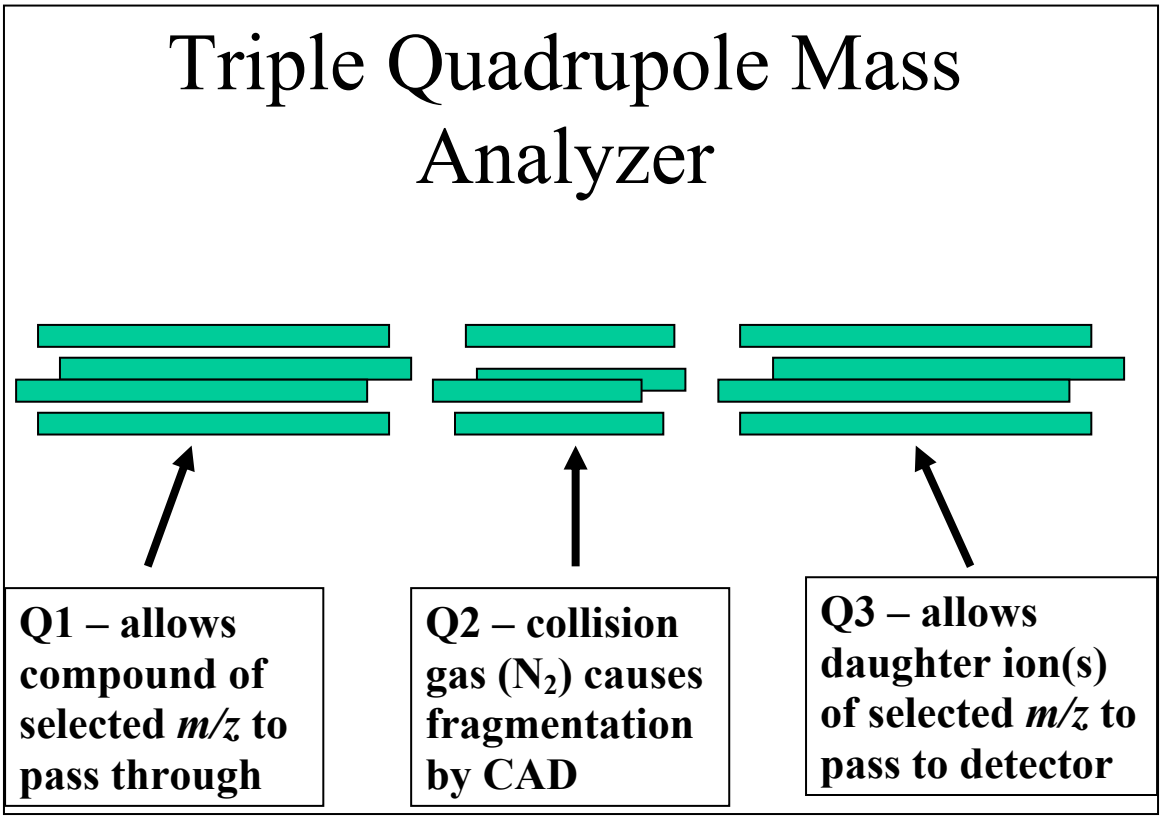

Figure 10: Example of Q1 scan versus MRM background signal. Sulfamethazine was analyzed by the author in (a) Q1 scan mode (background signal ca.5 x 10^7cps) and in (b) MRM mode (background signal ca. 200cps).

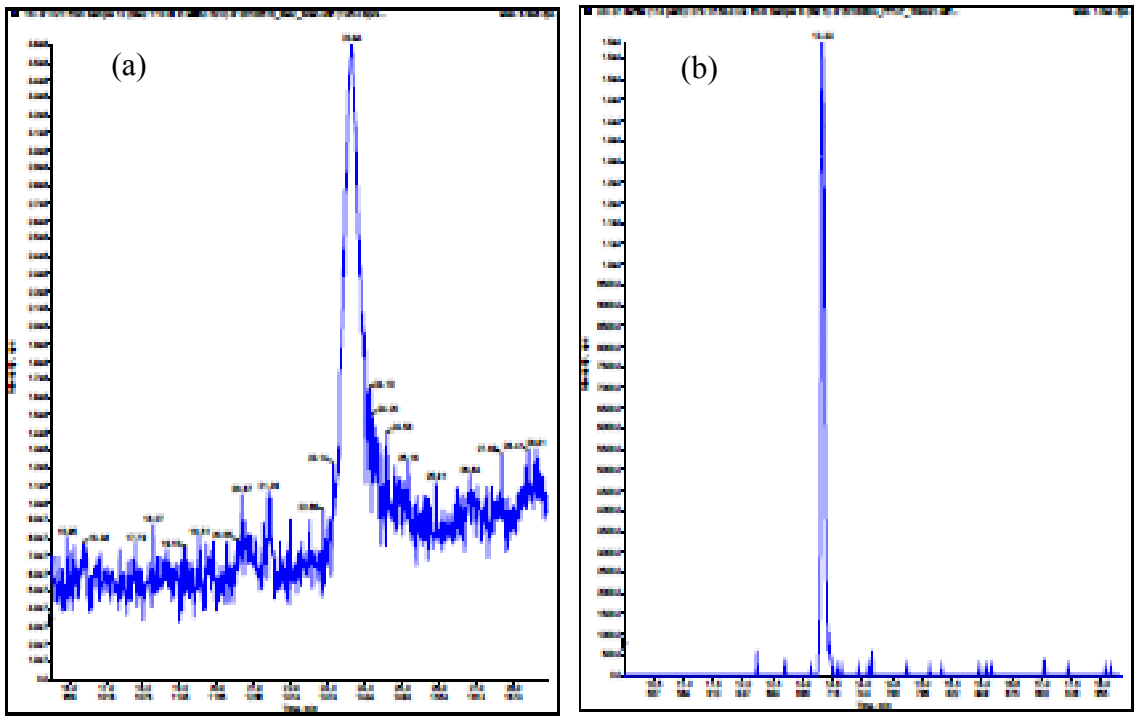

Figure 11: Schematic of the electron ionization process.

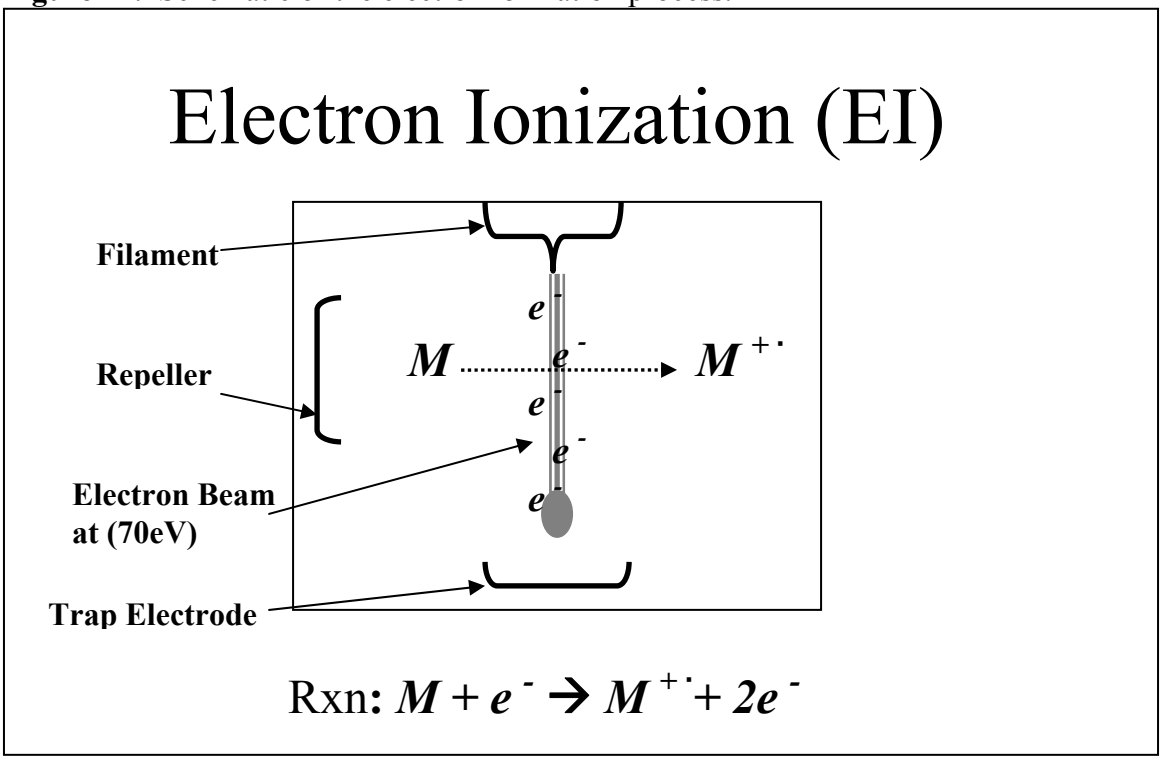

Figure 12: Electrospray ionization.

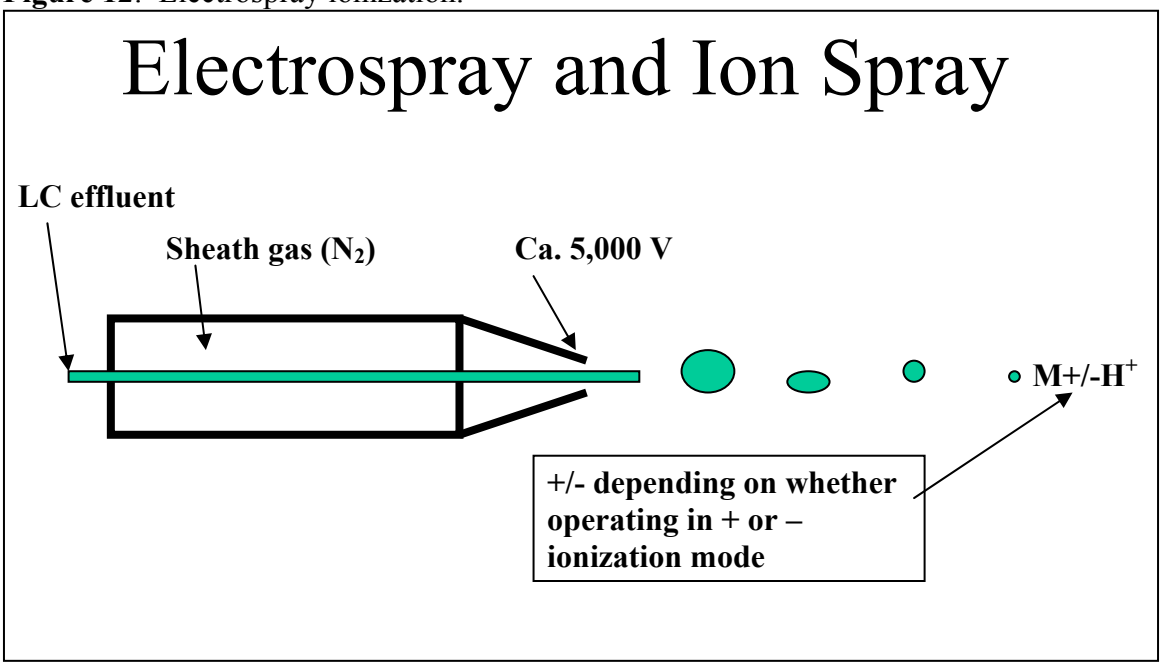

Figure 13: Atmospheric pressure chemical ionization.

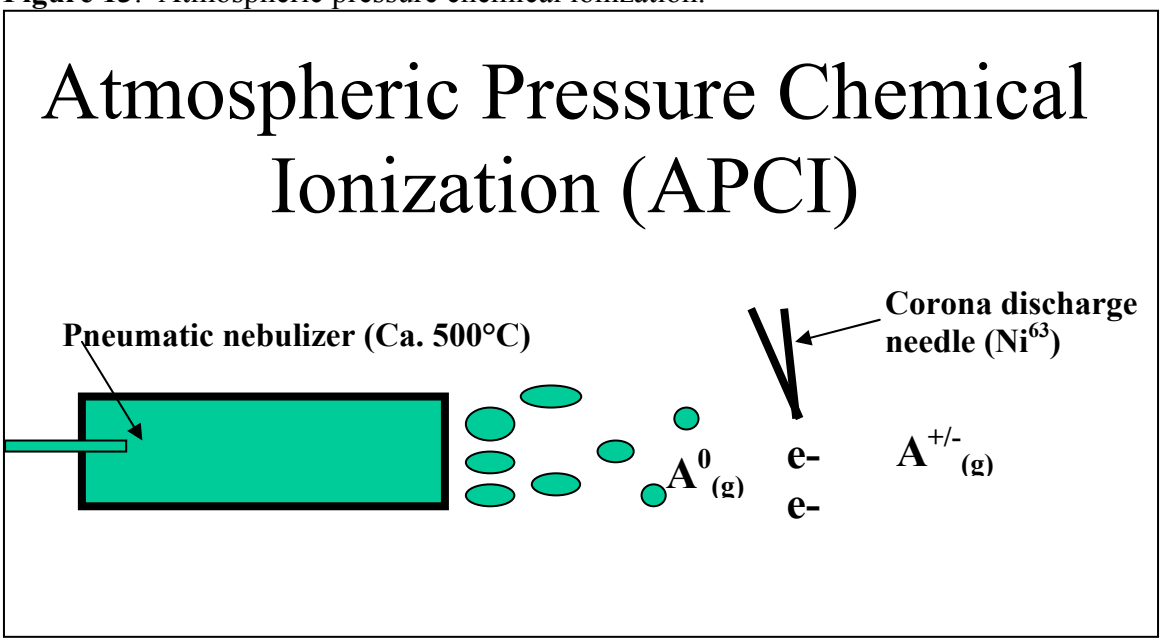

Figure 14: Atmospheric pressure photo ionization.

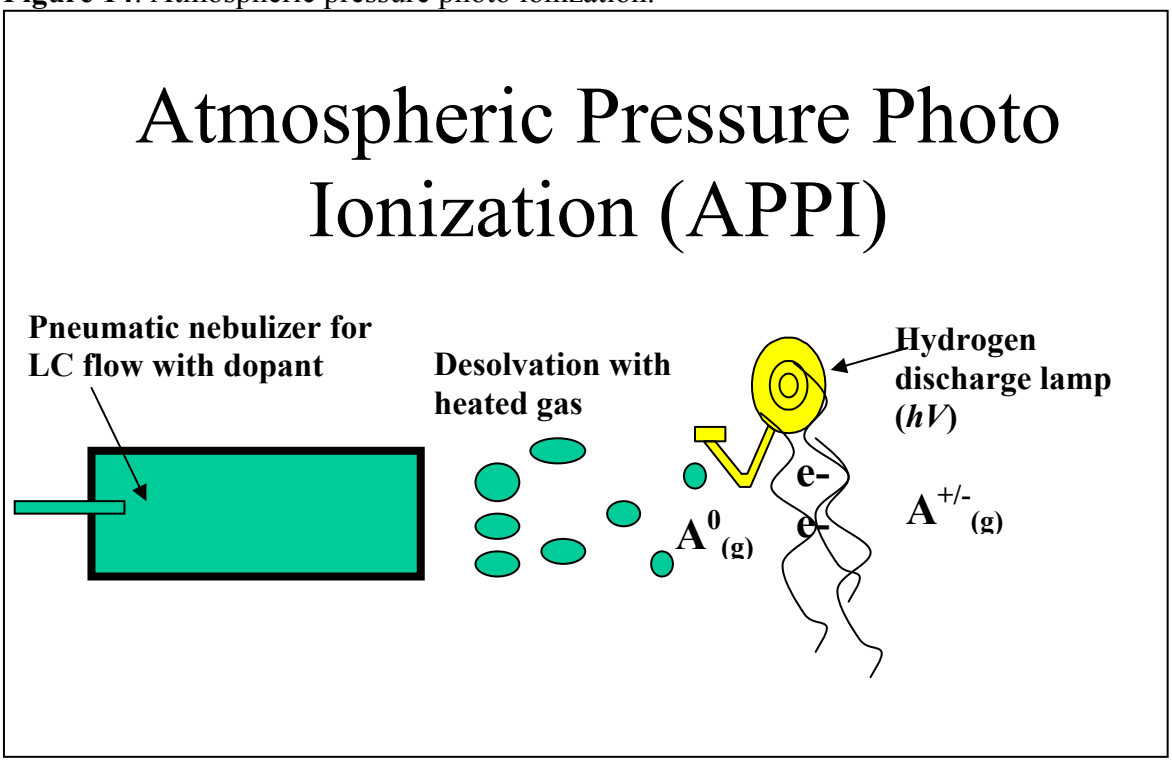

Chapter 2

Monitoring for Organic Compounds Emitted from Crumb Rubber Infill – Analytical Methodologies Employed for a Synthetic Turf Field Investigation in Connecticut

A version of this chapter will be submitted for publication to the *Journal of Occupational and Environmental Hygiene* with the following co-authors: Nancy Simcox, Erin Mani, Cheri Schwabe, Brandon Shelton, Jeff DeMinter, Mark Hudziak, and Derek Popp.

Evaluation of the quality of different analytical methods for measuring organic compounds emitted from crumb rubber infill used in synthetic turf.

Curtis Hedman[1], Nancy Simcox[2], Erin Mani[1], Cheri Schwabe[1], Brandon Shelton[1], Jeff DeMinter[1], Mark Hudziak[1], Derek Popp[1]

[1]Wisconsin State Laboratory of Hygiene, Madison WI, [2]University of Connecticut Health Center, Farmington CT

Key Words: Synthetic turf, crumb rubber, exposure assessment, environmental monitoring, VOCs, PAHs

Abstract

A variety of environmental analysis methods were used to monitor organic compounds emitted from crumb rubber infill used on synthetic turf fields. Sample types included area and personal air samples (on field and background), particulate matter (PM_{10}) generated during active play, and bulk crumb rubber material. Analytical methods used were based upon US CFR40, Part 50 for particulate matter (PM_{10}), US EPA Method TO-15 for 60 volatile organic compounds (VOCs), US EPA Method TO-13A for 114 semi-volatile organic compounds (SVOCs), NIOSH Method 2522 for seven N-nitrosamines, and NIOSH Method 2550 for benzothiazole and four other targeted rubber related compounds. In addition to the methods listed above, headspace analysis methods were also used to evaluate the compounds off-gassed from bulk crumb rubber samples supplied from the fields studied. Results from triplicate weighing and field blanks for PM_{10} analysis were within US CFR40, Part 50 method specifications. Recovery results for Method TO-15 VOC spikes were within 70 to 130 % of theoretical value, with the exception of acetone and methylene chloride for one batch. Spike recovery results were also used to determine correction factors to be applied to study samples for a small number of Method TO-13a SVOC compounds that were less than 75 % of

their theoretical value. Laboratory control sample recovery results ranged from 74.1 to 122.6 % for targeted rubber related compounds, and from 84.1 to 116 % for the seven N-nitrosamine compounds tested. Off-gas analysis spikes were all within 70% to 130% for VOC analytes and higher than 100% for rubber related SVOCs tested. A unique feature of this study was that the N-nitrosamine and targeted rubber related compound instrument analysis was performed by HPLC-MS/MS. The data generated was of sufficient quality to be used for the human health risk assessment study.

Introduction

The widespread use of bulk crumb rubber infill as a shock absorbing amendment to indoor and outdoor synthetic turf fields has led to concerns over chemical compounds that may leach or be off-gassed over time [1]. These concerns have led to several studies over the past decade to evaluate chemicals emitted from crumb rubber infill amended fields [2-5].

To extend this body of knowledge and to perform a human health risk assessment, the State of Connecticut commissioned a study to identify and monitor crumb rubber infill derived compounds of potential concern (COPC) in bulk crumb rubber, in area air samples, as well as in personal air monitoring samples [6]. The results of this study were used to determine the COPC to use for a human health risk assessment [7,8]. In order to achieve these goals, existing analytical methodology from both environmental (e.g., U.S. EPA) and occupational health (e.g., U.S. NIOSH/OSHA) sources were used. These established analytical methods were modified where necessary as described in Materials and Methods section below.

This paper presents information on the quality of the chemical data produced by analyzing the complex array of volatile organic compounds (VOCs), semi-volatile organic compounds (SVOCs), rubber-related chemicals (e.g., benzothiazole), and particulate matter in the various sample types from the study. The sample types included air sampling (personal and area) in fields with active play and inactive (background) fields. The quality of the results of analyses for off-gassing compounds from bulk crumb rubber samples collected from 11 athletic fields (including the six athletic fields where air monitoring occurred for this study) are also presented. The use of a new approach to measuring N-nitrosamines, benzothiazole and rubber related compounds that employs HPLC-MS/MS (in lieu of the prescribed GC methodologies) is given special attention. N-nitrosamines, benzothiazole and the other targeted rubber related compounds (2-mercaptobenzothiazole, 4-tert-octylphenol, butylated hydroxyanisole (BHA), and butylated hydroxytoluene (BHT)) were studied because these compounds are associated with rubber production [9] and were hypothesized to be of interest from a human health standpoint [10].

Sample Collection, Transport, and Storage

Although an evaluation of the sampling, transport, and storage of samples is not within the scope of this paper, some background on these topics is useful and relevant to the chemical analyses. Six athletic fields were sampled for this study: four outdoor fields, one indoor field, and one outdoor suburban grass area. Area samples were collected at 0.15 meter (six inches) and 0.91 meter (three feet) from turf surface both on and off (upwind) of the field of active play.

Additional area samples were collected in the neighborhood area away from the turf fields for background analyte concentration data. Three players were also equipped with personal sampling equipment at approximately one meter from the turf surface to monitor for selected target compounds (VOCs, N-nitrosamines, and rubber related targeted SVOCs) during active play. For further sampling information, a detailed description of the sampling design of this study has been published previously [6, 11].

Air Sampling

PM_{10} concentrations were measured using Harvard Impactors (Air Diagnostics and Engineering, Inc., Harrison, ME). Particulate matter was deposited onto 37 mm Teflon filter media (Pall Corporation, Ann Arbor, MI) according to US CFR40, Part 50 for particulate matter [12]. The completed sample filter was aseptically transferred to a foil lined Petri dish , which was transported back to the laboratory in coolers. Upon receipt at the laboratory, the PM_{10} sample filters were stored frozen until conditioned to constant temperature and humidity and weighed.

Air samples for VOCs were collected on 1.4 L (personal samples) and 6 L (for area samples) SUMMA canisters (ENTECH Instruments, Inc., Simi Valley, CA). The canisters were fitted with valves that were calibrated to sample for a two hour period. The VOC samples were shipped to the laboratory by overnight courier and stored at room temperature until analyzed. VOC samples were analyzed within 14 days per the US EPA TO-15 method [13].

PAHs and miscellaneous SVOCs were collected with Foam (PUF) Samplers (PS-1, Anderson Instruments, Inc., GA) according to EPA Method TO-13A [14]. Sampling heads were loaded with cylindrical glass PUF/XAD-2 cartridge (PUF Plug Part #20038, Supelco, Bellefonte, PA) and filter (Whatman Quartz Microfiber Filters, 102 mm, GE Healthcare Biosciences, Piscataway, NJ). Samples were transported to the laboratory by overnight courier in coolers with cool packs and stored refrigerated at 4 °C at the laboratory until analysis.

Targeted SVOC compounds were collected onto sorbent media as described in NIOSH Method 2522 for seven N-nitrosamines [15] and NIOSH Method 2550 for benzothiazole and four other targeted rubber related compounds [16]. Samples were transported back to the laboratory in coolers with ice packs and stored frozen at -20 °C until analysis. Because both of these methods have not been fully validated, trip blanks and trip spikes accompanied sample media throughout the process to assess recovery during sample transport and storage.

Bulk Rubber Sampling

Crumb rubber bulk samples were collected from eleven different fields as described in Simcox et al. [6,11]. Bulk samples were collected from five locations on each field. At each location, crumb rubber was placed in a pre-cleaned screw capped glass jar, covered to protect from light, and shipped to the laboratory (n=55). Upon receipt at the laboratory, the bulk samples were stored refrigerated at 4 °C until analysis.

Methods

Glassware, Reagent Chemicals, and Solvents

For methods requiring desorption of analytes from sampling media, glassware listed below was either solvent rinsed or furnace ashed at 550 °C for at least 6 hours prior to use. Reagent chemicals used were at least ACS grade or higher purity. Solvents listed below were ACS HPLC/GC/UV and spectrophotometry grade or higher quality.

Analytical Standards

For the 60 VOC compounds (**Table 1**) that were measured using the TO-15 method, reference standards (gas mixtures) were obtained from Restek Chromatography Products (Bellefonte, PA). For the 114 SVOC compounds monitored (**Table 2**), reference standards were obtained from SigmaAldrich (St. Louis, MO), Chiron (Trondheim, Norway), Accustandard (New Haven, CT), and Supelco (Bellefonte, PA). Seven N-nitrosamine compounds (**Table 3**) were analyzed and reference standards were obtained from ChemService, Inc. (West Chester, PA). Benzothiazole and associated compounds are listed in **Table 4**, and reference standards for these compounds were obtained from SigmaAldrich (St. Louis, MO).

PM10 Method

For PM_{10} analysis, samples were weighed according to CFR Title 40, Part 50 before and after sampling to determine particulate matter concentration [12]. Prior to shipment for field sampling, 37mm, 2 μm pore size Teflon filter media (Pall Corporation, Port Washington, NY) was conditioned in a temperature and humidity controlled room and pre-weighed in triplicate on a MT5 Microbalance (Mettler Toledo, Columbus, OH) using an Automated Weighing System (AWS) (Bohdan Automation, Inc., Vernon Hills, IL). Filters were shipped to the study site and used for sampling within 30 days of their tare date. Upon return of samples to the laboratory, the filters were stored at <4 °C pending gross weight analysis, which occurred within 30 days of the sampling date. Samples were conditioned in a temperature and humidity controlled room and analyzed for gross weight in triplicate using the AWS. To calculate the PM_{10} concentration in $\mu g/m^3$, the mean tare weight was subtracted from the mean gross weight, and that result was divided by the total air volume sampled in cubic meters.

Volatile Organic Compounds (VOCs) by GC/MS

All canisters (1.4 L and 6 L) were calibrated with a mass flow controller to collect air samples for up to 120 minutes. A modified version of U.S. EPA Method TO-15 by GC/MS was used to measure ambient-level concentrations for the VOC analytes [13]. Briefly, this method incorporates a multi-stage concentration process using an ENTECH 7100A Preconcentrator. This removes carbon dioxide, nitrogen, and water with a series of traps. The sample (500 mL) is

injected on a glass bead trap at a temperature of -150 °C. The trap temperature is then adjusted to 10 °C and purged gently with helium to transfer the VOCs and the carbon dioxide to a second trap. The second trap, which contains Tenax^{TM}, is adjusted to 10 °C, allowing the carbon dioxide to pass through the trap while retaining the VOCs. The second trap is heated and back-flushed with helium, sending the sample to the focusing trap, which is cooled to -160 °C. The focusing trap is then rapidly heated to 60 °C and the sample is injected onto the Rxi-lms (Restek Chromatography Products, Bellefonte, PA 16823), 60 m capillary column. Gas chromatographic separation conditions follow: inlet temp 250 °C; helium flow 1.0 mL/min, and average velocity 37 cm/second; initial oven temperature 35 °C hold for 2 minutes, ramp up at 8 °C/minute until 40 °C, then hold at 40 °C for 2 minutes, ramp from 40 °C to 200 °C at 6 °C/minute. Detection was achieved by mass spectrometric (MS) detection with electron ionization (EI) in scan mode (35 to 300 amu), capturing at least ten scans per chromatographic peak. For each analyte, a target ion and secondary ion(s) (if available) were extracted from the acquired MS scan data along with chromatographic retention time for identification and quantification. VOC concentrations were reported in ppbV and microgram per cubic meter (μg/m3) (Note: see the Supporting Materials section for this manuscript for further information regarding ppbV definition and calculations). Non-target compound peaks were identified by the National Institute of Standards and Technology (NIST) Database, if possible, and reported as non-quantified tentative identifications [17]. While a few non-targeted VOCs were tentatively identified, they are not the focus of this paper.

Semi-volatile Organic Compounds (SVOCs) by GC/MS

Samples were prepared and analyzed according to EPA Method TO-13A with the following modifications: (1) all samples were spiked with all internal standards pre-extraction, and (2) a rotary evaporator (Buchi, New Castle, DE) was used in place of a Kuderna-Danish concentrator [14]. Gas Chromatographic method parameters included: DB-5 MS column (30 m x 0.32mm), inlet temp 300 °C, helium flow 1.0 mL/min, and average velocity 37 cm/sec. Initial oven temperature 65 °C hold for 10 min, ramp up at 10 °C/min until 300 °C, then hold at 300 °C for 26.50 minutes. Detection was achieved by mass spectrometric (MS) detection with electron ionization (EI) in scan mode (35 to 500 amu), capturing at least five scans per chromatographic peak. For each analyte, a target ion and secondary ion(s) (if available) were extracted from the acquired MS scan data along with chromatographic retention time for identification and quantification.

Targeted Analysis for N-Nitrosamines, Benzothiazole and Other Rubber Related Compounds by HPLC-MS/MS

Special methodology was employed for monitoring specific rubber related organic compounds, including seven N-nitrosamines, benzothiazole, 2-mercaptobenzothiazole, 4-tert-octylphenol, butylated hydroxanisole (BHA), and butylated hydroxytoluene (BHT). For N-nitrosamines, samples were analyzed by a modified version of NIOSH Method 2522 [15,18]. In brief, air samples collected on Thermasorb/N media were desorbed with 3 mL of methylene chloride:methanol (75:25) solution. Aliquots of the desorbed samples were then analyzed by

reversed phase high-performance liquid chromatography (HPLC) employing a 0.1% formic acid:methanol linear gradient program. Detection was achieved by triple quadrupole mass spectrometry (MS/MS) using multiple reaction monitoring (MRM). Instrumental conditions for this method are summarized in the Supporting Materials section of this manuscript. The use of HPLC-MS/MS for this type of ambient air monitoring analysis has, to the author's knowledge, not been reported before. The HPLC-MS/MS method avoided the necessity of using a specialty GC detector (not available in the author's laboratory) and allowed for use of chromatography conditions more amenable to the polar nature of the compounds analyzed.

Targeted rubber related compounds were analyzed by an approach based upon NIOSH Method 2550 [16,19]. Bulk material or air samples collected on XAD-2 (vapor) and/or PTFE pre-filter (particulate) filter air sampling devices were desorbed in methanol with 10 minutes of sonication. Desorption volumes were 2 mL methanol for the particulate portion and 1 mL methanol for the vapor portion of each sample. Extracts were analyzed by reversed phase high-performance liquid chromatography employing a 0.1 % formic acid:methanol linear gradient program. Detection was achieved by triple quadrupole mass spectrometry using MRM. Instrumental conditions for this method are summarized in the Supporting Materials section of this manuscript. Again, HPLC-MS/MS detection was used instead of a GC method, taking account of the polar nature of the compounds.

Bulk Crumb Rubber Infill Off-gas Method

For VOC off-gassing of the bulk crumb rubber, the composited samples were analyzed by analysis of VOCs by GC/MS using ENTECH instrumentation (Simi Valley, CA), which is based upon OSHA Method PV2120 for the analysis of volatile organic compounds (VOCs) in air [20,21]. Samples were analyzed in an ENTECH 340 mL Large Volume Static Headspace (LVSH) container. A cleaned LVSH unit was heated to 70 °C overnight and then brought to room temperature in a clean room. A subsample (0.5 g) of each composited rubber infill was placed into the LVSH container, sealed with the stainless steel screw capped top/valve assembly, and heated in an oven at 70 °C for at least one hour. Immediately after the LVSH unit was removed from the oven, a 100 mL headspace air sample volume from within the LVSH unit was cryofocused by a liquid nitrogen cooled inlet and then injected into a GC/MS using a 60 meter RTX-624 capillary column (Restek Chromatography Products, Bellefonte, PA). Additional details for this method are summarized in the Supporting Materials section of this manuscript.

For bulk crumb rubber infill off-gassing analysis of targeted SVOCs and N-Nitrosamines, a Supelco (Bellefonte, PA) Adsorbent Tube Injector System (ATIS™) was utilized (**Figure 1**) [22]. A 0.5 g amount of bulk crumb rubber infill was weighed into the ATIS sample chamber, and the chamber was placed into the ATIS heating block assembly. The appropriate personal sampling media (XAD2 for SVOCs and Thermasorb/N for N-nitrosamines) was then affixed to the outlet of the sample chamber. A regulated flow of nitrogen gas (targeted flow = 1.0 L/min for N-Nitrosamines and targeted flow = 2.0 L/min for benzothiazole and 4-tert-octylphenol) was passed over the headspace in the sample chamber as it was heated to 60 °C, which allowed the

personal sampling media to collect the off-gassed analytes. The sample media was stored frozen at < -20 °C until analysis, where it was then desorbed and analyzed using the appropriate analytical methods as described above.

Quality Control (QC) Parameters

In general, quality control measures specified in the original methods (e.g., replicate analyses, spike recoveries, calibration checks) were employed. Details specific to the methods used are discussed below. Reporting limits, which are operationally defined limits, were typically set at the lowest acceptable (75% to 125% of the actual) concentration. Limits of detection and limits of quantification (three times the detection limit) were calculated using the U.S. EPA method detection limit calculation [23], based on statistics of replicate analyses, as specified in the referenced analytical methods. Reporting limits and Limits of Detection/Quantification for the study analytes are listed in **Table 1** through **Table 4**. While the U.S. EPA specified method was used to be consistent with the published analytical methods, we note that the LOD determination is conceptionally flawed [24].

PM 10 Evaluation

The balance used for weighing filters was calibrated with a traceable weight set prior to each use, and an internal weight calibration occurred after every ten weight measurements. Acceptance criteria per CFR Title 40, Part 50, for weight calibrations, must be $\pm$3 µg within the certified mass value. Room temperature must remain constant between 15 and 30 ^{o}C with a

variation of ±2 °C. Relative Humidity must remain at a constant level ±3 % that is less than 40 %. Results were the mean result from triplicate weight measurements. A field blank was analyzed with each analytical batch.

Volatile Organic Compounds (VOCs) by GC/MS

The quality control criteria of US EPA Method TO-15 were followed [13]. In summary, this involved a canister cleaning and certification protocol, recovery of calibration check standards, analysis of laboratory blanks, duplicate sample analysis, and the monitoring of compound and internal standard response and retention time values. It also involved the analysis of an instrument performance check standard (bromofluorobenzene (BFB)) prior to each run and after each 24 hours of run time to verify the mass spectrometer calibration is acceptable. A field spiked 6L SUMMA canister was also analyzed with the last sample batch for the study. Limits or detection (LOD) and quantification (LOQ) were determined by the U.S. EPA MDL method [23], using a Student's t test multiplier on the standard deviation of seven replicate low level spike analyses.

Semi-volatile Organic Compounds (SVOCs) by GC/MS

The quality control criteria of US EPA Method TO-13A were followed [14]. In summary, this involved recovery of calibration check standards and monitoring of compound and internal standard response and retention time values. It also included the analysis of laboratory blanks, field blanks, and laboratory control spikes at a rate of at least 5 % for the

samples analyzed. Reporting limits for the polyaromatic hydrocarbon (PAH) analytes were determined by the U.S. EPA MDL method [23], using a Student's t test multiplier on the standard deviation of seven replicate low level spike analyses. Reporting limits for the other SVOC analytes were determined from the lowest calibration standard analyzed with acceptable back calculated recovery (75 to 125 %).

Targeted Analysis for Rubber Related Compounds by HPLC-MS/MS

Quality control samples included laboratory reagent blanks, laboratory method blanks, and laboratory control spikes. Calibration check standards were also analyzed after every 10 samples analyzed. Reporting limits were determined from the lowest calibration standard analyzed with acceptable back calculated recovery (75 to 125 %). Duplicate blinded QC media spikes were also analyzed with each analytical sample batch, and results were verified to be within 30 % of theoretical value for acceptance. For benzothiazole and 4-tert-octylphenol, trip spikes and trip blanks accompanied the sample media and were analyzed along with the field samples. In addition, desorption efficiency spikes were also analyzed to evaluate the possible need for a desorption factor to be applied to the sample results. The reasons for the aforementioned trip spikes and blanks and desorption efficiency spikes are discussed in a later section.

Bulk crumb rubber infill

For crumb rubber VOC headspace analyses, method blank samples were run with each analytical batch – the LVSH chamber was analyzed empty and any VOC compounds detected above the reporting limit was noted in the analytical report. Reporting limits were determined as described above for rubber related compounds. Additional analytical QC parameters included daily calibration, linearity checks, detection limit verification, and desorption determination. The bulk crumb rubber samples were stored sealed in Teflon lined screw capped jars and were opened only when removing sample aliquots for analysis.

For targeted SVOC off-gas analyses, analytical QC parameters included daily calibration, linearity checks, and solvent blank analysis. In order to establish effective off-gassing and collection on media, Supelco Adsorbent Tube Injector System (ATIS™) spikes were run for the N-nitrosamine compounds, benzothiazole, 4-tert-octylphenol, BHA, and BHT. This involved spiking the ATIS chamber with a known amount of analyte, running the apparatus with the same conditions used for the bulk crumb rubber off-gassing tests, and capturing off-gassed compound onto sampling media. The lowest acceptable calibration standard was used for the reporting limit (**Table 1** through **Table 4**).

Results

The results discussed focus on the QC results and method performance parameters. For detailed field sample results and the human health risk assessment, refer to the sampling and analysis manuscript by Simcox et al. [6] and companion articles by Ginsberg et al. [7,8].

PM_{10} Quality

All weight calibrations made prior to each balance use were found to be within $\pm$3 µg of the certified mass value. Room temperature was verified to remain constant between 15 and 30 ^{o}C with a variation of $\pm$2 ^{o}C. Relative Humidity was less than 40 % and verified to remain at a constant level (within $\pm$3 %). Final PM_{10} concentrations for two of the six fields samples were blank corrected due to background (0.001 mg) detected in their associated field blank filters. All replicate analyses were within method specifications. Relative standard deviations and coefficients of variation for triplicate weighings ranged from 0 to 0.0035 and 0 to 0.003 %, respectively.

Volatile Organic Compounds (VOCs) by GC/MS

As mentioned above, canisters were subjected to a cleaning and pressure certification protocol [25] prior to use. One canister from each cleaning batch was analyzed and verified to be VOC free, and one canister was tested at approximately 30 psig to verify the canister seal was acceptable for use. All of these cleaning and pressure checks passed. Calibration check standards analyzed at the beginning and end of each analytical run gave recoveries that ranged between 60.5 % and 153% for all 60 compounds. Sample data was annotated for the small number of compounds that exceeded $\pm$30 % of the theoretical spike value (1,2,4-trichlorobenzene, 1,2-dichloropropane, acetone, and styrene) . Each analytical run included one

method blank per batch of samples (generally six samples, or less). Only one method blank had a compound (acetone) that exceeded its LOD, and the result for that analyte was flagged to indicate blank contamination. Duplicate analysis was performed on one sample per analytical batch. The relative percent difference (RPD) for each compound was within ±25 %, with the exception of one low methylene chloride duplicate result (41.5 % RPD). Retention time values were within Method TO-15 tolerance of ±0.3 minutes. Sample data for one batch of samples was annotated because the internal standard response exceeded the ±40 % of calibration response criteria set in Method TO-15. Otherwise, internal standards met this response criteria. Daily quality control checks were performed and were always within 30 % of the corresponding calibration standards. Bromofluorobenzene (BFB) instrument performance check standard results always passed Method TO-15 acceptance criteria. Recovery results for a 6L SUMMA canister that was spiked and shipped to and back from the field sampling site ranged from 78% to 126 %. All analyte calibration curves were calculated by external standardization and had a correlation coefficient (r) of 0.989 or greater, corresponding to a Coefficient of Determination (r^2) value of 0.980 or greater. Sample results that exceeded the highest calibration standard were annotated as estimated values. The LOD and LOQ values as determined by the U.S. EPA Method Detection Limit (MDL) method for each compound are listed in **Table 1** [23]. For all analytes, the calculated LOD was either 0.1, 0.2, or 0.5 ppbV.

Semi-volatile Organic Compounds (SVOCs) by GC/MS

The SVOC samples were analyzed in three separate batches of approximately six samples per batch. Internal standard response and retention time stability were within the

tolerances listed in Method TO-13A. A summary of the laboratory blank sample analysis is listed in **Tables 5 and 6**. Note that the method blanks showed that background concentrations were often present, although detections varied from batch to batch. Laboratory spike sample data performance for SVOCs is summarized in **Tables 7 and 8**. As the tables show, recoveries were generally within 75 % to 125 %. There was not, in general, a consistency among outliers between the filter and spike samples. For example, many of the higher alkanes (e.g., tricosane through dotriacontane) exceeded 125% recovery in one batch of filters, but did not exceed the acceptance criteria for other batches or the PUF samples (except for two of the PUF analytes from Batch 3). Calibration curves were calculated by mass labeled internal standardization. Internal standards used are listed in **Table 2**. The Coefficient of Determination (r^2) values of analyte calibration curves ranged from 0.9829 to 1.0. The reporting limits for the SVOC analytes are listed in **Table 2**. These limits ranged from 3.6 to 250 ng/sample.

Targeted Analysis for Rubber Related Compounds by HPLC-MS/MS

External standard calibration was used for these analytes, and correlation coefficients (r values) for standard curves ranged between 0.9981 and 0.9993 for N-nitrosamines, benzothiazole and other targeted rubber related compounds. Laboratory control spike (LCS) recovery results ranged from 84.1 to 116 % for the seven N-nitrosamine compounds tested, and from 74.1 to 122.6 % for targeted rubber related SVOCs. N-nitrosamine blanks were all less than reporting limit and all N-nitrosamine calibration checks were also within $\pm$15 % of the actual value. Background signals were often observed for the benzothiazole and other rubber related compounds in the laboratory reagent blanks and laboratory method blanks. These background

levels were < 50 % of the reporting limits in all cases. Calibration check standard recoveries observed were as follows: 80.5 % to 111 % (n=14) for benzothiazole; 88.4 % to 118 % (n=14) for 2-mercaptobenzothiazole; 83.5 % to 189 % (n=13) for 4-tert-octylphenol; 89.2 % to 219% (n=13) for butylated hydroxyanisole (BHA); and 73.0 % to 92.7 % for butylated hydroxytoluene (BHT). Laboratory desorption spike recovery results were below 75 % for Benzothiazole (filter mean recovery = 42 % (n = 3); XAD-2 mean recovery = 63 % (n=3)) and 2-mercaptobenzothiazole (filter mean recovery = 25 % (n = 3); XAD-2 mean recovery = 45 % (n=3)) , and desorption correction factors were applied to QC and sample results, accordingly, for these compounds. The field spike recovery for benzothiozole (vapor phase) after desorption factor correction was also incomplete (mean recovery = 72 %). However, the LCS samples analyzed were within range after desorption factor correction (74.1 to 122.6 %), as noted above. The reporting limit chosen for each analyte represented the lowest calibration standard that was not affected by background signal and resulted in acceptable back calculated recovery (within ±25 % of theoretical value). The reporting limits for these analytes are listed in **Table 3** and **Table 4**. The reporting limit for all of the N-nitrosamines was 100 ng/sample and 10 - 20 ng/sample for benzothiazole and related rubber compounds.

Bulk crumb rubber infill off-gas tests

For VOC headspace testing, laboratory blanks during analyses were below reporting limits for most compounds. Carbon disulfide, silyls, and siloxane-containing VOCs were frequently detected in trace amounts, however. Traces of these compounds were not thought to be components of the samples since they are common contaminants of the analytical system

(e.g., carbon disulfide is a solvent used often in the authors' laboratory). As an extra measure, a laboratory background VOC sample was collected in the walk-in cooler/sample storage area and analyzed. The following VOC compounds were reported in the laboratory background sample: 2-methyl-butane (31 ppb), acetone (830 ppb), benzene (18 ppb), methylene chloride (1030 ppb), methyl alcohol (790 ppb), and pentane (52 ppb). As in most laboratories, it is difficult to quantitate traces of these compounds in real samples due to the presence of these compounds in the laboratory. Other QC parameters for this test (daily calibration coefficients of determination were all greater than 0.9, linearity checks were all within 50% of the theoretical concentration, and report limit verification and desorption determination were all within method specifications.

For benzothiazole and related compounds measured from bulk sample off-gas, calibration coefficients (r value) and calibration check standard recoveries are given in **Table 9**. Note that recoveries for some compounds, including benzothiazole, tended to exceed 100%. Solvent blank samples were less than reporting limit for all compounds tested. Supelco Adsorbent Tube Injector System (ATIS™) spike results for targeted rubber related compounds are also summarized in **Table 9**. In all cases, the spike results exceeded 100% recovery.

Discussion

The measurement of particulate matter is a gravimetric analysis that produces high quality data. While it is not possible to run spiked samples, replicate weighings consistently produced reproducible results based upon the relative standard deviation and coefficients of variation

observed in the reported results. Sampling is the most difficult part of this analysis, but sampling techniques have been thoroughly evaluated [12], and these are not discussed in detail here.

The quality of the VOC data that was produced was also generally good, although contamination from laboratory air is a constant concern with TO-15 analysis. It was important to communicate the compounds that were observed in detectable levels in blanks, or that were outside of the TO-15 spike control percent recovery ranges, so these analytes could be given more scrutiny during the COPC selection process and comparison of air concentrations reported to toxicity thresholds. These types of out of specification QC sample results are indicative of potential issues with the analytical instrumentation or gas supplies as well as potential contamination from laboratory air. As follow up actions to these QC concerns, the instrument was checked for leaks in the flow path and a hydrocarbon trap in a gas supply line was replaced. With these analyses, there was not an opportunity to go back and reanalyze samples when out of specification QCs were encountered because of the smaller 1.4 L canisters that were used.

Similarly, in the TO-13A method for SVOCs the entire sample is extracted and analyzed so, other than re-injection of an extract, QC results can only be annotated with the issue and reported to the data user for consideration during data analysis. Certain SVOC analytes are ubiquitous in the environment and are also common laboratory contaminants, such as certain PAH compounds and organic acids. Some of the SVOC QC spike sample results required a correction factor to deal with spike sample recoveries that were below 75 %. These factors were applied in an effort to give a ‘worst case’ value for the evaluation and selection of COPC.

Conversely, correction factors for spike recovery values greater than 125 % were not reduced in order for the values to represent the 'worst case'.

One possible explanation for SVOC spike recoveries that were not within the specified acceptance range is that surrogate internal standardization was used for many of the analytes. Ideally, in a mass spectrometric method, each analyte would have its own mass labeled analog as an internal standard. This is because the mass labeled compound should act in an identical fashion to the native analyte in the extraction process and in the analytical system. When an analyte list becomes too large, however, this approach is generally too costly or many of the compounds are not available in the labeled form. Consequently, labeled internal standards were limited to one per class of compounds tested (shaded rows in **Table 2**). As a result of having to use surrogate compounds for many of the internal standards, there can be some discrepancy between an analyte's extraction efficiency and/or instrument response and the surrogate internal standard with which it is associated. This is especially true in complex matrices, such as the high volume air samples that were analyzed as part of this project. When dealing with so many analytes, finding proper surrogates for all compounds is difficult. Hence, the surrogate internal standard process may have caused some of the poor spike recoveries.

As noted previously the targeted analysis of rubber related compounds used a different type of instrumentation than prescribed in the NIOSH analytical methods referenced [15,16]. These modifications were made to determine if they improved the efficiency and flexibility of the methodology. In the case of N-nitrosamines, all blank and spike QC data were within

method prescribed acceptance limits. For the benzothiazole and related rubber compounds, however, blanks and spike QC data were not as good.

Some of the targeted rubber related compounds, especially benzothiazole and 2-mercaptobenzothiazole, were found to carry over from injection to injection in the analytical instrumentation. This carryover caused background concentrations in the blank QC samples. This carry over effect might have been alleviated by the use of stronger solvent for needle washes between injections. Regarding recoveries of spiked compounds, benzothiazole and 2-mercaptobenzothiazole tended to be low while BHA and 4-tert-octylphenol tended to be high. A possible explanation for the low recovery is binding of the compounds to active surfaces. Sulfur containing organic compounds (benzothiazole and 2-mercaptobenzothiazole contain sulfur while BHA and 4-tert-octylphenol do not) are known to bind to surfaces that are capable of carrying charge (active surfaces), such as silanol groups on glass (Si-OH) or metal oxide surfaces on stainless steel [26]. For BHA and 4-tert-octylphenol the reason for the high recoveries is unknown, but it is noted that no internal standards (labeled or surrogates) were used. The use of internal standardization in future work might improve spike recovery performance for these compounds. Recoveries for BHT were within acceptable range.

Because there has been little experience in analyzing benzothiazole and additional compounds (2-mercaptobenzothiazole, 4-tert-octylphenol, BHA, and BHT) in air, additional QC samples were analyzed (trip blanks trip spikes, and desorption efficiency spikes) with these samples.

Trip blanks for all rubber related compounds were positive, although generally less than 50 percent of the reporting limit. Trip spikes were run only for benzothiazole and 4-tert octylphenol. Benzothiazole recovery was low, possibly for the sulfur surface interaction discussed above. The trip spike recoveries for 4-tert octylphenol were within the acceptable range.

The desorption efficiency spikes were satisfactory except for the sulfur-containing benzothiazole and 2-mercaptobenzothiazole. The low desorption efficiency for these compounds (63 % and 45 % on XAD media, respectively) again could result from surface binding affinity for sulfur moieties. Strong surface binding could occur on the filter and XAD-2 media, among other sites.

Two methods were used to evaluate the organic compounds that off-gassed from bulk crumb rubber. For the VOC off-gas method, low levels of common laboratory solvents and suspected laboratory instrument contaminants were present in blank samples. Otherwise, the VOC method QC criteria were met. For the SVOC off-gas tests using the ATIS, spikes of target compounds recovered by the system were always in excess of 100%. This showed that the ATIS could successfully volatilize the SVOC compounds of interest and collect them with high efficiency on the air sampling media.

Regardless of the data limitations presented by the QC results, the data from the methods used for this study were of sufficient quality that COPCs could be identified and concentrations were reported with enough confidence that values could be compared to toxicity thresholds as

part of the human health risk assessment. Again, the results of these methods stress the need for a variety of QC sample types to be analyzed when monitoring for a wide variety of analytes in difficult matrices; especially for analytical methods that have not been fully validated.

The results for N-Nitrosamines, Benzothiazole and other targeted rubber related compounds show that HPLC-MS/MS can be used as an alternative to the GC methods prescribed in published NIOSH methods [15,16]. This is an important finding for laboratories that do not have access to specialty GC detectors, such as the thermal energy analyzer detector called for in the NIOSH N-Nitrosamines method [15]. The more polar nature of these analytes also makes them more amenable to HPLC-MS/MS analysis.

Acknowledgements

The authors are grateful for the advice of Dr. James Schauer during the study sampling design phase of the field sampling project. The authors also thank Mark Allen, Air Quality Chemist for the WI Department of Natural Resources, for the use of WI DNR high volume air sampling equipment and advice during the field sampling campaign. Funding for this project was provided by the Connecticut Department of Environmental Protection.

Literature Cited

[1] 2008. Synthetic Turf Health Debate Takes Root, *Environ Health Perspect* 116: A116-A122

[2] Dye, C., Bjerke, A., Schmidbauer, N. and Mano, S. Norwegian Pollution Control Authority, Norwegian Institute for Air Research (NILU). 2006. "Measurement of air pollution in indoor artificial turf halls." Norway:NILU, 82-425-1716-9.

[3] California Environmental Protection Agency. 2007. Evaluation of Health Effects of Recycled Tires in Playground and Track Products. Sacramento, CA: Office of Environmental Health Hazard Assessment.

[4] U.S. Environmental Protection Agency. 2009. *A scoping-level field monitoring study of synthetic turf fields and playgrounds.* EPA/600/R-09/135. Washington, DC: National Exposure Research Laboratory, Office of Research and Development. Available at http://www.epa.gov/nerl/documents/tire_crumbs.pdf .

[5] Vetrano, K. and Ritter, G. 2009. Air Quality Survey of Synthetic Turf Fields Containing Crumb Rubber Infill. Prepared for New York City Department of Health and Mental Hygiene, NY, NY. TRC Project No. 153896.

[6] Simcox, N., Bracker, A., Ginsberg, G., Toal, B., Golembiewski, B., Kurland, T., and Hedman, C. 2011. Synthetic turf field investigation in Connecticut. *J. Toxicol. Environ. Health A.* 74:1133-1149.

[7] Ginsberg, G., Toal, B., Simcox, N., Bracker, A., Golembiewski, B., Kurland, T., and Hedman, C. 2011. Human health risk assessment of synthetic turf fields based upon investigation of five fields in Connecticut. *J. Toxicol. Environ. Health A.* 74:1150-1174.

[8] Ginsberg, G., Toal, B., and Kurland, T. 2011. Benzothiazole toxicity assessment in support of synthetic turf field human health risk assessment. *J. Toxicol. Environ. Health A.* 74:1175-1183.

[9] CAES (Connecticut Agricultural Experimental Station). 2007. Examination of Crumb Rubber Produced from Recycled Tires. AC005 – 8/07.

[10] US Consumer Product Safety Commission Contract CPSC-C-94-1122: Sensory and Pulmonary Irritation Studies of Carpet System Materials and their Constituent Chemicals. Prepared by Air Quality Sciences, Atlanta GA, 1996.

[11] Simcox, N., Bracker, A., Meyer, J. 2010. Artificial Turf Field Investigation in Connecticut - Final Report. Accessed May 13, 2012. http://www.ct.gov/dep/lib/dep/artificialturf/uchc_artificial_turf_report.pdf

[12] U.S Environmental Protection Agency National Primary and Secondary Ambient Air Quality Standards, Title 40 CFR Part 50 Appendix J Reference Method for the Determination of Particulate Matter as PM_{10} in the Atmosphere. Accessed May 9, 2012. http://ecfr.gpoaccess.gov/cgi/t/text/text-idx?c=ecfr&rgn=div5&view=text&node=40:2.0.1.1.1&idno=40#40:2.0.1.1.1.0.1.18.11 .

[13] U.S. Environmental Protection Agency.1999. Compendium of Methods for the Determination of Toxic Organic Compounds in Ambient Air, Second Edition, Compendium Method TO-15 Determination Of Volatile Organic Compounds (VOCs) In Air Collected In Specially-Prepared Canisters And Analyzed By Gas Chromatography/Mass Spectrometry (GC/MS). Washington DC:Office of Research and Development, EPA/625/R-96/010b.

[14] U.S. Environmental Protection Agency. 1999. Compendium of Methods for the Determination of Toxic Organic Compounds in Ambient Air, Second Edition, Compendium Method TO-13A Determination of Polycyclic Aromatic Hydrocarbons (PAHs) in Ambient Air Using Gas Chromatography/Mass Spectrometry (GC/MS). Washington DC:Office of Research and Development, EPA/625/R-96/010b.

[15] National Institute of Occupational Safety and Health (NIOSH). 1994. Method 2522 Nitrosamines. In: Eller PM, Cassinelli ME. Eds. NIOSH Manual of Analytical Methods, 4th ed., Cincinnati, OH: NIOSH. Accessed April 2, 2012 at http://www.cdc.gov/niosh/docs/2003%2D154/pdfs/2522.pdf.

[16] National Institute of Occupational Safety and Health (NIOSH). 1998. Method 2550 Benzothiazole in Asphalt Fume. In: Eller PM, Cassinelli ME. Eds. NIOSH Manual of Analytical Methods, 4th ed., Cincinnati, OH: NIOSH. Accessed April 2, 2012 at http://www.cdc.gov/niosh/docs/2003-154/pdfs/2550.pdf.

[17] NIST/EPA/NIH. 2011. Mass Spectral Library with Search Program (Data Version: NIST 11, Software Version 2.0g.

[18] Wisconsin Occupational Health Laboratory (WOHL). 2006. Method WL096.1.0 Nitrosamine samples desorbed with dichloromethane:methanol 75:25 (v/v) and analyzed by HPLC using MS/MS detection.

[19] Wisconsin Occupational Health Laboratory (WOHL). 2008. Method WL100.2 Benzothiazole and 4-(tert-Octyl)phenol by LCMSMS.

[20] Wisconsin Occupational Health Laboratory (WOHL). 2008. Method WG086.2 Analysis of VOCs by GC/MS using ENTECH instrumentation.

[21] United States Department of Labor, Occupational Safety & Health Administration (OSHA) Method PV2120. 2003. Volatile organic compounds in air. Control No. T-PV2120-01-0305-ACT. Accessed April 2, 2012 at http://www.osha.gov/dts/sltc/methods/partial/pv2120.html .

[22] Supelco 2007. Adsorbent Tube Injector System (ATIS™) Operation Manual. Document T702019A. 16pp.

[23] CFR 40, Appendix B to Part 136 – Revision 1.11. 2011. Definition and Procedure for the Determination of the Method Detection Limit. Accessed May 9, 2012. http://www.gpo.gov/fdsys/search/pagedetails.action?st=citation%3A40+CFR+136&bread=true&granuleId=CFR-2011-title40-vol23-part136-appB&packageId=CFR-2011-title40-vol23 .

[24] Zorn, M.E., Gibbons, R.D., Sonzogni, W.C. 1999. Evaluation of approximate methods for calculating the limit of detection and limit of quantification. *Environmental Science and Technology*. 33:2291-2295.

[25] Wisconsin State Laboratory of Hygiene (WSLH). 2008. ESS ORG IOP 0420. Canister Cleaning. Organic Chemistry Department / Emergency Response, Revision 2.

[26] Restek Chromatography Products. 2011. Restek Application Note - Petrochemical Applications, Protect LNG Sample Integrity and Prevent Sulfur Loss with Sulfinert® Sample Cylinders. Lit. Cat.# PCAN1290

Table 1: U.S. EPA TO-15 volatile organic compound (VOC) target compounds, Chemical Abstracts Service (CAS) Numbers, and limits of detection (LOD) and quantitation (LOQ). PPB V = part per billion on volume basis.

VOC Compound	CAS Number	LOD/LOQ (ppbV)
1,1,1-trichloroethane	71-55-6	0.1/0.33
1,1,2,2-tetrachloroethane	79-34-5	0.1/0.33
1,1,2-trichloroethane	79-00-5	0.1/0.33
1,1,2-trichlorotrifluoroethane	76-13-1	0.1/0.33
1,1-dichloroethane	75-34-3	0.1/0.33
1,1-dichloroethene	75-35-4	0.1/0.33
1,2,4-trichlorobenzene	120-82-1	0.1/0.33
1,2,4-trimethylbenzene	95-63-6	0.1/0.33
1,2-dibromoethane	106-93-4	0.1/0.33
1,2-dichlorobenzene	95-50-1	0.1/0.33
1,2-dichloroethane	107-06-2	0.1/0.33
1,2-dichloropropane	78-87-5	0.1/0.33
1,2-dichlorotetrafluoroethane	76-14-2	0.1/0.33
1,3,5-trimethylbenzene	108-67-8	0.1/0.33
1,3-butadiene	106-99-0	0.1/0.33
1,3-dichlorobenzene	541-73-1	0.1/0.33
1,4-dichlorobenzene	106-46-7	0.1/0.33
1,4-dioxane	123-91-1	0.5/1.65
1-ethyl-4-methylbenzene	622-96-8	0.1/0.33
acetone	67-64-1	0.5/1.65
acrolein	107-02-8	0.5/1.65
benzene	71-43-2	0.1/0.33
bromodichloromethane	75-27-4	0.1/0.33
bromoform	75-25-2	0.1/0.33
bromomethane	74-83-9	0.1/0.33
carbon disulfide	75-15-0	0.1/0.33
carbon tetrachloride	56-23-5	0.1/0.33
chlorobenzene	108-90-7	0.1/0.33
chloroethane	75-00-3	0.1/0.33
chloroform	67-66-3	0.1/0.33
chloromethane	74-87-3	0.1/0.33
chloromethylbenzene (alpha)	100-44-7	0.1/0.33
cis-1,2-dichloroethylene	156-59-2	0.1/0.33
cis-1,3-dichloropropene	10061-01-5	0.1/0.33
cyclohexane	110-82-7	0.1/0.33
dibromochloromethane	124-48-1	0.1/0.33
dichlorodifluoromethane	75-71-8	0.1/0.33
ethyl acetate	141-78-6	0.1/0.33
ethylbenzene	100-41-4	0.1/0.33
halocarbon 11	75-69-4	0.1/0.33
heptane	142-82-5	0.1/0.33

hexachloro-1,3-butadiene	87-68-3	0.1/0.33
hexane	110-54-3	0.1/0.33
m/p-xylene	179601-23-1	0.2/0.66
methyl ethyl ketone	78-93-3	0.1/0.33
methyl isobutyl ketone	108-10-1	0.5/1.65
methyl n-butyl ketone	591-78-6	0.5/1.65
methylene chloride	75-09-2	0.1/0.33
o-xylene	95-47-6	0.1/0.33
propene	115-07-1	0.1/0.33
styrene	100-42-5	0.1/0.33
tert-butyl methyl ether	1634-04-4	0.1/0.33
tetrachloroethylene	127-18-4	0.1/0.33
tetrahydrofuran	109-99-9	0.5/1.65
toluene	108-88-3	0.1/0.33
trans-1,2-dichloroethylene	156-60-5	0.1/0.33
trans-1,3-dichloropropene	10061-02-6	0.1/0.33
trichloroethylene	79-01-6	0.1/0.33
vinyl acetate	108-05-4	0.1/0.33
vinyl chloride	75-01-4	0.1/0.33

Table 2: US EPA TO-13A (modified) SVOC target compounds, CAS Numbers, and reporting limits. Shaded rows show mass labeled internal standard compounds.

SVOC Compound	CAS Number	Reporting Limit (ng/sample)
naphthalene d8		
naphthalene	91-20-3	42.7
acenapthene d10		
acenaphthylene	208-96-8	91.9
1-methylnaphthalene	90-12-0	18.8
2-methylnaphthalene	91-57-6	14.9
acenaphthene	83-32-9	33.5
fluorine	86-73-7	7.57
2,6-dimethylnaphthalene	581-42-0	23.8
pyrene d10		
phenanthrene	85-01-8	3.6
anthracene	120-12-7	5.4
fluoranthene	206-44-0	5.7
acephenanthrylene	201-06-9	10.0
pyrene	129-00-0	6.0
benz[a]anthracene d12		
benzo(ghi)fluoranthene	203-12-3	10.0
cyclopenta(cd)pyrene	27208-37-3	8.4
benz(a)anthracene	56-55-3	10.4
chrysene	218-01-9	7.5
1-methylchrysene	3351-28-8	7.9
retene	483-65-8	26.0
benzo(b)fluoranthene	205-99-2	18.8
benzo(k)fluoranthene	207-08-9	9.3
benzo(j)fluoranthene	205-82-3	10.0
benzo(e)pyrene	192-97-2	6.0
benzo(a)pyrene	50-32-8	5.6
perylene	198-55-0	15.0
coronene d12		
indeno(1,2,3-cd)pyrene	193-39-5	10.8
benzo(ghi)perylene	191-24-2	16.9
dibenz(ah)anthracene	53-70-3	26.0
picene	213-46-7	30.0
coronene	191-07-1	20.0
dibenzo(ae)pyrene	192-65-4	40.0
cholestane d4		
17A(H)-22,29,30-trisnorhopane	51271-94-4	10.0
17B(H)-21A(H)-30-norhopane	81600-07-9	10.0
17A(H)-21B(H)-hopane	33281-23-1	10.0
22S-homohopane	60305-23-9	10.0
22R-homohopane	38706-31-9	10.0

22S-bishomohopane	67069-15-2	10.0
22R-bishomohopane	67069-25-4	10.0
22S-trishomohopane	67069-16-3	10.0
22R-trishomohopane	67069-26-5	10.0
ABB-20R-C27-cholestane	481-20-9	10.0
ABB-20S-C27-cholestane	69483-48-3	10.0
AAA-20S-C27-cholestane	41083-75-4	10.0
ABB-20R-C28-ergostane	67069-20-9	10.0
ABB-20S-C28-ergostane	71117-89-0	10.0
ABB-20R-C29-sitostane	101834-40-6	10.0
ABB-20S-C29-sitostane	101914-26-5	10.0
pentadecane d32		
nonane	111-84-2	100.0
decane	124-18-5	100.0
undecane	61193-21-3	100.0
dodecane	112-40-3	100.0
tridecane	629-50-5	100.0
tetradecane	629-59-4	100.0
pentadecane	629-62-9	100.0
hexadecane	544-76-3	100.0
eicosane d42	62369-67-9	
norpristane	3892-00-0	100.0
heptadecane	629-78-7	100.0
pristine	1921-70-6	100.0
octadecane	593-45-3	100.0
phytane	638-36-8	100.0
nonadecane	629-92-5	100.0
eicosane	112-95-8	100.0
heneicosane	629-94-7	100.0
docosane	629-97-0	100.0
tetracosane d50	16416-32-3	
tricosane	638-67-5	100.0
tetracosane	646-31-1	100.0
pentacosane	629-99-2	100.0
hexacosane	630-01-3	100.0
heptacosane	593-49-7	100.0
triacontane d62		
octacosane	630-02-4	100.0
nonacosane	630-03-5	100.0
triacontane	638-68-6	100.0
dotriacontane d66		
hentriacontane	630-04-6	100.0
dotriacontane	544-85-4	100.0
tritriacontane	630-05-7	100.0
tetratriacontane	14167-59-0	100.0

hexatriacontane d74		
pentatriacontane	630-07-9	250.0
hexatriacontane	630-06-8	250.0
heptatriacontane	7194-84-5	250.0
octatriacontane	7194-85-6	250.0
nonatriacontane	7194-86-7	250.0
tetracontane	4181-95-7	250.0
decylcyclohexane	1795-16-0	100.0
pentadecylcyclohexane	6006-95-7	100.0
hexadecylcyclohexane	6812-38-0	100.0
heptadecylcyclohexane	19781-73-8	100.0
octadecylcyclohexane	4445-06-1	100.0
nonadecylcyclohexane	22349-03-7	100.0
squalane	111-01-3	100.0
decanoic Acid d19		
octanoic acid	124-07-2	100.0
decanoic acid	334-48-5	100.0
tetradecanoic Acid d27		
dodecanoic acid	143-07-7	100.0
tetradecanoic acid	544-63-8	100.0
pentadecanoic acid	1002-84-2	100.0
heptadecanoic Acid d33		
hexadecanoic acid	57-10-3	100.0
heptadecanoic acid	506-12-7	100.0
octadecanoic acid	57-11-4	100.0
nonadecanoic acid	646-30-0	100.0
pinonic acid	61826-55-9	100.0
palmitoleic acid	373-49-9	100.0
oleic acid	112-80-1	100.0
linoleic acid	60-33-3	100.0
linolenic acid	463-40-1	100.0
eicosanoic Acid d39		
eicosanoic acid	506-30-9	100.0
heneicosanoic acid	2363-71-5	100.0
docosanoic acid	112-85-6	100.0
tricosanoic acid	2433-96-7	100.0
tetracosanoic Acid d59		
tetracosanoic acid	557-59-5	100.0
pentacosanoic acid	506-38-7	200.0
hexacosanoic acid	506-46-7	200.0
heptacosanoic acid	7138-40-1	200.0
octacosanoic acid	506-48-9	200.0
nonacosanoic acid	4250-38-8	200.0
triacontanoic acid	506-50-3	200.0
dehydroabietic acid	1740-19-8	100.0

Table 3: NIOSH Method 2522 (modified) N-nitrosamine target compounds, CAS Numbers, and reporting limit (RL).

N-nitrosamine Compound	CAS Number	Reporting Limit (ng/sample)
N-nitrosodimethylamine (NDMA)	62-75-9	100
N-nitrosomorpholine (NMOR)	59-89-2	100
N-nitrosopyrrolidine (NPYR)	930-55-2	100
N-nitrosodiethylamine (NDEA)	55-18-5	100
N-nitrosopiperdine (NPIP)	100-75-4	100
N-nitrosopropylamine (NDPA)	621-24-7	100
N-nitrosodibutylamine (NDBA)	924-16-3	100

Table 4: NIOSH Method 2550 (modified) rubber related target compounds, CAS Numbers, and reporting limit (RL).

Targeted SVOC Compound	CAS Number	Reporting Limit (ng/sample)
benzothiazole	95-16-9	20
2-mercaptobenzothiazole	149-30-4	20
4-tert-octylphenol	140-66-9	10
butylated hydroxyanisole (BHA)	25013-16-5	10
butylated hydroxytoluene (BHT)	128-37-0	20

Table 5: SVOC Method blank data for filter portion of samples. SVOC = semivolatile organic compound, NA = not analyzed, ND = not detected, DNQ = detected but not quantified.

SVOC in filter media	**Laboratory Method Blank Results**		
	Batch 1	**Batch 2**	**Batch 3**
	ng/filter	**ng/filter**	**ng/filter**
naphthalene	ND	ND	**11.5**
acenaphthylene	ND	ND	ND
1-methylnaphthalene	ND	ND	ND
2-methylnaphthalene	ND	ND	ND
acenaphthene	ND	ND	ND
fluorene	ND	ND	ND
2,6-dimethylnaphthalene	NA	ND	ND
phenanthrene	ND	**0.15**	ND
anthracene	ND	ND	ND
fluoranthene	ND	ND	ND
acephenanthrylene	ND	ND	ND
pyrene	ND	ND	ND
benzo(GHI)fluoranthene	ND	ND	ND
cyclopenta(cd)pyrene	ND	ND	ND
benz(a)anthracene	ND	ND	ND
chrysene	ND	ND	ND
1-methylchrysene	ND	ND	ND
retene	ND	ND	ND
benzo(b)fluoranthene	ND	ND	ND
benzo(k)fluoranthene	ND	ND	ND
benzo(j)fluoranthene	ND	ND	ND
benzo(e)pyrene	ND	ND	ND
benzo(a)pyrene	ND	ND	ND
perylene	ND	ND	ND
indeno(1,2,3-cd)pyrene	ND	ND	ND
benzo(GHI)perylene	ND	ND	ND
dibenz(ah)anthracene	ND	ND	ND
picene	ND	ND	ND
coronene	ND	ND	ND
dibenzo(ae)pyrene	ND	ND	ND
17A(H)-22,29,30-trisnorhopane	ND	ND	ND
17B(H)-21A(H)-30-norhopane	**1.90**	ND	ND
17A(H)-21B(H)-hopane	**2.67**	ND	ND
22S-homohopane	ND	ND	ND

22R-homohopane	ND	ND	ND
22S-bishomohopane	ND	ND	ND
22R-bishomohopane	ND	ND	ND
22S-trishomohopane	ND	ND	ND
22R-trishomohopane	ND	ND	ND
ABB-20R-C27-cholestane	ND	ND	ND
ABB-20S-C27-cholestane	ND	ND	ND
AAA-20S-C27-cholestane	ND	ND	ND
ABB-20R-C28-ergostane	ND	ND	ND
ABB-20S-C28-ergostane	ND	ND	ND
ABB-20R-C29-sitostane	ND	ND	ND
ABB-20S-C29-sitostane	ND	ND	ND
undecane	ND	ND	ND
dodecane	ND	ND	ND
tridecane	ND	ND	ND
tetradecane	ND	ND	ND
pentadecane	ND	ND	ND
hexadecane	**52.7**	**31.9**	ND
norpristane	ND	ND	ND
heptadecane	ND	**DNQ**	**7.03**
pristane	ND	ND	ND
octadecane	ND	ND	ND
phytane	ND	ND	ND
nonadecane	ND	ND	**2.45**
eicosane	**33.9**	ND	ND
heneicosane	**19.9**	ND	ND
docosane	**203**	ND	ND
tricosane	**186**	ND	ND
tetracosane	**345**	ND	ND
pentacosane	**265**	**27.0**	ND
hexacosane	**295**	**32.1**	ND
heptacosane	**278**	**34.3**	ND
octacosane	**241**	**25.8**	ND
nonacosane	**191**	**30.8**	ND
triacontane	**174**	**30.9**	ND
hentriacontane	**131**	**39.6**	ND
dotriacontane	**142**	**27.8**	ND
tritriacontane	**91.7**	ND	ND
tetratriacontane	**77.6**	ND	ND

pentatriacontane	**56.7**	ND	ND
hexatriacontane	ND	ND	ND
heptatriacontane	ND	ND	ND
octatriacontane	ND	ND	ND
nonatriacontane	ND	ND	ND
tetracontane	ND	ND	ND
decylcyclohexane	ND	ND	ND
pentadecylcyclohexane	ND	ND	ND
hexadecylcyclohexane	ND	ND	ND
heptadecylcyclohexane	ND	ND	ND
octadecylcyclohexane	ND	ND	ND
nonadecylcyclohexane	ND	ND	ND
squalane	ND	ND	ND
octanoic acid	**121**	**103**	ND
decanoic acid	**87.6**	**68.3**	**60.9**
dodecanoic acid	**66.9**	**73.4**	**68.4**
tetradecanoic acid	**119**	**101**	**89.0**
pentadecanoic acid	**47.3**	**38.3**	**23.4**
hexadecanoic acid	**529**	**387**	**417**
heptadecanoic acid	**19.5**	**17.8**	**19.8**
octadecanoic acid	**436**	**318**	**519**
nonadecanoic acid	**2.88**	**7.58**	ND
pinonic acid	ND	ND	ND
palmitoleic acid	**31.3**	**17.0**	ND
oleic acid	**47.5**	**25.3**	ND
linoleic acid	**42.7**	ND	ND
linolenic acid	ND	ND	ND
eicosanoic acid	**11.4**	**11.1**	**4.55**
heneicosanoic acid	ND	**4.14**	ND
docosanoic acid	**17.2**	**15.2**	**13.6**
tricosanoic acid	**11.4**	**0.97**	ND
tetracosanoic acid	**27.9**	**25.7**	**16.4**
pentacosanoic acid	**16.0**	**19.2**	ND
hexacosanoic acid	**16.4**	**20.4**	ND
heptacosanoic acid	ND	ND	ND
octacosanoic acid	ND	ND	ND
nonacosanoic acid	ND	ND	ND
triacontanoic acid	ND	ND	ND
dehydroabietic acid	**DNQ**	**DNQ**	ND

Table 6: SVOC Method blank data for polyurethane foam (PUF) portion of samples. SVOC = semivolatile organic compound, AG = analysis group, NA = not analyzed, ND = not detected, DNQ = detected but not quantified.

SVOC in filter media	**Laboratory Method Blank Results**		
	Batch 1	**Batch 2**	**Batch 3**
	ng/PUF	**ng/PUF**	**ng/PUF**
naphthalene	**243**	**149**	**54.7**
acenaphthylene	ND	ND	ND
1-methylnaphthalene	**49.8**	**44.2**	ND
2-methylnaphthalene	**19.1**	**16.5**	ND
acenaphthene	ND	ND	ND
fluorene	**14.4**	ND	ND
2,6-dimethylnaphthalene	NA	ND	ND
phenanthrene	**15.4**	**6.34**	**2.18**
anthracene	ND	ND	ND
fluoranthene	**12.6**	**12.0**	ND
acephenanthrylene	ND	ND	ND
pyrene	ND	**2.80**	ND
benzo(GHI)fluoranthene	ND	ND	ND
cyclopenta(cd)pyrene	ND	ND	ND
benz(a)anthracene	ND	ND	ND
chrysene	ND	ND	ND
1-methylchrysene	ND	ND	ND
retene	ND	ND	**54.3**
benzo(b)fluoranthene	ND	**19.4**	ND
benzo(k)fluoranthene	ND	**11.0**	ND
benzo(j)fluoranthene	ND	**17.9**	ND
benzo(e)pyrene	ND	**15.7**	ND
benzo(a)pyrene	ND	ND	ND
perylene	ND	ND	ND
indeno(1,2,3-cd)pyrene	ND	ND	ND
benzo(GHI)perylene	ND	ND	ND
dibenz(ah)anthracene	ND	ND	ND
picene	ND	ND	ND
coronene	ND	ND	ND
dibenzo(ae)pyrene	ND	ND	ND
17A(H)-22,29,30-trisnorhopane	ND	ND	ND
17B(H)-21A(H)-30-norhopane	ND	ND	**24.4**
17A(H)-21B(H)-hopane	**25.7**	ND	**23.5**

22S-homohopane	ND	ND	ND
22R-homohopane	ND	ND	ND
22S-bishomohopane	ND	ND	ND
22R-bishomohopane	ND	ND	ND
22S-trishomohopane	ND	ND	ND
22R-trishomohopane	ND	ND	ND
ABB-20R-C27-cholestane	ND	ND	ND
ABB-20S-C27-cholestane	ND	ND	ND
AAA-20S-C27-cholestane	ND	ND	ND
ABB-20R-C28-ergostane	ND	ND	ND
ABB-20S-C28-ergostane	ND	ND	ND
ABB-20R-C29-sitostane	ND	ND	ND
ABB-20S-C29-sitostane	ND	ND	ND
undecane	ND	ND	ND
dodecane	ND	ND	ND
tridecane	ND	**414**	ND
tetradecane	**328**	**328**	**75.6**
pentadecane	ND	**187.66**	**DNQ**
hexadecane	**788**	**277**	**56.0**
norpristane	ND	ND	ND
heptadecane	**349**	**DNQ**	**46.3**
pristane	**DNQ**	ND	ND
octadecane	**344**	**DNQ**	**DNQ**
phytane	**DNQ**	ND	ND
nonadecane	**270**	**DNQ**	**DNQ**
eicosane	**276**	**31.6**	**DNQ**
heneicosane	**367**	**157**	**41.1**
docosane	**964**	**626**	**50.3**
tricosane	**1139**	**896**	**385**
tetracosane	**817**	**798**	**565**
pentacosane	**411**	**440**	**745**
hexacosane	**273**	**228**	**701**
heptacosane	**255**	**165**	**859**
octacosane	**168**	ND	**722**
nonacosane	**163**	ND	**714**
triacontane	**205**	ND	**542**
hentriacontane	ND	ND	**501**
dotriacontane	ND	ND	**258**
tritriacontane	ND	ND	**270**

tetratriacontane	ND	ND	ND
pentatriacontane	ND	ND	ND
hexatriacontane	ND	ND	ND
heptatriacontane	ND	ND	ND
octatriacontane	ND	ND	ND
nonatriacontane	ND	ND	ND
tetracontane	ND	ND	ND
decylcyclohexane	ND	ND	ND
pentadecylcyclohexane	ND	ND	ND
hexadecylcyclohexane	ND	ND	ND
heptadecylcyclohexane	ND	ND	ND
octadecylcyclohexane	ND	ND	ND
nonadecylcyclohexane	ND	ND	ND
squalane	ND	ND	ND
octanoic acid	**2179**	**607**	ND
decanoic acid	**829**	**270**	**462**
dodecanoic acid	**1173**	**168**	**677**
tetradecanoic acid	**729**	**321**	**512**
pentadecanoic acid	**312**	**110**	**186**
hexadecanoic acid	**3194**	**1626**	**5448**
heptadecanoic acid	**73.9**	**54.8**	**79.5**
octadecanoic acid	**1990**	**1127**	**3247**
nonadecanoic acid	**17.91**	ND	ND
pinonic acid	ND	ND	ND
palmitoleic acid	**136**	ND	ND
oleic acid	**330**	**79.0**	**96.8**
linoleic acid	ND	ND	ND
linolenic acid	ND	ND	ND
eicosanoic acid	**12.2**	**31.9**	**45.7**
heneicosanoic acid	ND	ND	ND
docosanoic acid	**138**	**126**	**140**
tricosanoic acid	**116**	ND	ND
tetracosanoic acid	**246**	**212**	**166**
pentacosanoic acid	**152**	ND	ND
hexacosanoic acid	**171**	ND	ND
heptacosanoic acid	ND	ND	ND
octacosanoic acid	ND	ND	ND
nonacosanoic acid	ND	ND	ND
triacontanoic acid	ND	ND	ND

dehydroabietic acid	**DNQ**	**DNQ**	**10005**

Table 7: SVOC method spike performance data data for filter portion of samples. SVOC = semivolatile organic compound, NA = not analyzed.

SVOC in filter media	% Recovery		
	Batch 1	**Batch 2**	**Batch 3**
naphthalene	81.5	88.6	87.1
acenaphthylene	91.5	107	107
1-methylnaphthalene	83.8	89.0	95.6
2-methylnaphthalene	61.0	70.7	76.2
acenaphthene	67.8	75.6	72.3
fluorene	86.5	93.1	82.8
2,6-dimethylnaphthalene	NA	72.5	84.6
phenanthrene	92.7	93.5	96.5
anthracene	61.1	69.7	82.8
fluoranthene	97.6	101	102
pyrene	100	103	102
benzo(GHI)fluoranthene	95.0	104	101
cyclopenta(cd)pyrene	28.7	32.9	38.6
benz(a)anthracene	93.5	103	98.5
chrysene	99.2	108	96.1
1-methylchrysene	99.5	104	101
retene	98.4	116	102
benzo(b)fluoranthene	93.2	94.4	102
benzo(k)fluoranthene	84.4	98.0	96.1
benzo(e)pyrene	99.9	98.9	103
benzo(a)pyrene	78.2	84.3	89.1
perylene	15.4	19.5	55.9
indeno(1,2,3-cd)pyrene	71.5	67.4	93.9
benzo(GHI)perylene	101	105	99.3
dibenz(ah)anthracene	102	102	99.0
picene	103	107	95.1
coronene	113	113	110
dibenzo(ae)pyrene	119	118	121
17A(H)-22,29,30-trisnorhopane	99.0	98.8	94.0
17B(H)-21A(H)-30-norhopane	101	114	97.6
17A(H)-21B(H)-hopane	108	107	105
22S-homohopane	116	114	107
ABB-20R-C27-cholestane	102	104	102
ABB-20S-C27-cholestane	102	98.4	81.2
ABB-20R-C28-ergostane	101	100	95.5
ABB-20R-C29-sitostane	105	111	103

undecane	107	115	135
dodecane	75.6	76.7	101
tridecane	115	105	119
tetradecane	112	102	108
pentadecane	124	119	117
hexadecane	112	121	119
norpristane	97.7	93.4	100
heptadecane	90.6	87.0	98.3
pristane	92.2	91.8	102
octadecane	103	102	108
phytane	100	97.4	103
nonadecane	102	101	106
eicosane	105	110	117
heneicosane	110	113	119
docosane	109	119	120
tricosane	101	110	149
tetracosane	103	119	183
pentacosane	100	113	178
hexacosane	99.6	113	191
heptacosane	103	115	174
octacosane	101	116	195
nonacosane	104	118	178
triacontane	103	112	172
hentriacontane	103	109	151
dotriacontane	101	109	152
tritriacontane	102	106	134
tetratriacontane	103	109	129
pentatriacontane	105	112	124
hexatriacontane	103	110	118
heptatriacontane	105	110	112
octatriacontane	107	112	112
nonatriacontane	106	110	112
tetracontane	104	107	115
decylcyclohexane	88.2	89.3	101
pentadecylcyclohexane	103	109	110
nonadecylcyclohexane	104	102	97.2
squalane	115	117	119
octanoic acid	89.5	89.8	102
decanoic acid	101	99.7	101

dodecanoic acid	95.5	97.6	96.1
tetradecanoic acid	106	104	102
hexadecanoic acid	124	119	112
octadecanoic acid	116	114	108
pinonic acid	25.7	20.7	35.9
palmitoleic acid	95.7	86.7	89.6
oleic acid	90.2	80.5	84.1
linoleic acid	81.4	77.6	86.4
linolenic acid	75.4	66.7	71.0
eicosanoic acid	99.2	95.8	94.5
docosanoic acid	99.9	96.1	93.0
tetracosanoic acid	105	99.4	102
octacosanoic acid	105	99.3	101
triacontanoic acid	106	104	107
dehydroabietic acid	91.7	92.2	108

Table 8: SVOC method spike performance data data for PUF portion of samples. PUF = polyurethane foam, SVOC = semivolatile organic compound, NA = not analyzed.

SVOC in PUF media	% Recovery		
	Batch 1	**Batch 2**	**Batch 3**
naphthalene	85.5	90.3	87.7
acenaphthylene	63.7	74.2	82.2
1-methylnaphthalene	58.4	59.4	58.9
2-methylnaphthalene	41.7	44.9	45.7
acenaphthene	42.9	45.4	44.9
fluorene	52.4	52.8	50.2
2,6-dimethylnaphthalene	NA	75.9	81.7
phenanthrene	97.6	97.5	91.4
anthracene	66.1	82.0	89.4
fluoranthene	102	101	100
pyrene	103	100	99.1
benzo(GHI)fluoranthene	97.9	99.6	103
cyclopenta(cd)pyrene	36.8	54.2	83.3
benz(a)anthracene	96.6	101	100
chrysene	103	99.3	102
1-methylchrysene	104	102	99.5
retene	116	109	106
benzo(b)fluoranthene	102	98.7	105
benzo(k)fluoranthene	99.0	98.2	105
benzo(e)pyrene	105	99.0	103
benzo(a)pyrene	91.1	92.2	95.1
perylene	89.6	92.3	101
indeno(1,2,3-cd)pyrene	102	102	103
benzo(GHI)perylene	98.8	106	103
dibenz(ah)anthracene	94.0	99.2	99.3
picene	109	107	100
coronene	109	113	112
dibenzo(ae)pyrene	118	112	119
17A(H)-22,29,30-trisnorhopane	106	100	90.1
17B(H)-21A(H)-30-norhopane	101	100	99.8
17A(H)-21B(H)-hopane	116	105	106
22S-homohopane	115	108	104
ABB-20R-C27-cholestane	99.9	103	104
ABB-20S-C27-cholestane	102	98.2	87.3
ABB-20R-C28-ergostane	102	99.2	98.4
ABB-20R-C29-sitostane	107	104	105

undecane	139	100	118
dodecane	91.3	101	102
tridecane	107	125	105
tetradecane	108	111	107
pentadecane	134	125	107
hexadecane	119	118	112
norpristane	106	108	107
heptadecane	96.0	93.1	97.1
pristane	97.3	99.0	99.3
octadecane	106	105	103
phytane	103	99.7	100
nonadecane	107	103	105
eicosane	109	111	109
heneicosane	118	117	112
docosane	124	128	114
tricosane	125	131	107
tetracosane	122	127	108
pentacosane	111	113	108
hexacosane	101	102	105
heptacosane	99.8	103	108
octacosane	105	109	112
nonacosane	105	107	114
triacontane	103	104	120
hentriacontane	105	106	141
dotriacontane	108	104	128
tritriacontane	107	104	117
tetratriacontane	106	108	109
pentatriacontane	110	109	111
hexatriacontane	111	105	108
heptatriacontane	113	106	108
octatriacontane	114	108	106
nonatriacontane	115	109	104
tetracontane	114	105	103
decylcyclohexane	103	108	103
pentadecylcyclohexane	101	106	107
nonadecylcyclohexane	99.6	94.6	101
squalane	108	107	117
octanoic acid	107	95.1	104
decanoic acid	107	102	97.4

dodecanoic acid	106	103	110
tetradecanoic acid	110	106	97.7
hexadecanoic acid	140	129	146
octadecanoic acid	118	117	110
pinonic acid	61.6	82.5	93.4
palmitoleic acid	93.6	95.1	161
oleic acid	93.3	87.4	156
linoleic acid	92.9	92.4	160
linolenic acid	82.6	82.7	151
eicosanoic acid	94.3	92.5	76.2
docosanoic acid	95.5	93.3	69.9
tetracosanoic acid	101	98.8	79.5
octacosanoic acid	106	106	83.6
triacontanoic acid	115	111	96.4
dehydroabietic acid	102	96.9	481

Table 9: QC results summary for off-gas analysis of benzothiazole and other rubber related compounds. N/A = not analyzed.

Rubber Related Compound	Correlation Coefficient (r value)	Calibration Check Standard Recovery Ranges (n = 7) (%)	ATIS Spike Result (% Recovery)
benzothiazole	0.9998	110 – 126 %	131%
2-mercaptobenzothiazole	0.9987	109 – 130 %	NA
4-tert-octylphenol	0.9984	149 – 184 %	283 %
butylated hydroxyanisole (BHA)	0.9996	117 – 173 %	141 %
butylated hydroxytoluene (BHT)	0.9968	181 – 230 %	166 %
N-nitrosodimethylamine (NDMA)	1.000	84.8 – 98.2 %	114 %
N-nitrosomorpholine (NMOR)	0.9999	91.1 – 103 %	129 %
N-nitrosopyrrolidine (NPYR)	0.9996	93.8 – 103 %	119 %
N-nitrosodiethylamine (NDEA)	0.9998	76.4 – 99.5 %	112 %
N-nitrosopiperdine (NPIP)	0.9990	101 – 108 %	151 %
N-nitrosopropylamine (NDPA)	1.000	95.5 – 102 %	144 %
N-nitrosodibutylamine (NDBA)	0.9997	95.4 – 106 %	145 %

Figure 1: Schematic for the Supelco Adsorbent Tube Injection System (ATIS). Samples are placed within the heated chamber, spiked through the port if necessary and a known volume of gas is collected on appropriate sorbent media to collect off-gassing SVOC compounds.

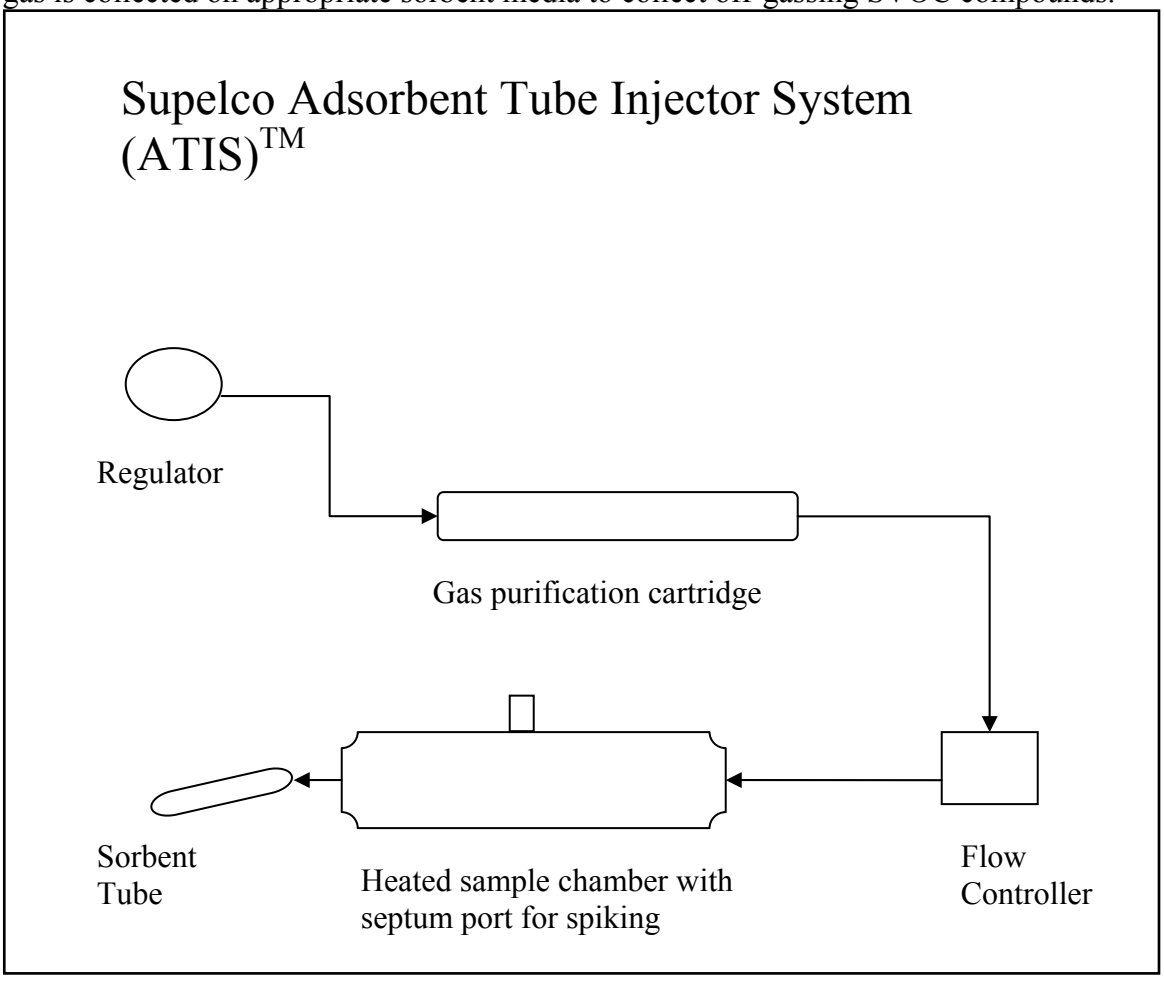

Chapter 3

Evaluation of Estrogenic and Androgenic Active Compounds Present in CAFO Environmental Samples using Bioassay Directed Fractionation Techniques

A version of this chapter will be submitted for publication to *Chemosphere* with the following co-authors: Jocelyn C. Hemming, Sonya Havens, Mark Mieritz, James Schauer, and William C. Sonzogni.

.Evaluation of Estrogenic and Androgenic Active Compounds Present in CAFO Environmental Samples using Bioassay Directed Fractionation Techniques

Curtis J. Hedman[*,1,2], Jocelyn C. Hemming[1], Sonya Havens[1], Mark Mieritz[1], James Schauer[1,2], William C. Sonzogni[2]

[1]Wisconsin State Laboratory of Hygiene, 2601 Agriculture Drive, Madison, Wisconsin, 53718, [2]Department of Environmental Chemistry and Technology, University of Wisconsin–Madison, Madison, Wisconsin, 53706

[*]Corresponding author telephone: (608) 224-6210; e-mail: cjhedman@facstaff.wisc.edu.

Keywords: hormones, CAFO, TIE, EDA, E-screen, A-screen HPLC-MS/MS, GC/MS.

ABSTRACT

Natural and synthetic steroids and their metabolites are released in animal urine and feces, and have been detected in runoff from Concentrated Animal Feeding Operations (CAFOs), raising concern over potential endocrine disrupting effects on benthic organisms and aquatic species. The current study evaluated the estrogenic and androgenic biological activity of extracts of liquid and solid samples from CAFO environmental samples. These extracts were fractionated by fraction collection liquid chromatography (FCLC) and analyzed by bioassays (E-screen and A-screen) and chemical analysis methods, such as high-performance liquid chromatography – ultraviolet – fluorescence – tandem mass spectrometry (HPLC-UV-FL-MS/MS) and gas chromatography – mass spectrometry (GC/MS) to determine fractions containing endocrine disrupting compounds and the identity and concentration of these compounds, where possible. Estrogenic bioactivity levels observed in the E-screen assay results were between 20 and 35 ng/L estrogen equivalents (Eeq) for the runoff samples. Androgenic bioactivity levels observed in the A-screen assay results were between ND and 10 ng/L androgen

equivalents (Aeq) for the runoff samples, 65 ng/L Aeq for the digester slurry sample, and 16 ng/g (dry wt.) Aeq for the manure sample tested. Hormones detected in the HPLC-MS/MS target compound analysis were 17beta-estradiol, 4-androstene-1,17-dione, progesterone, 17,20-dihydroprogesterone, nandrolone, and zearalenone. As part of an investigation to determine additional compounds potentially causing endocrine disrupting activity, triazine and phthalate related compounds were identified by derivitization GC/MS of E-screen and A-screen active fractions.

INTRODUCTION

Large scale confined livestock feeding operations generate more than 500 million tons of animal waste annually in the U.S.[1]. The trend in agriculture is toward CAFOs that confine a large number of animals in a small area and may have limited land available for effective manure disposal. Both natural and synthetic steroids and their metabolites are released in animal waste and have been detected in runoff from CAFOs [2-5]. In regards to biological effects, estrogen, androgen, and progestin agonistic and antagonistic activities have been associated with CAFO effluents [5-7] and female fish downstream from CAFOs have been masculinized [8-12].

The potential for hormone contamination of environmental compartments from CAFO-derived waste has led to many studies directed toward understanding the occurrence, fate, transport, and environmental effects from exposures resulting from releases of natural and synthetic steroid hormones in animal waste from CAFOs [13-21]. The hormones that are present

in animal manure can potentially enter the environment through direct discharge, spills, or leaching from holding tanks and ponds, animal confinement areas, waste handling, and containment systems, or through surface runoff from agricultural land where manure is applied as fertilizer or deposited in a rangeland grazing setting [22-29]. Even at relatively low environmental levels, natural and synthetic hormones and their metabolites have been shown to have effects on aquatic organisms. For example, trenbolone has been shown to be a potent reproductive toxicant in fathead minnows [9,30] and has adversely affected wild fathead minnow populations below a cattle feedlot [10]. Progesterone has also recently been shown to have adverse effects on fathead minnows [31].

To determine the potential impact of CAFO-generated waste on surrounding ecosystems, samples from various environmental compartments are collected and analyzed by various bioassays and chemical analysis methods. One of the advantages of bioassays is that endocrine disrupting activity can be detected, regardless of the chemical source. Comparing this bioactivity with targeted chemical analysis can usually account for some of the bioactivity, but often not all of it. One way to expand this bioactivity and chemical analysis is to run bioassay-directed fractionation experiments. In this technique, an extract is run through a HPLC separation, and timed fractions of the eluate are collected. These fractions are then reanalyzed by the bioassay and chemical methodology to help determine where the compound(s) eliciting toxicity reside in a complex mixture. The U.S. EPA developed a battery of tests based upon this methodology termed Toxicity Indicator Evaluation (TIE) in the late 1980s [32]

Snyder et al. [33] used bioassay-directed fractionation with a cell culture assay for estrogenicity (one type of toxicity endpoint that has received much attention of late due to interest in environmental causes of endocrine disruption), and were able to attribute 88 to 99.5 % of the total estrogen equivalents observed to beta estradiol and ethynyl estradiol concentrations detected in the same five liter surface water samples. Estrogen equivalents (Eeq) and androgen equivalents (Aeq) are a way of relating the potency of compounds that have estrogenic or androgenic properties to beta estradiol (E2), the most potent estrogen, and dihydrotestosterone (DHT), the most potent androgen, respectively (**Table 1**). The use of estrogen and androgen equivalents allows the summation of different compounds that cause estrogenic effects to get the total or cumulative potency of the mixture- similar to dioxin equivalents used to sum the contributions of different dioxin congeners to the overall toxicity [7]. Burnison and colleagues used a recombinant yeast estrogen screen bioassay to evaluate hog manure runoff in concentrated animal feeding operation (CAFO) drain tile samples [34]. They reported confirmation of 17-β-estradiol, estrone, and equol in the hog manure fractions and observed estrogenicity in drain tile samples from fields that had been recently amended with hog manure. Schlenk et al. (2005) used fish bioassay-guided fractionation of marine sediment extracts from the Southern California Bight, but the bioassay results did not always correlate with the compounds they measured in the samples [35]. They further noted that unknown compounds of relatively high polarity were in the bioactive fractions. More recently, this research group observed evidence of the same polar compounds in samples taken over a period of several years, indicating temporal and spatial stability of these compounds [36].

In Europe bioassay-directed fractionation studies are often termed Effect Directed Analysis or EDA [37-39]. Houtman et al. [40] utilized a TIE approach to identify estrogenic compounds in fish bile from bream in Dutch surface waters. They found native hormones (17-β-estradiol, estrone, estriol) and xenobiotic chemicals (17-α-ethinylestradiol, triclosan, chloroxylenol, clorophene) in both bream bile and the surface waters they came from. Although the natural estrogens and 17-α-ethinylestradiol helped to explain the observed elevated plasma vitellogenin and high incidence of intersex gonads in these fish, the other xenobiotic chemicals identified were not known to cause significant estrogenicity. In addition, estrogenic activity detected in their in vitro assay in the most non-polar fraction could not be assigned to any causative chemical(s) [40]. Kuch et al. [41] studied an effects directed analysis approach to identify estrogen-like compounds in groundwater adjacent to abandoned landfills. They reported that groundwater downstream from three out of seven landfill sites tested exhibited E-screen activity higher than the provisional benchmark of 0.5 ng estradiol equivalents per liter, but the xenoestrogens identified were not present in concentrations that explained the estrogenic activity observed [41].

The main goals of this study were to identify the estrogenic and androgenic activity of liquid and solid CAFO extracts, attribute the amount of this activity that is due to any target compounds present in the extracts, and to identify other compounds present that could help explain any remaining endocrine disrupting activity not accounted for by target compound analysis. A bioassay-directed fractionation approach was used to accomplish these goals.

STUDY SITE AND SAMPLING PARAMETERS

Study sites – Sampling was performed at farms participating in the Wisconsin Discovery Farms program, which is a unit of the University of Wisconsin and administered through the UW-Extension and College of Agriculture and Life Sciences at UW-Madison. The goal of this program is to support and facilitate research on best management practices at operating private farms. Samples were collected from three different farming operations. Farm site A is a 300 acre steer facility housing 600 animals, farm site B is a 4000 acre permitted CAFO dairy operation with 1,400 cows and an on-site manure digester system, and farm site C is a semi-confined dairy and steer facility housing approximately 200 animals. The study sites are maintained by Discovery Farms personnel, as well as staff contracted by the United States Geological Survey (USGS).

Sampling Parameters – Two to four liter surface water and tile drainage system samples were taken by grab sampling or by automated liquid samplers (Teledyne ISCO, Lincoln, NE) deployed on the study site into silanized glass containers. These samples were acidified to a pH of 2 with concentrated sulfuric acid, transported to the lab within 24 hours of collection, split into aliquots in silanized glass bottles at the laboratory, refrigerated, and processed within 14 days of sampling due to the potential for analyte losses [42]. Digester and manure samples were taken by grab sampling into two quart glass Mason Jars and were frozen as soon as possible pending extraction and analysis.

MATERIALS AND METHODS

Reagent chemicals – Hormone compounds were obtained from Sigma-Aldrich (St Louis, MO) with the exception of 17α-trenbolone, which was purchased from Hayashi Pure Chemical Inc. (Osaka, Japan). The isoptopically labeled standards 17β-estradiol-*d*5, 17α-estradiol-*d*2, estrone-*d*4, estriol-*d*3, testosterone-*d*5, 5α-androstan-17β-ol-3-one-*d*4, 4-androstene-3,17-dione-*d*7, nandrolone-*d*3, and progesterone-*d*9 were purchased from C/D/N Isotopes (Pointe-Claire, Quebec, Canada) and melengestrol-*d*3, melengestrol acetate-*d*3, 17β-trenbolone-*d*3 and α-zearalenol-*d*4 were obtained from the European Union Reference Laboratory at the National Institute for Public Health and the Environment (RIVM; Bilthoven, The Netherlands). Solvents and additives were obtained from the following companies: trace analysis grade methanol and dichloromethane from Burdick and Jackson (Morristown, NJ), ethyl alcohol from AAPER Alcohol (Shelbyville, KY), ethyl acetate, toluene, sulfuric acid (H_2SO_4) and copper sulfate pentahydrate ($CuSO_4$) from Fisher Scientific (Pittsburgh, PA) and sodium azide (NaAz) from Sigma-Aldrich (St. Louis, MO). All of the liquid samples were stored in 200 mL amber glass vials (Fisher Scientific, Hannover Park, IL) that received a silanization treatment to deactivate the glass surface to prevent hormone adsorption to the vial wall. The silanization treatment included: one rinse with 5% dimethyldichlorosilane (in toluene; Supelco, Bellefonte, PA), two rinses with toluene, and three rinses with methanol.

Liquid Sample Solid Phase Extraction for Bioassays - The surface water runoff samples intended for the E-screen bioassays were extracted using Empore™ SDB-RPS Extraction Disk Cartridges (3M, St. Paul, MN). The disks were swelled by soaking in 3 mL acetone and 3 mL isopropyl alcohol for three minutes each. The disks were then sequentially rinsed with 10 mL dichlormethane:ethyl acetate (1:1, v/v), 10 mL methanol and 20 mL 18 Mohm-cm water. The filtered surface water samples (1 L) were then filtered through the preconditioned extraction

disks, and the hormones were subsequently eluted with 5 mL ethyl acetate, 5 mL dichloromethane-ethyl acetate (1:1, v/v) and 5 mL dichloromethane.

Liquid Sample Solid Phase Extraction for Isotope Dilution HPLC-MS/MS Analysis - Each surface water sample was spiked with 50 µL of 1 µg/mL internal standard mix stock solution to account for extraction inefficiency [21]. The hormones were then extracted from the runoff samples using Isolute® ENV+ polypropylene solid phase extraction (SPE) cartridges (6 mL capacity, 200 mg sorbent bed mass, Biotage, USA). The SPE cartridges were preconditioned with 6 mL of methanol:ethyl acetate (1:1, v:v), 6 mL of methanol and 6 mL of 18Mohm-cm water at a flow rate of 3 mL/min. The sample (200 to 1000 mL) was then loaded onto the SPE cartridges at 3 mL/min, followed by a rinse with 10 mL of 18 Mohm-cm water and dried with a stream of air for five minutes. The hormones were then eluted from the cartridge with 6 mL of methanol followed by 6 mL of methanol:ethyl acetate (1:1, v:v) at a flow rate of 0.5 mL/min into methanol-rinsed collection vials. The extracts were concentrated with a gentle stream of nitrogen gas to a volume of approximately 100 µL and reconstituted to a final volume of 1.0 mL using methanol in 2.0 mL amber glass vials (Target LoVial; National Scientific, USA).

Solid Sample Accelerated Solvent Extraction - Both the manure samples and the digester solids samples were extracted using accelerated solvent extraction (ASE). The 11 mL stainless steel extraction cells (Dionex, Sunnyvale, CA, USA) used were sealed with stainless steel screw caps equipped with Teflon O-rings. For the soil samples, the assembled extraction cells were layered, from the bottom up, with two 19 mm muffled glass fiber filters (GF/A, Dionex), 2 g of muffled Ottawa sand and 5.0 ± 0.1 g of soil sample. Soil samples intended for liquid chromatography were spiked with 50 µL of 1 µg/L or 10 µg/mL internal standard mix stock

solution (in methanol), mixed with at least 2g Na_2SO_4 and then the methanol was allowed to evaporate. The soil samples intended for the E-screen bioassays were mixed with at least 2 g Na_2SO_4 without spiking. The mixed soil was then topped with 1 g of 110 °C oven baked Ottawa sand followed by one 19 mm GF/A filter. A stainless steel perforator was used to obtain eight 18 mm circular punches from each of the GF/B filters that were used to filter the surface water samples. Four of the punches were designated for liquid chromatography and the other four were intended for the E-screen bioassays. The filter punches for the E-screen were not spiked, whereas the four punches for the liquid chromatography were spiked with 50 μL of of 1μg/L internal standard mix stock solution that was equally distributed onto the punches. Two 19 mm GF/A filters were placed on the bottom of the assembled extraction cells followed by alternating layers of Na_2SO_4 and the GF/B filter punches and topped with one 19 mm GF/A filter. After tamping the material within the cell down and affixing the cell's top screw cap, the cells were loaded onto the ASE, preheated to 120 °C and held for five minutes without solvent. The solvent (1:1 acetone-hexane) was then added, and maintained at 120 °C and 1500 psi for 5 minutes. After a five-minute equilibration period, the solvent was eluted with a single flush of nitrogen into a 60 mL amber glass collection vial (I-CHEM, Rockwood, TN). Method blanks, consisting of three 19 mm GF/A filter disks, muffled Ottawa sand and Na_2SO_4, were extracted after every five soil sample extractions to ensure there was no analyte carry over.

HPLC-MS/MS analysis – The hormone concentrations in the extracts were analyzed using high-performance liquid chromatography (Agilent Technologies 1100 HPLC system, Santa Clara, California) with tandem mass spectrometric detection (Applied Biosystems/SCIEX API 4000 Foster City, California; MS/MS) operating in positive Atmospheric Pressure Chemical Ionization (APCI) mode. In summary, a sample injection volume of 15 μL was applied to a 4

μm, 4.6 x 250 mm Synergi MAX-RP column (Phenomenex, Torrance, CA) and separated with a reversed phase binary mobile phase gradient (channel A = 0.1 % formic acid; channel B = methanol) at 0.8 $mL \cdot min^{-1}$. Relevant multiple reaction monitoring (MRM) mass spectrometer settings included IonSpray ™ voltage at 5500 Volts, collision gas at 6 arbitrary units, curtain gas at 25 psig, nebulization gas at 40 psig, drying gas at 15 psig and source temperature at 450 °C. HPLC-MS/MS conditions are listed in the supporting materials section for this manuscript.

Fraction Collection Liquid Chromatography (FCLC) – Extracts were fractionated using an integrated FCLC system (Agilent Technologies 1200, Waldbronn, Germany) consisting of a refrigerated autosampler, a quaternary gradient pump, a refrigerated fraction collector, and integrated UV-diode array and fluorescence detection modules. LC separation parameters were the same as described for the HPLC-MS/MS section above, with the exception that 25 μL was injected instead of 15 μL per analysis. UV-diode array signal was collected discretely at 254 nm as well as in full scan mode from 100 to 400 nm. Where used, fluorescence detection parameters included excitation wavelength of 250 nm and an emission wavelength of 450 nm. The capillary dwell time from detector to fraction collector was calibrated by a standard protocol using a delay calibration standard [43].

Semi-volatile Organic Compounds (SVOCs) by GC/MS - Samples were analyzed by GC/MS parameters according to EPA Method TO-13a [44]. GC method parameters include: inlet temp 300 °C, flow 1.0 ml/min, and average velocity 37 cm/sec. Initial oven temperature 65 °C hold for 10 min, ramp up at 10 °C/min until 300 °C, then hold at 300 °C for 26.50 minutes. To screen for more polar compounds that might be present, an aliquot of extract was derivatized

by silylation with N,O-bis(trimethylsilyl)trifluoroacetamide (BSTFA) prior to analysis. Detection was achieved by mass spectrometric (MS) detection with electron ionization (EI) in scan mode (35 to 300 amu), capturing at least ten scans per chromatographic peak. The GC/MS peaks present in the tested fractions were evaluated with National Institute of Standards and Technology (NIST) mass spectral library [45].

E-screen and A-screen Bioassays - The E-screen uses MCF-7 breast cancer cells that proliferate in response to estrogenic compounds. The A-screen uses MCF7-AR1 cells, which are stable transfectants of MCF-7 cells that express the wild-type human androgen receptor [46] and respond to androgens by decreasing their proliferation rate. The MCF-7 and MCF7-AR1 cells were obtained from Drs. Sonnenschein and Soto at Tufts University (Boston, MA), maintained using methods described elsewhere [47] and cultured in Dulbecco's modified eagle's medium (DME; ICN Biomedicals, Aurora, OH) with 5 % fetal bovine serum (FBS; Hyclone Laboratories, Logan, UT) and incubated at 37 °C and 6.5 % CO_2 in 75 cm^2 tissue culture flasks.

The methods for the E-screen and A-screen are based on those described in [7]. Briefly, the MCF-7 and MCF7-AR1 cells were seeded into 24-well plates to achieve 2-3×10^4 cells per well. Twenty-four hours after seeding, the media was replaced with experimental media (charcoal dextran [CD] media), which consisted of DME devoid of phenol red (Irvine Scientific, Irvine CA) and 5 % FBS that was stripped of hormones using CD stripping procedures. Standard curves for estrogenic activity were prepared by exposing the CD-media containing MCF-7 cells to 15 concentrations of 17β-estradiol, ranging from 0.027 to 2724 ng/L, in quadruplicate. For the androgenic activity standard curve, 15 concentrations of testosterone

ranging from 0.29 to 2900 ng/L were exposed to CD-media containing MCF7-AR1 cells and supplemented with 27.2 ng/L 17β-estradiol. After five days of incubation, the cell proliferation was measured using the sulphorhodamine B dye (SRB; Sigma-Aldrich, St. Louis, MO) protein assay, which evaluates the total cell numbers by measuring the total protein content. The SRB-stained cells were read at a wavelength of 515 nm on a microplate reader (Molecular Devices, Sunnyvale, CA). The standard curve was fit with a four-parameter logistic equation with Softmax PRO v 2.6 (Molecular Devices, Sunnyvale, CA).

Dose-response curves spanning eight concentrations in quadruplicate were analyzed by E-screen and A-screen assays for each of the natural and synthetic hormone compounds studied (Table 1) to determine the potency of each of the target analytes. The concentration causing 50 % of the maximum cell proliferation (EC_{50}) was calculated using Microcal Origin v. 4.1 (Microcal, Northampton, MA). The potency of each target analyte (Table 1) was then determined relative to the EC_{50} of 17β-estradiol and 5α-androstan-17β-ol-3-one (dihydrotestosterone) for estrogenic and androgenic activity, respectively.

The estrogenic and androgenic activity in the samples was evaluated by adding the sample extract (in ethanol) to the CD-media, containing either MCF-7 cells or MCF-7-AR1, respectively, at a concentration no higher than 1 % in a dilution series to ensure that the activity in the samples fell within the linear portion of the standard curves. Cell proliferation was measured after a five day incubation using the SRB assay described above. The Eeqs and Aeqs of the samples were determined by interpolating the results from the standard curves and

correcting for the dilution and concentration of the samples. The limit of detection was 0.04 ng/L for estrogenic activity and 5.5 ng/L for androgenic activity.

Toxicity Indicator Evaluation (TIE) Methodology - Runoff samples from concentrated animal feeding operations were split and analyzed following the generalized schematic in **Figure 1**. Samples were split and then concentrated/cleaned up by solid phase extraction (SPE). Two other sub-samples of the SPE concentrate from Split 1 were each subjected to HPLC separations. For one sub-sample the fractions were collected and subjected to individual E-screen testing. The other sub-sample was passed through the HPLC and a qualitative analysis performed using in-line detectors. The detectors were arranged sequentially so that the eluent was analyzed by a UV detector, a fluorescence detector and a tandem mass spectrometer (in that order). The UV and fluorescence detectors are non-destructive, but may provide information on non-target compounds in the sample. The tandem mass spectrometer set up allows qualitative identification of targeted compounds (the mass spectrometer is optimized for detection of targeted compounds). **Table 1** lists the targeted compounds studied. The second split of the original sample (**Figure 1**) was dosed with mass-labeled target compounds. It was then subjected to SPE, and then isotope dilution quantitation of targeted compounds was performed. Isotope dilution provides highly accurate quantitation of analytes, accounting for extraction inefficiencies and mass spectrometer ionization matrix effects. All samples were run on the same column under the same chromatographic conditions to maintain a constant retention time for each compound over different sample runs.

Quality Control – For isotope dilution HPLC-MS/MS analysis, standard curves with a minimum of five points were generated with a correlation coefficient threshold of >0.990. Reagent and method blanks were analyzed with each analytical batch. Standard check samples were analyzed after every 10 samples analyzed, and were verified to be $^{+}$20 % of theoretical value. For FCLC runs, methanol blanks were run between field samples until UV and FL signals were free of extraneous peaks. For E-screen and A-screen analysis, a positive control sample (17β-estradiol for E-screen and dihydrotestosterone for A-screen) was fractionated and analyzed to ensure response occurred at the anticipated fraction.

RESULTS

The HPLC-MS/MS isotope dilution assay results, E-screen assay results, and A-screen assay results for samples from fractionation analysis of Farm A: Site 1 and Farm C: Site 5 runoff sample extracts are summarized in **Figure 2**. A-screen results from digester sample and manure sample solids extracts are shown in **Figure 3** and **Figure 4**, respectively.

Estrogenic bioactivity levels observed in the E-screen assay results were between 20 and 35 ng/L Eeq for the runoff samples (**Figure 2)**. Androgenic bioactivity levels observed in the A-screen assay results were between ND and 10 ng/L Eeq for the runoff samples (**Figure 2)**, 65 ng/L Eeq for the digester slurry sample (**Figure 3)**, and 16 ng/g (dry wt.) Eeq for the manure sample tested (**Figure 4)**. Hormones detected in the HPLC-MS/MS target compound analysis of the runoff samples were, 17-beta-estradiol, 4-androstene-1,17-dione, progesterone, 17,20-dihydroprogesterone, nandrolone, and zearalenone. When the target compound concentrations

observed in the runoff samples were normalized to E2 equivalent activity with corresponding potency factors (**Table 3**) and compared to the bioassay results, detected hormones accounted for between 40 and 100+% of the E-screen bioactivity observed. Potential endocrine disrupting compounds (EDCs) detected by derivatiztion GC/MS analysis of bioactive fractions were as follows: a triazine related compound (1,3,5-Triazine, 2-chloro-4,6-bis(methylthio)-, and and a substituted phthalate (Phthalic acid, 3,4-dimethylphenylmethyl ester).

DISCUSSION

Again, to summarize this bioassay directed fractionation process, two liter runoff grab samples were split and extracted by two different methods (**Figure 1**). In one method mass-labeled compounds were added to the sample, extracted by cartridge SPE, and analyzed by HPLC-MS/MS. In the second method, the same sample was analyzed by extracting the unaltered (no mass labeled compounds added) sample by disk SPE. This extracted sample was bioassayed using the whole extract or fractioned portions of the extract. The extracted whole sample was also analyzed by HPLC with UV-diode array, fluorescence, and mass spectrometric detection. GC/MS analysis was also performed on the bioassay-determined bioactive fractions in order to identify non-targeted compounds that may account for the additional endocrine disrupting activity detected. In general, hormones detected using the extraction cartridge and isotope dilution HPLC-MS/MS analysis were also detected using the disk SPE and the HPLC using an assortment of detectors. A noted exception was the presence of nandrolone observed in the cartridge SPE split from one sample, but not in the disk SPE split from that same sample.

Overall, from a qualitative standpoint, hormones detected or not detected by either extraction used were in agreement.

The additive bioassay results of the fractions were compared to the bioassay on the whole extract, and found to be similar. While, in this case, this suggests that the fractionation process was able to effectively parse out the compounds responsible for the overall toxicity without losses, it is important to note that the fractionation process results may not always agree with the total bioactivity observed. This is due to the fact that the fractionation process may separate two or more compounds from the whole extract that cause synergistic or antagonistic endocrine disrupting effects when present together.

To probe the efficacy of the entire process, the runoff sample results were subjected to the entire bioassay-directed fractionation process. The fractions were reanalyzed by the E-screen bioassay, and results compared to the original E-screen results, as well as the target compound analysis results. By multiplying the observed values of estrogenic target compounds present by potency factors (**Table 3**), the estradiol equivalent results could be compared to the values observed for the E-screen analysis. In the case of the Farm A: Site 1 sample from the March 2008 sampling event, the normalized estradiol equivalents observed (4.8 ng/L Eeq.) correlated well with the target compound (zearlenone) in fraction 7 that included that compound (4.7 ng/L Eeq.) (**Table 4 and Table 5**). The total estrogenicity also compared well between that observed for all fractions (11.9 ng/L Eeq.) (**Table 5**) and the E-screen result from the total extract (13 ng/L Eeq.) (**Figure 2**). The estrogenicity observed in fraction #8 could not be attributed to any of the target compounds from the MS/MS target hormones and metabolites analysis, and several peaks

observed in the fluorescence detection chromatogram suggest that unknown compound(s) contributed to the total estrogenicity of this extract.

Fractions that exhibited E-screen or A-screen activity that was not linked to the HPLC-MS/MS target compound concentrations present in them were analyzed by GC/MS, both with and without derivitization, in an attempt to identify the unknown compounds attributing to the additional bioassay activity observed. NIST database analysis of these runs tentatively identified two compounds that might help to explain the extra bioassay activity observed [45]. Certain triazine pesticides and phthalate compounds are known to cause endocrine disruption. To confirm that these compounds caused a portion of the unknown endocrine disrupting activity, putative standards will need to be purchased and tested by the bioassay. If they are confirmed EDCs, then these standards can be used to quantitate the amount present in the sample and to determine potency factors in order to compare quantitative results to the bioassay equivalents.

Certainly, there may be compounds present in bioactive fractions that may not be GC amenable, even with derivatization. This is especially true of earlier fractions from a reversed phase FCLC run, as the compounds that elute early in this type of chromatography are generally more polar in nature. Another potential way to identify these more polar unknown compounds that are endocrine disrupting compounds would be to run them, either by direct probe, infusion, or by HPLC introduction, on a high resolution mass spectrometer, such as a magnetic sector MS or a Fourier transform – ion cyclotron resonance (FT-ICR) MS. If a mass spectrum with enough resolution (>10,000) can be acquired, the number of possible molecular formulae can be limited to a few candidate structures. Acquiring the C13 and C14 peaks with high resolution, as well,

and using algorithms like that developed at U.S. EPA [48], can often reduce this list to one molecular formula. If enough unknown compound concentration is present in the fraction, nuclear magnetic resonance NMR analysis may also be performed to confirm the compound's structure.

Similar trends were observed for the two solid sample extracts tested by this TIE fractionation technique. Androgenic bioactivity was observed in the digester sample in both early (8-10) and later (12-14) fractions (**Figure 3**), suggesting compounds with more polar as well as less polar properties are responsible for the total androgenicity of this sample. Some of the bioactivity in these extracts was attributable to target compounds observed in the HPLC-MS/MS analysis, but the A-screen analysis suggests additional unknown compounds contribute to the overall androgenic activity of the extract. The majority of Aeq bioactivity in the manure sample (**Figure 4**) was observed in fraction 13 and lesser amounts were observed in fractions 9 and 12. This general pattern was also observed for the digester sample that was analyzed. Efforts are underway to apply the same chemical analysis methods used on the runoff samples to account for compounds (targeted and unknown) that are causing the endocrine disrupting effects in these samples.

The Eeq and Aeq concentrations observed in all three sample types (runoff, digester, and manure) were at levels that can elicit endocrine disrupting effects in biota. This highlights the importance of continued monitoring for the occurrence of these compounds in CAFO runoff and for further study of the efficacy of farm digester and other mitigation strategies to limit hormone and other endocrine disrupting compound release to the environment.

CONCLUSION

The estrogenicity and androgenicity of extracts from both liquid and solid CAFO generated samples was successfully characterized by use of E-screen and A-screen methodology. Fractionation of these extracts by FCLC showed that targeted compounds and some unknown compounds are causing endocrine disrupting effects. The use of isotope dilution HPLC-MS/MS allowed for quantification of targeted endocrine disrupting compounds present in samples, and the use of HPLC-UV-FL-MS/MS and GC/MS on sample fractions helped to determine the plausible identity of some unknown peaks that potentially contributed to the biological activity detected by A-screen and E-screen in those fractions. The development of potency factors for target compounds using these bioassays allowed for normalization of bioassay response that facilitated direct comparisons to concentrations of target compounds quantified by HPLC-MS/MS.

ACKNOWLEDGEMENT

This research presented in this manuscript was funded by the United States Environmental Protection Agency (U.S. EPA), Center for Environmental Research, Science To Achieve Results (STAR) program under grant number R833421 and the Wisconsin Department of Natural Resources Bureau of Drinking and Groundwater. The authors are grateful for the participation of University of Wisconsin Discovery Farms and United States Geological Survey personnel that coordinated sampling events and maintained monitoring stations.

LITERATURE CITED

[1] U.S. EPA 2009. *Compliance and Enforcement National Priority: Concentrated Animal Feeding Operations (CAFOs).* Accessed on April 2, 2012 at http://www.epa.gov/compiance/resources/publications/data/planning/priorities/fy2008prioritycwacafo.pdf .

[2] Schiffer, B., Daxenberger, A., Meyer, K., Meyer, H.H. 2001. The fate of trenbolone acetate and melengestrol acetate after application as growth promoters in cattle: Environmental studies. *Environmental Health Perspectives.* 109:1145-1151.

[3] Lange, I.G., Daxenberger, A., Schiffer, B., Witters, H., Ibarreta, D., Meyer H.H.D. 2002. Sex hormones originating from different livestock production systems: fate and potential disrupting activity in the environment. In *4th International Symposium on Hormone and Veterinary drug Residue Analysis*, Antwerp, Belguim, pp 27-37.

[4] Shore, L.S., Reichmann, O., Shemesh, M., Wenzel, A., Litaor, M.I. 2004. Washout of accumulated testosterone in a watershed. *Science of the Total Environment*. 332:193-202.

[5] Wilson, V.S., Lambright, C., Ostby, J., Gray, L.E.J. 2002. In vitro and in vivo effects of 17 betatrenbolone: a feedlot effluent contaminant. *Toxicological Sciences*. 70:202-211.

[6] Durhan, E.J., Lambright, C.S., Makynen, E.A., Lazorchak, J., Hartig, P.C., Wilson, V.S., Gray, L.E., Ankley, G.T. 2006. Identification of metabolites of trenbolone acetate in androgenic runoff from a beef feedlot.

[7] Soto, A. M., Calabro, J. M., Prechtl, N. V., Yau, A. Y., Orlando, E. F., Daxenberger, A., Kolok, A. S., Guillette, L. J., le Bizec, B., Lange, I. G., Sonnenschein, C. 2004. Androgenic and estrogenic activity in water bodies receiving cattle feedlot effluent in eastern Nebraska, USA. *Environmental Health Perspectives.* 112:346-352.

[8] Gray, L.E., Jr., Wilson, V.S., Stoker, T., Lambright, C., Furr, J., Joriega, N., Howdeshell, K., Ankley, G.T., Guillette, L. 2006. Adverse effects of environmental antiandrogens and androgens on reproductive development in mammals. *International Journal of Andrology*. 29:96-104.

[9] Ankley, G. T., Jensen, K. M., Makynen, E. A., Kahl, M. D., Korte, J. J., Hornung, M. W., Henry, T. R., Denny, J. S., Leino, R. L., Wilson, V. S., Cardon, M. C., Hartig, P. C., Gray, L. E. 2003. Effects of the androgenic growth promoter 17-beta-trenbolone on fecundity and reproductive endocrinology of the fathead minnow. *Environmental Toxicology and Chemistry.* 22:1350-1360.

[10] Orlando, E. F., Kolok, A. S., Binzcik, G. A., Gates, J. L., Horton, M. K., Lambright, C. S., Gray, L. E., Jr., Soto, A. M., Guillette, L. J. J. 2004. Endocrine disrupting effects of cattle feedlot effluent on an aquatic sentinel species, the fathead minnow. *Environmental Health Perspectives.* 112:353-358.

[11] Fenske, M., Maack, G., Schäfers, C., Segner, H. 2005. An environmentally relevant concentration of estrogen induces arrest of male gonad development in zebrafish, *Danio rerio*. *Environmental Toxicology and Chemistry.* 24:1088-1098.

[12] Gross-Sorokin, M. Y., Roast, S. D., Brighty, G. C. 2006. Assessment of feminization of male fish in English rivers by the environment agency of England and Wales. *Environmental Health Perspectives.* 114:147-151.

[13] Lee, L. S., Strock, T. J., Sarmah, A. K., Rao, P. S. 2003. Sorption and dissipation of testosterone, and estrogens, and their primary transformation products in soils and sediments. *Environmental Science and Technology.* 37:4098-4105.

[14] Casey, F. X. M., Simůnek, J., Lee, J., Larsen, G. L., Hakk, H. 2005. Sorption, mobility, and transformation of estrogenic hormones in natural soil. *Journal of Environmental Quality.* 34:1372-1379.

[15] Jacobsen, A. M., Lorenzen, A., Chapman, R., Topp, E. 2005. Persistence of testosterone and 17beta-estradiol in soils receiving swine manure or municipal biosolids. *Journal of Environmental Quality.* 34:861-871.

[16] Khanal, S. K., Xie, B., Thompson, M. L., Sung, S., Ong, S. K., Van Leeuwent, J. 2006. Fate, transport, and biodegradation of natural estrogens in the environment and engineered systems. *Environmental Science and Technology.* 40:6537-6546.

[17] Arnon, S., Dahan, O., Elhanany, S., Cohen, K., Pankratov, I., Gross, A., Ronen, Z., Baram, S., Shore, L. S. 2008. Transport of Testosterone and Estrogen from Dairy-Farm Waste Lagoons to Groundwater. *Environmental Science and Technology.* 42:5521-5526.

[18] Fan, Z., Casey, F. X. M., Hakk, H., Larsen, G. L. 2008. Modeling of coupled degradation, sorption, and transport of 17beta-estradiol in undisturbed soil. *Water Resources Research.* 44:456-467.

[19] Stumpe, B., Marschner, B. 2009. Factors controlling the biodegradation of 17 beta-estradiol, estrone and 17 alpha-ethinylestradiol in different natural soils. *Chemosphere.* 74:556-562.

[20] Khan, B., Lee, L.S. 2010. Soil temperature and moisture effects on the persistence of synthetic androgen 17alpha-trenbolone, 17beta-trenbolone and trendione. *Chemosphere.* 79:873-879.

[21] Mansell, D. S., Bryson, R. J.; T., H., Webster, J. P., Kolodziej, E. P., Sedlak, D. L. 2011. Fate of endogenous steroid hormones in steer feedlots under simulated rainfall-induced runoff. *Environmental Science and Technology.* 45:8811-8818.

[22] Finlay-Moore, O., Hartel, P. G., Cabrera, M. L. 2000. 17 beta-estradiol and testosterone in

soil and runoff from grasslands amended with broiler litter. *Journal of Environmental Quality.* 29:1604-1611.

[23] Lange, I. G., Daxenberger, A., Schiffer, B., Witters, H., Ibarreta, D., Meyer, H. H. D. 2002. Sex hormones originating from different livestock production systems: fate and potential disrupting activity in the environment. In *4th International Symposium on Hormone and Veterinary Drug Residue Analysis*, Antwerp, Belgium, pp. 27-37.

[24] Hanselman, T. A., Graetz, D. A., Wilkie, A. C. 2003. Manure-borne estrogens as potential environmental contaminants: a review. *Environmental Science and Technology.* 37:5471-5478.

[25] Kolodziej, E. P., Sedlak, D. L. 2007. Rangeland grazing as a source of steroid hormones to surface waters. *Environmental Science and Technology.* 41:3514-3520.

[26] Combalbert, S., Hernandez-Raquet, G. 2010. Occurrence, fate, and biodegradation of estrogens in sewage and manure. *Applied Microbiology and Biotechnology.* 86:1671-1692.

[27] Chen, T. S., Chen, T. C., Yeh, K. J., Chao, H. R., Liaw, E. T., Hsieh, C. Y., Chen, K. C., Hsieh, L. T., Yeh, Y. L. 2010. High estrogen concentrations in receiving river discharge from a concentrated livestock feedlot. . *Science of the Total Environment.* 408:3223-3230.

[28] Gadd, J. B., Tremblay, L. A., Northcott, G. L. 2010. Steroid estrogens, conjugated estrogens and estrogenic activity in farm dairy shed effluents. *Environmental Pollution.* 158:730-736.

[29] Gall, H. E., Sassman, S. A., Lee, L. S., Jafvert, C. T. 2011. Hormone discharges from a Midwest tile-drained agroecosystem receiving animal wastes. *Environmental Science and Technology.* 45:8755-8764.

[30] Jensen, K. M., Makynen, E. A., Kahl, M. D., Ankley, G. T. 2006. Effects of the feedlot contaminant 17alpha-trenbolone on reproductive endocrinology of the fathead minnow. *Environmental Science and Technology.* 40:3112-3117.

[31] DeQuattro, Z. A., Peissig, E. J., Antkiewics, D., Lundgren, E. J., Hedman, C. J., West, D. W., Hemming, J. C., Barry, T. P. 2012. Effects of progesterone exposure on fathead minnow (*Pimephales promelas*) reproduction. *Environmental Toxicology and Chemistry.* 31:851-856.

[32] U.S. EPA. 1991. Methods for aquatic toxicity identification evaluations - phase I toxicity characterization procedures. 2nd ed. Office of Research and Development, Report number: 600/6-91/003.

[33] Snyder, S. A., Villeneuve, D. L., Snyder, E. M., Giesy, J. P. 2001. Identification and quantification of estrogen receptor agonists in wastewater effluents. *Environmental Science and Technology.* 35:3620-3625.

[34] Burnison, B. K., Harmann, A., Lister, A., Servos, M. R., Ternes, T. A., Van Der Kraak, G.

2003. A toxicity identification evaluation approach to studying estrogenic substances in hog manure and agricultural runoff. *Environmental Toxicology and Chemistry.* 22:2243-2250.

[35] Schlenk, D., Sapozhnikova, Y., Irwin, M. A., Lingtian, X., Hwang, W., Reddy, S., Brownawell, B. J., Armstrong, J., Kelly, M., Montagne, D. E., Kolodzief, E. P., Sedlak, D., Snyder, S. 2005. In vivo bioassay-guided fractionation of marine sediment extracts from the Southern California Bight, USA, for estrogenic activity. *Environmental Toxicology and Chemistry.* 24:2820-2826.

[36] Lavado, R., Loyo-Rosales, J. E., Floyd, E., Kolodziej, E. P., Snyder, S. A., Sedlak, D., Schlenk, D. 2009. Site-specific profiles of estrogenic activity in agricultural areas of California's inland waters. *Environmental Science and Technology.* 43:9110-9116.

[37] Brack, W., Klamer, H., de Ada, M., Barcelo, D. 2007. Effect-directed analysis of key toxicants in European river basins - A review. *Environmental Science and Pollution Research.* 14:30-38.

[38] Scheurell, M., Franke, S., Huhnerfuss, H. 2007. Effect-directed analysis: a powerful tool for the surveillance of aquatic systems. *International Journal of Environmental Analytical Chemistry.* 87:401-413.

[39] Barceló, D. 2009. Applying combinations of chemical analysis and biological effects to environmental and food samples. *TrAC Trends in Analytical Chemistry.* 28:519-520.

[40] Houtman, C., Van Oostveen, A., Brouwer, A., Lamoree, M., Legler, J. 2004. Identification of estrogenic compounds in fish bile using bioassay-directed fractionation. *Environmental Science and Technology.* 38:6415-6423.

[41] Kuch, B., Kern, F., Metzger, J., von der Trenck, K. 2010. Effect-related monitoring: estrogen-like substances in groundwater. *Environmental Science and Pollution Research International.* 17:250-260.

[42] Havens, S. M., Hedman, C. J., Hemming, J. D. C., Mieritz, M. G., Shafer, M. M., Schauer, J. J. 2010 Stability, preservation, and quantification of hormones and estrogenic and androgenic activities in surface water runoff. *Environmental Toxicology and Chemistry.* 29:2481-2490.

[43] Agilent Technologies. 2003. *Innovative fraction collection with the Agilent 1100 Series purification platform*. Publication Number 5988-9250EN. 4pp. Accessed on April 2, 2012 at http://www.chem.agilent.com/library/applications/5988_9250EN.pdf .

[44] U.S. Environmental Protection Agency. 1999. Compendium of Methods for the Determination of Toxic Organic Compounds in Ambient Air, Second Edition, Compendium Method TO-13A Determination of Polycyclic Aromatic Hydrocarbons (PAHs) in Ambient Air Using Gas Chromatography/Mass Spectrometry (GC/MS). Washington DC:Office of Research and Development, EPA/625/R-96/010b.

[45] NIST/EPA/NIH. 2011. Mass Spectral Library with Search Program (Data Version: NIST 11, Software Version 2.0g.

[46] Szelei, J., Jimenez, J., Soto, A.M., Luizzi, M.F., Sonnenschein, C. 1997. *Endocrinology.* 138:1406-1412.

[47] Drewes, J. E., Hemming, J., Ladenburger, S. J., Schauer, J., Sonzogni, W. 2005. An assessment of endocrine disrupting activity changes during wastewater treatment through the use of bioassays and chemical measurements. *Water Environment Research.* 77:12-23.

[48] Grange, A. H., L. Osemwengie, G. Brilis and G. W. Sovocool (2001). "Ion Composition Elucidation (ICE): An investigative tool for characterization and identification of compounds of regulatory importance." International Journal of Environmental Forensics 2: 61-74.

Table 1: Target analyte list by class with compound's origin, associated CAS Number, and mass labeled internal standard used for isotope dilution quantitation.

Class	Origin	Target Analyte [CAS #]	Mass Labeled Standard
Estrogen	Natural	17-β-estradiol [50-28-2]	17-β-estradiol-d5
″	″	estrone [53-16-7]	″
″	″	estriol [50-27-1]	estriol-d3
″	Synthetic/ Fungal	α-zearalenol [36455-72-8]	α-zearalenol-d4
″		zearalanone [5975-78-0]	″
″	‟	zearalenone [17924-92-4]	″
Androgen	Natural	testosterone [58-22-0]	testosterone-d5
″	″	androsterone [53-41-8]	″
″	″	5-α-androstane-3,17-dione [846-46-8]	″
″	″	4-androstene-3,17-dione [63-05-8]	″
″	″	1-dehydrotestosterone (boldenone) [846-48-0]	″
″	″	17-β-nortestosterone (nandrolone) [434-22-0]	nandrolone-d3
″	Synthetic	17-β-trenbolone [10161-33-8]	17β-trenbolone-d3
Progestogen	Natural	progesterone [57-83-0]	progesterone-d9
″	″	17,20 dihydroxyprogesterone [1662-06-2]	″
″	Synthetic	melengestrol acetate [2919-66-6]	melengestrol acetate-d3
″	″	melengestrol [5633-18-1]	melengestrol-d3

Table 2: Targeted compounds detected in CAFO runoff HPLC-MS/MS sample extracts and identification of targeted compounds in CAFO runoff E-screen sample extracts by FCLC with MS/MS detection. ND = not detected, + = compound identified by MS/MS, (RT) = retention time of compound detected.

Analyte	Farm A Site 1 3/14/08		Farm C Site 5 3/14/08	
	Analytical Isotope Dilution HPLC-MS/MS Result	E-screen Extract HPLC-MS/MS Conf. (RT)	Analytical Isotope Dilution HPLC-MS/MS Result	E-screen Extract HPLC-MS/MS Conf. (RT)
Estriol	ND	ND	ND	ND
Estrone	ND	ND	ND	ND
Estradiol	ND	ND	89 ng/L	+ (19.5 min)
Testosterone	ND	ND	ND	ND
beta Trenbolone	ND	ND	ND	ND
Androsterone	ND	ND	ND	ND
Dihydrotestosterone	ND	ND	ND	ND
5-alpha-androstane-3,17-dione	ND	ND	ND	ND
11-beta-hydroxy-etiocholanolone	ND	ND	ND	ND
4-androstene-3,17-dione	ND	ND	55 ng/L	+ (19.0 min)
Progesterone	32 ng/L	+ (24.9 min)	360	+ (24.9 min)
17,20-dihydroxyprogesterone	ND	ND	109	+ (20.7 min)
Boldenone	ND	ND	ND	ND
Zearalanol	ND	ND	ND	ND
alpha Trenbolone	ND	ND	ND	ND
Nandrolone	ND	ND	12 ng/L	ND
Zearalenone	240 ng/L	+ (19.8 min)	ND	ND
Melengestrol	ND	ND	ND	ND
Melengestrol acetate	ND	ND	ND	ND
Zearalanone	ND	ND	ND	ND

Table 3: E-screen and A-screen relative potency factors.

Compound Class	Compound Name	Relative Potency Factor
Estrogens	**17-β-estradiol**	**1.00**
	α-zearalenol	0.29
	estriol	0.26
	α-zearalanol	0.15
	estrone	0.12
	zearalanone	0.067
	17-α-estradiol	0.035
	zearalenone	0.020
	β-zearalanol	0.017
Androgens	**dihydroestosterone**	**1.00**
	testosterone	0.25
	androsterone	0.00081
	5α-androstane-3,17-dione	0.0041
	4-androstene-3,17-dione	0.0047
	1-dehydrotestosterone (boldenone)	0.039
	17β-nortestosterone (nandrolone)	0.82
	17β-trenbolone	1.1

Table 4: Calculated potency of zearalenone observed in Sample Farm A, Site 1 - 3/14/08 in E-screen estrogen equivalents.

	Potency Relative to 17b-Estradiol	**Concentration in Sample (ng/L)**	**Estrogen Equivalents (ng/L)**
zearalenone	0.020	240	4.8*

* Zearalenone was detected in HPLC fraction 7 by HPLC-MS/MS at 240ng/L (see **Table 2**).

Table 5: E-screen results from HPLC Fractionation of Runoff Sample from Farm A, Site 1. Normalized Eeq. are corrected to concentration in runoff sample from amount of extract injected on column.

FCLC Fraction Number	**17b-Estradiol Eq. (ng/mL)**	**Normalized 17b-Estradiol Eq. (ng/L)**
Fraction #1 (0-3 min.)	<0.027	<0.027
Fraction #2 (3-6 min.)	<0.027	<0.027
Fraction #3 (6-9 min.)	<0.027	<0.027
Fraction #4 (9-12 min.)	<0.027	<0.027
Fraction #5 (12-15 min.)	<0.027	<0.027
Fraction #6 (15-18 min.)	<0.027	<0.027
Fraction #7 (18-21 min.)	.039	4.7
Fraction #8 (21-24 min.)	.06	7.2
Fraction #9 (24-27 min.)	<0.027	<0.027
Fraction #10 (27-30 min.)	<0.027	<0.027
Total	0.099	**11.9**

** The calculated potency of zearalenone, detected in fraction 7, was 4.8 ng/L as estrogen equivalents (see **Table 4**).

Figure 1: Analysis scheme used by author and colleagues for bioassay directed fractionation analysis of concentrated animal feeding operation (CAFO) samples. HPLC conditions (column and mobile phase gradient) are equivalent for different HPLC runs so data can be compared by retention time.

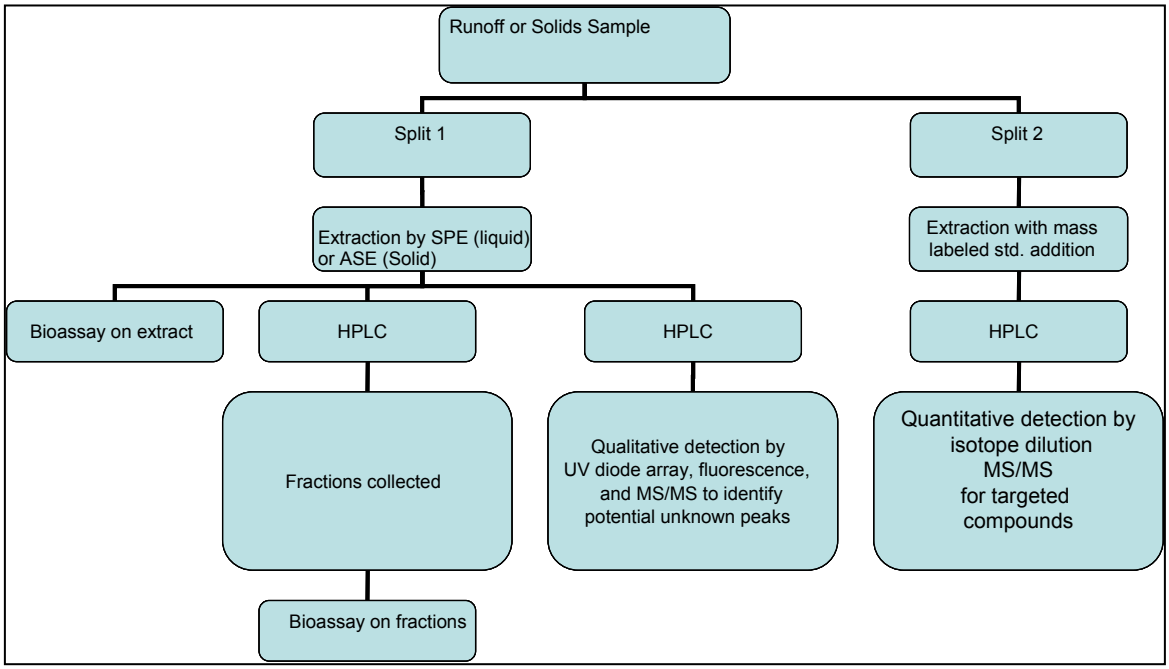

Figure 2: Results from HPLC-MS/MS target analysis of hormones and metabolites, E-screen, and A-screen results from representative CAFO runoff samples.

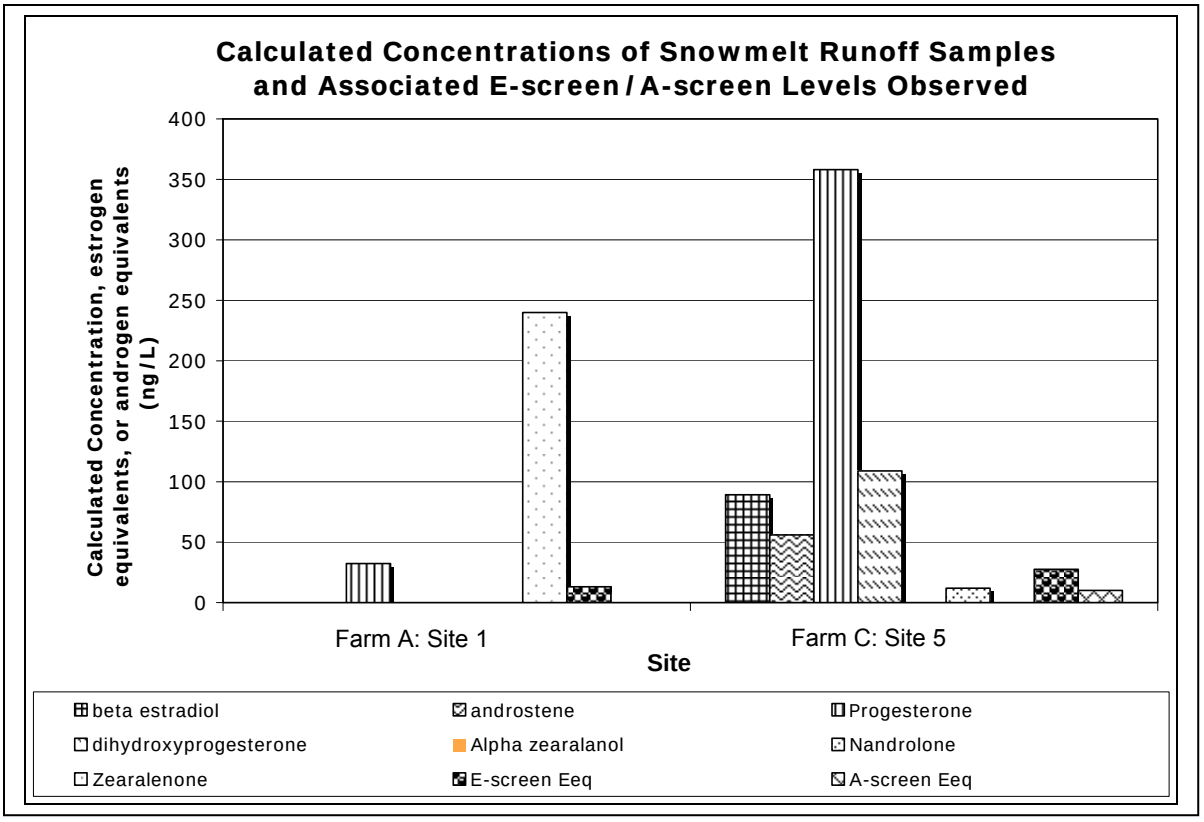

Figure 3: A-screen results (Aeq.) from HPLC fractionation of digester sample FU721. Note: F = fraction number.

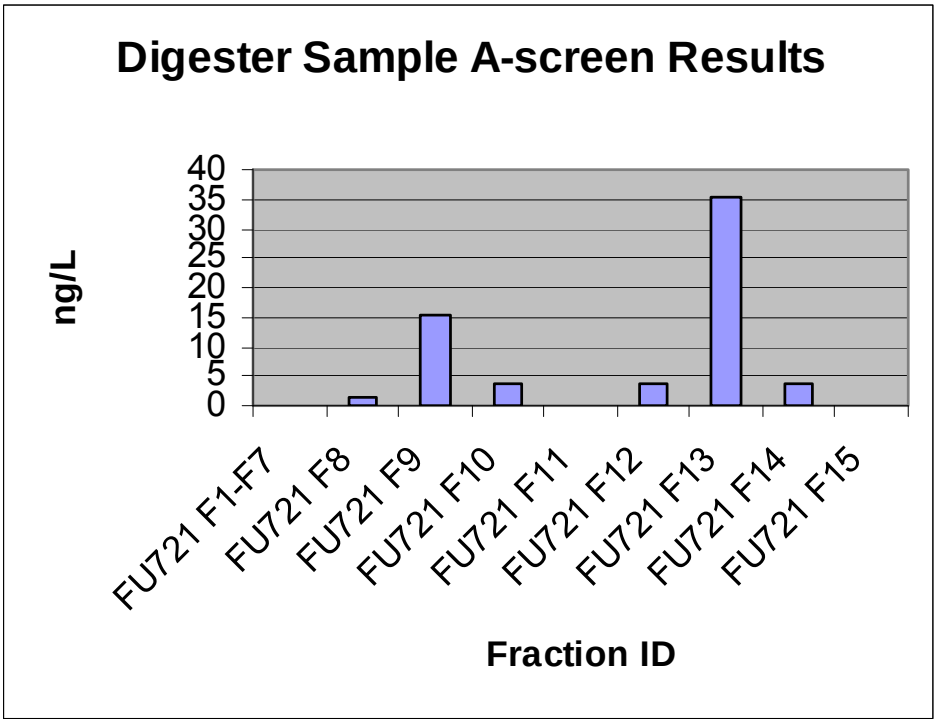

Figure 4: A-screen results (Aeq.) from HPLC fractionation of manure sample 22. Note: F = fraction number.

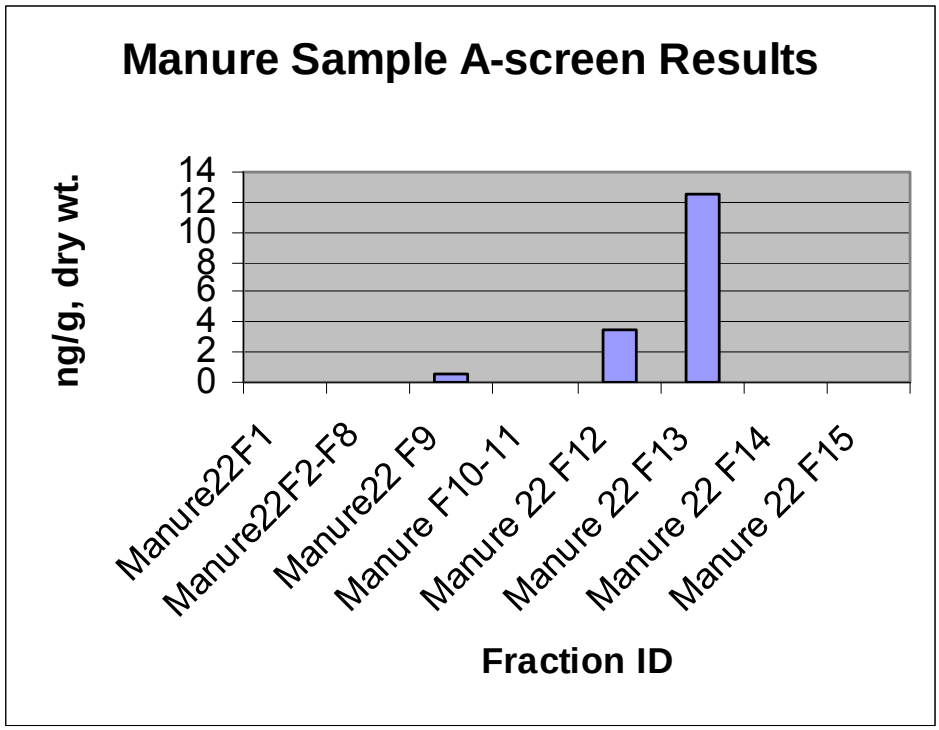

Chapter 4

Transformation of Sulfamethazine by Manganese Oxide in Aqueous Solution

Notes:

This chapter was published as Gao, J.; Hedman, C.; Liu, C.; Guo, T.; Pedersen, J.A. Transformation of sulfamethazine by manganese oxide in aqueous solution. *Environ. Sci. Technol.* **2012**, *46*, 2642-2651.

A version of pages 121-146 and 189-213 of this dissertation appeared in Dr. Juan Gao's dissertation entitled "Sorption and Transformation of Sulfonamide Antimicrobial Agents", 2007.

Contributions: Curtis Hedman contributed the setup and analysis of birnessite (δ-MnO_2)/sulfamethazine (SMZ) reaction solutions by HPLC-UV-MS/MS, interpretation of UV and MS/MS data for proposed reaction product identification, and the execution and analysis for $H_2{}^{18}O$ and ${}^{18}O_2$ mass labeling (δ-MnO_2)/sulfamethazine (SMZ) reaction experiments. Juan Gao contributed the physicochemical characterization of δ-MnO_2, the determination of SMZ degradation rate constants with and without oxygen and under different pH conditions, interpretation of UV and MS/MS data for proposed reaction product identification, and proposal of SMZ transformation reaction schemes. Tan Guo contributed mass spectral peak interpretation, reaction product structure elucidation, and reviewed proposed SMZ transformation reaction schemes. Cun Liu contributed an evaluation of the feasibility of the proposed transformation products and δ-MnO_2/SMZ reaction schemes by gas phase density functional theory (DFT) calculations. Joel Pedersen oversaw all aspects of the work from conception and design to manuscript preparation.

Transformation of Sulfamethazine by Manganese Oxide in Aqueous Solution

Juan Gao[1,2], Curtis Hedman[3,4], Cun Liu[5], Tan Guo[6], and Joel A. Pedersen[,2,3]*

[1]State Key Laboratory of Pollution Control and Resource Reuse, School of the Environment, Nanjing University, P.R. China, 210093

[2]Department of Soil Science, University of Wisconsin, Madison, WI, 53706

[3]Wisconsin State Lab of Hygiene, Madison, WI, 53718

[4] Environmental Chemistry and Technology Program, University of Wisconsin, Madison, WI, 53706

[5]Department of Crop and Soil Sciences, Michigan State University, East Lansing, Michigan 48824

[6]Sequoia Foundation/Department of Toxic Substances Control

* Corresponding author: Department of Soil Science, University of Wisconsin, Madison, WI, 53706; phone (608) 263-4971; fax (608) 265-2595; e-mail japedersen@soils.wisc.edu

TOC Art

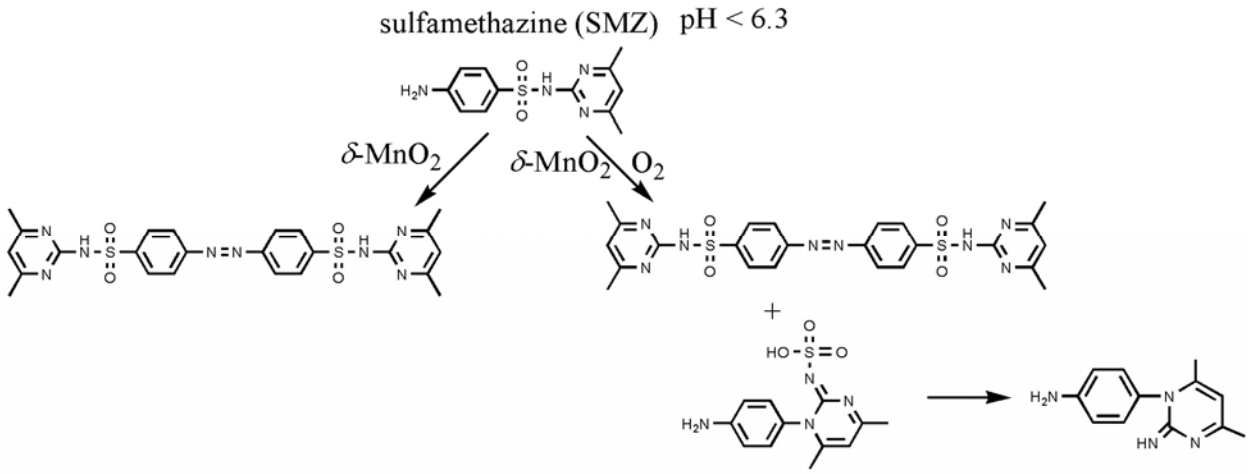

Abstract. The transformation of the sulfonamide antimicrobial sulfamethazine (SMZ) by a synthetic analog of the birnessite-family mineral vernadite (δ-MnO_2) was studied. Observed pseudo-first-order reaction constants (k_{obs}) decreased as pH decreased from pH 5.6 to 4.0, consistent with the decline in δ-MnO_2 reduction potential with increasing pH. Molecular oxygen accelerated SMZ transformation by δ-MnO_2 and influenced transformation product distribution. Increases in Na^+ concentration produced declines in k_{obs}. Transformation products identified by tandem mass spectrometry and the use of ^{13}C-labeled SMZ included an azo-dimer self-coupling product and SO_2-extrusion products. Product analysis and density functional theory calculations are consistent with surface precursor complex formation followed by single electron transfer from SMZ to δ-MnO_2 to produce SMZ radical species. Sulfamethazine radicals undergo further transformation by at least two pathways: radical-radical self-coupling or a Smiles-type rearrangement with O addition and then extrusion of SO_3. Experiments conducted in $H_2{}^{18}O$ or in the presence of $^{18}O_2$(aq) demonstrated that activated oxygen both from the lattice of as-synthesized δ-MnO_2 and initially present as dissolved oxygen reacted with SMZ. Study results suggest that the oxic state of acidic soil and sediment environments can be expected to influence manganese oxide-mediated transformation of sulfonamide antimicrobials.

Introduction

Sulfonamide antimicrobials comprise a class of pharmaceuticals widely applied in both livestock production and human medicine[1]. Sulfonamides inhibit the growth of susceptible bacteria by competitively inhibiting the enzyme dihydropteroate synthetase, thereby disrupting folate synthesis[2]. A major route of sulfonamide introduction into the environment is via land application of manure from treated animals. The main concern with introducing antimicrobial agents into environment is that they may exert selective pressure on microbial communities, potentially leading to the transfer of antibiotic resistance genes to pathogenic organisms[3,4].

Assessing the potential risks posed by the presence of sulfonamide antimicrobial agents in the environment requires an understanding of the processes influencing their fate and transport. The sorption of sulfonamide antimicrobials to soils and sediments has received considerable attention.[5-11] In contrast, transformations of sulfonamide antimicrobials in soils and sediments have received substantially less study. Several transformation processes may contribute to the degradation of sulfonamides in soils and sediments. Soil may contain microorganisms capable of degrading sulfonamide antimicrobials;[12] photodegradation may

contribute to sulfonamide transformation within ~0.5 mm of the soil surface[13,14] and is influenced by pH, sunlight intensity, and DOM composition. Extracellular phenoloxidases (e.g., peroxidase, laccase) can facilitate the covalent coupling of sulfonamides with humic substances[15-17]. Sulfonamide antimicrobials have been shown to undergo transformation in the presence of manganese oxide (MnO_2);[17-19] however, rate data for environmentally important forms of MnO_2 are limited, and the products of manganese oxide-mediated sulfonamide transformation have not been reported.

Manganese hydroxides/oxides rank among the strongest natural oxidants in soil and sediment environments. The standard reduction potential of MnO_2 at pH 7 and 25°C, E_H^0(W) is 0.464 V.[20,21] Manganese hydroxides/oxides influence the transport and transformation of organic contaminants via adsorption, direct oxidation, and surface catalysis.[22] Synthetic Mn hydroxides/oxides can oxidize phenol, hydroquinone, aniline and their substituted derivatives, as well as a variety of antimicrobial agents (viz. fluoroquinolones, triclosan, chlorophene, and tetracyclines).[23-33] Organic reductants are hypothesized to be oxidized by Mn hydroxides/oxides via a three-step process: (1) reductant diffusion to and precursor formation on the mineral surface, (2) electron transfer from the precursor complex to $Mn^{III/IV}$, and (3) release of reaction products and Mn^{II} from the mineral surface.[22] The rate-determining step is generally regarded as either the formation of surface precursor complex[34] or the transfer of electrons.[22-24] For most organic reductants studied,[26-28,35] MnO_2-mediated transformation appears to be independent of O_2. When the presence of O_2 promotes MnO_2-mediated reactions, its role is typically attributed to the reoxidation of Mn^{2+} to $Mn^{III/IV}$, leading to less release of Mn^{II} into solution in the presence of O_2(aq) than in its absence.[36,37]

The objectives of this study were to examine the influence of O_2(aq), pH, and NaCl concentration on the initial reaction rates and products of MnO_2-mediated transformation of sulfamethazine (SMZ, *N*1-(4,6-dimethyl-2-pyrimidinyl)sulfanilamide, Figure S1). To accomplish these objectives, we followed δ-MnO_2-mediated transformation of SMZ in completely mixed reactors by high-performance liquid chromatography with UV detection (HPLC-UV), characterized major SMZ transformation products by mass spectrometry, and tracked Mn^{II} release by inductively coupled plasma-optical emission spectrometry (ICP-OES).

Materials and Methods

Chemicals. Chemicals used, and their suppliers and purities are described in the Supporting Information (SI).

Manganese Oxide Synthesis and Characterization. We synthesized a poorly crystalline manganese oxide by the method of Murray.[38] The manganese oxide resembled δ-MnO_2, equivalent to the birnessite-family mineral vernadite,[39] defined as randomized z-axis birnessite (Figures S2 and Table S1). Synthesis and characterization of the δ-MnO_2 are detailed in the SI. The δ-MnO_2 had an average oxidation state of +3.94. The δ-MnO_2 was stored in aqueous suspension at 4 °C. All experiments were conducted within 2 weeks of δ-MnO_2 synthesis.

Reactor Setup. To examine δ-MnO_2-mediated SMZ transformation, freshly synthesized δ-MnO_2 stock suspension (~90 mM) was added to 10 mM sodium acetate buffer (ionic strength, I = 10 mM, adjusted with NaCl) at desired pH and equilibrated for 2 h. SMZ stock solution was then added into an aluminum foil-covered 100 mL glass bottle under continuous stirring. The molar ratio of δ-MnO_2 (stoichiometry: $MnO_{1.92}\cdot 0.88H_2O$)[40] to SMZ (initial concentration $[SMZ]_0$ = 0.007, 0.018 and 0.036 mM) was 10:1, and the total solution volume was 50 mL. Aliquots (~1

mL) were removed at desired time points after SMZ addition, and the reaction was quenched by either addition of 25 μL of 0.9 M oxalic acid or filtration through a 0.2-μm PTFE filter (Nalge Nunc International, Rochester, NY). Samples used to determine SMZ transformation kinetics and identify transformation products were quenched by the oxalic acid method; samples used to measure Mn^{II} release during reaction with SMZ were quenched by microfiltration. The SI contains details on the quenching procedures and information on SMZ adsorption to δ-MnO_2. After quenching, the SMZ concentration was determined by HPLC-UV (λ = 254 and 265 nm). Dissolved Mn was measured by ICP-OES (Perkin-Elmer Optima 4300 DV, Wellesley, MA) in samples quenched by filtration. Dissolved Mn was operationally defined as Mn passing the 0.2-μm filter and was assumed to be composed primarily of Mn^{II} (aq) released due to reduction of $Mn^{IV/III}$ by SMZ. All experiments were conducted in triplicate, and control reactors lacking MnO_2 were processed in parallel.

For O_2-free conditions, SMZ solutions and δ-MnO_2 suspensions were purged with argon for ~1 h before SMZ addition. Purging was continued during these reactions. The dissolved oxygen concentration, $[O_2]_{aq}$, was measured using an Orion 3 Star Meter (ThermoElectron, Beverly, MA). The influence of Na^+ concentration on reaction was studied at pH 5.0 in 10 mM sodium acetate buffer.

Product Identification. To facilitate identification of products of δ-MnO_2-mediated transformation of SMZ, reactions were conducted at higher initial reactant concentrations (0.144 and 1.44 mM for SMZ and δ-MnO_2). The products identified in reactions carried out at high SMZ concentration were also observed at lower concentrations more representative of environmental conditions (e.g., 0.018 mM or 0.3 μM; data not shown)[8,#]. After quenching, products and any remaining SMZ were separated by HPLC and analyzed by tandem mass

spectrometry (MS/MS) on an Applied Biosystems/MDS SCIEX API 4000 triple quadrupole mass spectrometer (Q3-MS) and by time-of-flight mass spectrometry (TOF-MS) on an Applied Biosystems Voyager DE-Pro MALDI-TOF Mass Spectrometer. Instrumental parameters are detailed in the SI. To elucidate transformation product structures, some reactions were conducted in $H_2{}^{18}O$, purged with $^{18}O_2$, or employed [phenyl-$^{13}C_6$]-SMZ (M = 284.4). All experiments conducted to elucidate transformation product structure were performed in duplicate.

Computational Methods. Gas phase density functional theory (DFT) calculations were conducted to evaluate possible structures of SMZ radical intermediates and the products associated with the proposed degradation pathway using the Gaussian03 software package.[41] Solvent effects were included by using polarizable continuum model (PCM).[42] Full geometry optimizations of all species were performed using the Becke three-parameter exchange functional (B3)[43] and the Lee−Yang−Parr correlation functional (LYP)[44] with 6-31+G* basis set. The Gibbs free energy for all structures was calculated using the standard equations of statistical mechanics. The combination of B3LYP method with PCM has been successfully applied for many aqueous phase reaction studies of many groups of organic compounds and shown to reliably reproduce the structural and energetic properties of reaction intermediates.[45] The optimized structures of SMZ species with their electrostatic potentials are shown in Figure S1. We also calculated atomic spin densities of the SMZ radical intermediates by natural bond orbital (NBO) scheme.[46]

Results and Discussion

Influence of Solution pH on SMZ Transformation Kinetics. Sulfamethazine reacted rapidly with δ-MnO_2 at pH 4.0 and I = 10 mM; 62 ± 4 % of the antimicrobial was transformed within 8 minutes when the initial SMZ and δ-MnO_2 concentrations ($[SMZ]_0$ and $[\delta\text{-}MnO_2]_0$)

were 0.036 mM and 0.360 mM, respectively (Figure 1a). These data were collected in the presence of ambient oxygen ($[O_2]_{aq}$ = 0.27 mM). Sulfamethazine was stable in aqueous solution for at least 2 weeks at room temperature in the absence of δ-MnO_2.

Rates of SMZ transformation by δ-MnO_2 declined as solution pH increased (Figure 1a). After 8 minutes, the amount of SMZ transformed declined from 62 ± 4 % at pH 4 to 30 ± 2 % at pH 5 to 20 ± 2 % at pH 5.6 under the conditions described above. Preliminary experiments conducted at pH 5.6 indicated that rates did not differ for reactions conducted in 10 mM sodium acetate buffer and those in distilled deionized water (ddH_2O; 18 MΩ-cm resistivity) ($p > 0.05$). In the absence of buffer, solution pH increased by 0.1 unit after 15-min reaction. No SMZ transformation was observed over 20 min at pH 6.3 and 7.6 (pH buffered with 3-*N*-morpholino propanesulfonic acid (MOPS), pK_a = 7.2). Sulfamethazine degradation kinetics were fitted to a pseudo-first-order kinetic model:

$$\ln\left(\frac{[\mathrm{SMZ}]_t}{[\mathrm{SMZ}]_0}\right) = -k_{obs}t \qquad (1)$$

where $[SMZ]_0$ and $[SMZ]_t$ are the sulfamethazine concentrations (μM) at time 0 and at time t (min), and k_{obs} (min^{-1}) is the observed pseudo-first-order reaction rate constant. The k_{obs} were estimated from first three sampling time points; R^2 ranged from 0.88 to 0.99. Observed pseudo-first-order reaction rate constants were 0.075 ± 0.014 min^{-1} for pH 4.0, and 0.055 ± 0.008 min^{-1} for pH 5.0, 0.032 ± 0.005 min^{-1} for pH 5.3, and 0.016 ± 0.011 min^{-1} for pH 5.6 (Figure 1b).

Influence of O_2(aq) on SMZ Transformation Kinetics. The presence of dissolved molecular oxygen O_2(aq) accelerated SMZ transformation kinetics at pH 4.0 and 5.0 (Figure 1b). Purging reaction vessels with argon reduced the amount of SMZ transformed after 8 minutes at pH 4 to 34 ± 4 % compared to 62 ± 4 % for reactions conducted in the presence of ambient

O_2(aq) ($[O_2]_{aq}$ = 0.27 mM). This corresponded to a lower k_{obs} (0.039 ± 0.006 min^{-1}) in the absence vs. in the presence of O_2(aq) (0.066 ± 0.010 min^{-1}) at pH 4.0. At pH 5.0 in the absence of oxygen, the amount of SMZ transformed after 8 minutes was insignificant, while in the presence of ambient O_2 ($[O_2]_{aq}$ = 0.27 mM) 30 ± 2 % SMZ reacted (Figure 1b). These results suggested that δ-MnO_2-mediated SMZ proceeded by at least two reaction pathways.

Release of Mn^{II} during Reaction of Sulfamethazine with δ-MnO_2. The amount of Mn^{II} released into solution during SMZ reaction with δ-MnO_2 depended on the presence of O_2(aq) and pH (Figure 1c). At pH 4.0 after 8-minute reaction, the Mn^{II} concentration, $[Mn^{II}]_{aq}$, was 0.63 ± 0.02 μM under Ar-purged conditions or 0.90 ± 0.06 μM in the presence of O_2(aq) (Figure 1c). These Mn^{II} concentrations are much lower than stoichiometric based on the quantity of SMZ transformed (i.e., $[Mn^{II}]_{aq}$ expected for a 1:1 ratio of SMZ transformed to Mn^{II} released is 12.3 μM under Ar-purged conditions or 22.3 μM in the presence of O_2). The Ar-purged reactions lacked O_2(aq), so the low $[Mn^{II}]_{aq}$ under these conditions cannot be attributed to reoxidation of liberated Mn^{II} by molecular oxygen. This suggests that Mn^{II} formed in the reaction adsorbed to δ-MnO_2 surfaces, or Mn reduced in the reaction remained in the crystal lattice, or both.[28,36] At pH 5.0, SMZ transformation was not detected in the absence of O_2(aq). In the presence of O_2(aq) at pH 5 after 8-minute reaction, $[Mn^{II}]_{aq}$ was below the limit of detection (0.04 μM) despite a marked decline in SMZ. No Mn^{III}(aq) was detected at either pH in preliminary experiments employing capillary electrophoresis with UV-Vis detection.[47,48] Molecular oxygen may have participated in these reactions by reoxidizing Mn^{II} to $Mn^{IV/III}O_2$ or via reaction with SMZ.[36,37] To our knowledge, activation of molecular oxygen at MnO_2 surfaces has not been explored.

The decreasing reactivity of δ-MnO_2 toward SMZ as pH increases is consistent with the decline in δ-MnO_2 reduction potential as proton activity drops. The reduction potential, E_H, for

Mn^{IV} in δ-MnO_2 in water at 25°C and pH 5.0 and 4.0 are 1.0 V and 1.1 V; those for Mn^{III} in δ-MnO_2 are 1.2 V and 1.4 V (In all cases, $[Mn^{II}]_{aq} = 10^{-10}$ M; calculations based on E_H^0 values for δ–MnO_2 and γ-MnOOH of 1.29 V and 1.50 V).[20] Increased SMZ adsorption to the δ-MnO_2 surface may have also contributed to the increase in reaction rate as pH declined. The aniline moiety of SMZ has a pK_a value of 2.3[49] as pH declines from 5.0 to 4.0, SMZ present as the cationic species ($SMZ+H^+$) in solution increases from 0.068 μM to 0.673 μM. Over the same pH decrement, MnO_2 surface charge density decrease to a smaller extent, from −13.3 to −10.4 $\mu mol_c \cdot m^{-2}$.[50] Higher adsorption of $SMZ+H^+$ would lead to the expectation of higher relative abundance of transformation products for which reaction was initiated by oxidation of the aniline moiety (e.g., product **5**, *vide infra*) at pH 4 vs. pH 5.

Influence of Na^+ Concentration on SMZ Transformation Kinetics. The rate of SMZ transformation by δ-MnO_2 decreased as the Na^+ concentration increased from 10 mM to 40 mM at pH 5.0 (Figure 1d). The observed reaction rate constant k_{obs} declined from 0.055 ± 0.0077 min^{-1} to 0.004 ± 0.0001 min^{-1} as $[Na^+]$ increased from 10 to 40 mM. This result is consistent with Na^+ ions occupying or blocking sites of SMZ adsorption and reaction[26,51] or the screening of electrostatic interactions between $SMZ+H^+$ and the MnO_2 surface. Molar Na^+-to-SMZ ratios when I was 10, 20, 30, and 40 mM were 329, 607, 885 and 1163. Using published δ-MnO_2 charge density[50] (−13.3 $\mu mol_c \cdot m^{-2}$), the specific surface area measured in this study (333.28 $m^2 \cdot g^{-1}$, Table S1), and the amount of δ-MnO_2 used in these experiments, the molar ratios of Na^+ to negative surface charges were 129, 238, 347, and 456; the ratio of SMZ to surface negative charge was 0.39. If only SMZ adsorbed to the δ-MnO_2 surface is assumed to react, these data indicate that SMZ had higher affinity for the δ-MnO_2 surface than did Na^+ and suggest that mechanisms in addition to electrostatic attraction contribute to the higher adsorption affinity of

SMZ, such as SMZ complexation with $Mn^{III/IV}$, hydrophobic exclusion from solution, or hydrogen bonding.

Transformation Products. The reaction of SMZ with δ-MnO_2 yielded seven to ten chromophore-bearing transformation products (designated **1**-**10**; Figure S4) depending on reaction conditions (e.g., pH, presence of O_2(aq), temperature). The chromatogram obtained at pH 4.0 in the absence of O_2(aq) contained seven major peaks (Figure S4a). Reactions conducted at pH 4.0 or 5.0 in the presence of O_2(aq) contained an additional early eluting product (**8**; Figures S3b,c); those conducted at pH 5.0 produced a further transformation product (**9**; Figure S4c). With the exception of **8** and **9**, reaction products were present at lower concentrations at pH 5.0 than at pH 4.0. During 48-h storage after quenching reaction at room temperature in the dark, **8** appeared to partially transform into **10**, **7** was completely degraded (Figures S4b and S5), and other products peaks decreased. Elevating temperature to 40°C in the pH 5.0 reaction resulted in the diminution of the peak associated with **8** and the appearance of the peak corresponding to **10** (Figure S4d).

Products **1**-**10** were absent in control reactions (i.e., reactors containing only SMZ or δ-MnO_2), including those conducted at 40°C. We selected three major product peaks **5**, **8** and **10** for structural elucidation (Figure 3).

*Product **5*** (*m*/*z* 553.1357, $[M+H]^+$) was tentatively identified as a dimer composed of two SMZ molecules connected via a dimidine (azo) linkage (Figures 3, S6). In full-scan mode, molecular ions of unlabeled and [phenyl-$^{13}C_6$]-labeled **5** differed by 12.3 *u*, indicating the product contained the carbon atoms from phenyl rings of two SMZ molecules. Based on the exact masses determined by LC-TOF-MS, the most probable elemental composition of **5** was $C_{24}H_{25}N_8O_4S_2$, equivalent to two molecule ions $[SMZ+H]^+$ minus 5 H (Figure 3). Subjection of

the molecular ion to collisionally activated dissociation (CAD) at a collision energy of 50 eV in Q3-MS experiments yielded a MS^2 spectrum exhibiting high intensity fragment ion peaks with *m/z* 123.4 ($[M\text{-}C_{18}H_{16}N_5O_4S_2]^+$, 39.6%), 186.1 ($[M\text{-}C_{18}H_{17}N_5O_2S]^+$, 16.0%), 198.5 ($[M\text{-}C_{12}H_{13}N_5O_4S_2]^+$, 100%), 263.1 ($[M\text{-}C_{12}H_{12}N_5O_2S]^+\cdot$, 36.8%) and 367.2 ($[M\text{-}C_6H_8N_3O_2S]^+$, 6.6%) (Figure S6b). The MS^2 spectrum obtained at 25 eV contained two major peaks: *m/z* 553.4 ($[M+H]^+$) and 198.2 ($[SMZ\text{-}NH_2\text{-}SO_2]^+$) (Figure S6a). A proposed fragmentation pathway for **5** is presented in Figure S6b. Taken together, these data are consistent with the azosulfamethazine structure in Figure 3.

*Product **8*** (*m/z* 295.0768, $[M+H]^+$) was formed in reactions with δ-MnO_2 in the presence of O_2(aq) (Figure S4), and appeared to slowly decompose in solution to yield **10** (Figure S5). The earlier elution of **8** relative to SMZ during reverse phase chromatography suggests the former was more polar. Products **8** and **10** exhibited similar HPLC retention times (Figure S4) and UV spectra (Figure S7).

The full-scan mass spectrum of **8** (Figure S7a) contained a series of ion peaks with *m/z* values exceeding that of $[SMZ+H]^+$ (*m/z* 279.3), many of which were consistent with clusters containing *m/z* 294 subunits: 428.5 (3.4%), 509.4 ($[2M+H\text{-}SO_3]^+$, 24.5%), 611.5 ($[2M+Na]^+$; 6.5%), and 905.7 ($[3M+Na]^+$; 6.9%) (Figure S7a). The ion peak at *m/z* 428.5 may correspond to a dimer formed from two *m/z* 215.4 ions ($215.4 + 215.4 - 2H^+$). Three ion cluster peaks were selected for CAD (25 eV): *m/z* 509.5, 611.5, and 905.7 (Figure S8). The *m/z* 509.5 ion lost a *m/z* 294.3 fragment to form a *m/z* 215.2 daughter ion; the *m/z* 611.0 ion lost 2×80 (SO_3) neutral fragments to form a *m/z* 451.1 ($214 + 214 + Na^+$) fragment ion, as well as *m/z* 215.2 and 237.3 ($215.2 - H^+ + Na^+$) fragment ions; the *m/z* 905.7 ion easily lost a 294 neutral fragment (*m/z* of **8**) and 2×80 (SO_3) to form *m/z* 610.9 and 451.1 ions. These results suggest that the majority of the

peaks in mass spectrum of **8** were ion clusters of *m/z* 294 with H^+ and Na^+, the low abundance (1.43%) *m*/*z* 295.4 ion corresponds to the molecular ion ($[M+H]^+$) for **8** (Figure S7a), and the *m*/*z* 215.4 ion was a stable fragment ion of **8** resulting from SO_3 extrusion. Low abundance molecular ions are uncommon in the API-(+)-TIS mode, suggesting **8** was thermally unstable and decomposed during heating at the nebulizer interface (400 °C).[52] The putative molecular ion for **8** is 16 *u* larger than that for SMZ, suggesting addition of an O atom during δ-MnO_2-mediated transformation of SMZ in the presence of O_2(aq).

In the full-scan mass spectrum of **8** from reactions employing [phenyl-$^{13}C_6$]-SMZ (Figure S9), the molecular ion peak shifted to *m*/*z* 301.4, the *m*/*z* 215.4 peak shifted to *m*/*z* 221.5, and cluster ion peaks *m/z* 509.5, 611.0, and 905.7 shifted to *m*/*z* 521.6 (12 *u* larger than *m*/*z* 509.5), *m*/*z* 623.7 (12 *u* larger than *m*/*z* 611.0), and *m*/*z* 923.7 (18 *u* larger than *m*/*z* 905.7). These results are consistent with **8** containing an intact phenyl ring from the aniline moiety in its structure (further supported by the fragmentation pattern of **10**, *vide infra*).

Based on the exact masses (*m*/*z* 295.0768) determined by LC-TOF-MS, the most probable elemental composition of **8** was $C_{12}H_{15}N_4O_3S$ (Figure 3), and the most intense ion peak (*m/z* 215.1351) was $C_{12}H_{15}N_4$. Daughter ion peak *m*/*z* 215.4 had the same fragmentation pattern as did **10**, corresponding to **8** losing SO_3. The most probable structure for the *m*/*z* 215.4 daughter ion (product **10**) was 4-(2-imino-4,6-dimehtylpyrimidin-1(2*H*)-yl)aniline (*vide infra*).

The mass spectrometric data indicate that **8** corresponds to a thermally labile SMZ transformation product having a single O atom added to the parent structure, possessing an intact phenyl ring from the aniline moiety, and readily decomposing by SO_3 extrusion to form product **10**. We conducted DFT/PCM calculations to determine likely positions of O addition to the $SMZ+H^+$ and SMZ^0 radicals. Spin density analysis (NBO) indicated four positions with spin

density exceeding 0.1: N4 on aniline group, N1 on −SO_2−NH−, *para*-C on the dimethylpyrimidine group, and N on the dimethylpyrimidine group. Free energies of reaction ($\Delta_r G$) were calculated for the addition of O to the possible positions leading to the formation of **8** (Table S2). Mass spectra for **8** indicated that it possessed an intact aniline moiety, so N4 on aniline group was not a position where O was added. Addition of O to the N1 position had $\Delta_r G$ = +47.3 kJ·mol^{-1} relative to the stable reference state SMZ + ½O_2 and was therefore not favored. The $\Delta_r G$ of O addition to the *p*-C of the pyrimidine moiety was favorable (−117.7 kJ·mol^{-1}), but the resulting structure would not readily yield **10** upon decomposition. The remaining possible high spin density position for simple O addition was a pyrimidine N (slightly unfavorable relative $\Delta_r G$, +26.6 kJ·mol^{-1}). However, the resulting SMZ-N→O structure (Table S2) was not expected to elute as early as did product **8** (shortly after solution peak) or to readily decompose to yield **10**. A further possibility, and one that would yield **10** as a SO_3 extrusion product of **8**, is the intramolecular (Smiles-type) rearrangement of the SMZ-H^0· (N1) radical followed by oxidation of the SO_2 group (Figure 3). Such *ipso*-substitution reactions have been reported for sulfonamides in the organic synthesis literature.[53,54,55] Solvated DFT calculations suggested that the formation of this product ($\Delta_r G$ = −102.4 or −149.5 kJ·mol^{-1} depending on the conformer, Table S2) was favored over that of the SMZ-N→O structure. We therefore tentatively assign **8** to (1-(4-aminophenyl)-4,6-dimethylpyrimidin-2(1*H*)-yl idene)sulfamic acid.

Comparison of products formed from reactions conducted in $H_2{}^{16}O$ and $H_2{}^{18}O$ indicated that the oxygen added in **8** did not originate from the solvent (data not shown). The mass spectrum of **8** for reactions conducted in the presence of $^{18}O_2$(aq) contained peaks for putative molecular ions with *m*/*z* 295.4 and 297.2 (at approximately a 2:1 ratio), and cluster ions with *m*/*z* 611.4, 613.5, and 615.5 (at approximately a 1:1:0.3 ratio), and *m*/*z* 905.6 and 907.6 (at

approximately a 1:1.3 ratio). A similar mass shift for the *m/z* 215.2 daughter ion was not observed or expected. No peak with *m/z* 297.2 was detected in reactions conducted under ambient O_2 conditions ($^{18}O_2$ natural abundance is 0.2%). These results provide direct evidence that both ^{16}O from the lattice of as-synthesized δ-MnO_2 and ^{18}O from dissolved oxygen reacted with SMZ. Consumption of O_2(aq) has been reported in manganese oxide-mediated degradation of glyphosate, and reformation of reactive MnO_2 surfaces via oxidation of Mn^{II} (aq) by molecular oxygen was invoked to account for the dependence of the reaction of O_2(aq). These results also suggest that oxygen added to SMZ at a location other than the two aromatic rings: the proposed structure of *m/z* 215.2 daughter ion (product **10**) contains both aromatic rings and no oxygen (*vide infra*).

*Product **10*** (*m/z* 215.1351, $[M+H]^+$) appeared to form from **8** during storage at 22°C and in reactions conducted at 40 °C and pH 5.0 in the presence of O_2(aq) (Figures S4d and S5). The UV spectra of **8** and **10** differed slightly (Figure S7). The most intense peak corresponded in the full-scan mass spectrum of **10** was the *m/z* 215.3 ion (Figure S7b) and appeared to correspond to the molecular ion $[M+H]^+$. Based on the exact masses determined by LC-TOF-MS for **10** $[M+H]^+$, the most probable elemental composition was $C_{12}H_{15}N_4$ (Figure 3), identical to that of the stable *m/z* 215.4 daughter ion of **8**. Collisionally activated dissociation at 50 eV of the putative molecular ion of **10** produced major fragment ions with *m/z* = 64.9 ($[M\text{-}C_7H_8N_4]^+$, 76.5%), 92.3 ($[M\text{-}C_6H_7N_3]^+$, 100%), 133.4 ($[M\text{-}C_4H_6N_2]^+$, 25.5%), and 157.9 ($[M\text{-}CH_3N_3]^+$, 42.4%) (Figure 2a), identical to those of the *m/z* 215.4 daughter ion of **8** (Figure 2b). The identical elemental compositions and fragmentation patterns suggest that **10** and the *m/z* 215.4 daughter ion of **8** share the same structure. In reactions using [phenyl-$^{13}C_6$]-SMZ, the masses of *m/z* 221.5 fragments shifted to *m/z* 69.9 ($[M\text{-}C_7H_8N_4]^+$, 26.5%), 97.9 ($[M\text{-}C_6H_7N_3]^+$, 100%),

139.5 ([M-$C_4H_6N_2$]$^+$, 13.2%), 164.6 ([M-CH_3N_3]$^+$, 17.1%) and 179.1 ([M-CH_2N_2]$^+$, 13.7%) (Figure S10). These data indicate that the phenyl ring of the aniline moiety is intact in **10** [M+H]$^+$. Based on the above data, two structures for **10** are possible: *N*-(4,6-dimethylpyrimidin-2-yl)benzene-1,4-diamine and 4-(2-imino-4,6-dimehtylpyrimidin-1(2*H*)-yl)aniline. The HPLC retention time (18 min) and UV spectrum (Figure S11) of an authentic standard for the former did not correspond to those of **10**. The most probable the structure for **10** was therefore 4-(2-imino-4,6-dimethylpyrimidin-1(2*H*)-yl)aniline. This SO_2-extrusion product of SMZ was reported as a major product in indirect photolysis of SMZ in aqueous solution.[57] Confirmation of the structure of **10** requires further experimentation (e.g., nuclear magnetic resonance and Fourier transform infrared spectroscopy of the isolated compound). We provisionally propose the structure and fragmentation pathway for **10** in Figure 2a .

Proposed Transformation Pathways. The cationic and neutral SMZ species predominated over the pH range for which δ-MnO_2-mediated transformation of SMZ occurred (Figure S1). The more rapid rate of reaction at pH 4.0 is consistent with a higher affinity of the cationic species for the negatively charged δ-MnO_2 surface. Initial single electron transfer from SMZ to δ-MnO_2 generates a SMZ radical, which can exist as either a cationic or neutral species (Scheme S1). The cationic radical species ($SMZ^{+}\cdot$) can be formed via the loss of one proton and one electron from SMZ+H^+ or through SMZ^0 losing one electron. The neutral radical species (SMZ-$H^0\cdot$) can be formed via loss of one proton and one electron from SMZ^0 (or through SMZ-H^- losing one electron, although this was likely unimportant in the present study). A macroscopic acid dissociation constant (pK_a') of 5.2 has been reported for the equilibrium between $SMZ^{+}\cdot$ and SMZ-$H^0\cdot$.[58] Cationic radicals would have therefore dominated between pH 4.0 and 5.2 (Figure 1b). If production of SMZ radicals is assumed to proceed at the same rate as

SMZ disappearance (viz. k_{obs}) (Scheme S1), a strong linear correlation would be apparent between k_{obs} and the fraction of cationic radical $SMZ^{+\bullet}$ ($\alpha_{SMZ+\cdot}$, eq S1) in solution, as was indeed the case: k_{obs} = 0.081 (± 0.007) · $\alpha_{SMZ+\cdot}$ (R^2 = 0.96). This result supports the idea that SMZ transformation leads to the production of $SMZ^{+\bullet}$.

Proposed pathways for SMZ transformation by δ-MnO_2 are shown in Figure 3. After $SMZ+H^+$ or SMZ^0 forms a surface complex with δ-MnO_2, a single electron is transferred from SMZ to $Mn^{III/IV}$.[27,28] Calculated spin density distributions for the cationic and neutral SMZ radicals indicate that electron transfer would be most facile from the amino N4 atom of cationic species, and from the N4 or amide N1 atoms of the neutral species (Figure S12). The SMZ radicals could undergo coupling and rearrangement reactions.

*Product **5*** could form via the coupling of two $SMZ^{+\bullet}$ (N4) or $SMZ\text{-}H^{0\bullet}$ (N4) radicals to produce a hydrazo intermediate, which loses two protons and a further two electrons to δ-MnO_2 to produce azosulfamethazine (product **5**) and Mn^{II} (Figure 3).[59] An alternative pathway involving a second, one-electron oxidation of $SMZ\text{-}H^{0\bullet}$ to form a nitrene radical may also be possible.[60] Solvated DFT/PCM calculations suggested that the hydroazo intermediate was more stable relative to the triplet nitrene intermediate (Table S3). However, the later species might be stabilized by complexing $Mn^{II/III}$ on MnO_2 surface, lowering the nitrene radical energy status. Because overall reactions of two pathways were energetically favorable (calculated $\Delta_r G$ = −311.4 kJ mol^{-1}), both routes were possible. Analogous azosulfonamide products have been reported in the electrochemical oxidation of sulphapyridine and in the reaction of sulfamethoxazole with HOCl.[61] Azobenzene and 4,4'-dimethylazobenzene products also form in the δ-MnO_2-mediated transformation of aniline.[62]

*Products **8** and **10***. The SMZ-H^{0}• (N1) radical would relocate to an N in dimethylpyrimidine, which could subsequently engage in nucleophilic attack at *ipso*-position of SMZ. This reversible intramolecular nucleophilic substitution reaction (Smiles-type rearrangement)[63,64] could form a *N*-(1-(4-aminophenyl)-4,6-dimethylpyrimidin-2(1H)-ylidene)sulfonamide radical (SMZ^{+}•-Smiles) (Figure 3). The free energy of formation of the SMZ-H^{0}•-Smiles radical is lower than that of SMZ-H^{0}• by 81.6 kJ·mol^{-1} (Figure 4). The unpaired electron in resulting SMZ-H^{0}•-Smiles radical is expected to reside on sulfone group (Figure 3). The sulfone could be further oxidized and O added to the sulfur atom to form product **8**. Experiments conducted in the presence of $^{18}O_2$(aq) indicate that the O can originate from the crystal lattice of the as-synthesized δ-MnO_2, or from molecular O_2. Product **8** could extrude SO_3 to form **10**.

The proposed structures of **8** and **10** were consistent with their early elution times in HPLC in that they should exist as ions in mobile phase (pH 3.54). The sulfamic group of **8** is expected to be strongly acidic (e.g., the estimated pK_a of benzylsulfonic acid is −2.8)[65] and would completely dissociate in the mobile phase; it could also ion pair with Na^{+} and form clusters in MS/MS chamber. The dissociation constant for the conjugate acid of the imino group in **10** is unknown, but expected to be around 4.9 (at mobile phase pH 3.54, 95% imino group would then be protonated) based on data for related compounds.[66] Product **10** is therefore expected to exist as a cation in the mobile phase. The proposed reaction pathways are consistent with quantum calculations (Text S3). The products that were not identified in the present study may form via additional reaction pathways.

Environmental Significance. Birnessite-family minerals are the most commonly occurring manganese oxides and rank among the strongest natural oxidants in soils and

sediments.[67] Transformation of the sulfonamide antimicrobial sulfamethazine by a synthetic analog for the birnessite-family mineral vernadite appears to proceed through the formation of radical intermediates. The radical SMZ species can self-couple (product **5**) or undergo rearrangement reactions. Similar reactions are expected for other sulfonamide anitmicrobials. In the environment, radical coupling of SMZ to NOM molecules would be expected to be a more important process than self-coupling reactions.[17] Stable SMZ transformation products identified in this study (**5**, **10**) are expected to exhibit diminished ability to inhibit dihydropterate synthetase, the mode of action of sulfonamide antimicrobials. Nonetheless, their bioactivities by other modes of action may warrant future study.

This study suggests that naturally occurring manganese oxides may contribute to the dissipation of sulfonamide antimicrobials in acidic soil environments. We observed SMZ transformation by MnO_2 at pH $\leq$ 5.6. The pH of soil solutions span a wide range and encompass the acidic pH values used in the present study. Arable soils in humid temperate regions have pH values from 7 to slightly below 5, while those of forest soils can be as low as ~3.5. Fertilization with sulfur or ammonia forms of nitrogen and application of sewage sludge or animal manures can depress soil pH. Rhizosphere pH values can be lower than those of the bulk soil by as much as two units. The contribution of MnO_2-mediated transformation to the fate of these antimicrobials is expected to depend on the availability of reactive MnO_2 surfaces, pH and O_2(aq) of the soil solution, and presence of competing cations. The importance of O_2(aq) in δ-MnO_2-mediated SMZ transformation implies that sulfonamide degradation would proceed more rapidly in aerobic surface soils than under anaerobic conditions.

Acknowledgments. This research was supported by USDA CSREES Project WIS04621 and Water Resource Institute Project R/UW-CTR-005. We thank Walt Zeltner for surface area measurements, Huifang Xu for use of the XRD instrument, Kevin Metz for SEM images,

Kennedy Rubert and Soren Eustis for helpful discussions, and three anonymous reviewers for their helpful comments.

Supporting Information Available

Text, tables and figures addressing materials and methods and supporting data and discussion. This information is available free of charge via the Internet at http://pubs.acs.org/.

Literature Cited

1. Mellon, M.; Benbrook, C.; Benbrook, K.L. *Hogging It: Estimates of Antimicrobial Abuse in Livestock. UCS Publications.* Union of Concerned Scientists: Cambridge, MA, 2001.
2. Hardman, J.G.; Limbrid, L.E.; Gilman, A.G.E. *Goodman & Gilman's The Pharmacological Basis of Therapeutics*. McGraw Hill: New York, 2001.
3. Heuer, H.; Smalla, K. Manure and sulfadiazine synergistically increased bacterial antibiotic resistance in soil over at least two months. *Environ. Microbiol.* **2007,** *9* (3), 657-666; DOI: 10.1111/j.1462-2920.2006.01185.x.
4. Pei, R.T.; Kim, S.C.; Carlson, K.H.; Pruden, A. Effect of river landscape on the sediment concentrations of antibiotics and corresponding antibiotic resistance genes (Arg). *Water Res.* **2006,** *40* (12), 2427-2435; DOI: 10.1016/j.watres.2006.04.017.
5. Thiele-Bruhn, S.; Seibicke, T.; Schulten, H.R.; Leinweber, P. Sorption of sulfonamide pharmaceutical antibiotics on whole soils and particle-size fractions. *J. Environ. Qual.* **2004,** *33* (4), 1331-1342; DOI:10.2134/jeq2004.1331.
6. Gao, J.; Pedersen, J. A. Adsorption of sulfonamide antimicrobial agents to clay minerals. *Environ. Sci. Technol.* **2005,** *39* (24), 9509-9516; DOI: 10.1021/es050644c.
7. ter Laak, T.L.; Gebbink, W.A.; Tolls, J. The effect of pH and ionic strength on the sorption of sulfachloropyridazine**,** tylosin, and oxytetracycline to soil. *Environ. Toxicol. Chem.* **2006,** *25* (4), 904-911; DOI: 10.1897/05-232R.1
8. Burkhardt, M.; Stamm, C. Depth distribution of sulfonamide antibiotics in pore water of an undisturbed loamy grassland soil. *J. Environ. Qual.* **2007,** *36* (2), 588-596; DOI: 10.2134/jeq2006.0358
9. Richter, M.K.; Sander, M.; Krauss, M.; Christl, I.; Dahinden, M.G.; Schneider, M.K.; Schwarzenbach, R.P. Cation binding of antimicrobial sulfathiazole to leonardite humic acid. *Environ. Sci. Technol.* **2009**, *43* (17), 6632-6638; DOI**:** 10.1021/es900946u
10. Geddes J.; Miler, G.C. Photolysis of organics in the environment. In *Perspectives in Environmental Chemistry*, Macalady, D.L. Ed., Oxford University Press: New York, 1998; pp. 195-209.
11. Silvia Díaz-Cruz, M.; Barceló, D. LC–MS^2 trace analysis of antimicrobials in water, sediment and soil. *TrAC Trends Analyt. Chem*. **2005**, *27* (7), 645-657; DOI:10.1016/j.trac.2005.05.005.
12. Gao, J.; Pedersen, J.A. Sorption of sulfonamide antimicrobial agents to humic-clay complexes. *J. Environ. Qual.* **2010**, *39* (1), 228-235; DOI:10.2134/jeq2008.0274.
13. Perez, S.; Eichhorn, P.; Aga, D.S. Evaluating the biodegradability of sulfamethazine, sulfamethoxazole and trimethoprim at different stages of sewage treatment. *Environ. Toxicol. Chem.* **2005,** *24* (6), 1361-1367; DOI: 10.1897/04-211R.1.
14. Hebert, V.R.; Miller, G.C. Depth dependence of direct and indirect photolysis on soil surfaces. *J. Agric. Food Chem.* **1990**, *38* (3), 913-918; DOI: 10.1021/jf00093a069.

15. Bialk, H.M.; Pedersen, J.A. NMR investigation of enzymatic coupling of sulfonamide antimicrobials with humic substances. *Environ. Sci. Technol.* **2008,** *42* (1), 106-112; DOI: 10.1021/es070779d.
16. Bialk, H.M.; Hedman, C.; Castillo, A.; Pedersen, J.A. Laccase-mediated michael addition of N-15-sulfapyridine to a model humic constituent. *Environ. Sci. Technol.* **2007,** *41* (10), 3593-3600; DOI: 10.1021/es0617338.
17. Bialk, H.M.; Simpson, A.J.; Pedersen, J.A. Cross-coupling of sulfonamide antimicrobial agents with model humic constituents. *Environ. Sci. Technol*. 2005, 39 (12), 4463-4473; DOI: 10.1021/es0500916.
18. Dong, J.; Li, Y.; Zhang, L,; Liu, C.; Zhuang, L.; Sun, L.; Jianmin, J. The oxidative degradation of sulfadiazine at the interface of α-MnO2 and water. *J. Chem. Technol. Biotechnol*. **2009**, *84* (12), 1848-1853; DOI: 10.1002/jctb.2256.
19. Liu, C.; Zhang, L.; Li, F.; Wang, Y.; Gao, Y.; Li, X.; Cao, W.; Feng, C.; Dong, J.; Sun, L. Dependence of sulfadiazine oxidative degradation on physicochemical properties of manganese dioxides. *Ind. Eng. Chem. Res*. **2009**, *48* (23), 10408-10413; DOI: 10.1021/ie900812j.
20. Bricker, O.P. Some stability relations in the system MnO_2-H_2O at 25°C and one atmosphere total pressure. *Am. Mineral.* **1965**, 50, 1296-1354.
21. Schwarzenbach, R.P.; Gschwend, P.M.; Imboden, D.M. *Environmental Organic Chemistry*, 2nd ed.; John Wiley & Sons: New York, 2002.
22. Wang, D.; Shin, J.Y.; Cheney, M.A; Sposito, G.; Spiro, T.G. Manganese dioxide as a catalyst for oxygen-independent atrazine dealkylation. *Environ. Sci. Technol*. **1999**, *33* (18), 3160-3165; DOI: 10.1021/es990419t.
23. Stone, A.T. Reductive dissolution of manganese(III/IV) oxides by substituted phenols. *Environ. Sci. Technol*. **1987**, *21* (10), 979-988; DOI: 10.1021/es50001a011.
24. Zhang, H.C.; Huang, C.H. Reactivity and transformation of antibacterial N-oxides in the presence of manganese oxide. *Environ. Sci. Technol.* **2005,** *39* (2), 593-601; **DOI:** 10.1021/es048753z.
25. Rubert, K.F.; Pedersen, J.A. Kinetics of oxytetracycline reaction with a hydrous manganese oxide. *Environ. Sci. Technol.* **2006,** *40* (23), 7216-7221; **DOI:** 10.1021/es060357o.
26. Zhang, H.C.; Huang, C.H. Oxidative transformation of triclosan and chlorophene by manganese oxides. *Environ. Sci. Technol.* **2003,** *37* (11), 2421-2430; DOI: 10.1021/es026190q.
27. Zhang, H.C.; Huang, C.H. Oxidative transformation of fluoroquinolone antibacterial agents and structurally related amines by manganese oxide. *Environ. Sci. Technol.* **2005,** *39* (12), 4474-4483; DOI: 10.1021/es048166d.
28. Stone, A.T.; Morgan, J.J. Reduction and dissolution of manganese(III) and manganese(IV) oxides by organics. 1. Reaction with hydroquinone. *Environ. Sci. Technol.* **1984,** *18* (6), 450-456; DOI: 10.1021/es00124a011.
29. Stone, A.T.; Ulrich, H.J. Kinetics and reaction stoichiometry in the reductive dissolution of manganese(IV) dioxide and Co(III) oxide by hydroquinone. *J. Colloid Interface Sci.* **1989,** *132* (2), 509-522; DOI:10.1016/0021-9797(89)90265-8.
30. Ukrainczyk, L.; McBride, M.B. The oxidative dechlorination reaction of 2,4,6-trichlorophenol in dilute aqueous suspensions of manganese oxides. *Environ. Toxicol. Chem.* **1993,** *12* (11), 2005-2014; DOI: 10.1002/etc.5620121106.

31. Ukrainczyk, L.; McBride, M.B. Oxidation and dechlorination of chlorophenols in dilute aqueous suspensions of manganese oxides: Reaction products. *Environ. Toxic. Chem.* **1993,** *12* (11), 2015-2022; DOI: 10.1002/etc.5620121107.
32. Zhang, H.C.; Chen, W.R.; Huang, C. H. Kinetic modeling of oxidation of antibacterial agents by manganese oxide. *Environ. Sci. Technol.* **2008,** *42* (15), 5548-5554; DOI: 10.1021/es703143g.
33. Forrez, I.; Carballa, M.; Fink, G.; Wick, A.; Hennebel, T.; Vanhaecke, L.; Ternes, T.; Boon, N.; Verstraete, W. Biogenic metals for the oxidative and reductive removal of pharmaceuticals, biocides and iodinated contrast media in a polishing membrane bioreactor. *Water Res.* **2011**, *45* (4), 1763 – 1773; DOI:10.1016/j.watres.2010.11.031.
34. Zhang, H.C.; Huang, C.H. Oxidative transformation of fluoroquinolone antibacterial agents and structurally related amines by manganese oxide. *Environ. Sci. Technol.* **2005,** *39* (12), 4474-4483; DOI: 10.1021/es048166d.
35. Matocha, C.J.; Sparks, D.L.; Amonette, J.E.; Kukkadapu, R.K. Kinetics and mechanism of birnessite reduction by catechol. *Soil Sci. Soc. Am. J.* **2001,** *65* (1), 58-66; DOI: 10.2136/sssaj2001.65158x.
36. Barrett, K.A.; McBride, M.B. Oxidative degradation of glyphosate and aminomethylphosphonate by manganese oxide. *Environ. Sci. Technol.* **2005,** *39* (23), 9223-9228; DOI: 10.1021/es051342d.
37. McBride, M.B. Oxidation of dihydroxybenzenes in aerated aqueous suspensions of birnessite. *Clays Clay Miner.* **1989,** *37* (4), 341-347.
38. Murray, J.W. Surface chemistry of hydrous manganese-dioxide. *J. Colloid Int. Sci.* **1974,** *46* (3), 357-371; DOI:10.1016/0021-9797(74)90045-9.
39. Villalobos, M.; Toner, B.; Bargar, J.; Sposito, G. Characterization of the manganese oxide produced by pseudomonas putida strain Mnb1. *Geochim. Cosmochim. Acta.* **2003,** *67* (4), 2649-2662; DOI:10.4491/eer.2010.15.4.183.
40. Klausen, J.; Haderlein, S.B.; Schwarzenbach, R.P. Oxidation of substituted anilines by aqueous MnO_2: Effect of co-solutes on initial and quasi-steady-state kinetics. *Environ. Sci. Technol.* **1997,** *31* (9), 2642-2649; DOI:10.1080/02678290412331314950.
41. Frisch, M. J.; Trucks, G. W.; Schlegel, H. B.; Scuseria, G. E.; Robb, M. A.; Cheeseman, J. R.; Montgomery, J. A., Jr.; Vreven, T.; Kudin, K. N.; Burant, J. C.; Millam, J. M.; Iyengar, S. S.; Tomasi, J.; Barone, V.; Mennucci, B.; Cossi, M.; Scalmani, G.; Rega, N.; Petersson, G. A.; Nakatsuji, H.; Hada, M.; Ehara, M.; Toyota, K.; Fukuda, R.; Hasegawa, J.; Ishida, M.; Nakajima, T.; Honda, Y.; Kitao, O.; Nakai, H.; Klene, M.; Li, X.; Knox, J. E.; Hratchian, H. P.; Cross, J. B.; Bakken, V.; Adamo, C.; Jaramillo, J.; Gomperts, R.; Stratmann, R. E.; Yazyev, O.; Austin, A. J.; Cammi, R.; Pomelli, C.; Ochterski, J. W.; Ayala, P. Y.; Morokuma, K.; Voth, G. A.; Salvador, P.; Dannenberg, J. J.; Zakrzewski, V. G.; Dapprich, S.; Daniels, A. D.; Strain, M. C.; Farkas, O.; Malick, D. K.; Rabuck, A. D.; Raghavachari, K.; Foresman, J. B.; Ortiz, J. V.; Cui, Q.; Baboul, A. G.; Clifford, S.; Cioslowski, J.; Stefanov, B. B.; Liu, G.; Liashenko, A.; Piskorz, P.; Komaromi, I.; Martin, R. L.; Fox, D. J.; Keith, T.; Al-Laham, M. A.; Peng, C. Y.; Nanayakkara, A.; Challacombe, M.; Gill, P. M. W.; Johnson, B.; Chen, W.; Wong, M. W.; Gonzalez, C.; Pople, J. A. Gaussian 03, revision E.01; Gaussian, Inc.: Wallingford, CT, 2004.
42. Miertus, S.; Scrocco, E.; Tomasi, J. Electrostatic interaction of a solute with a continuum. A direct utilization of AB initio molecular potentials for the prevision of solvent effects. *Chem. Phys.* **1981**, *55* (1), 117-129; DOI: 10.1016/0301-0104(81)85090-2.

43. Becke, A.D. Density-functional thermochemistry. III. The role of exact exchange. *J. Chem. Phys.* **1993**, *98* (7), 5648– 5652; DOI:10.1063/1.464913.
44. Lee, C.; Yang, W.; Parr, R.G. Development of the Colle-Salvetti correlation-energy formula into a functional of the electron density. *Phys. Rev. B.* **1988**, *37* (2), 785– 789; DOI: 10.1103/PhysRevB.37.785.
45. Tomasi J, Mennucci B, Cammi R. Chem Rev. Quantum mechanical continuum solvation models. *Chem Rev*. **2005,** *105* (8), 2999-3093; DOI: 10.1021/cr9904009.
46. Glendening, E. D.; Reed, A. E.; Charpenter, J. E.; Weinhold, F. Gaussian NBO program, version 3.1. Theoretical Chemistry Institute, University of Wisconsin: Madison, WI, 2001.
47. Wang, Y.; Stone, A.T. The citric acid-$Mn^{III,IV}O_2$(birnessite) reaction. Electron transfer, complex formation, and autocatalytic feedback. *Geochim. Cosmochim. Acta.* **2006,** *70* (17), 4463-4476; DOI:10.1016/j.gca.2006.06.1551.
48. Wang, Y.; Stone, A.T. Reaction of Mn^{III},Mn^{IV} (hydr)oxides with oxalic acid, glyoxylic acid, phosphonoformic acid, and structurally-related organic compounds. *Geochim. Cosmochim. Acta.* **2006,** *70* (17), 4477-4490; DOI:10.1016/j.gca.2006.06.1548.
49. Lin, C.E.; Chang, C.C.; Lin, W.C. Migration behavior and separation of sulfonamides in capillary zone electrophoresis III. Citrate buffer as a background electrolyte. *J. Chromatogr.* . **1997**, *768* (1-2), 105-112; DOI:10.1016/S0021-9673(96)00771-6.
50. McKenzie, K. Manganese oxides and hydroxides. In *Minerals in Soil Environments*, 2nd ed.; Soil Science Society of America: Madison, WI, 1989; pp 456-465.
51. Murray, J. The surface chemistry of hydrous manganese dioxide. *J. Coll. Int. Sci.* **1974**, 46 (3), 357-371; DOI: 10.1016/0021-9797(74)90045-9.
52. Bruins, A.P. Atmospheric-pressure-ionization mass-spectrometry. 2. Applications in pharmacy, biochemistry and general chemistry. *TrAC-Trends in Analyt. Chem.* **1994,** *13* (2), 81-90; DOI: 10.1016/0165-9936(94)85069-0.
53. Ryokawa, A., and H. Tōgō. Synthetic use of 1,1,2,2-tetraphenyldisilane for the preparation of biaryls through the intramolecular free radical ipso-substitution of N-(2-bromoaryl)arenesulfonamides. *Tetrahedron*. **2001**, *57* (28), 5915-5921, DOI: 10.1016/S0040-4020(01)00560-9.
54. Tōgō, H. *Advanced Free Radical Reactions for Organic Synthesis*. Elsevier: Amsterdam, 2004.
55. Kitsmiller, M. Radical Smiles rearrangement of sulfonamide. *Nihon Kagakkai*. **2001**, *81* (2), 1368.
56. Lanci, M.; Brinkley, D.W.; Stone, K.L.; Smirnov, V.V.; Roth, J.P. Structure of transition states in metal-mediated O_2-activation Reactions. *Angew. Chem. Int. Ed.* **2005**, *44*, 7273-7276. DOI: 10.1002/anie.200502096.
57. Boreen, A.L.; Arnold, W.A.; McNeill, K. Triplet-sensitized photodegradation of sulfa drugs containing six-membered heterocyclic groups: identification of an SO_2 extrusion photoproduct. *Environ. Sci. Technol.* **2005,** *39* (10), 3630-3638; DOI: 10.1021/es048331p.
58. Voorhies, J.D.; Adams, R.N. Voltammetry at solid electrodes. Anodic polarography of sulfa drugs. *Anal. Chem.* **1958**, *30* (3), 346-350; DOI: 10.1021/ac60135a010.
59. Goyal, R.N.; Mittal, A. Electrochemical oxidation of sulphapyridine at a pyrolytic graphite electrode. *Anal. Chim. Acta.* **1990**, *228*, 273-278; DOI:10.1016/S0003-2670(00)80504-8.
60. Cauquis, G., G. Pierre, M.H. Elnagdi, and H.M. Fahmy. Electrochemical behaviour of heterocyclic amidines I. Anodic oxidation of 2-amino-5-ethoxycarbonyl-4-methylthiazole. *J. Heterocycl. Chem.* **1979**, *16* (2), 413-414; DOI: 10.1002/jhet.5570160248.

61. Dodd, M.C.; Huang, C.H. Transformation of the antibacterial agent sulfamethoxazole in reactions with chlorine: kinetics, mechanisms, and pathways. *Environ. Sci. Technol.* **2005**, *38* (21), 5607–5615; DOI: 10.1021/es035225z.
62. Laha, S.; Luthy, R.G. Oxidation of aniline and other primary aromatic-amines by manganese-dioxide. *Environ. Sci. Technol.* **1990,** *24* (3), 363-373; DOI: 10.1021/es00073a012.
63. Knipe, A. C.; Lound-Keast, J. Kinetics of desulphonative double smiles' rearrangement of N-(2-hydroxyalkyl)-*p*-nitrobenzenesulphonamides. *J. Chem. Soc., Perkin Trans.2.* **1976,** *14*, 1741-1748; DOI: 10.1039/P29760001741.
64. Tada, M.; Shijima, H.; Nakamura, M., Smile-type free radical rearrangement of aromatic sulfonates and sulfonamides: Syntheses of arylethanols and arylethylamines. *Org. Biomol. Chem.* **2003,** *1* (14), 2499-2505; DOI: 10.1039/B303728B.
65. Guthrie, J.P. Hydrolysis of esters of oxy acids: pK_a values for strong acids; Brønsted relationship for attack of water at methyl; free energies of hydrolysis of esters of oxy acids; and a linear relationship between free energy of hydrolysis and pK_a holding over a range of 20 pK units. *Can. J. Chem.* **1978**, *56* (17), 2342-2354; DOI: 10.1139/v78-385.
66. Brown, D.J. *The Pyrimidines.* In *The Chemistry of Heterocyclic Compounds (Weissberger).* John Wilcy and Sons: New York, London. 1962; p. 472.
67. Taylor, R.M.; McKenzie, R.M.; Norrish, K. The mineralogy and chemistry of manganese in some Australian soils. *Aust. J. Soil Res.* **1964,** *2* (2), 235-248; DOI: 10.1071/SR9640235.

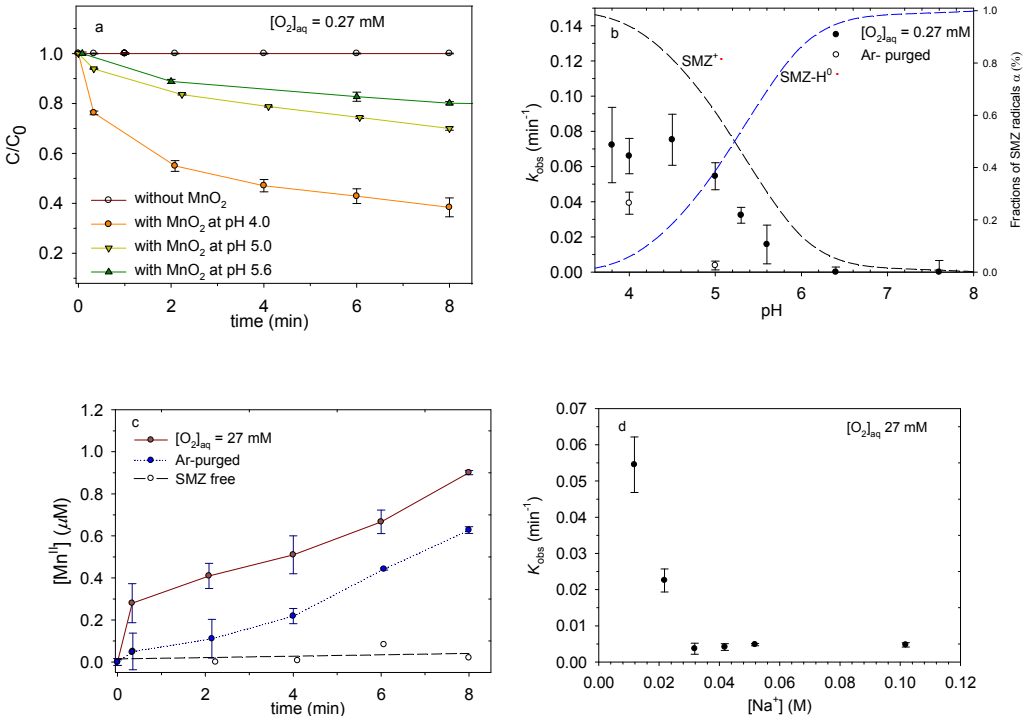

Figure 1. MnO_2-mediated sulfamethazine (SMZ) transformation: (a) reaction under ambient O_2 conditions; (b) pH influence on observed reaction rate constant and SMZ radical species fraction, $pK_a' = 5.2$ for $SMZ^{+}\cdot$ and $SMZ\text{-}H^{0}\cdot$; (c) Mn^{II} released in reaction at pH 4.0 in presence and absence of oxygen, no detectable Mn^{II} (aq) was present in δ-MnO_2 suspensions lacking SMZ under the same conditions (Mn^{II} (aq) detection limit = 0.04 μM); (d) effect of Na^+ concentration on SMZ transformation at pH 5.0 in ambient O_2 conditions. Initial concentrations: $[SMZ]_0$ = 36 μM, $[\delta\text{-}MnO_2]_0$ = 360 μM, under ambient conditions, $[O_2]_{aq}$ = 0.27 mM. Reactions were conducted in 10 mM Na acetate with ionic strength (I) adjusted with of NaCl (I = 10 mM for panels a-c, I = 10 to 100 in panel d). Symbols and bars represent mean values; error bars indicate one standard deviation of triplicate measurements; some error bars are obscured by symbols.

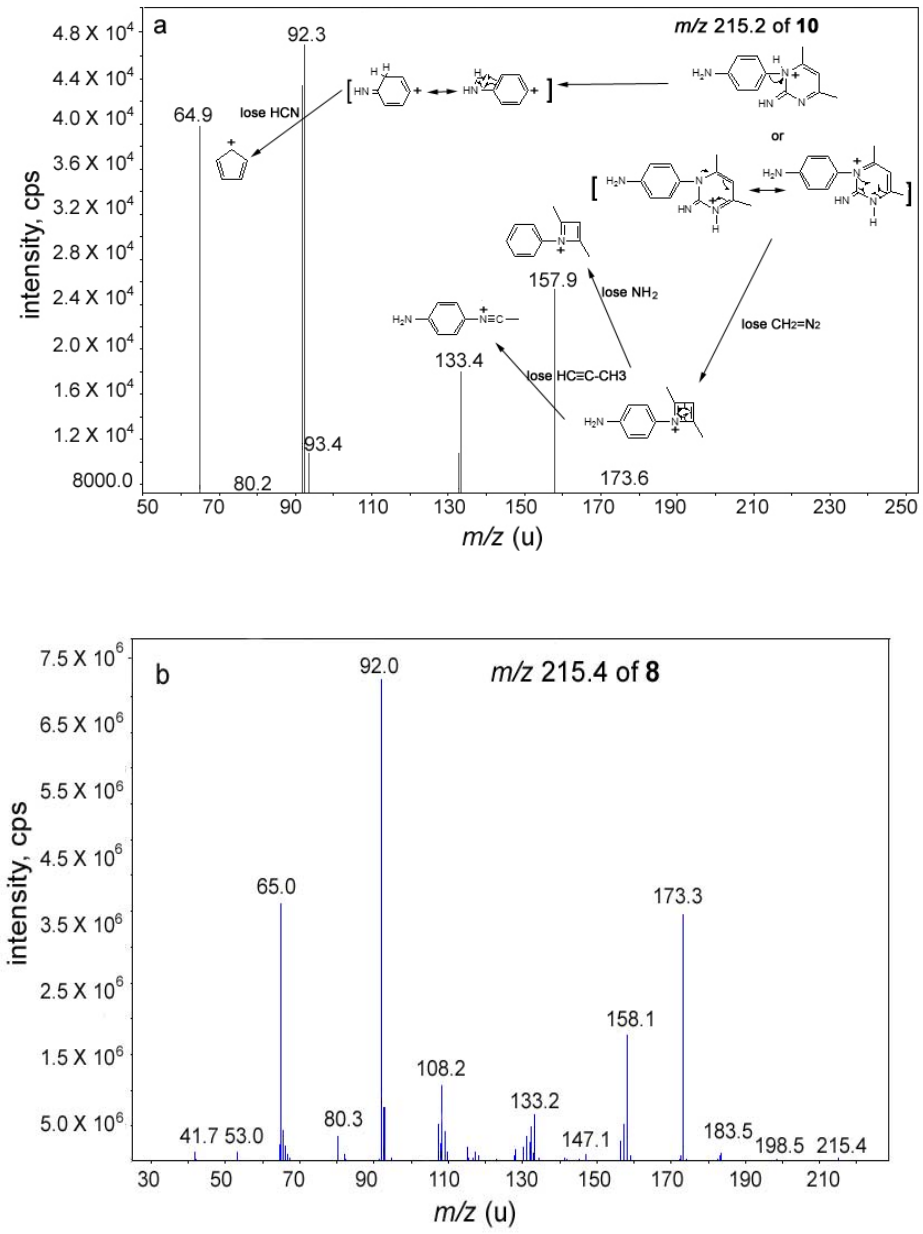

Figure 2. MS^2 spectra of (a) **10** (molecular ion, $[M+H]^+$, *m/z* = 215.2) and (b) daughter ion of **8** *m/z* 215.4 obtained at CAD at 50 eV. The fragment ions with *m/z* = 64.9 (65.0), 92.3 (92.0), 108.2, 157.9 (158.1) and 173.3 were shifted to *m/z* 69.9, 97.9, 114.3, 139.6, 164.7 and 178.9 in MS^2 spectra of products from [phenyl-$^{13}C_6$]-labeled SMZ transformation, which indicated that these ions contained benzene ring and that **10** and daughter ion *m/z* 215.4 of **8** contained an intact aniline moiety in their structures (*cf.* Figures S9 and S10). Multiple protonation sites are possible for **10**.

Step 1. SMZ surface complex formation and single electron transfer to $Mn^{III}/Mn^{IV}O_2$

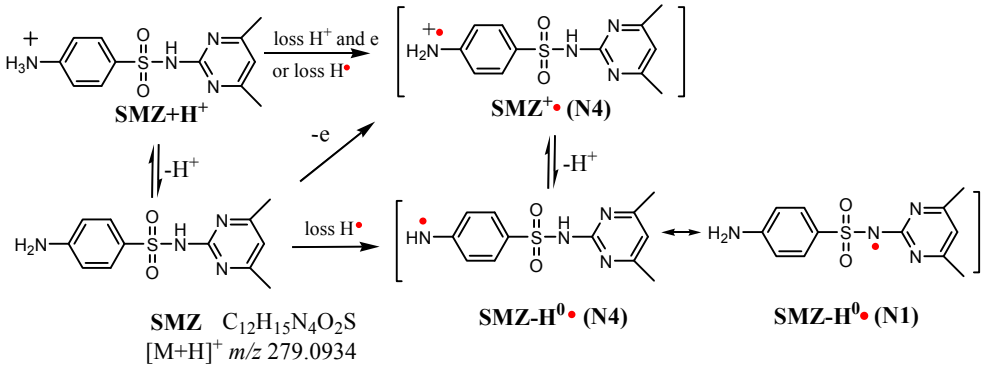

Step 2, Pathway A. Two $SMZ^{+}\cdot$ (N4) or $SMZ^{0}\cdot$ (N4) radicals couple to form a hydrazo-dimer which is further oxidized to an azo-dimer.

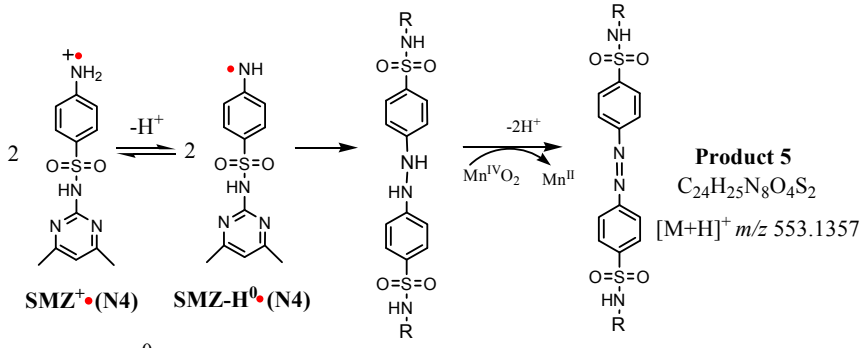

Step 2, Pathway B. $SMZ^{0}\cdot$ undergoes structural rearrangement and reacts with MnO_2 (or activated O_2) to form **8** and then **10** by losing $–SO_3$.

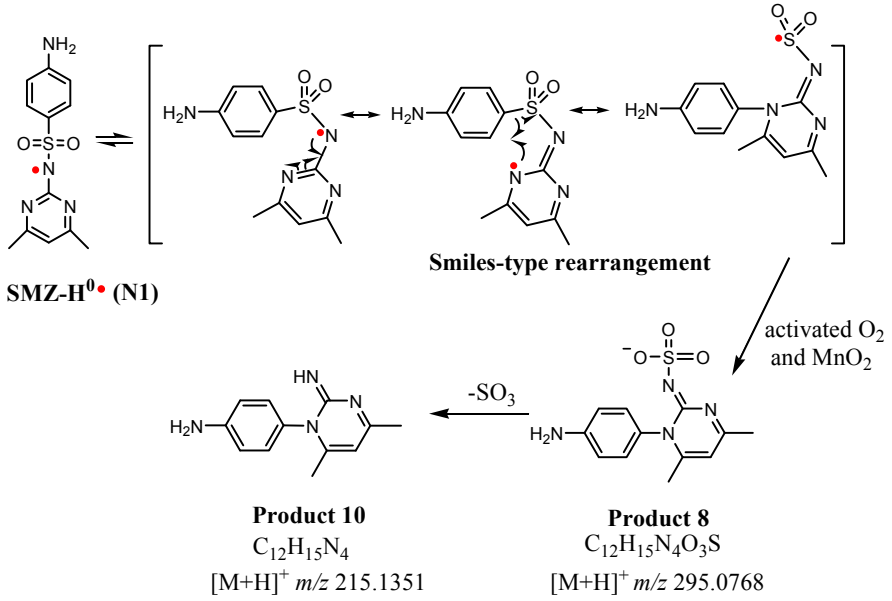

Figure 3. Proposed scheme for pathways of δ-MnO_2-mediated transformation of SMZ. In Step 2, Pathway A, the possibility exists for the $SMZ\text{-}H^{0}\cdot$ (N4) radical to further lose one electron and one proton to form a nitrene radical. Two SMZ nitrene radicals can self-condense to form **5**.[58] Mass-to-charge (*m*/*z*) ratios determined by TOF-MS and abundances relative to $[M+H]^{+}$ ion of

$[M+1+H]^+$ and $[M+2+H]^+$ ions: SMZ (280.0900, 14.26%; 281.0885, 5.04%), **5** (554.1336, 23.522%; 555.1324, 9.588%), **8** (not available due to low intensity), and **10** (216.1281, 12.15%; 217.1405, 0.6569%). Error (ppm) between accurate mass and molecular formula: −0.62659 (SMZ), −1.75659 (**5**), 2.57967 (**8**), and −0.57199 (**10**).

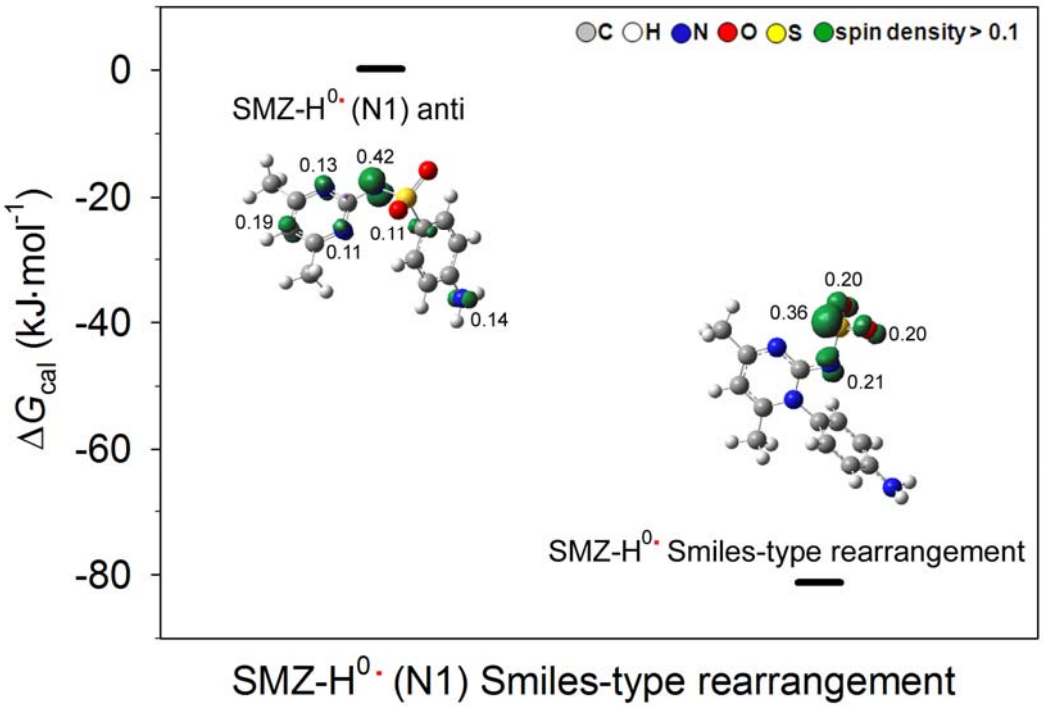

Figure 4. Relative free energies of formation in aqueous phase (calculated by PCM/DFT method) for SMZ-H$^{0\cdot}$ and Smiles-type rearrangement product. The structures represent ball-stick stereoisomers of SMZ-H$^{0\cdot}$ and Smiles-type rearrangement product with spin density isosurface at 0.0675 e Å^{-3} plotted. Numbers are atomic spin densities calculated by NBO analysis.

Chapter 5

Mass Spectrometry of Environmental Samples –

Discussion, Study Conclusion, and Future Directions

Mass Spectrometry for Environmental Analysis

Modern mass spectrometry equipment has made it possible to monitor emerging contaminants in complex environmental matrices, such as biosolids, WWTP influent, and manure, in parts per trillion or lower quantities. This has allowed resource managers to become more aware of potential hazards that were not apparent even 10 to 15 years ago [1]. The research performed and reported within this thesis document showcases the utility of mass spectrometers to address a variety of environmental analysis needs, such as quantitative target compound analysis, qualitative evaluation of complex environmental chemical mixtures, and unknown environmental organic compound identification problems.

Environmental Mass Spectrometry for Quantitative Target Compound Analysis

The utility of GC/MS and HPLC-MS/MS instruments to perform multi compound residue analysis with analyte monitoring capabilities of >100 compounds per sample has greatly increased awareness and knowledge of how organic compounds of interest interact with the environment. However, some key parameters need to be kept in mind when performing quantitative analysis with this instrumentation to ensure accurate and high quality results.

Labeled Internal Standards - One of these key parameters is the use of mass labeled internal standard compounds. Adding these internal standards pre-extraction has been shown to greatly increase the accuracy of GC/MS and HPLC-MS/MS quantitative results [2,3]. Because the mass

labeled compounds are essentially the target compound with the exchange of several deuterium, ^{13}C, or ^{15}N atoms, the compound behaves similarly in both extraction efficiency and behavior in the presence of matrix suppressing and/or enhancing substances within the ionization source of the mass spectrometer. This was shown to be of great importance for the analysis of hormones in CAFO samples [2].

Laboratory Control Spikes - Because there are instances where a mass labeled internal standard is not available, the questions of extraction efficiency and matrix effects must be addressed in another fashion. This was the case for the analysis of targeted rubber-related compounds in the artificial turf study [3]. A series of negative and positive controls were utilized for this purpose. Multiple laboratory-prepared desorption spikes were analyzed along with the samples to establish extraction efficiency, and the mean result was used to develop a factor which was applied to the field sample results. This concept was extended with the addition of several trip spikes, which were prepared and shipped with the field sampling media, to validate the recovery of the compounds of interest through the sampling, transport, and storage aspects of the project. In fact, it is a good practice to extract and run duplicate Laboratory Control Spikes (LCSs) with each batch of field samples processed to ensure acceptable recovery of anlaytes is routinely achieved.

Reagent and Method Blanks - Although positive controls are important to ensure good performance and recovery of the analytes in a GC/MS or HPLC-MS/MS quantitative assay, the use of negative controls is also very important. This is especially true of assays that are monitoring these compounds at trace levels in the environment. The analysis of reagent and method blanks help to show when certain compounds exhibit background contamination. In the artificial turf study, it was

found that the sulfur-containing compounds, benzothiazole and 2-mercaptobenzothiazole interacted with stainless steel components of the HPLC equipment, and therefore had a significant carryover effect into subsequent blanks [3]. To address this effect, multiple methanol blanks were run before field samples and after injections of standards containing high concentrations of the analyte. The reporting limit of these compounds was also raised to a level that was above the observed carry over contamination effect in the method blanks.

Confirmation Ions – Although the use of multiple reaction monitoring (MRM) allows for extremely selective detection, the potential for co-eluting compounds to cause interfering signal exists. This effect is called isobaric interference, and it is where two compounds with the same unit mass pass through a mass analyzer together and interfere with each other. This is possible due to the fact that quadrupole MS instruments operate at unit mass resolution. There is therefore a need to monitor more than one MRM transition and make a comparison of the ratio of these responses as a quality control measure. A rule of thumb is to monitor one quantitative MRM channel and at least one confirmatory MRM channel as part of a HPLC-MS/MS analytical method. The use of this quality control principal served our group well in a study of cyanobacterial toxin, Anatoxin-A [4]. Comparison of quantitative and confirmatory MRM ratio alerted us to a field sample that did not match this ratio well, even though all three MRM transitions monitored were present. Further investigation showed that the compound detected was actually phenylalanine [4]. This example highlights the need for confirmatory ion monitoring. This concept is also important in GC/MS analysis, where quantitative and several qualifying ions at different m/z values are monitored for each analyte [4].

Environmental Mass Spectrometry for Unknown Environmental Organic Compound Identification Problems

The use of mass spectrometry, especially when coupled with orthogonal detection methods, is a powerful tool for the elucidation of unknown compounds. Recent work by the author has demonstrated this by several different techniques. By running MS/MS experiments like product ion scans, where a precursor *m/z* is fragmented and its products detected in scan mode, the product ion peaks present in the mass spectrum can be used to deduce structure from their *m/z* values. This technique along with the method of first principles was used to elucidate the structure of an unknown contaminant peak in algal toxin monitoring [4]. The tentatively identified peak, phenylalanine, was confirmed by purchasing and running a putative standard.

By running ultraviolet-diode array detection (UV-DAD) in line with MS/MS detection, some transformation products of oxytetracycline and chlortetracycline were identified and assigned tentative structures [5]. Some of these structures were then confirmed by the purchase and analysis of putative standards. This in-line UV-DAD-MS/MS detection technique was also employed to identify and assign tentative structures to several abiotic transformation products of sulfamethazine by a synthetic analog of the birnessite-family mineral vernadite (δ-MnO_2) [6]. Finally, in a collaborative study with Bialk et al., the addition of nuclear magnetic resonance (NMR) analysis off-line to this UV-DAD-MS/MS technique, allowed for further characterization of compound identity for a reaction of 15N-labeled sulfapyridine to a model humic constituent (protocatechuic acid) [7].

Environmental Mass Spectrometry for Qualitative Evaluation of Complex Environmental Chemical Mixtures

In Chapter One of this thesis, the topic of advanced scan functions in hybrid mass spectrometry systems was introduced. The main examples, neutral loss scan, precursor ion scan, and product ion scan, were described. Two of these advanced scan MS/MS functions were utilized for a project that characterized the chemical character of water soluble organic carbon compounds in atmospheric samples [8]. Using a specialized type of chromatography called Hydrophobic Interaction Liquid Chromatography (HILIC), a separation was able to be made which separated groups by compound class (or functional group). By doing this, detection of groups of compounds could then be made by use of these advanced MS/MS scan functions. For example, a neutral loss scan of 44 amu was used to determine the presence of compounds that contain a carboxylic acid group. Another example was the use of precursor ion scan of 97 amu, which was used to probe the samples for the presence of organosulphate compounds [8].

Environmental Mass Spectrometry in High Resolution Mode for Organic Compound Structural Identification and Fragmentation Pathway Analysis

The use of high resolution MS can be very useful when unambiguous compound structural assignment is required. A magnetic sector MS was used with ethyl chloroformate derivatization and gas chromatographic separation to study the fragmentation pathway of beta-methylamino-L-alanine (BMAA) [9]. The unambiguous assignment of fragmentation structures allowed fragmentation

pathways to be proposed that corrected previously published fragmentation pathways determined by lower resolution MS methodology.

Environmental Mass Spectrometry with Derivatization and Mass Labeling for the Study of Organic Compound Transformation Pathways

In the study by Gao et al. discussed previously [6], the use of [phenyl-$^{13}C_6$]-labeled sulfamethazine (SMZ) helped in the interpretation of fragments from transformation products. Reactions were run with both natural SMZ and mass labeled SMZ. By comparing product ion scan mass spectra between the two experiments, the six Dalton mass difference in mass labeled compound m/z could be tracked. This mass labeled element tracking method also helped determine the mechanism by which the SMZ was transformed. By running one SMZ birnessite reaction with mass labeled water ($H_2{}^{18}O$) and another by purging with mass labeled oxygen ($^{18}O_2$) prior to HPLC-UV-DAD-MS/MS analysis, the additional mass could be tracked to determine if oxygen from water or from dissolved oxygen was reacting to form the SMZ transformation products [6]. In the BMAA fragmentation pathway study by Guo discussed previously [9], the derivatization of BMAA with ethyl chloroformate not only made the compound amenable for the GC chromatography and sample introduction to the MS, but it also created fragmentation mass spectra that also helped in the unambiguous determination of the BMAA fragmentation pathway. It did so because it reacts on a specific functional group, and the ethyl chloroformate *m/z* could then be tracked throughout the fragmentation process.

Dissertation Study Conclusions

With the work described in the preceding chapters and previous publications, the author has successfully shown evidence to support the following overarching thesis goal statements:

1. The use of HPLC-MS/MS and GC/MS is practicable for multi residue analysis of trace organic compound contaminants in complex environmental extracts (Chapter 2) [3].
2. HPLC-MS/MS and GC/MS can be successfully employed for unknown organic compound determinations in environmental samples (Chapter 3) [4-7].
3. Advanced MS/MS scans, such as precursor ion scan and neutral loss scan, can be used to generate useful data for the characterization of complex environmental extracts [8].
4. High resolution MS data can outperform unit resolution MS generated data for the elucidation of organic compound structure and fragmentation pathway analysis (Chapter 4) [9].
5. Derivitization and mass labeling are important aids when using mass spectrometry to study chemical transformation pathways (Chapter 4) [6, 9].

In addition, the work presented in Chapters 2 through 4 of this dissertation provided evidence in support of the following hypothesis statements:

1. Chapter 2
    a) By the evaluation of quality control results, HPLC-MS/MS is a viable alternative to GC with thermal energy analyzer (TEA) detection for the analysis of N-nitrosamine compounds in air samples as referenced in NIOSH Method 2522 [11].

b) By the evaluation of quality control results, HPLC-MS/MS can effectively be used in place of GC with sulfur chemiluminescence detection for the analysis of benzothiazole compounds in air samples as referenced in NIOSH Method 2550 [12].

2. Chapter 3
    a) Using HPLC-MS/MS with isotope dilution targeted analysis and bioassays with potency factors for targeted analysis compounds, it is possible to quantitatively account for the bioactivity observed in fractionated environmental extracts.
3. Chapter 4
    a) The influence of oxygen in organic compound transformation product reactions can be determined by the use of $^{18}O_2$ and $H_2{}^{18}O$ in reactions along with the analysis of reaction products by HPLC-UV-MS/MS.

Future Directions for Environmental Mass Spectrometry

Advanced Instrumentation - The newest generation of mass spectrometers have a high resolution time of flight (TOF) mass analyzer that is coupled to a quadrupole, ion mobility, and/or another TOF mass analyzer in front of it, separated by a collision cell. Examples include the SYNAPT-G2 QTOF (Waters Corporation, Milford, MA), the 6550 Q-TOF (Agilent Technologies, Santa Clara, CA), and the 5600 Q/TOF from AB/SCIEX (Framingham, MA). These instruments can easily achieve >10,000 resolution, and are therefore capable of assigning compound formula to unknown small molecules. Recent advances in TOF mass analyzer technology have extended their quantitative linear range, making them viable alternatives to quadrupole mass analyzers for trace quantitative analysis. These new MS/MS instruments also have the ability to acquire all masses all of

the time, so data can be mined later for the presence of unknown compounds. These instruments therefore have the ability to generate trace quantitation of analytes while also allowing for the identification of unknown compounds encountered in the same sample. This is a powerful advance in technology that could improve environmental analysis, because non-targeted compounds, metabolites, and breakdown products of environmental contaminants can feasibly be identified from the same target compound sample extract. Adjusting environmental analysis methodology to look for these additional compounds will allow scientists to gain a much better understanding of how polar organic compounds behave in the environment.

Linking environmental exposures to human health effects - Recent work by the author provided concentrations of xenoestrogenic compounds in human serum to researchers who compared these concentrations to mammographic breast cell density measurements for a cohort of post menopausal women. Positive correlations were made between two of the target compounds (monoethyl phthalate and bisphenol A) and breast cell density, showing a statistically significant increase in breast cancer risk with elevated levels of these compounds (**Appendix C).** This highlights the capability of mass spectrometry studies to be able to link environmental exposures to human health effects. The use of mass spectrometry in 'omics' studies (proteomics, metabolomics, and lipidomics) shows potential as a means to identify and monitor for biomarkers of environmental exposure. A new branch of omics study (exposomics) suggests a way for environmental scientists to monitor for and study the aggregate exposure to environmental toxicants [10].

Mass spectrometry has most certainly come a long way since its inception in the late 19th century. With the rate of development in mass spectrometer designs and applications over the past 20 years,

this technique is sure to have a primary role in the future of environmental monitoring. Its ability to interface with a variety of separation techniques, or to operate by direct analysis, lends itself well to the myriad of different organic compounds and matrices that are analyzed in environmental science.

Literature Cited

[1] Daughton, C. G. 2004. PPCPs in the environment: Future research - Beginning with the end always in mind. Pharmaceuticals in the environment. K. Kümmerer, Springer**:** 463-495.

[2] Havens, S. M., Hedman, C.J.,Hemming, J.D.C.,Mieritz, M.M,Shafer, M.M., Schauer, J.J. 2010. Stability, preservation, and quantification of hormones and estrogenic and androgenic activities in surface water runoff. *Environ. Toxicol. Chem.* **29**: 2481-2490.

[3] Simcox, N., Bracker, A., Ginsberg, G., Toal, B., Golembiewski, B., Kurland, T., and Hedman, C. 2011. Synthetic turf field investigation in Connecticut. *J. Toxicol. Environ. Health A.* 74:1133:1149.

[4] Hedman, C., Krick, W., Karner, D., Harrahy, E., Sonzogni, W. 2008. New measurements of cyanobacterial toxins in Wisconsin waters. *J. Environ. Qual*. 37:1817-1824 (2008).

[5] Rubert, K.F., IV, Hedman, C.J., Pedersen, J.A. 2009. Influence of MnO2 on the transformation of oxy- and chlortetracycline in pond water. In Veterinary Pharmaceuticals in the Environment, ACS Symposium Series No. 1018; Coats, J.R.; Henderson, K.L. (eds.); Oxford University Press: New York, pp. 45-65.

[6] Gao, J., C. Hedman, C. Liu, T. Guo, and J.A. Pedersen. Transformation of sulfamethazine by manganese oxide in aqueous solution. Environ. Sci. Technol. 46:2642-2651, 2012.

[7] Bialk, H., Hedman, C., Castillo, A., Pedersen, J. 2007. Laccase-mediated Michael addition of ^{15}Nsulfapyridine to a model humic constituent. *Environ. Sci. Technol*., 41:3593-3600.

[8] Stone, E.A., Hedman, C.J., Sheesley, R,J., Shafer, M.M., Schauer, J.J. 2009. Investigating the chemical nature of humic-like substances (HULIS) in North American atmospheric aerosols by liquid chromatography tandem mass spectrometry. *Atmospheric Environment*. 43:4205-4213.

[9] Guo, T., Geis, S., Hedman, C., Arndt, M., Krick, W., Sonzogni, W. 2007. Characterization of ethyl chloroformate derivative of beta-methylamino-L-alanine. *J. Am. Soc. Mass Spectrom*., 18:817-825 2007.

[10] Lioy P.J., Rappaport S.M. 2011. Exposure science and the exposome: an opportunity for coherence in the environmental health sciences. *Environ Health Perspect*ives, 119:A466–A467.

[11] National Institute of Occupational Safety and Health (NIOSH). 1994. Method 2522 Nitrosamines. In: Eller PM, Cassinelli ME. Eds. NIOSH Manual of Analytical Methods, 4th ed., Cincinnati, OH: NIOSH. Accessed April 2, 2012 at http://www.cdc.gov/niosh/docs/2003%2D154/pdfs/2522.pdf.

[12] National Institute of Occupational Safety and Health (NIOSH). 1998. Method 2550 Benzothiazole in Asphalt Fume. In: Eller PM, Cassinelli ME. Eds. NIOSH Manual of Analytical Methods, 4th ed., Cincinnati, OH: NIOSH. Accessed April 2, 2012 at http://www.cdc.gov/niosh/docs/2003-154/pdfs/2550.pdf.

Appendix A

Supporting Material from Chapter 2

File Name: WL096.1.0

Procedure: **Nitrosamine samples are desorbed with dichloromethane:methanol 75:25 (v/v) and analyzed by HPLC using MS/MS detection.**

Cover Letter: 756
Analyte(s):

NAME	IDC	CAS	Reporting Limit
N-nitrosodimethylamine (NDMA)	1942	62-75-9	100 ng/sample
N-nitrosomorpholine (NMOR)	1943	59-89-2	100 ng/sample
N-nitrosopyrrolidine (NPYR)	1950	930-55-2	100 ng/sample
N-nitrosodiethylamine (NDEA)	1947	55-18-5	100 ng/sample
N-nitrosopiperdine (NPIP)	1949	100-75-4	100 ng/sample
N-nitrosodipropylamine (NDPA)	1948	621-24-7	100 ng/sample
N-nitrosodibutylamine (NDBA)	1944	924-16-3	100 ng/sample
Nitrosamines Scan	9707		100 ng/sample

A. Principle of Method: Nitrosamine samples are desorbed with dichloromethane:methanol 75:25 (v/v) and analyzed by HPLC using MS/MS detection.

B. Health and Safety:

1. NDMA is a Class 1 carcinogen, and other nitrosoamines are suspected carcinogens. Handle only in hood.
2. Formic acid:
   - **a.** Exposure Routes: inhalation skin absorption, ingestion, skin and/or eye contact
   - **b.** Symptoms: ingestion may cause burning sensation, coughing wheezing, laryngitis, shortness of breath, headache, nausea, and vomiting; inhalation may cause spasm, inflammation and edema of the larynx and bronchi, chemical pheumonitis, and pulmonary edema; extremely destructive to tissue of the mucous membranes and upper respiratory tract, eyes, and skin
   - **c.** Target Organs: eyes, skin, respiratory system, gastrointestinal tract, central nervous system, blood, liver, kidneys
3. Dichloromethane
   - **a.** Exposure Routes: inhalation, skin absorption, ingestion, skin and/or eye contact
   - **b.** Symptoms: inhalation may cause irregular breathing, pulmonary edema (effects may be delayed); eye contact may cause redness, tearing, blurred vision, and conjunctivitis; ingestion may cause gastrointestinal irritation, nausea, and vomiting; repeated skin exposure can cause defatting and dermatitis; DCM metabolizes in the body to form carbon monoxide which irreversibly binds hemoglobin to cause oxygen depletion
   - **c.** Target organs: eyes, skin, respiratory system, gastrointestinal tract, central nervous system, blood, liver, pancreas, heart, central nervous system
4. Methanol
   - **a.** Exposure Routes: inhalation, skin absorption, ingestion, skin and/or eye contact

b. Symptoms: irritation to eyes, skin, upper respiratory system; headache, drowsiness, dizziness, nausea, vomiting, dermatitis, visual disturbance, optic nerve damage, blindness
c. Target Organs: eyes, skin respiratory system, central nervous system, gastrointestinal tract

C. Sampling Information:
1. Sampling Media: Thermosorb N tubes
2. Sample collection:
a. Flow Rate: 0.2 to 2 liter per minutes
b. Air Volume: Up to 75 liters the larger the collection volume better it is.
3. Sample Storage: Protect all samples from light. Store in freezer until ready to analyze.
4. Interferences: No information available.

D. Chemicals and Reagents:
1. Reagents:
a. Methanol
b. Formic Acid
c. High purity water
d. Glacial acetic acid
e. Dichloromethane
f. Desorption solution is composed of 75% dichloromethane and 25% methanol by volume.
2. Standards are prepared over the range from 100-2,000 ng/ml in dichloromethane:methanol 75:25 (v/v). Protect standards from light and store frozen.

E. Equipment and Supplies:
1. Liquid Chromatograph
2. Detector: Tandem Mass Spectrometer

F. Sample Preparation:
1. Thermosorb N tubes are transferred to scintillation vials and desorbed with 4 ml of 75/25 dicoloromethane/methanol desorption solution.
2. The desorption eluent is collected in a 10 ml graduated cylinder, measured for a total volume, and an aliquot is transferred to an injection vial.

G. Calibration and Sample Analysis:
1. LC Conditions:
a. Column Type: RP-C18 Reverse phase, 4.6 mm ID x 25cm long
b. Mobile Phase:
1) Solvent A : 0.1% Formic Acid
2) Solvent B: Methanol
c. Probe Height Setting: 6
d. Injection Volume: 20 µl

2. Run Conditions:

a. Agilent 1100 LC Pump Method Properties

1) Pump Model: Agilent 1100 LC Binary Pump

Minimum Pressure (psi)	0.0
Maximum Pressure (psi)	5801.0
Dead Volume (µl)	40.0
Maximum Flow Ramp (ml/min²)	100.0
Maximum Pressure Ramp (psi/sec)	290.0
Left Compressibility	50.0
Right Compressibility	115.0
Left Dead Volume (µl)	40.0
Right Dead Volume (µl)	40.0
Left Stroke Volume (µl)	-1.0
Right Stroke Volume (µl)	-1.0
Left Solvent	A1 (0.1% Formic Acid)
Right Solvent	B2 (Methanol)

2) Step Table:

Step	**Total Time (min)**	**Flow Rate (µl/min)**	**A (%)**	**B (%)**
0	0.00	500	97.0	3.0
1	4.00	500	97.0	3.0
2	6.00	500	50.0	50.0
3	10.00	500	5.0	95.0
4	19.00	500	5.0	95.0
5	19.50	500	97.0	3.0
6	29.50	500	97.0	3.0

b. Agilent 1100 Autosampler Properties

Autosampler Model	Agilent 1100 Wellplate Autosampler
Syringe Size (µl)	100
Injection Volume (µl)	20.00
Draw Speed (µl/min)	200.0
Eject Speed (µl/min)	200.0
Needle Level (mm)	0.00
Temperature Control	Not Used
Wash	Not Used
Automatic Delay Volume Reduction	Not Used
Equilibration Time (sec)	2
Enable Vial/Well Bottom Sensing	No
Use Custom Injector Program	No

c. Agilent 1100 Column Oven Properties

Left Temperature (°C)	20.00
Right Temperature (°C)	20.00
Temperature Tolerance ±(°C):	1.00
Start Acquisition Tolerance ±(°C)	0.50
Time Table	(Not Used)
Column Switching Valve	Not Installed
Position for first sample in the batch	N/A
Use same position for all sample in the batch	

d. Quantitation Information:

1) Sample Type: Unknown
2) Dilution Factor: 1.000000

e. Custom Data: None

f. MS Method Properties:

1) Period 1:

Scans in Period:	938
Relative Start Time:	0.00 msec
Experiments in Period:	1

2) Period 1 Experiment 1:

Scan Type:	MRM (MRM)
Polarity:	Positive
Scan Mode:	N/A
Ion Source:	Turbo Spray
Resolution Q1:	Unit
Resolution Q3:	Unit
Intensity Thres.:	0.00 cps
Settling Time:	0.0000 msec
MR Pause:	5.0070 msec
MCA:	No
Step Size:	0.00 amu

3)

Analyte ID	Q1 Mass (amu)	Q3 Mass (amu)	Dwell (msec)	Param	Start	Stop
NDBA 1	159.23	57.10	40.00	DP	66.00	66.00
				CE	23.00	23.00
				CXP	8.00	8.00
NDEA 1	103.19	75.10	40.00	DP	66.00	66.00
				CE	19.00	19.00
				CXP	12.00	12.00
NDMA 1	75.17	42.64	40.00	DP	71.00	71.00
				CE	23.00	23.00
				CXP	10.00	10.00

Analyte ID	Q1 Mass (amu)	Q3 Mass (amu)	Dwell (msec)	Param	Start	Stop
N-Nitrosodiphenyl amine 1	109.17	57.00	40.00	DP	36.00	36.00
				CE	21.00	21.00
				CXP	4.00	4.00
NDPA-1	131.24	89.20	40.00	DP	66.00	66.00
				CE	17.00	17.00
				CXP	10.00	10.00
N-Nitrosomethylethyl amine 1	89.21	70.90	40.00	DP	76.00	76.00
				CE	21.00	21.00
				CXP	4.00	4.00
N-Nitrosomorpholine 1	117.18	87.10	40.00	DP	51.00	51.00
				CE	17.00	17.00
				CXP	4.00	4.00
NPIP	115.21	68.60	40.00	DP	71.00	71.00
				CE	21.00	21.00
				CXP	12.00	12.00
NPYR	101.21	84.2	40.00	DP	61.00	61.00
				CE	17.00	17.00
				CXP	6.00	6.00
NDBA 2	159.23	103.40	40.00	DP	66.00	66.00
				CE	17.00	17.00
				CXP	8.00	8.00
NDEA 2	103.19	56.90	40.00	DP	66.00	66.00
				CE	13.00	13.00
				CXP	10.00	10.00
NDMA 2	75.17	46.80	40.00	DP	71.00	71.00
				CE	17.00	17.00
				CXP	8.00	8.00
N-Nitrosodiphenyl amine 2	109.17	104.00	40.00	DP	36.00	36.00
				CE	13.00	13.00
				CXP	16.00	16.00
NDPA-2	131.24	42.70	40.00	DP	66.00	66.00
				CE	19.00	19.00
				CXP	16.00	16.00
N-Nitrosomethylethyl amine 2	89.21	44.70	40.00	DP	76.00	76.00
				CE	29.00	29.00
				CXP	16.00	16.00
N-Nitrosomorpholine 2	117.18	86.10	40.00	DP	51.00	51.00
				CE	19.00	19.00
				CXP	4.00	4.00
NPIP 2	115.21	40.80	40.00	DP	71.00	71.00
				CE	35.00	35.00
				CXP	6.00	6.00

Analyte ID	Q1 Mass (amu)	Q3 Mass (amu)	Dwell (msec)	Param	Start	Stop
NPYR 2	101.21	55.00	40.00	DP	61.00	61.00
				CE	25.00	25.00
				CXP	10.00	10.00

				DP	36.00	36.00
d^8 Naphthalene 1	137.14	79.10	40.00	CE	11.00	11.00
				CXP	12.00	12.00
				DP	36.00	36.00
d^8 Naphthalene 2	137.14	122.6	40.00	CE	11.00	11.00
				CXP	12.00	12.00
				DP	66.00	66.00
NDEA 3	103.19	47.00	40.00	CE	23.00	23.00
				CXP	8.00	8.00
				DP	61.00	61.00
NPYR 3	101.21	40.70	40.00	CE	33.00	33.00
				CXP	8.00	8.00
				DP	71.00	71.00
NDMA 3	75.17	58.00	40.00	CE	19.00	19.00
				CXP	10.00	10.00
				DP	76.00	76.00
N-Nitrosomethylethyl amine 3	89.21	42.50	40.00	CE	33.00	33.00
				CXP	7.00	7.00

4) Parameter Table (Period 1 Experiment 1):

CAD:	10.00
CUR:	25.00
GS1:	20.00
GS2:	60.00
IS:	5500.00
TEM:	500.00
ihe:	ON
EP:	10.00

g. Retention Times:

Compound	**Time (min)**
NDMA	13.3
NMOR	13.6
NPYR	14.3
NDEA	15.1
NPIP	15.5
NDPA	6.3
NDBA	17.1

H. QC Procedures:

1. Acceptance criteria for STDS and repeats:
2. Check Standards:
   - **a.** Continuing calibration verification (CCV) will be run at least one in every ten injections. An independently prepared (second source) standard shall be verified each day or at each start of an analytical run.
   - **b.** Acceptance criteria are $^{\pm}$10% for CCV and $^{\pm}$15% for second source.
3. Blank sample results are not subtracted from the results.
4. Sample Duplicates or Replicates:
   - **a.** Minimum of 10% of samples will be analyzed in duplicate.
   - **b.** Acceptance criteria are $^{\pm}$20%.

I. Confirmatory Technique: GC-HRMS, per OSHA 27.

J. Calculation of Results:

1. Results are calculated by instrument software as mass per sample.
2. Spreadsheet calculations are completed by LIMS as follows: $mg/m^3 = \frac{\mu g/sample}{Air\ volume\ (L)}$

K. Method Development/Validation:

1. Reporting Levels: 100 ng/mL
2. Interference: Multiple Reaction Monitoring (MRM) MS/MS detection is highly selective for target analytes, however, co-eluting moieties could potentially cause signal suppression/enhancement for the analyte(s). If this is suspected, a standard additions experiment should be performed on the sample in question to verify results.
3. Validation Data:
   a. Desorption Data: M:\EHD\ESS(4900)\ESS Org(4940)\LC-MS\Data Archive\Nitrosamines (WOHL)
   b. Stability Data: ..\..\..\..\..\..\ESS(4900)\ESS Org(4940)\LC-MS\Data Archive\Nitrosamines (WOHL)\Stability Desorption Data.xls

L. Reference: OSHA Method 27

M. Procedure by: Curtis Hedman **Date:** 04/06

N. Procedure Approved by: Terry Burk **Date**: 7/25/07

O. Procedure Modified by: **Date:**

P. Modified Procedure Approved by: **Date:**

File Name: WL100.2

Procedure: **Benzothiazole and 4-(tert-Octyl)phenol by LCMSMS**

Cover Letter:
Analyte(s):

NAME	IDC	CAS	Reporting Limit
Benzothiazole vapor	B506V	95-16-9	100 ng/sample
4-(tert-Octyl)phenol vapor	9922V	140-66-9	100 ng/sample
Benzothiazole particulate	B506	95-16-9	100 ng/sample
4-(tert-Octyl)phenol particulate	9922	140-66-9	100 ng/sample

Q. Principle of Method: Benzothiazole and 4-(tert-Octyl)phenol samples are desorbed with methanol and analyzed by HPLC using MS/MS detection.

R. Health and Safety:

1. Target compounds may be irritating to mucous membranes and upper respiratory tract. May be harmful if inhaled. Handle only in hood.
2. Formic acid:
   a. Exposure Routes: inhalation skin absorption, ingestion, skin and/or eye contact
   b. Symptoms: ingestion may cause burning sensation, coughing wheezing, laryngitis, shortness of breath, headache, nausea, and vomiting; inhalation may cause spasm, inflammation and edema of the larynx and bronchi, chemical pheumonitis, and pulmonary edema; extremely destructive to tissue of the mucous membranes and upper respiratory tract, eyes, and skin
   c. Target Organs: eyes, skin, respiratory system, gastrointestinal tract, central nervous system, blood, liver, kidneys
3. Methanol
   a. Exposure Routes: inhalation, skin absorption, ingestion, skin and/or eye contact
   b. Symptoms: irritation to eyes, skin, upper respiratory system; headache, drowsiness, dizziness, nausea, vomiting, dermatitis, visual disturbance, optic nerve damage, blindness
   c. Target Organs: eyes, skin respiratory system, central nervous system, gastrointestinal tract

B. Sampling Information:

1. Sampling Media: 37-mm PTFE filter and XAD tube in series (see WOHL Sampling Guide for details).
2. Sample collection:
   a. Flow Rate: Up to 2 liters per minute.
   b. Air Volume: Up to 960 liters the larger the collection volume better it is.
3. Sample Storage: Protect all samples from light. Store in freezer until ready to analyze.
4. Interferences: No information available.

C. Chemicals and Reagents:

1. Reagents:
   - **a.** Methanol
   - **b.** Formic Acid
   - **c.** High purity water
   - **d.** Desorption solution is composed 100% methanol.
2. Standards are prepared over the range from 100-5,000 ng/ml in methanol. Protect standards from light and store frozen. Below what is being done for making standards change it to fix your needs.
3. Calibration and check standard preparation: A 10.0 µg/ml pool dilution is prepared as follows.
   - **a.** Weigh a known amount of analyte using an analytical balance into a volumetric flask.
   - **b.** Make subsequent dilutions using variable volume pipette and volumetric flasks to bring to required concentration.
   - **c.** Record standard preparation into LC standard preparation logbook.
4. Make the following dilutions of standard:

Standard Name	µl of 10 µg/ml Standard	µl of Desorbing Solution	Concentration (µg/ml)
1000 µl Std	1000	0	10
500 µl Std	500	500	5
200 µl Std	200	800	2
100 µl Std	100	900	1
50 µl Std	50	950	0.5
20 µl Std	20	980	0.2
10 µl Std	10	990	0.1
8 µl LOQ Std	8	992	0.08
4 µl LOQ Std	4	996	0.06
2 µl LOQ Std	2	998	0.02

D. Equipment and Supplies:

1. Liquid Chromatograph
2. Detector: Tandem Mass Spectrometer

E. Sample Preparation:

1. XAD tube contents and/or Teflon filters are transferred to scintillation vials and desorbed with 3 ml of methanol desorption solution.
2. The methanol is collected in a 15 ml glass conical tube.
3. Steps (1) and (2) are repeated two additional times for a total of three desorptions.
4. The combined methanol fractions are evaporated on a TurboVap set at 40^{o}C and 5-15 psi Nitrogen flow to <0.5 ml. NOTE: Recovery losses are observed if the methanol completely evaporates from the tubes.

F. Calibration and Sample Analysis:

1. LC Conditions for Benzothiazole:
   - **a.** Column Type: Zorbax Stable Bond C_8, 4.6 mm ID x 15 cm long
   - **b.** Mobile Phase:

1) Solvent A : 0.1% Formic Acid
2) Solvent B: Methanol

c. Probe Height Setting: 6

d. Injection Volume: 20 µl

2. Run Conditions for Benzothiazole:

a. Agilent 1100 LC Pump Method Properties

1) Pump Model: Agilent 1100 LC Binary Pump

Minimum Pressure (psi)	0.0
Maximum Pressure (psi)	5801.0
Dead Volume (µl)	40.0
Maximum Flow Ramp (ml/min²)	100.0
Maximum Pressure Ramp (psi/sec)	290.0
Left Compressibility	50.0
Right Compressibility	115.0
Left Dead Volume (µl)	40.0
Right Dead Volume (µl)	40.0
Left Stroke Volume (µl)	-1.0
Right Stroke Volume (µl)	-1.0
Left Solvent	A1 (0.1% Formic Acid)
Right Solvent	B2 (Methanol)

2) Step Table:

Step	Total Time (min)	Flow Rate (µl/min)	A (%)	B (%)
0	0.00	800	5.0	95.0
1	4.00	800	5.0	95.0

b. Agilent 1100 Autosampler Properties

Autosampler Model	Agilent 1100 Wellplate Autosampler
Syringe Size (µl)	100
Injection Volume (µl)	20.00
Draw Speed (µl/min)	200.0
Eject Speed (µl/min)	200.0
Needle Level (mm)	0.00
Temperature Control	Not Used
Wash	Not Used

Automatic Delay Volume Reduction	Not Used
Equilibration Time (sec)	2
Enable Vial/Well Bottom Sensing	No
Use Custom Injector Program	No

c. Agilent 1100 Column Oven Properties

Left Temperature (°C)	25.00
Right Temperature (°C)	25.00
Temperature Tolerance ±(°C):	1.00
Start Acquisition Tolerance ±(°C)	0.50
Time Table	(Not Used)
Column Switching Valve	Not Installed
Position for first sample in the batch	N/A
Use same position for all sample in the batch	

d. Quantitation Information:
1) Sample Type: Unknown
2) Dilution Factor: 1.000000

e. Custom Data: None

f. MS Method Properties:
1) Period 1:

Scans in Period:	238
Relative Start Time:	0.00 msec
Experiments in Period:	1

2) Period 1 Experiment 1:

Scan Type:	MRM (MRM)
Polarity:	Positive
Scan Mode:	N/A
Ion Source:	Turbo Spray
Resolution Q1:	Unit
Resolution Q3:	Unit
Intensity Thres.:	0.00 cps
Settling Time:	0.0000 msec
MR Pause:	5.0070 msec
MCA:	No
Step Size:	0.00 amu

3)

Analyte ID	Q1 Mass (amu)	Q3 Mass (amu)	Dwell (msec)	Param	Start	Stop
Benzothiazole 1	136.03	109.20	500	DP	76.00	76.00
				CE	37.00	37.00
				CXP	8.00	8.00
Benzothiazole 2	136.03	64.92	500	DP	76.00	76.00
				CE	47.00	47.00
				CXP	10.00	10.00

4) Parameter Table (Period 1 Experiment 1):

CAD:	10.00
CUR:	10.00
GS1:	20.00
GS2:	20.00
IS:	3500.00
TEM:	500.00
ihe:	ON
EP:	10.00

g. Retention Time for Benzothiazole = 2.24 min.

3. LC Conditions for 4-(tert-Octyl)phenol:

a. Column Type: Zorbax Stable Bond C_8, 4.6 mm ID x 15 cm long

b. Mobile Phase:
1) Solvent A : 0.1% Formic Acid
2) Solvent B: Methanol

c. Probe Height Setting: 6

d. Injection Volume: 20 µl

4. Run Conditions for 4-(tert-Octyl)phenol:

a. Agilent 1100 LC Pump Method Properties

1) Pump Model: Agilent 1100 LC Binary Pump

Minimum Pressure (psi)	0.0
Maximum Pressure (psi)	5801.0
Dead Volume (µl)	40.0
Maximum Flow Ramp (ml/min²)	100.0
Maximum Pressure Ramp (psi/sec)	290.0
Left Compressibility	50.0
Right Compressibility	115.0
Left Dead Volume (µl)	40.0
Right Dead Volume (µl)	40.0
Left Stroke Volume (µl)	-1.0
Right Stroke Volume (µl)	-1.0
Left Solvent	A1 (0.1% Formic Acid)
Right Solvent	B2 (Methanol)

2) Step Table:

Step	Total Time (min)	Flow Rate (µl/min)	A (%)	B (%)
0	0.00	800	0.0	100.0
1	4.00	800	0.0	100.0

b. Agilent 1100 Autosampler Properties

Autosampler Model	Agilent 1100 Wellplate Autosampler
Syringe Size (µl)	100
Injection Volume (µl)	20.00
Draw Speed (µl/min)	200.0
Eject Speed (µl/min)	200.0
Needle Level (mm)	0.00
Temperature Control	Not Used
Wash	Not Used

Automatic Delay Volume Reduction	Not Used
Equilibration Time (sec)	2
Enable Vial/Well Bottom Sensing	No
Use Custom Injector Program	No

c. Agilent 1100 Column Oven Properties

Left Temperature (°C)	25.00
Right Temperature (°C)	25.00
Temperature Tolerance ±(°C):	1.00
Start Acquisition Tolerance ±(°C)	0.50
Time Table	(Not Used)
Column Switching Valve	Not Installed
Position for first sample in the batch	N/A
Use same position for all sample in the batch	

d. Quantitation Information:

1) Sample Type: Unknown
2) Dilution Factor: 1.000000

e. Custom Data: None

f. MS Method Properties:

1) Period 1:

Scans in Period:	238
Relative Start Time:	0.00 msec
Experiments in Period:	1

2) Period 1 Experiment 1:

Scan Type:	MRM (MRM)
Polarity:	Negative
Scan Mode:	N/A
Ion Source:	Turbo Spray
Resolution Q1:	Unit
Resolution Q3:	Unit
Intensity Thres.:	0.00 cps
Settling Time:	0.0000 msec
MR Pause:	5.0070 msec
MCA:	No
Step Size:	0.00 amu

3)

Analyte ID	Q1 Mass (amu)	Q3 Mass (amu)	Dwell (msec)	Param	Start	Stop
				DP	-85.00	-85.00
4-(tert-Octyl)phenol 1	205.15	133.10	500	CE	-30.00	-30.00
				CXP	-9.00	-9.00
				DP	-85.00	-85.00
4-(tert-Octyl)phenol 2	205.15	134.20	500	CE	-26.00	-26.00
				CXP	-9.00	-9.00

4) Parameter Table (Period 1 Experiment 1):

CAD:	6.00
CUR:	10.00
GS1:	20.00
GS2:	10.00
IS:	-4500.00
TEM:	250.00
ihe:	ON
EP:	-10.00

g. Retention Time for 4-(tert-Octyl)phenol = 2.37 min.

G. QC Procedures:

1. Acceptance criteria for STDS and repeats:

2. Check Standards:

a. Continuing calibration verification (CCV) will be run at least one in every ten injections. An independently prepared (second source) standard shall be verified each day or at each start of an analytical run.

b. Acceptance criteria are $^{\pm}$10% for CCV and $^{\pm}$15% for second source.

3. Blank sample results are not subtracted from the results.

4. Sample Duplicates or Replicates:
   a. Minimum of 10% of samples will be analyzed in duplicate.
   b. Acceptance criteria are $^{+}$20%.

H. Confirmatory Technique: GC with sulfur chemiluminescence detection, per NIOSH 2550.

I. Calculation of Results:
1. Results are calculated by instrument software as mass per sample.
2. Spreadsheet calculations are completed by LIMS as follows: $mg/m^3 = \frac{\mu g/sample}{\text{Air volume (L)}}$

J. Method Development/Validation:
1. Reporting Levels: 100 ng/ml
2. Interference: Multiple Reaction Monitoring (MRM) MS/MS detection is highly selective for target analytes, however, co-eluting moieties could potentially cause signal suppression/enhancement for the analyte(s). If this is suspected, a standard additions experiment should be performed on the sample in question to verify results.
3. Validation Data:
   a. Desorption Data: M:\EHD\ESS(4900)\ESS Org(4940)\LC-MS\Data Archive\B 4T (WOHL)
   b. Stability Data:R:\ESS(4900)\ESS Org(4940)\LC-MS\Data Archive\B 4T (WOHL)\Stability Desorption Data.xls

K. Reference: NIOSH Method 2550, NMAM 4th ed. 1998.

L. Signatures:

1. **Procedure by:** Curtis Hedman **Date:** 09/30/08
2. **Procedure Approved by:** Terry Burk **Date:**
3. **Procedure Modified by:** **Date:**
4. **Modified Procedure Approved by:** **Date:**

File Name: WG086.2
Method: Analysis of VOCs by GC/MS Using ENTECH Instrumentation
Cover Letter: Customized for each study

NAME	CAS	SYNONYMS
Benzene*	000071-43-2	
Bromomethane*	000074-83-9	
1-Butanethiol	000109-79-5	n-Butyl Mercaptan
2-Butanethiol	000513-53-1	sec-Butyl Mercaptan
Carbon Disulfide	000075-15-0	
Carbon Tetrachloride*	000056-23-5	
Chlorobenzene*	000108-90-7	
Chloroethene*	000075-01-4	Vinyl Chloride
Chloroform*	000067-66-3	
Chloromethane*	000074-87-3	
1,2-Dibromoethane*	000106-93-4	Ethylene Bromide; Ethylene Dibromide
1,2-Dichlorobenzene*	000095-50-1	o-Dichlorobenzene
1,3-Dichlorobenzene*	000541-73-1	m-Dichlorobenzene
1,4-Dichlorobenzene*	000106-46-7	p-Dichlorobenzene
Dichlorodifluoromethane*	000075-71-8	Freon 12
1,1-Dichloroethane*	000075-34-3	
1,2-Dichloroethane*	000107-06-2	Ethylene Chloride
1,1-Dichloroethene*	000075-35-4	Vinylidene Chloride
(Z)-1,2-Dichloroethylene*	000156-59-2	cis-1,2-Dichloroethylene
Dichloromethane*	000075-09-2	Methylene Chloride
1,2-Dichloropropane*	000078-87-5	Propylene Chloride
(E)-1,3-Dichloropropene*	010061-02-6	trans-1,3-Dichloropropene
(Z)-1,3-Dichloropropene*	010061-01-5	cis-1,3-Dichloropropene
Dichlorotetrafluoroethane*	000076-14-2	Freon 114
Dimethyl Disulfide	000624-92-0	
Dimethyl Sulfide	000075-18-3	
Ethanethiol	000075-08-1	Ethyl Mercaptan
Ethylbenzene*	000100-41-4	
Ethyl Chloride*	000075-00-3	
Hexachloro-1,3-butadiene*	000087-68-3	
Methanethiol	000074-93-1	Methyl Mercaptan
2-Methyl-2-propanethiol	000075-66-1	tert-Butyl Mercaptan
1-Propanethiol	000107-03-9	n-Propyl Mercaptan
2-Propanethiol	000075-33-2	Isopropyl Mercaptan
Styrene*	000100-42-5	Phenylethylene
1,1,2,2-Tetrachloroethane*	000079-34-5	Acetylene Tetrachloride
Tetrachloroethylene*	000127-18-4	PERK; Perchloroethylene
Toluene*	000108-88-3	
1,1,1-Trichloroethane*	000071-55-6	Methyl Chloroform
1,2,4-Trichlorobenzene*	000120-82-1	
1,1,2-Trichloroethane*	000079-00-5	
Trichloroethylene*	000079-01-6	

Trichloromonofluoromethane*	000075-69-4	Freon 11
NAME	**CAS**	**SYNONYMS**
1,2,4-Trimethylbenzene*	000095-63-6	Pseudocumene
1,3,5-Trimethylbenzene*	000108-67-8	Mesitylene
1,1,2-Trichloro-1,2,2-trifluoroethane*	000076-13-1	Freon 113
o-Xylene*	000095-47-6	
p-& m-Xylene*		

*This VOC is present in a commercial calibration mix used for general solvent screening. Other VOCs not present in this calibration mix or listed in the above table may be used to quantitate samples as per client request.

A. Principle of Method: This procedure is used to identify and quantitate volatile organic compounds (VOCs) present in air or bulk samples using gas chromatography with mass-selective detection (GC/MS). Air samples are collected into bags or evacuated Silonite-coated metal canisters. Bulk liquid or solid samples are placed into Large Volume Static Headspace (LVSH) containers. Using the ENTECH 7032AQ Autosampler, an assigned volume of either the air sample or the headspace from the bulk sample is introduced into the ENTECH 7100A Preconcentrator. After a three-stage modification, the sample is injected into a GC/MS analytical system. Identification and quantitation of the VOCs detected in the sample are performed with calibration standards as well as NIST library searches of the spectral data. Results are reported as either confirmed quantitations or tentatively-identified estimations.

B. Health Hazards:

1. Typical hazards associated with working with organic VOCs. Consult MSDS's of each VOC of interest for safety information.
2. Liquid nitrogen can cause severe damage when it comes in contact with the skin. Use caution when opening/closing valves and when hooking tanks up to the ENTECH instruments.
3. The ENTECH 3100A MiniCans™ blanket mantle will heat MiniCans™ up to 80^{o}C during the can cleaning process. When removing cleaned cans from the 3100A, use caution to avoid burning fingers.

C. Sampling Information:

1. Sampling Media:
   - **a.** Tedlar™ or foil bags, 0.5 - 10 liter, SKC 232-08A, or equivalent.
   - **b.** MiniCan™ with Quick-Connect (QC) valve, 380-m1, Silonite®-coated, ENTECH no. 29-MC400S, or equivalent.
2. Sample collection:
   - **a.** Tedlar™ or foil bags: Fill using typical industrial hygiene sampling techniques for VOC collection into bags.
   - **b.** MiniCans™:
     1) Instantaneous (grab sample) using the Filtered Quick-Fill Sampler (FQFS):
        a) Remove the metal cap from a clean, evacuated MiniCan™.
        b) Place the FQFS over the exposed tip (male end) of the MiniCan™.
        c) Push down firmly and hold for approximately 20 seconds.
        d) Remove FQFS and re-cap the MiniCan™.
     2) 15-30 minute area sample using the Restrictor Sampler-6 (RS-6):

a) Remove the metal cap from a clean, evacuated MiniCan™.
b) Push back the Quick-Connect ring on the RS-6. Insert the exposed tip (male end) of the MiniCan™ firmly into the Quick-Connect on the RS-6. Push down hard to make the connection.
c) Release the Quick-Connect ring on the RS-6. Wait until desired sampling time has elapsed.
d) Remove the MiniCan™ from the RS-6 by pushing back the Quick-Connect ring on the RS-6 and pulling the MiniCan™ out of the Quick-Connect. Re-cap the MiniCan™. Record the elapsed time.

3) 2-hour or 8-hour area sample using the CS1200P Flow Controller (Sampler):
   a) Make certain the Sampler has the correct critical orifice.
      (1) For a 2 hour sample- use critical orifice# 4.
      (2) For an 8 hour sample- use critical orifice# 5.
   b) Calibrate the Sampler:
      (1) Attach the Sampler to the Alicat Scientific Precision Gas Flow Meter using a 9/16" wrench. Attach an evacuated MiniCan™ to the Sampler's Quick-Connect.
      (2) Remove the set screw in the center of the Sampler with an Allen wrench.
      (3) Adjust the flow with the Allen wrench to the desired rate.
         (a) For a 2 hour sample, the flow should be approximately 3.16 cc/min.
         (b) For an 8 hour sample, the flow rate should be approximately 0.79 cc/min.
      (4) When desired flow rate is achieved, remove the MiniCan™ from the Quick-Connect. Using the Allen wrench, replace the set screw.
   c) Attach the Area Sampler Modification (ASM) to the collection port of the Sampler with a 9/16" wrench.
   d) Begin area sampling by attaching a clean, evacuated MiniCan™ to the Sampler's Quick-Connect.
      (1) The MiniCan™ begins to fill the moment it is attached to the Sampler. As the MiniCan™ fills; the gauge on the Sampler should start near 30 and slowly move toward 0.
      (2) The can will automatically stop filling on its own due to the action of the critical orifice. Remove the MiniCan™ from the Sampler when the desired time has elapsed. Recap the MiniCan™.
4) 2-hour or 8-hour personal sample using the CS1200P Flow Controller (Sampler):
   a) Follow instructions as listed in the area sampling section above *except* instead of using the ASM, attach a Teflon™ personal sampling line with filter to the Sampler's collection port.
   b) When sampling, place the Sampler in the holster and belt arrangement worn around the worker's waist. Pin the filter end of the Teflon™ personal sampling line to the collar of the worker's shirt, as close to the breathing zone as possible.
   c) Attach a MiniCan™ to the Sampler as outlined above. Remove the MiniCan™ from the Sampler when the desired sampling time has elapsed. Recap the MiniCan™.

c. Bulk liquid or solid sample: Place sample into air-tight and leak-proof container. Ship to WOHL for use in the LVHS container.

D. Reagents:

1. Liquid or Gas Analyte of Interest: Neat; Chromatographic Grade. *Note: Solid reagents are generally not compatible with the Entech system.*
2. Specialty Gases (diluted) or commercial Gas Mixtures: Chromatographic Grade, if possible. A single-analyte gas may be obtained at a concentration of approximately 1000 ppm (balanced with nitrogen). Commercial gas mixtures may be obtained at a concentration of 1 ppm (balanced with nitrogen).
3. Calibration Standard Preparation using Dynamic Dilution (for gas cylinders only): Prepare a working standard containing analytes of interest from which several calibrations standards can be readily obtained. A typical working standard is usually at a concentration of 10 ppb and can be prepared as follows:
   a. Attach a gas cylinder containing analytes of interest to the back of the Entech 4600A Dynamic Diluter. Make certain the isolation valve on the front of the 4600 Dynamic Diluter is closed. Open the gas cylinder.
   b. Open the Entech 4600A Dynamic Dilution program. Then open the method new*100x.m45* and hit 'go' on the computer screen to start equilibrating flows. *Note: The new100x.m45 method results in a 100 fold dilution of the concentration in the attached gas cylinder. Other dilutions may be obtained by modifying the new100x.m45 program as needed.*
   c. After equilibrating for approximately 5 minutes, open the isolation valve on the front of the 4600A Dynamic Diluter. Wait approximately 5 minutes, and then close the isolation valve. *Note: This step "flushes" the isolation valve and the fill port.*
   d. Attach a clean, evacuated 6 liter can to the Dynamic Diluter's fill port. Open the Nupro valve on the can. Check the pressure in absolute pressure per square inch (psia) at the bottom right of the computer screen; it should be at 0.
   e. Open the isolation valve. The pressure listed on the computer screen should slowly increase as the 6 liter can fills with diluted standard. When the pressure reached 24.7 psia, immediately close the Nupro valve on the 6-liter can. Then close the isolation valve and hit 'stop' on the computer screen.
   f. Remove the can from the fill port and close the gas cylinder attached to the back of the 4600A. Close down the new*100.m45* program.
   g. Label the 6 liter can with the contents, concentration, date prepared, and initials of preparer. Let the can sit for approximately 4 hours before analyzing to allow its contents to equilibrate.
   h. Calibration standard cans are typically attached to the ENTECH instrumentation using a sampling line connected to the calibration port. Calibration standards may also be fitted with a male Quick-connect adapter and attached to the ENTECH 7032AQ sampling port.
4. Calibration Standard Preparation using ESP software and Static Dilution: Prepare a working standard containing analytes of interest from which several calibrations standards can be readily obtained. A typical working standard is usually at a concentration of 10 ppb and can be prepared as follows:
   a. Record the barometric pressure and the room temperature. *(Example: 28.92 inches Hg pressure and 23.2^{o}C temperature).*
   b. Open the Entech Standards Preparation (ESP) computer program. The *Standards Preparation Calculation* screen will appear. Select *Static* and then *Cocktail Inventory*. A

drop-down list of VOCs is available for selection. *Note: Additional VOCs not present in the drop-down list may be added to the list using the Edit button*. Select the desired VOC from the list. *(Example: toluene).*

c. Enter a weighing factor. For a typical single VOC analysis, the weighing factor is 1. If a multiple VOC mixture is desired, weighing factors may be increased for select VOCs in that mixture, as needed, to increase the concentrations of those VOCs. *(Example: A calibration standard consisting of 10 ppb toluene, 10 ppb acetone, and 20 ppb styrene is prepared using a weighing factor of 1 for toluene, 1 for acetone, and 2 for styrene)*.

d. After a weighing factor is entered, click on 'add to vial'. Continue selecting VOCs from the drop-down list, choosing the appropriate weighing factors, and 'adding to vial', as needed, until selection of the components in the calibration standard mixture is complete. This mixture is now known as the *cocktail*. Then click on the 'Analysis' button. The *Static Dilution* screen will appear.

e. Enter chemist's initials, barometric pressure, room temperature, and required concentration (ppb) in the spaces provided. *Note: For a calibration standard that contains multiple VOCs at different concentrations, the required concentration value entered must be the lowest concentration in the mixture. In the preceding example, for a calibration standard that contains 10 ppb toluene, 10 ppb acetone, and 20 ppb styrene; enter a value of 10 ppb in the required concentration space*.

f. This calibration procedure defaults to using a 1-liter glass bulb at 50^{o}C for standard preparation. The defaults also assume the use of a 6-liter evacuated can at 30 pounds per square inch gauge (psig). Adjust any of these parameters, as desired, for calibration standard preparation. *Note: The final pressure in the can for most calibration standard preparation is usually 24.7 psia (equals 10 psig).*

g. In the cell identified as 'V 1-2', enter the amount of the cocktail you wish to spike into the glass bulb, typically 0.5-1.0 µl. Then click on the cell 'V 2-3'. The ESP program will calculate the amount, in cc, of the vaporized contents of the glass bulb that will be injected into the evacuated canister. *Note: The amounts in cells 'V 1-2' and 'V 2-3' may be adjusted, one at a time, as needed, to achieve realistic amounts to syringe.* To ensure that saturation of the glass bulb does not occur, press the 'read' button in the middle of the screen. This button will calculate the concentration in the glass bulb and send an alert if saturation is possible. *Note: If saturation is possible, reduce the µl amount spiked into the glass bulb, and then recalculate 'V 2-3"*.

h. If gas reagents are used to make calibration standards, click on the picture of the syringe on the *Static Dilution* screen. Click on 'Choose Cylinder', select the desired gas reagent from the cylinder inventory, hit 'ok', and then click on the compound line to highlight the selected reagent. *Note: Additional gas reagents may be added to the cylinder inventory by going back to the Standards Preparation Calculation screen and opening 'Edit', and then 'Cylinder Inventory'.* The concentration of the gas reagent cylinder, in ppb, will be listed at the right. In the last cell at the bottom of the injection volume column, enter the desired concentration, in ppb, of the diluted gas, and then hit the 'process' key. The amount of reagent needed to spike into the evacuated can in order to obtain the desired final concentration will appear on the screen.

i. Click 'Exit' to return to the *Static Dilution* screen and then click on the print button to print out a copy of the information needed to perform standard preparation. *Note: If only gas reagents are needed to prepare a calibration standard, the print button will not work.*

Information for this type of preparation must therefore be handwritten from the computer screen into the appropriate lab notebook.

j. Follow the ESP instructions to prepare the calibration standard:
1) Using calibrated pipettes, prepare the cocktail mixture in a GC vial and cap. Shake vigorously to mix well.
2) Flush a gas bulb with nitrogen for approximately 30 minutes before sealing off.
3) Using a syringe, spike the required amount of the cocktail mixture into the glass bulb. Heat the bulb in a GC oven at the required temperature for at least 30 minutes. *Note: If very polar substances are present in the cocktail mixture, the glass bulb must be heated for a longer period of time to ensure that all of the spiked cocktail mixture has vaporized in the bulb.*
4) Open the NT4600A computer program and click on 'Flush' and then 'dilute to target pressure'. Enter desired pressure (in psia) in box (generally 24.7 psia). Click on the 'go' button on the computer screen. The 4600 diluter is now under manual control.
5) Press and hold the 'flush' button on the diluter *until it clicks*. The diluter line will flush for approximately 10 seconds. Repeat 2 or 3 times.
6) Attach a clean, evacuated 6-liter can to the diluter. Open the Nupro valve on the can.
7) Using a syringe, inject the required amount of the glass bulb's vaporized contents through the diluter's injection port into the evacuated can. Then inject the appropriate amount of any gas standard reagent, if applicable. Finish by injecting approximately 50 µl of water into the can. *Note: If can contains sulfurous reagents,* ***do not*** *add water*.
8) Press and hold the 'pressurize' button on the diluter *until it clicks*. The can will slowly fill with nitrogen to the desired pressure. When the pressurization is complete, close the Nupro valve on the can and remove from the diluter. Flush the line as before, then hit the 'stop' button on the computer screen and exit the program.
9) Label the 6-liter can with the contents, concentration, date prepared, and initials of preparer. Let the can sit for approximately 4 hours before analyzing to allow its contents to equilibrate.

k. Calibration standard cans are typically attached to the ENTECH instrumentation using a sampling line connected to the calibration port. Calibration standards may also be fitted with a male Quick-connect adapter and attached to the ENTECH 7032AQ sampling port.

5. Check Standard Preparation: Check standards to confirm the validity of the calibration may be prepared by either dynamic or static dilution techniques as outlined in sections D.3 or D.4. Whenever possible, second source reagents should be used.

6. Internal Standard Mixture Preparation: The internal standard mixture is prepared as described in section **D.4** using n-Nonane-$_d$20 as the internal standard and Acetone-$_d$6 as a performance indicator. The internal standard mixture is prepared in concentrations of 20 ppb n-Nonane-$_d$20 and 100 ppb Acetone-$_d$6 at 24.7 psia. However, during analysis, **only 50 mL** of the internal standard mixture is used for each injection, so that the final concentration of n-Nonane-$_d$20 = 10 ppb and the final concentration of Acetone-$_d$6 = 50 ppb for each injection. The internal standard canister is attached to a sampling line connected to the ENTECH 7100A internal standard sampling port.

7. Blank canister: A 6 liter canister is typically filled with nitrogen to 24.7 psia and attached to the ENTECH 7100A blank sampling port.

E. Equipment and Supplies:

1. Automated gas chromatograph equipped with a mass-selective detector (GC/MS) and an RTX-624 capillary column
2. ENTECH 7100A/7032AQ Autosampler and Preconcentrator equipped with cryofocusing and interfaced to the GC/MS
3. ENTECH 4600A Diluter
4. ENTECH 3100A Automated Can Cleaning System
5. Silonite-coated ENTECH MiniCans™ and 6-liter cans, or equivalent
6. Glass bulbs, syringes, GC vials, and other common laboratory glassware and equipment

F. Cleaning Canisters:

1. Cleaning MiniCans:
   - **a.** Turn on rough pump that is connected to cleaning system.
   - **b.** Turn on power to ENTECH NT 3100A high vacuum cleaner (switch is located on the back panel of the unit).
   - **c.** Load MiniCans onto the cleaning board and cover with the heating mantle.
   - **d.** Flip the "start" toggle on the front panel of the NT3100A. The high vacuum pump will begin to rev up. **Wait until the rpm green light on the front panel of the NT3100A is glowing** (high vacuum pump is completely revved up) **before proceeding further. This process may take several minutes.**
   - **e.** After rpm green light is glowing, click on the "shortcut to NT3100A" icon on the computer screen.
   - **f.** Go to "open", then select canclean1.m30.
   - **g.** Hit the "run" button at the top of the screen. Then hit the "go" button on the computer screen. The cleaning process will begin. In general, it takes about 3 hours to clean 50 cycles. If cans are very dirty, additional cleaning cycles may be added before hitting the "go" button on the computer screen.
   - **h.** The cleaning process will end when the programmed cycles are completed. When it ends, "idle" is highlighted.
   - **i.** Remove heating mantle from cans. Remove cans from cleaning board and place in clean can drawer. **Careful: cans are sometimes hot when touched.**
   - **j.** Go to the computer screen and hit "stop", then "exit", then "exit" again. Hit the "stop" toggle switch on the front panel of the NT3100A. The high vacuum pump will **slowly** begin to rev down. This process may take up to 30 minutes.
   - **k.** Shut off the power to the NT3100 only after the high vacuum pump is **completely** revved down. Then turn off the rough pump.
2. Cleaning 6 liter or other canisters:
   - **a.** Follow the cleaning procedure outlined above for Minicans except attach a female-to-male adapter (allows canister to attach to Quick-Connect valves) before loading onto the cleaning board. **It is recommended that only 1 canister be cleaned at a time.**
   - **b.** *Note: If very dirty cans were cleaned, a representative of the cleaned batch should be checked to ensure all contamination was removed before assuming that the cleaning process was valid. To check can cleanliness, pressurize a cleaned can to 14.7 psia as outlined in section G, and analyze as if it were an actual sample. Cans are properly cleaned if all detected peaks are less than the Reporting Limit (RL).*

G. Sample Preparation:

1. For MiniCans™: Pressurize to 15 psia using the ENTECH 4600A diluter. **Record the dilution factor**. Insert the MiniCans™ into the appropriate sampling port on the ENTECH 7032AQ. Allow sample to equilibrate at room temperature for approximately 4 hours before analysis.
2. For Tedlar™ or foil bag: Attach the appropriate Quick-Connect adapter to the bag's sampling port. Insert the bag into the appropriate sampling port on the ENTECH 7032AQ. Open the bag.
3. For bulk solid or liquid: Allow the LVHS to come to room temperature in a clean room. For bulk liquids, fill a scintillation vial approximately ½ full. Do not cap the scintillation vial. While in the clean room, place either bulk solid or scintillation vial of bulk liquid into LVHS. Screw the LVSH lid on to seal. Insert the LVSH into the appropriate sampling port on the ENTECH 7032AQ. Allow sample to equilibrate at room temperature for approximately 4 hours before analysis.

H. Tuning the GCMS: Tune the MS as follows:

1. Open the GCMSD3 session
2. Go to the instrument control screen in the GCMSD3 session. Click on 'View', then highlight 'Tune and Vacuum Control'.
3. Under 'Tune', highlight 'Autotune'. The MS will then perform an autotune (takes about 5 minutes).
4. After tune is completed, go back to 'Tune' and highlight "Tune Evaluation". The tune values and a corresponding air and water leak check will be automatically compared to parameters pre-set by the manufacturer. When evaluation is complete, a report will be produced that documents current parameters and notes whether they passed or failed manufacturer criteria. Address any failures by performing maintenance, replacing parts, or re-running tunes, as needed, to achieve passing tune values. If tune cannot pass criteria, consult with supervisor before analyzing samples.
5. Save tune values to method, and save copies of tune and evaluation to lab notebook and also with sample paperwork packet.

I. Leak-checking the ENTECH: Check for leaks in the ENTECH 7100A as follows:

1. Attach cans containing calibration standard, internal standard, and blank to their designated ports on the 7100A, but keep the Nupro valves on the cans closed at this point.
2. Open the 'Shortcut to SL7100.exe' session.
3. Click on the 'manual' button at the top of the screen. A screen will appear that shows fields labeled as 'stream select', 'auto1', 'auto2', 'auto3', and buttons labeled 'update', 'exit', 'vacuum', 'press.', and 'isolate', as well as a timer.
4. Start by setting the stream select to 1 (blind stream-leak check) and hitting the 'update' button.
5. Hit the 'vacuum' button and wait approximately 30 seconds. The displayed pressure should decrease to 0.4-0.6 psia.
6. Press the 'isolate' button and wait approximately another 30 seconds. The pressure should remain between 0.4-06 psia for this length of time. If pressure keeps increasing, a leak is present in the system and remedial action must be taken (tightening lines, valves etc.) After remedial action is taken, repeat steps 4-6 until pressure holds.

7. Next set the stream select to 3 (internal standard). Hit the 'update' button and then follow steps 5-6 above.
8. Repeat steps 4-6, setting the stream select to 4 (for calibration standard) and then 7 (for blank).
9. Next set the stream select to 5 and the autosample 1 position (auto1) to 1. Insert a plug in sample injection port 1-1 and hit the 'update' button. Follow steps 5-6 above.
10. If pressure is ok (no leak detected), keep stream select on 5 but advance auto1 to 2. Insert plug in sample injection port 1-2 and hit the 'update' button. Continue on as in steps 5-6.
11. Continue, keeping the stream select at 5 but changing the auto1 from 3 through 12, inserting the plug in turn in sample injection ports 1-3 through 1-12, leak checking as outlined in steps 5-6.
12. Repeat steps 9-11, except set the stream select to 6 and alternate auto1 position sequentially from 1 through 9, inserting the plug in sample ports 2-1 through 2-9 and checking for leaks as outlined in steps 10-11.
13. When leak checking is complete, exit the system by hitting the 'exit' button.

J. Calibration and Sample Analysis:

1. GC Analytical Conditions: A method must be devised that maximizes resolution of desired analytes while minimizing interferences. The chemist must be able to adjust parameters, as needed, to optimize chromatography. Some typical GC parameters are as follows:
   - **a.** Initial temperature: 35^{o}C
   - **b.** Initial time: 5.0 minutes
   - **c.** Temperature program rate:
     1) 4^{o}C per minute to 150^{o}C, then
     2) 6^{o}C per minute to 240^{o}C, then hold for 2.0 minutes
   - **d.** Front Inlet Initial temperature: 240^{o}C
   - **e.** Mode: Constant Flow
   - **f.** Thermal Aux 2 Use: MSD transfer line heater
   - **g.** Initial temperature MSD transfer line heater: 200^{o}C
   - **h.** Acquisition mode: Scan
   - **i.** MS Quad: 150^{o}C and MS Source: 230^{o}C
   - **j.** *Note: See C:\HPCHEM\1\METHODS\split.m for full details of a typical GC analytical method.*
2. ENTECH 7100A Analytical Conditions: A method must be devised that results in the maximum resolution of desired analytes while minimizing interferences. The chemist must be able to adjust parameters, as needed, to optimize chromatography. Some typical ENTECH method parameters are as follows:
   - **a.** Module 1: trap 150^{o}C, preheat 10^{o}C, desorb 10^{o}C, and bake 150^{o}C for 10 minutes
   - **b.** Module 2: desorb 180^{o}C, time 3.5 minutes, and bake 190^{o}C
   - **c.** Module 3: focus 160^{o}C, inject for 2 minutes, bake for 3 minutes, wait time 50 minutes
   - **d.** Preflush: Internal and analytical standards = 5 sec; sample = 10 sec; sweep/purge = 2 sec
   - **e.** M1 to M2: trap 40 ml at 10 ml/minute
   - **f.** Sweep/purge: trap 75 ml at 100 ml/minute
   - **g.** *Note: See C:\Smart \splitAIR624HT.mpt for full details of a typical ENTECH analytical method.*
3. Instrument Calibration:

a. At least 3 levels of calibration standards are run as needed. **One of these levels must be at or below the reporting limit.**

b. Typically, a single 10 ppb calibration standard is run as follows: 20 ml, 50 ml, 100 mL, 200 ml, 400 ml, and 800 ml of the same 10 ppb calibration standard are individually analyzed, corresponding to 2 ppb, 5 ppb, 10 ppb, 20 ppb, 40 ppb, and 80 ppb, respectively.

c. After standards are run, calibration curves for each analyte are constructed using Chemstation software as follows:

1) Open an off-line copy of Chemstation Data Analysis.
2) Go to 'calibrate' and then 'edit compounds'. A database of the 39 VOCs in the calibration mix has already been constructed. To edit any of the listed VOCs, simply click on the desired VOC and click on 'view'. Three pages are then accessible for modification.
   a) Page 1 contains specific information about an analyte. Fill in the fields for
      (1) name of analyte
      (2) units: select 'ppb'
      (3) RT
      (4) RT extraction range (generally defaults to +/-0.5 min)
      (5) Quantitation signal: select 'target ion'
      (6) % uncertainty: select 'relative'
      (7) m/z data for target ions, their relative responses, and % uncertainty.
         (a) This data can be found in the NIST database for each VOC. Simply locate the VOC in the NIST database, find the 4 most abundant ions for that VOC and their corresponding m/z responses (in percent), and enter them in the spaces provided on page 1. *Note: for relative uncertainty, default to 35%.*
         (b) Example: for benzene, the most abundant m/z ions are: target = 78, Q1= 77, Q2= 51, and Q3= 50. The corresponding m/z relative responses for each ion are: 100, 22.7, 12.3, and 10.7, respectively. The uncertainty is set to 35% for all ions.

NAME	Primary	Secondary		Tertiary		Quaternary	
		Target	%	Target	%	Target	%
Acetone-d6	46	64	38.4				
Benzene*	78	77	22.7	51	12.3	50	10.7
Bromomethane*	94	96	95.6	79	9	93	19.6
1-Butanethiol	56.1	90	84.8	41.1	74.2	47	31.8
2-Butanethiol	57	41	81.8	61	88.7	90	114.5
Carbon Disulfide	76	44	16.3	78	7.5		
Carbon Tetrachloride*	117	119	97.7	121	31.7	82	17.7
Chlorobenzene*	112	77	44	114	32.9	51	11.6
Chloroethene*	62	64	32.5				
Chloroform*	83	85	65.6	47	16.8	35	5.1
Chloromethane*	50	52	33	49	9.6		
1,2-Dibromoethane*	107	109	95.6	81	4	79	3.9
1,2-Dichlorobenzene*	146	148	64.4	111	32.7	75	17.6
1,3-Dichlorobenzene*	146	148	64.1	111	31.2	75	17.2

1,4-Dichlorobenzene*	146	148	64.2	111	30	75	17.8
Dichlorodifluoromethane*	85	87	32.7	101	9.7		
1,1-Dichloroethane*	63	65	32.4	62	6.2	83	14.5
1,2-Dichloroethane*	62	64	33	49	25.8	63	17.3
1,1-Dichloroethene*	61	96	84.5	98	55.2	63	32.9
(Z)-1,2-Dichloroethylene*	61	96	105.4	35	5.3	63	32.9
Dichloromethane*	49	84	109.9	86	70.8	51	31.2
1,2-Dichloropropane*	63	62	70.8	27	5.0	41	43.1
(E)-1,3-Dichloropropene*	75	39	33.5	77	32.2	110	29.9
(Z)-1,3-Dichloropropene*	75	77	32.5	39	33.1	110	33.2
Dichlorotetrafluoroethane*	85	135	92.4	87	32.5	137	30
Dimethyl Disulfide	94	79	59.4	45	62.6	96	8.6
Dimethyl Sulfide	62	47	95.4	61	33.3	45	40.8
Ethanethiol	62	47	68.6	45	15.4	61	14.8
Ethylbenzene*	91	106	36.7	51	6.5		
Ethyl Chloride*	64	66	32.7	49	20.1		
Hexachloro-1,3-butadiene*	225	223	62.6	227	64	190	37.9
Methanethiol	47	48	75.8	45	61.4	46	14.7
2-Methyl-2-propanethiol	41	57	122.6	90	97.8	39	30.1
n-Nonane-d20	66.1	50.1	97.8	98.15	46.8	46.1	41.5
1-Propanethiol	76	43	50	47	55.1	42	47.3
2-Propanethiol	43	41	96.2	76	98.5		
Styrene*	104	103	46.2	78	34.2	51	16.1
1,1,2,2-Tetrachloroethane*	83	85	65.1	95	15.2	60	8
NAME	**Primary**	**Secondary**		**Tertiary**		**Quaternary**	
		Target	**%**	**Target**	**%**	**Target**	**%**
Tetrachloroethylene*	166	164	77.8	131	56.5	129	58.3
Toluene*	91	92	61.7	65	9.2	39	5.8
1,1,1-Trichloroethane*	97	99	64.8	61	32	117	15.8
1,2,4-Trichlorobenzene*	180	182	95.7	145	23.6	184	30.6
1,1,2-Trichloroethane*	97	83	76.7	61	42.9	99	63.6
Trichloroethylene*	95	130	134.5	132	130	97	65.5
Trichloromonofluoromethane*	101	103	65.8	66	9.2	105	10.9
1,2,4-Trimethylbenzene*	105	120	54.3	77	9.5	119	13.6
1,3,5-Trimethylbenzene*	105	120	58.3	119	13.7	77	10
1,1,2-Trichloro-1,2,2-trifluoroethane*	101	151	111.7	103	65	85	37.3
o-Xylene*	91	106	55.7	105	17.7	39	3.7
p-& m-Xylene*	91	106	58.4	105	25	77	11.5

(8) Quantitation type: select ‘target’
(9) Measure response: by ‘area’.
(10) ID: by ‘best RT match’.
(11) Maximum # of hits: generally 1
(12) Subtraction method: select ‘extend area quantitation’.
(13) Curve fit: select ‘linear force through 0’.
(14) Weight: select ‘equal’.

b) Page 2 has fields for additional VOC information and for special parameters. Fill in the following:

(1) CAS #.
(2) Compound type: use 'T' for target
(3) Ignore all other fields on this page.

c) Page 3 contains the levels for concentration and response. Select level ID for each concentration of standard. When calibrating, the response will fill in automatically.
d) To remove any VOCs from the database, click on the analyte in the list and hit 'delete'. To add to the database, click on the VOC whose RT elutes just after the desired VOC and click on 'insert above'. Then fill in the necessary data on pages 1-3 as described above.
e) When the database is completed, click on 'exit' and save the method.

3) Load the data file from the first standard injected. Go to 'calibrate', then 'update', then 'update one level'.
4) A screen will appear with fields needed to complete the calibration. Select 'recalibrate', the select the appropriate calibration level ID from the drop box, and then select 'replace' for both responses and RTs. Then click on 'do update'. The software will automatically enter the responses, based on the rations of the selected target ions and their relative responses, for the concentration of each analyte as listed on page 3.
5) Repeat steps 3-4 as listed above for each level of the standard. When complete, go to page 3 for each analyte, confirm that the concentration and response is properly entered, and click on 'plot' to examine the plot for each analyte. **A valid plot must have a coefficient of determination of 0.9 or greater**. If plots are not valid, additional standards must be prepared and analyzed, or RL values must be raised, in order to pass the valid plot criteria.
6) When calibration is complete, exit the calibration module and save the method.

d. See D:\lab\org\msd3\meth\39VOC-8-22-07.m for full details of a typical calibrated method.

4. Sample Analysis:

a. Re-boot the Chemstation and all instrument sessions. (The GCMS configuration with the ENTECH operating system is prone to crashes.)
b. Bring up the MS session and tune the MS as outlines in section H.
c. Check for leaks in the ENTECH 7100A as outlined in section I.
d. Create, save, and print out an ENTECH 7100A sequence.
e. Create, save, and print out an Agilent GCMS sequence. *Note: In general, sequences are written in the flowing order:*

1) *warm-up run*
2) *blank*
3) *Calibration standards (from least to most concentrated)*
4) *Blank*
5) *ICV (independent calibration verification) standard*
6) *QC spike*
7) *blank*
8) *sample1 study1*
9) *sample2 study1; etc*
10) *blank*

11) *sample1 study2*
12) *sample2 study 2; etc*
13) *blank*
14) *repeat of calibration standard at RL level*
15) *repeat of calibration standard at mid level*
16) *blank*

f. *Note: Repeat steps 7-10 as needed, depending on the number of samples in a study and the number of studies in a sequence. Be sure to inject at least 1 repeat of a calibration standard after every 10 samples in the sequence.*

g. *Note: At least 10% of all samples (excluding MiniCans) must be injected twice (2x).Typically, 2 injections cannot be performed on MiniCans because the resultant loss in can pressure after the first injection results in poor reproducibility.*

h. Open any valves, if necessary, on any of the sample or standard canisters.

i. Set the printer to 'pink'.

j. Check that the amount of liquid nitrogen is sufficient to complete the sequence.

k. Start the GCMS sequence first. When the 'system ready' box appears on the computer screen, start the ENTECH 7100A sequence by clicking on 'go'.

l. *Note: Once the 7100A sequence begins, it **cannot** be modified in any way. Doing so will **crash** the system and stop the analysis.*

K. QC Procedures:

1. Check Standards: An ICV (independent calibration verification) standard shall be injected at least once in a sequence. In addition, repeated injections from the calibration standard are used as 'check' standards. All check standards are valid if they agree within 50-150% of the actual values ($^{+}$50%).
2. Sample Duplicates or Replicates: Repeat injection and analysis are performed for at least 10% of the samples (excluding MiniCans) in an analytical batch. The repeat analysis must agree to within 50%-150% ($^{+}$50%) of the original calculation. Any failures must be investigated. If the failures cannot be adequately explained, the "worst-case" or higher value must be reported to the client with a comment.
3. Media Blank: Media blanks are generally meaningless with this method. Clean, evacuated cans may be pressurized with nitrogen (like the samples) and analyzed for any can contamination before sampling.
4. Blind QC sample pairs are prepared for each analytical batch and the acceptance criteria is set by the QC department.

L. Confirmatory Technique: Since a MSD is used for sample analysis, no additional confirmatory techniques are needed.

M. Calculation of Results:

1. All results are reported as parts per billion (ppb).
2. For VOCs with valid calibration curves, use Chemstation curve data to calculate all sample results. Remember to multiply all results by the dilution factor, if necessary. Results that exceed the upper limit of the calibration may be diluted and re-analyzed or may be reported out with a comment stating: Result is approximated because the amount of the analyte present in the sample exceeded the calibration range.

3. For uncalibrated VOCs, an estimated result is reported based on the area of the VOC compared to the average area of the n-Nonane-$_d$20 internal standard, as derived from Blank injections. Remember to multiply all results by the dilution factor, if necessary. All estimated results must be qualified with a comment stating the limitations of the accuracy and identity of the result.

N. Method Development/Validation:

1. Reporting Limits (RL): RLs are verified with each batch of samples through the use of the calibration standard. Typical LRLs are 10 ppb for most VOCs in the calibration mix.
2. Interferences: Analytes which have similar retention times can cause interferences. In addition, the internal standard VOC n-Nonane-$_d$20 needs to be free and clear for accurate calibrated and estimated calculations. Any potential interference will result in approximated values.
3. Validation and Stability Data: OSHA PV2120 has stability data for a limited number of VOCs. The canister method currently remains a partially-validated method.

O. Reference: OSHA PV2120 May 2003.

P. Signatures:

1. **Method developed by:** Shari Schwabe **Date:** 12/18/07
2. **Method approved by:** Terry Burk, CIH **Date:** 5/14/08
3. **Method modified by:** Shari Schwabe **Date:** 9/14/2009
4. **Modified method approved by:** Steve Strebel **Date:** 9/24/09

Information regarding ppbV definition and calculations

When dealing with air concentrations, one cannot use the convenient assumption used in dilute aqueous systems that at room temperature and 1 atmosphere of pressure, 1 liter (L) of water weighs 1 kilogram (kg). As a result, the units of ppm and ppb in gas systems are computed on a volume-per-volume ratio, such as ppbV.

The following example is taken from the U.S. EPA EPA On-line Tools for Site Assessment Calculation [S1].

For example:

$$1\ ppmV = \frac{1\ volume\ of\ gaseous\ contaminant}{1{,}000{,}000\ \ volumes\ of\ air + contaminant}$$

So, how do we convert between the mass-per-volume units and ppmV or ppbV in a gas system?

- First, we must use the ideal gas law to convert the measured contaminant mass to a volume. The ideal gas law (PV=nRT) relates pressure, volume, temperature and mass of a gaseous contaminant:

1. $$P_{air} \times V_{contaminant} = \#\ moles_{contaminant} \times R \times T_{air}$$

   where P_{air} is air pressure
   $V_{contaminant}$ is the volume occupied by the contaminant
   R is the universal gas constant, and
   T_{air} is air temperature.

   Any units for pressure, volume and temperature may be used, as long as the universal gas constant is in consistent units. Noting that # $moles_{contaminant}$ = $mass_{contaminant}$ / molecular $weight_{contaminant}$, and using pressure, temperature and volume in units of [kPa], [K] and [L], we can solve the preceding relationship for the volume of our contaminant, given its mass in grams:

2. $$V_{contaminant}[L] = \frac{Mass_{contaminant}[g]}{Molecular\ Weight_{contaminant}[g/mole]} \times 8.3144\left[\frac{L \cdot kPa}{mol \cdot K}\right] \times T_{air}[K] \times \frac{1}{P_{air}[kPa]}$$

   Note that T[K] = T[°C] + 273.15.

- Now that we have the mass of the contaminant converted to a volume, we simply need to divide by the volume of the sample measurement, and work out the units. For example, ppmV is equivalent to 1 mL/m^3 and ppbV is equivalent to 1 $\mu L/m^3$. Or in equation form:

3.

$$ppmV = \frac{V_{contaminant}[mL]}{V_{sample}[m^3]} \quad \text{and} \quad ppbV = \frac{V_{contaminant}[\mu L]}{V_{sample}[m^3]}$$

- So, to convert from µg/m³ to ppmV, we plug in our mass values in equation 2 above, making sure to convert our µg to units of grams required by the equation. This will give us the volume of our contaminant in liters. We must now convert this into mL for equation 3. Then we simply divide by the sample volume in m³ to obtain our result in ppmV. Likewise, to convert µg/m³ to ppbV, we would follow the same procedure, except we'd convert the volume of the contaminant to µL instead of mL.

Reference

Weaver, J., Socik, C., Washington, J., Owensby, C. 2012. U.S. EPA EPA On-line Tools for Site Assessment Calculation. Accessed May 12, 2012. http://www.epa.gov/athens/learn2model/part-two/onsite/ia_unit_conversion_detail.html

Appendix B

Supplementary Material for Chapter 4

Notes:

This chapter was published as Gao, J.; Hedman, C.; Liu, C.; Guo, T.; Pedersen, J.A. Transformation of sulfamethazine by manganese oxide in aqueous solution. *Environ. Sci. Technol.* **2012**, *46*, 2642-2651.

A version of pages 121-146 and 189-213 of this dissertation appeared in Dr. Juan Gao's dissertation entitled "Sorption and Transformation of Sulfonamide Antimicrobial Agents", 2007.

Contributions: Curtis Hedman contributed the setup and analysis of birnessite (δ-MnO_2)/sulfamethazine (SMZ) reaction solutions by HPLC-UV-MS/MS, interpretation of UV and MS/MS data for proposed reaction product identification, and the execution and analysis for $H_2{}^{18}O$ and $^{18}O_2$ mass labeling (δ-MnO_2)/sulfamethazine (SMZ) reaction experiments. Juan Gao contributed the physicochemical characterization of δ-MnO_2, the determination of SMZ degradation rate constants with and without oxygen and under different pH conditions, interpretation of UV and MS/MS data for proposed reaction product identification, and proposal of SMZ transformation reaction schemes. Tan Guo contributed mass spectral peak interpretation, reaction product structure elucidation, and reviewed proposed SMZ transformation reaction schemes. Cun Liu contributed an evaluation of the feasibility of the proposed transformation products and δ-MnO_2/SMZ reaction schemes by gas phase density functional theory (DFT) calculations. Joel Pedersen oversaw all aspects of the work from conception and design to manuscript preparation.

Supporting Information for

Sulfamethazine Transformation by Manganese Oxide in Aqueous Solution

Juan Gao[1,2], Curtis Hedman[3,4], Cun Liu[5], Tan Guo[6], and Joel A. Pedersen[,2,3]*

[1]State Key Laboratory of Pollution Control and Resource Reuse, School of the Environment, Nanjing University, Nanjing, PR China, 210093,

[2]Department of Soil Science, University of Wisconsin, Madison, WI, 53706

[3]Wisconsin State Lab of Hygiene, Madison, WI, 53718

[4] Environmental Chemistry and Technology Program, University of Wisconsin, Madison, WI, 53706

[5]Department of Crop and Soil Sciences, Michigan State University, East Lansing, Michigan 48824

[6]Sequoia Foundation/Department of Toxic Substances Control, Berkeley, CA 94710

Text S1. Supporting Information for the Materials and Methods

Chemicals. Sulfamethazine (SMZ), manganese chloride, sodium permanganate, potassium permanganate, sodium acetate, formic acid, and ammonium formate were purchased from Acrōs Organics (Fairland, NJ). A 0.36 mM SMZ stock solution was prepared in 10 mM sodium acetate buffer. [Phenyl-$^{13}C_6$]-SMZ was obtained from Cambridge Isotope Laboratories, Inc. (Andover, MA). *N*-(4,6-dimethylpyrimidin-2-yl) benzene-1,4-diamine was obtained Oakwood Products, Inc. (West Columbia, SC). Hydrochloric acid (12 M), NaCl, and methanol (HPLC grade) were obtained from Fisher Chemicals (Fair Lawn, NJ); glacial acetic acid was acquired from Sigma Chemical Co. (St. Louis, MO); sodium hydroxide was procured from Mallinckrodt Specialty Chemicals Co. (Paris, KY); and oxalic acid was bought from Mallinckrodt Chemical Works (St. Louis, MO). Argon (Ultra high purity, 99.999%) and oxygen (Ultra high purity, 99.995%) were purchased from Linde Gas, LLC. (Independence, OH). Unless otherwise specified, the purities of all chemicals were > 99%.

MnO_2 Synthesis. Manganese oxide was synthesized by the method of Murray.[1] Briefly, 3.2 mmol NaOH was added to 400 mL of 4 mM $NaMnO_4$ under constant stirring, followed by dropwise addition of 24 mL of 0.1 M $MnCl_2$ at room temperature (Mn^{VII}:Mn^{II} = 0.67). After the MnO_2 precipitate formed, the suspension was centrifuged at 6500*g* for 15 min. The precipitate was washed six times with distilled deionized water (ddH_2O; 18 MΩ-cm resistivity; NANOpure Ultrapure Water System, Barnstead, Dubuque, Iowa) to achieve an electrical conductivity < 0.06 $\mu S \cdot cm^{-1}$ at 22.7 °C. The δ-MnO_2 was stored in aqueous suspension at 4 ºC.

MnO_2 Characterization. Scanning electron microscopy (SEM) images were taken using a LEO Supra 1555 VP field emission scanning microscope (Carl Zeiss SMT Ltd, German). Surface area was determined by N_2 adsorption using the Brunauer-Emmett-Teller (BET) method at room temperature on a Micrometrics ASAP 2010 multi-gas volumetric adsorption analyzer. The ζ-potential and aggregate hydrodynamic diameter of the MnO_2 particles were determined by electrophoretic and dynamic light

scattering using a Zetasizer Nano ZS (Malvern Instruments, Southborough, MA). The pH_{zpc} of δ-MnO_2 is < 2.4.[1] X-ray diffractometry was conducted on a Scintag PAD V diffractometer (Cupertino, CA) using CuKα radiation and continuous scanning from 2° to 70° 2θ at 0.05°·sec^{-1}. The x-ray diffraction pattern of the poorly crystalline manganese oxide synthesized resembled that of δ-MnO_2. The oxidation status of δ-MnO_2 was determined by back titration. Briefly, a predetermined amount of δ-MnO_2 was dissolved in excess 0.2 M sodium oxalate. The remaining oxalate was oxidized by dropwise addition of 0.1 M pre-titrated fresh potassium permanganate. The oxidation state of δ-MnO_2 was calculated from the amount of oxalate oxidized prior to permanganate addition.

The δ-MnO_2 produced using the method employed[1] was reported to have hexagonally symmetrical unit cells with random stacked layers.[2] Scanning electron microscopy indicated that the δ-MnO_2 formed aggregates composed of primary particles with diameters of 30 to 70 nm (Figure S2). Back titration of δ-MnO_2 with sodium oxalate and potassium permanganate[3] indicated the average oxidation state of the Mn was +3.94. If the δ-MnO_2 is assumed to contain no Mn^{II}, 94% of the manganese was present as Mn^{IV}, a result consonant with the findings of Villalobos et al.[2] Figure S2 provides further characteristics of the synthesized δ-MnO_2.

Quenching Methods. When oxalic acid was used to halt the δ-MnO_2-mediated reaction, the quench time was defined as the time needed to dissolve 90% of MnO_2,[4] 7 s in these experiments. Quenching by filtration took 2 s to remove remaining MnO_2. The end of a time interval was defined as the sampling time plus the quench time. Preliminary experiments indicated no detectable reaction of SMZ with oxalic acid and lack of significant SMZ sorption to syringe filters ($p > 0.05$).

Adsorption of SMZ to δ-MnO_2. The degree of SMZ adsorption to δ-MnO_2 was determined by comparing the difference in SMZ concentrations between samples quenched by filtration and by oxalic acid dissolution. The amount SMZ in sample filtrates corresponded to the (operationally defined) free

antimicrobial, while that in samples quenched by oxalic acid addition was the total amount of SMZ (sorbed + free). Results from these experiments are presented in Figure S3.

Influence of Temperature. To examine the influence of temperature on SMZ transformation, reactors were housed in an incubator, and all solutions used were pre-equilibrated to the desired temperature.

HPLC-UV Analyses. In kinetics experiments, sample aliquots were analyzed on a Gilson HPLC (pump model 302, manometric module model 802B, sample injector 231) equipped with EC 4.0 mm × 250 mm Nucleosil C18/5 μm column (Macherey-NAGEL Inc., Germany) and Spectra SYSTEM UV2000 detector (Thermo Separation Products, San Jose, CA) set at λ = 254 and 265 nm. An isocratic mobile phase composed of 31% methanol and 69% aqueous formic acid (0.07%) and ammonium formate (10 mM) was used at a 0.8 mL·min^{-1} flow rate.

For product identification, HPLC-UV with full UV scan (λ = 190-400 nm) was used to monitor the disappearance of SMZ and the evolution of chromophore-bearing transformation products. Quenched samples (10 μL) were injected directly on to a Phenomenex Luna 3u C18 (2) column (150 × 3.0 mm) in a Hewlett Packard Series 1050 HPLC equipped with an Agilent 1100 diode array detector. UV spectra for λ = 190-400 nm were collected every 2 s for each 38-min chromatographic run. A binary mobile phase at a flow rate 0.3 mL·min^{-1} was used: mobile phase A was 90:10 water/acetonitrile (v/v) with 10 mM ammonium formate and 0.07% formic acid, and mobile phase B consisted of acetonitrile. The mobile phase gradient was as follows: 0-5 min, 100% A; 5-15 min, 90% A; 15-25 min, 70% A; 25-30 min, 55% A; 30-34 min, 100% A; 34-38 min, 100% A. After each sample, a method blank was run to minimize carryover between runs.

HPLC-tandem mass spectrometry. HPLC-MS/MS was used to elucidate the structures of SMZ transformation products. The Agilent 1100 HPLC (consisting of an autosampler, column oven, diode array detector, and a binary gradient pump) was interfaced to an Applied Biosystems/MDS SCIEX API

4000 triple quadrupole mass spectrometer. Mobile and stationary phases were identical to those used for HPLC-UV analysis of transformation products; the elution rate was 0.36 $mL \cdot min^{-1}$. Positive ionization mode TurboIonSpray (TIS) mass spectra (25-1000 *m*/*z*, mass resolution = 0.7 *u* FWHM) were collected with a 1-s scan time. MS acquisition parameters included the following: curtain gas pressure = 20 psi, nebulizer gas pressure = 35 psi, drying gas pressure = 30 psi, declustering potential = 51 V, entrance potential = 10 V, collision cell exit potential = 10 V, source temperature = 400 ºC, and capillary voltage = 5500 V. Product Ion Scan MS/MS experiments were conducted under the same HPLC conditions listed above at collision energies of 25 and 50 eV.

HPLC-time-of-flight-mass spectrometry. HPLC-TOF-MS was used to obtain accurate masses and the most probable elemental composition of selected products. A 5 μL aliquot of the filter-quenched reaction mixture was injected directly onto an Agilent Zorbax 1.8 μM SB-C18 (2.1 × 50 mm) column in an Agilent 1100 series HPLC with capillary-LC pumps. The binary mobile phase (flow rate = 0.20 $mL \cdot min^{-1}$) consisted of 0.1% formic acid in ddH_2O for mobile phase A and 0.1% formic acid in acetonitrile for mobile phase B. The mobile phase gradient was as follows: 0-30 min, B increasing linearly from 1.0% to 100%; 30-32 min, B decreasing linearly from 100% to 1.0%; and 32-35 min, 1.0% B. Samples were ionized in positive electrospray mode at 4.0 kV. The reference masses 922.009798 (HP-0921, $[C_{18}H_{18}O_6N_3P_3F_{24}+H]^+$) and 121.050873 (purine, $[C_5H_4N_4+H]^+$) (Agilent API-TOF reference mass solution kit) were used as locked mass standards, and mass accuracy was 3 ppm.

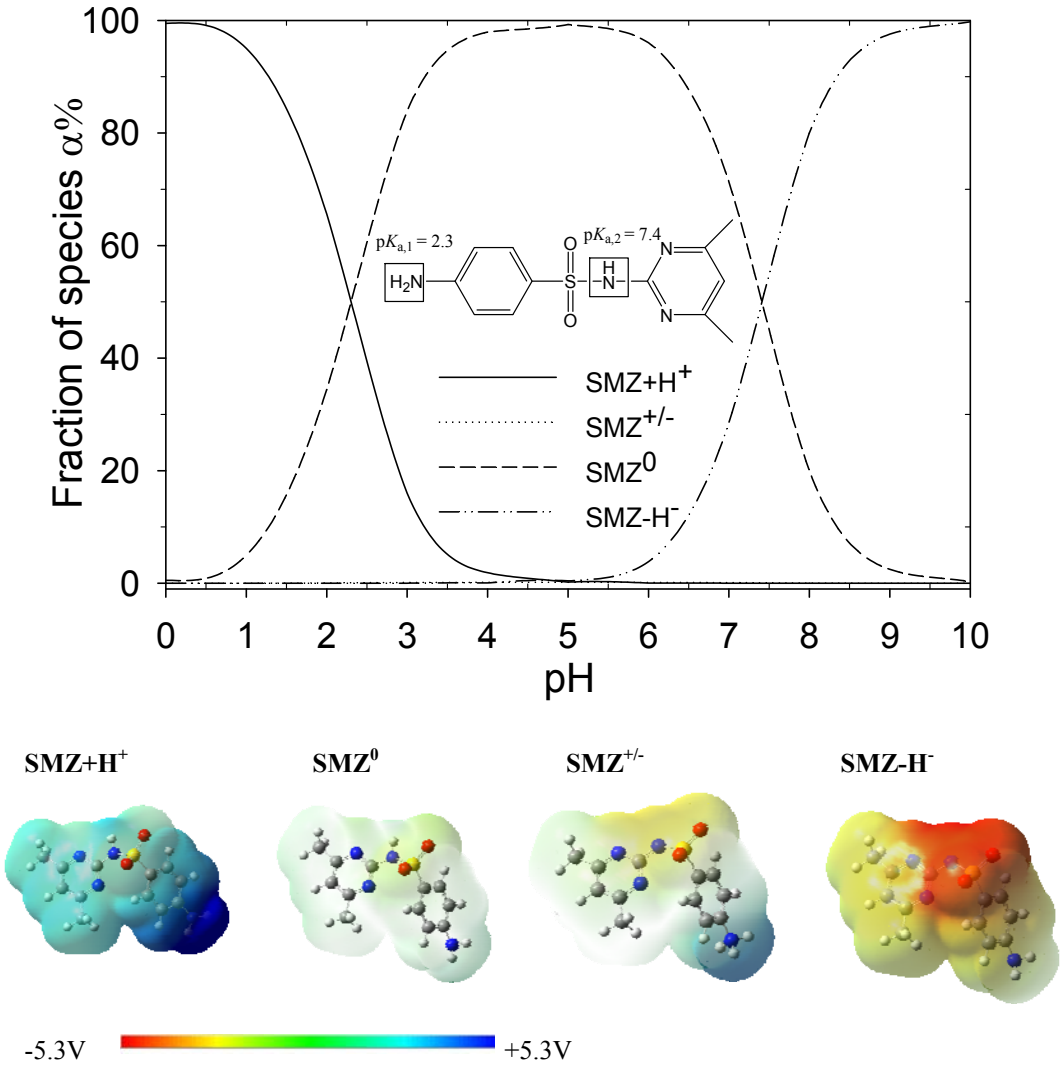

Figure S1. Speciation as a function of pH, skeletal formulae and molecular electrostatic potentials (MEPs) of cationic ($SMZ+H^+$), neutral (SMZ^0), zwitterionic ($SMZ^{\pm}$) and anionic ($SMZ-H^-$) sulfamethazine species. Macroscopic dissociation constants (pK_a) for SMZ was taken from Lin et al.[5] Molecular electrostatic potentials were calculated along the $\rho = 0.0004$ $e/Å^3$ electron density isosurface corresponding approximately to the molecular van der Waals radius. Atoms in the ball-and-stick structures are color-coded as follows: white, H; grey, C; blue, N; red, O; and yellow, S.

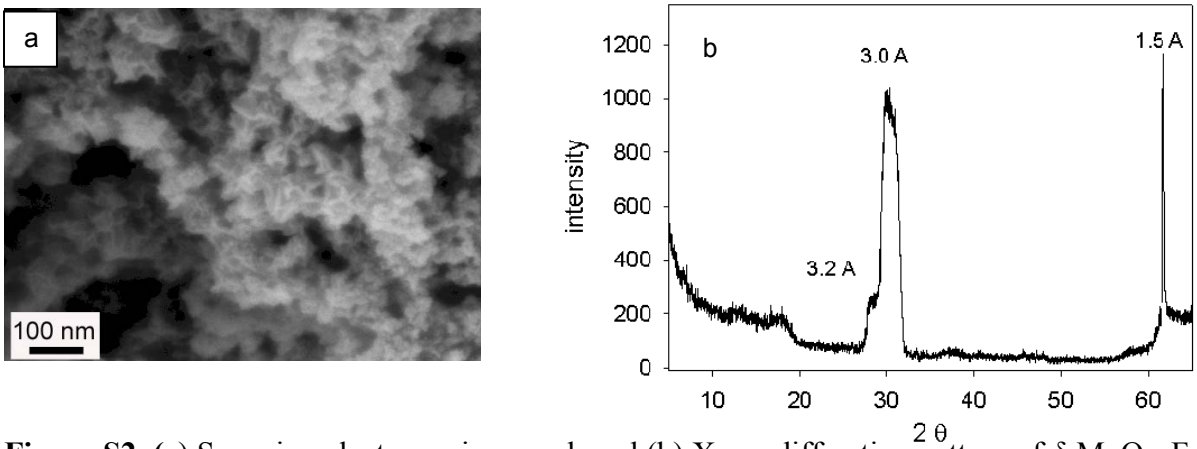

Figure S2. (a) Scanning electron micrograph and (b) X-ray diffraction pattern of δ-MnO_2. For (b), a few drops of aqueous MnO_2 suspension were pipetted onto glass slides and dried at room temperature prior to analysis. The x-ray diffractogram lacked a peak at 7.2 Å, indicating that the *c*-axis of the synthesized δ-MnO_2 was disordered.

20

Table S1. Properties of the synthesized *δ*-MnO_2.

parameter	value
hydrodynamic diameter at pH 5.0 (nm)[a]	390 ± 10
A_{surf} ($m^2 \cdot g^{-1}$) [b]	333.28
ζ-potential at pH 5.0 (mV)	-34 ± 5
Mn oxidation state	+3.94
x-ray diffraction peaks (Å)	3.2, 3.0, 1.5

[a] Z-average hydrodynamic diameter determined by dynamic light scattering.

[b] BET surface area determined by N_2 adsorption at room temperature.

21

22

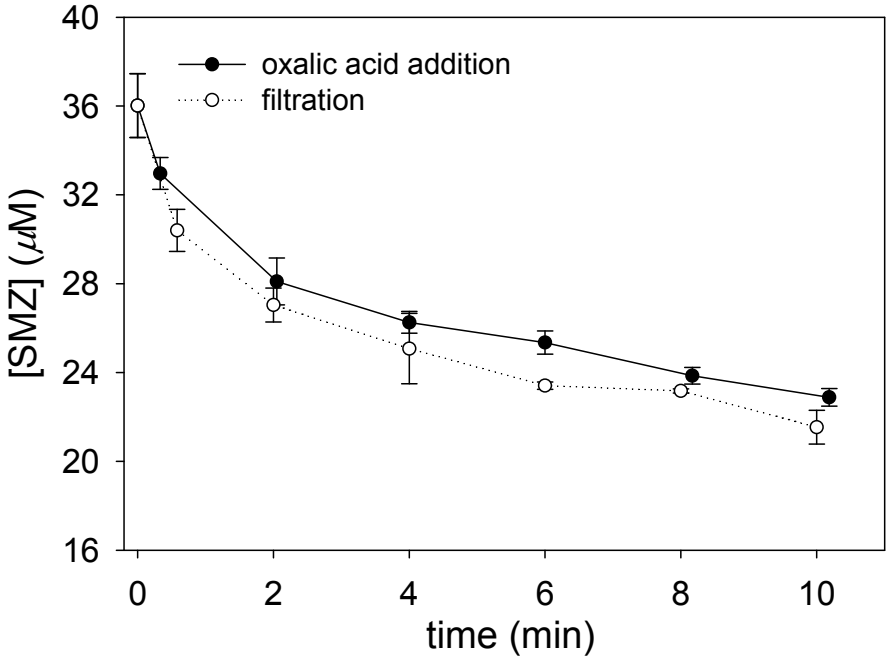

Figure S3. Adsorption of SMZ to δ-MnO_2 at pH 5.0. The amount of SMZ in samples quenched by oxalic acid addition corresponds to the total amount (sorbed + dissolved) of SMZ; the amount of SMZ passing the 0.2-μm filter represents the operationally defined dissolved fraction. Initial concentrations: $[SMZ]_0$ = 36 μM, $[\delta\text{-}MnO_2]_0$ = 360 μM. Reactions were conducted in 10 mM Na acetate with I adjusted to 10 mM by addition of NaCl. Error bars indicate one standard deviation of triplicate measurements.

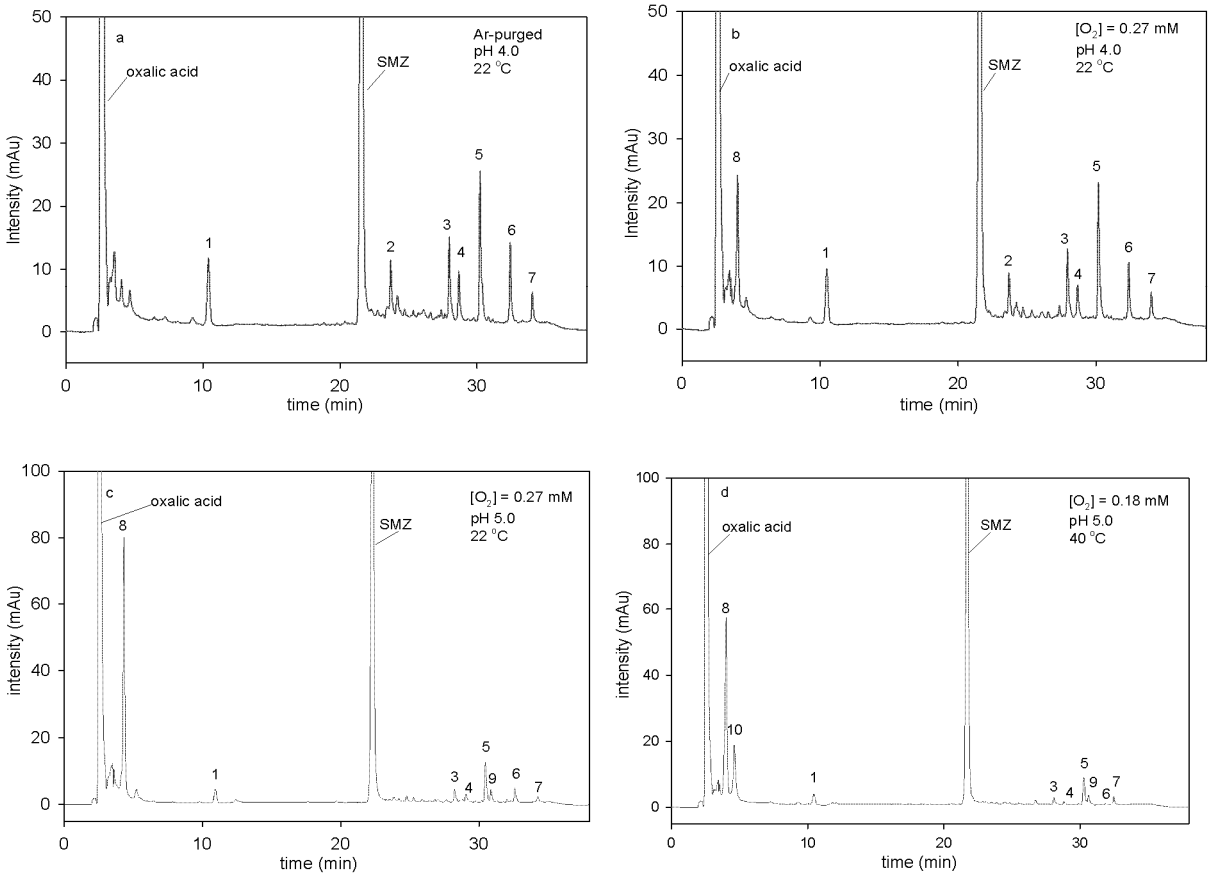

Figure S4. HPLC-UV chromatograms (λ = 254 nm) for δ-MnO_2-mediated transformation of SMZ (t = 10 min) conducted under (a) Ar-purged (O_2-free) conditions at pH 4.0 and 22ºC; (b) ambient O_2 conditions at pH 4.0 and 22ºC; (c) ambient O_2 conditions at pH 5.0 and 22ºC; (d) ambient O_2 conditions at pH 5.0 and 40ºC. For each set of reaction conditions, products profiles were the same at 1 min and 10 min. Comparison of product profiles quenched either by filtration or oxalic acid addition indicated that products **1, 6** and **7** were extensively adsorbed to δ-MnO_2, while **5** and **8** were not (data not shown). At room temperature, **7** and **8** were unstable. During 48-h storage at room temperature in the dark, **8** appeared to partially transform into **10**, **7** was completely degraded (Figure S5), and other product peaks decreased. For all reactions shown, initial concentrations $[SMZ]_0$ = 0.144 mM and $[MnO_2]_0$ = 1.44 mM. Initial dissolved oxygen concentrations for reactions conducted under ambient O_2 conditions: $[O_2]_{aq,\ 22\ °C}$ = 0.27 mM, $[O_2]_{aq,\ 40\ °C}$ = 0.18 mM.

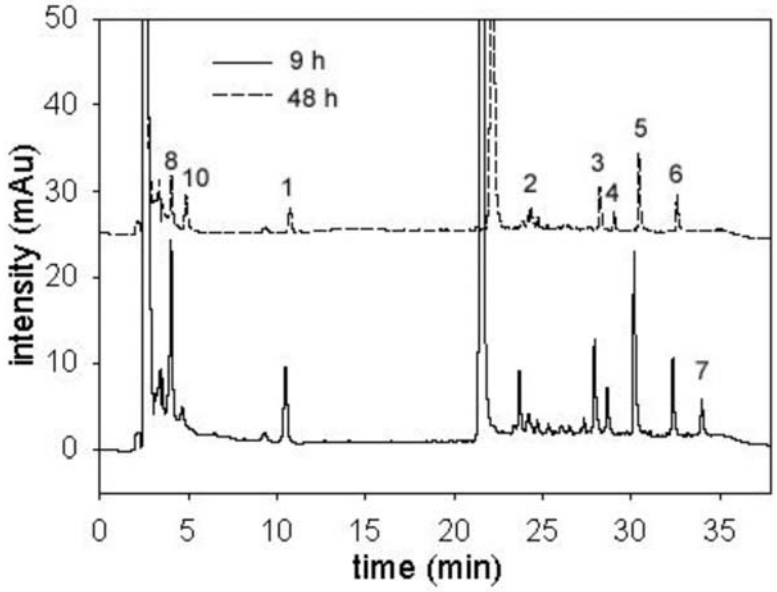

Figure S5. Stability of SMZ transformation products over 48 h. δ-MnO_2-mediated transformation of SMZ was conducted at pH 4, $[O_2]_{aq}$ = 0.27 mM, and 22 ºC. Reactions were quenched at t = 10 min with oxalic acid and stored at room temperature for 9 and 48 h in dark. HPLC-UV profiles were constructed for λ = 254 nm.

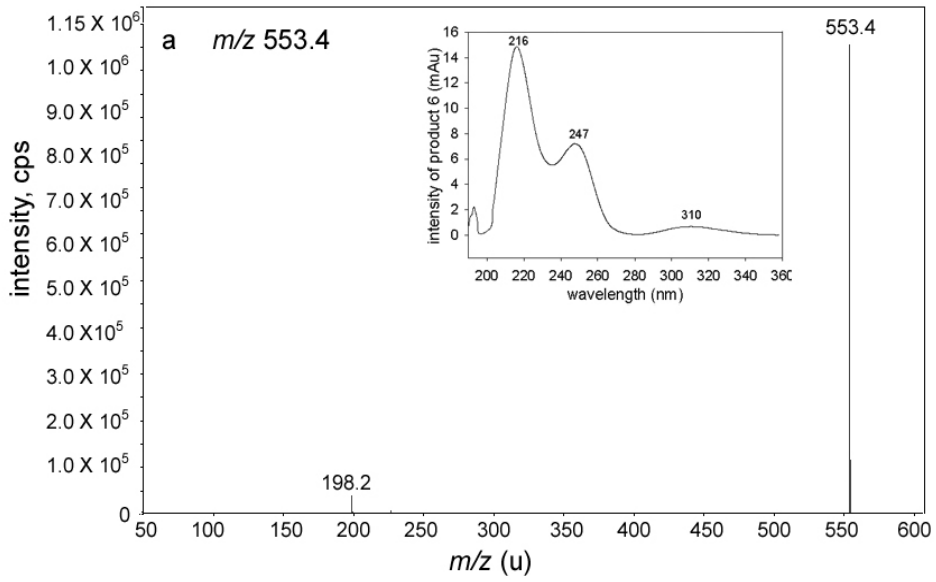

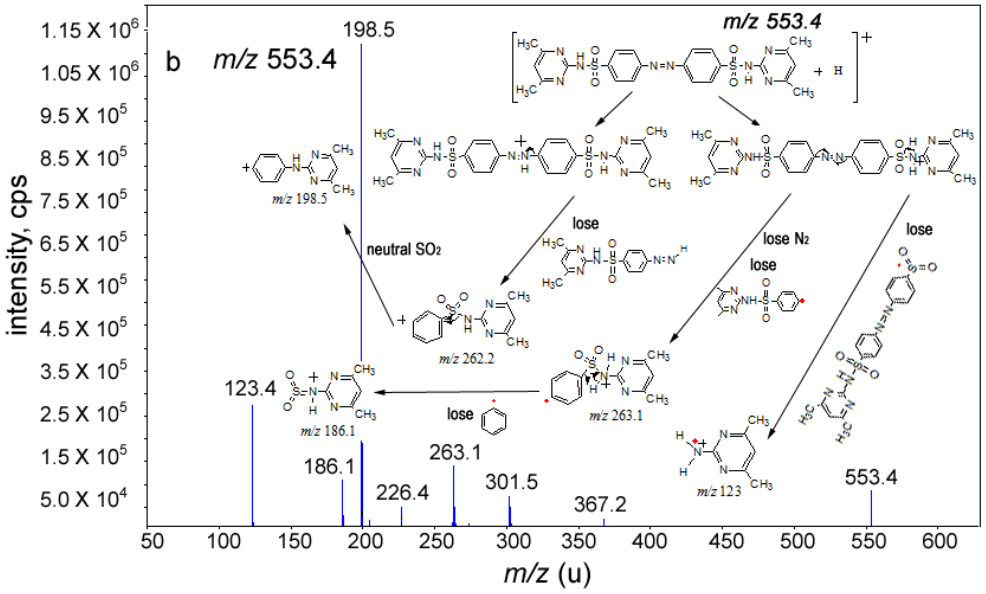

Figure S6. MS^2 spectra of **5** (*m/z* 553.4) obtained by CAD at (a) 25 eV and (b) 50 eV. The inset in (a) shows the UV spectrum for **5** in 10 mM ammonium formate; the inset in (b) shows proposed detailed fragmentation pathways for **5** with a 50 eV collision energy. Multiple protonization sites (azo-N and sulfonal-amide-N) were possible for **5**.

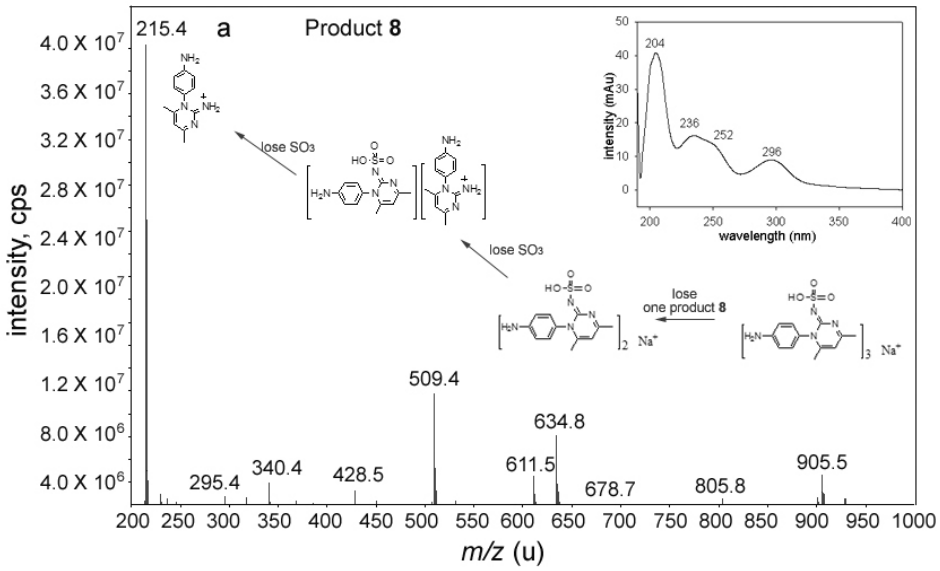

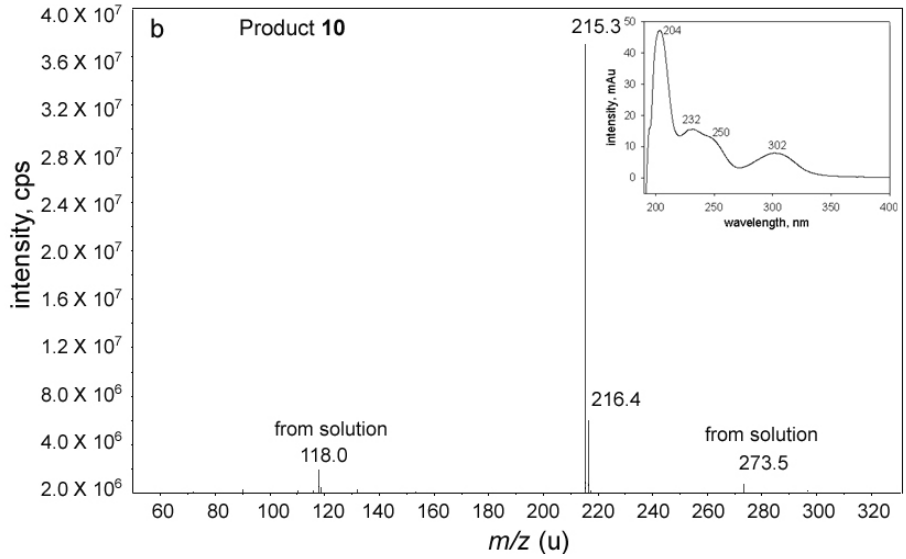

Figure S7. Full-scan mass spectra of (a) Product **8** and (b) Product **10**. The insets contain the corresponding UV spectra (with maximum absorbance wavelengths noted).

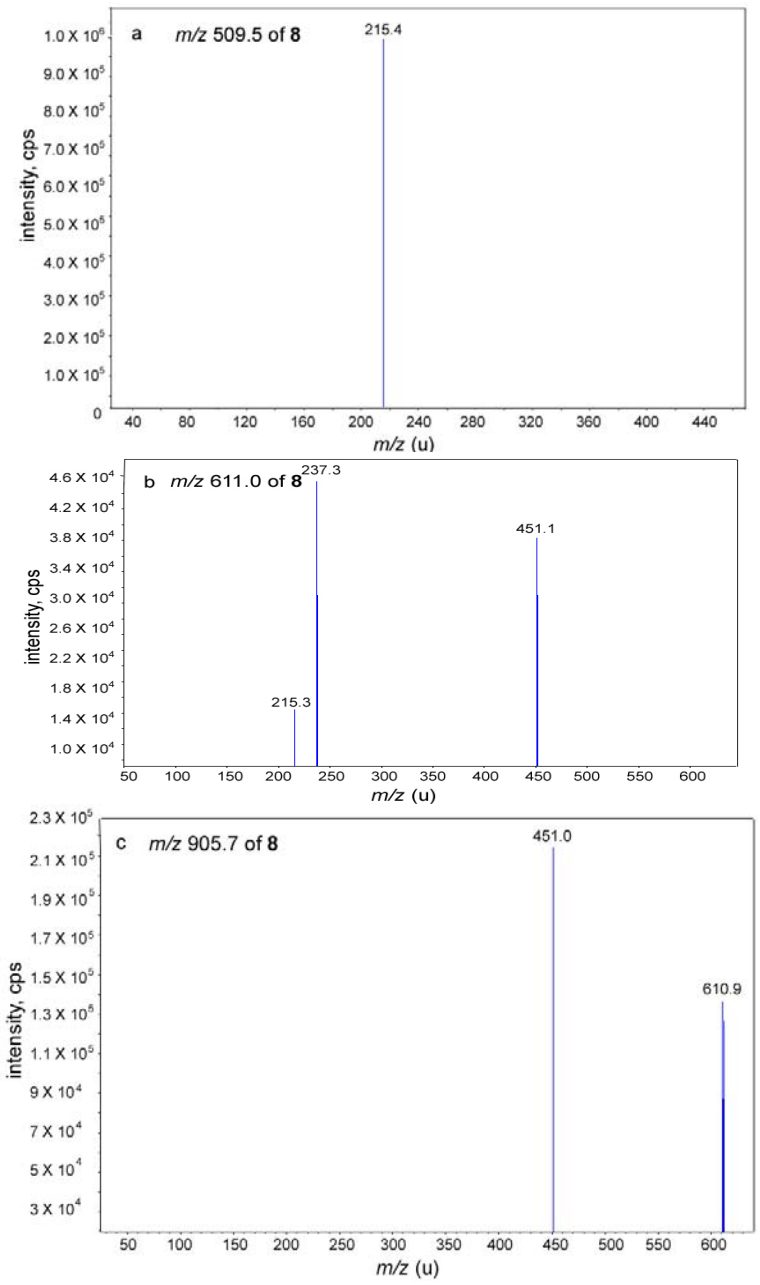

Figure S8. MS^2 spectra of selected ion clusters in the full-scan mass spectrum of **8** (*cf*. Figure S7a): (a) *m*/*z* 509.5, (b) *m*/*z* 611.0 and (c) *m*/*z* 905.7. CAD was conducted at 25 eV.

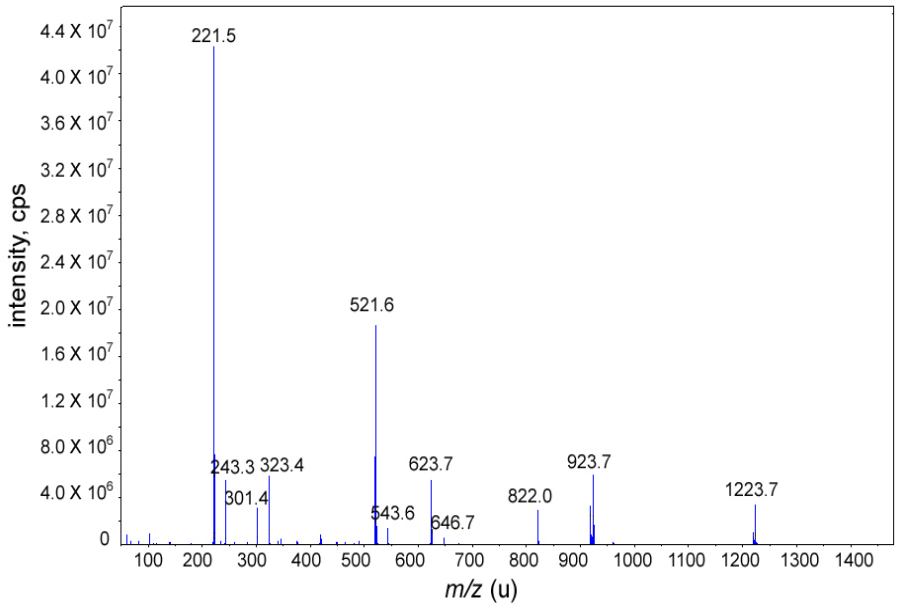

Figure S9. Full-scan mass spectra of phenyl-$^{13}C_6$ labeled **8**. MS^2 spectra of the *m/z* 221.5 daughter ion are shown in Figure S10.

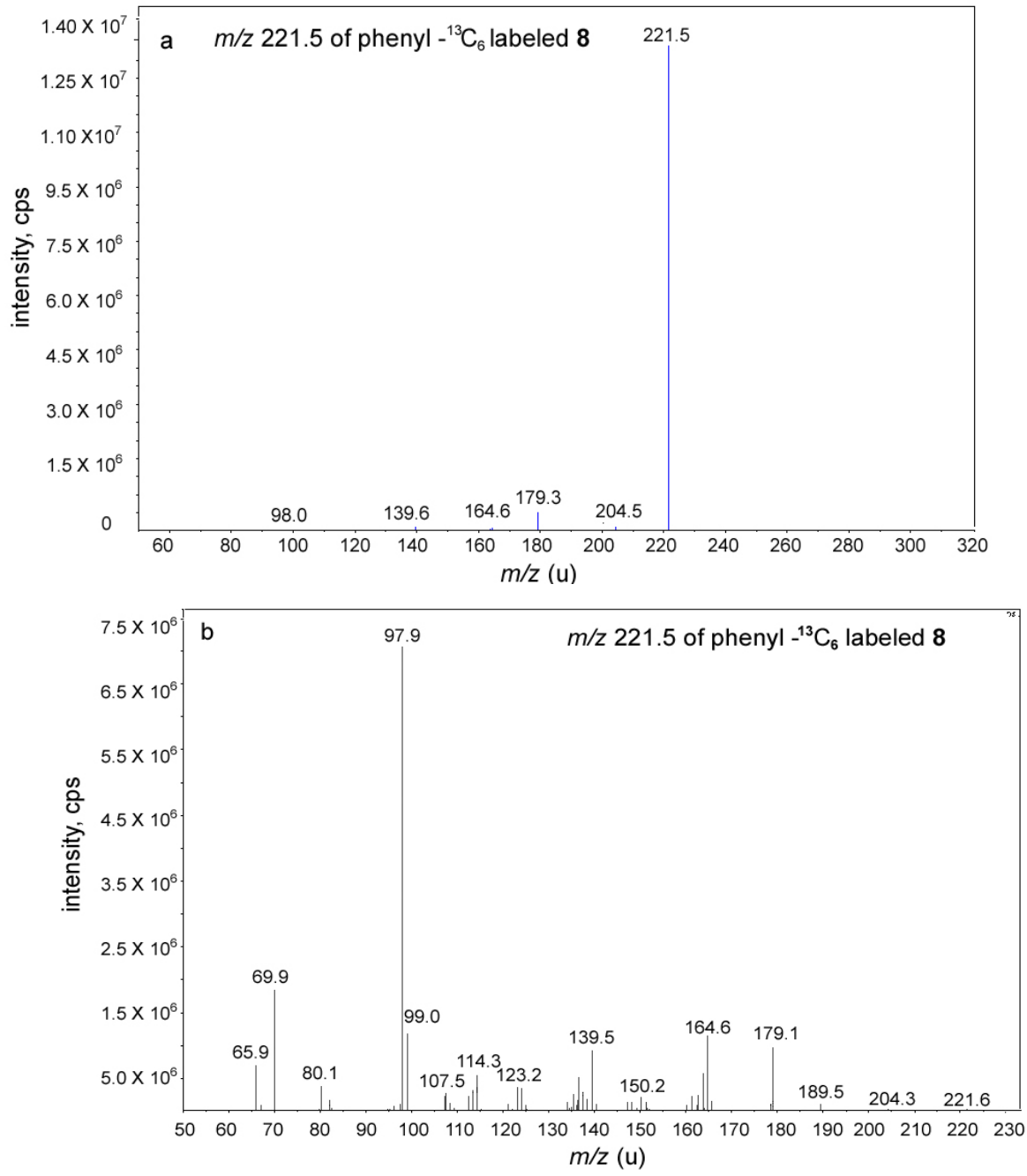

Figure S10. MS^2 spectra of the *m/z* 221.5 daughter ion phenyl-$^{13}C_6$-labeled **8** obtained with CAD conducted at (a) 25 eV and (b) 50 eV. The fragment ions with *m/z* = 139.6, 164.6, 179.3 and 204.5 were 6 *u* heavier than those with *m/z* 133.2, 158.3, 173.3 and 198.7 appearing in the MS^2 spectra of daughter ion *m/z* = 215.4 of **8** (*cf*. Figure 2b).

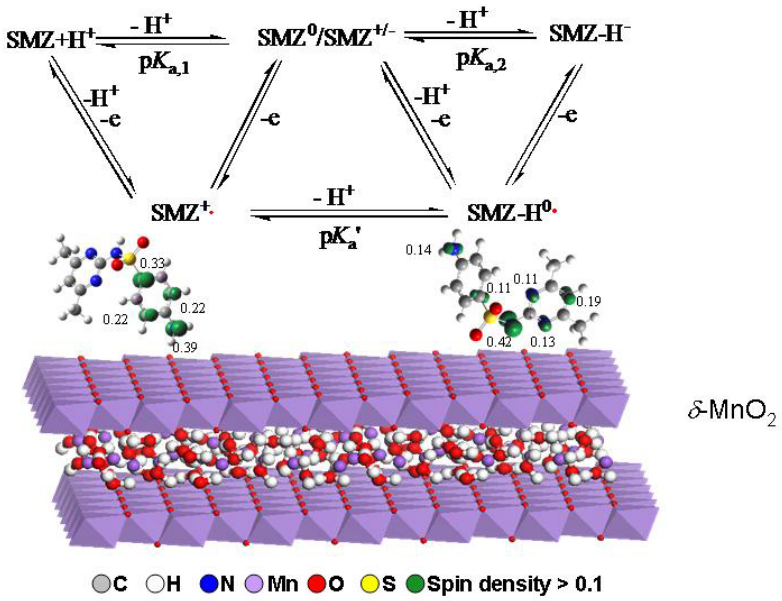

Scheme S1. Speciation of SMZ and SMZ radicals. The p$K_{a,1}$ and p$K_{a,2}$ were from Lin et al.[5] The macroscopic proton dissociation constant for the radical species of pK_a' = 5.2 has been reported.[6] The DFT/PCM optimized radical structures are shown in ball and stick representation with spin density isosurface at 0.0675 e Å^{-3} plotted. Numbers are atomic spin densities calculated by NBO analysis.

Text S2. Relative energy among SMZ radical resonance structures.

One electron (e^-) could be transferred from SMZ aniline N (N4) group or sulfonal amide (N1) group to Mn^{III}/Mn^{IV} on δ-MnO_2 surface to form an SMZ radical species (Scheme S1). The equilibrium between cationic and neutral radical species is pH dependent, and the fraction of the cationic radical ($SMZ^{+}\cdot$), $\alpha_{SMZ+\cdot}$, can be expressed as:

$$\alpha_{SMZ^{+}\cdot} = \frac{1}{1+10^{pH-pK'_a}} \qquad S1$$

Due to rotation about the S−N1 bond, two stable conformational isomers of SMZ or SMZ radicals are possible: an anti rotamer (dimethylpyrimidine and 2 O on different sides of S-N1 bond) and a syn rotamer (dimethylpyrimidine and 2 O on the same side of S-N1 bond). Solvated DFT/PCM calculations indicated that the relative free energies of formation were lowest for the anti rotamers of the N4 radicals for both $SMZ^{+}\cdot$ and $SMZ\text{-}H^{0}\cdot$ (Figure S13; $SMZ^{+}\cdot$ (N4) syn could not be located). $SMZ^{+}\cdot$ (N4) anti was therefore predicted to be the dominant radical cationic species (Figure S13a). For the neutral radical, the relative free energy differences among the $SMZ\text{-}H^{0}\cdot$ (N1) anti, $SMZ\text{-}H^{0}\cdot$ (N1) syn, $SMZ\text{-}H^{0}\cdot$ (N4) anti and $SMZ\text{-}H^{0}\cdot$ (N4) syn species were less than 11.0 $kJ\cdot mol^{-1}$, and co-existence of all four radicals were expected.

Table S2. Evaluation of possible structures for Product 8.

Label	Structure	Name	$\Delta_r G^{\dagger}$ (kJ·mol^{-1})
SMZ-N1-OH	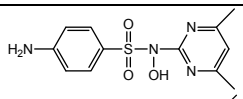	4-amino-*N*-(4,6-dimethylpyrimidin-2-yl)-*N*-hydroxybenzenesulfonamide	+47.3
SMZ-N→O	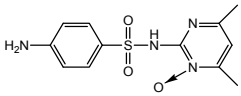	sulfamethazine-*N*-oxide	+20.6
SMZ-*p*-OH	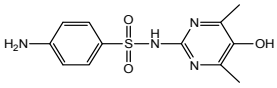	4-amino-*N*-(5-hydroxy-4,6-dimethylpyrimidin-2-yl)benzenesulfonamide	−117.7
SMZ-Smiles	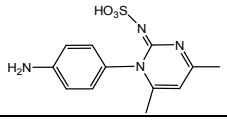	1-(4-aminophenyl)-4,6-dimethylpyrimidin-2(1*H*)-ylidenesulfamic acid	−120.4 (SMZ-Smiles-SO_3 conformer 1) −149.5 (SMZ-Smiles-SO_3 conformer 2)

† Free energies of reaction ($\Delta_r G$) of the evaluated structure relative to the reference state, SMZ+½O_2, computed using B3LYP/6-31+G* with the PCM solvent model. See main text for further details.

$MnO_2 + 4H^+ + 2e^- \rightarrow Mn^{2+} + 2H_2O$ ($E_H^0 = 1.29$V)[7] has the similar standard reduction potential as ½O_2 + $2H^+$ + 2e → H_2O ($E_H^0 = 1.23$V),[8] so O_2 was used to simplify the calculation. PCM, polarizable continuum model.

Table S3. Free energies of reaction ($\Delta_r G$) for formation of Product 5 computed using B3LYP/6-31+G* with the PCM solvent model.

Proposed reaction pathway	$\Delta_r G^{\dagger}$ (kJ·mol^{-1})
Hydrazo route	
2 SMZ-H^{0}· (N4) → azoHH-SMZ	−183.6
azoHH-SMZ + $^{1}/_{2}$ O_2 → azo-SMZ + $H_2O^{\ddagger}$	−127.9
Nitrene route	
2 SMZ-H^{0}· (N4) +$^{1}/_{2}$ O_2 → 2[SMZ-nitrene triplet rad]^{0}·· +H_2O	−11.8
2[SMZ-nitrene triplet rad]^{0}·· → azo-SMZ	−299.7

† Free energies of reaction ($\Delta_r G$) for the proposed pathways computed using B3LYP/6-31+G* with the PCM solvent model. See main text for further details.

$^{\ddagger}MnO_2 + 4H^+ + 2e^- \rightarrow Mn^{2+} + 2H_2O$ ($E_H^0 = 1.29$V)[7] has the similar standard reduction potential as $^{1}/_{2}$ $O_2 + 2H^+ + 2e^- \rightarrow H_2O$ ($E_H^0 = 1.23$V)[8], so in this calculation O_2 is used to simplify the calculation.

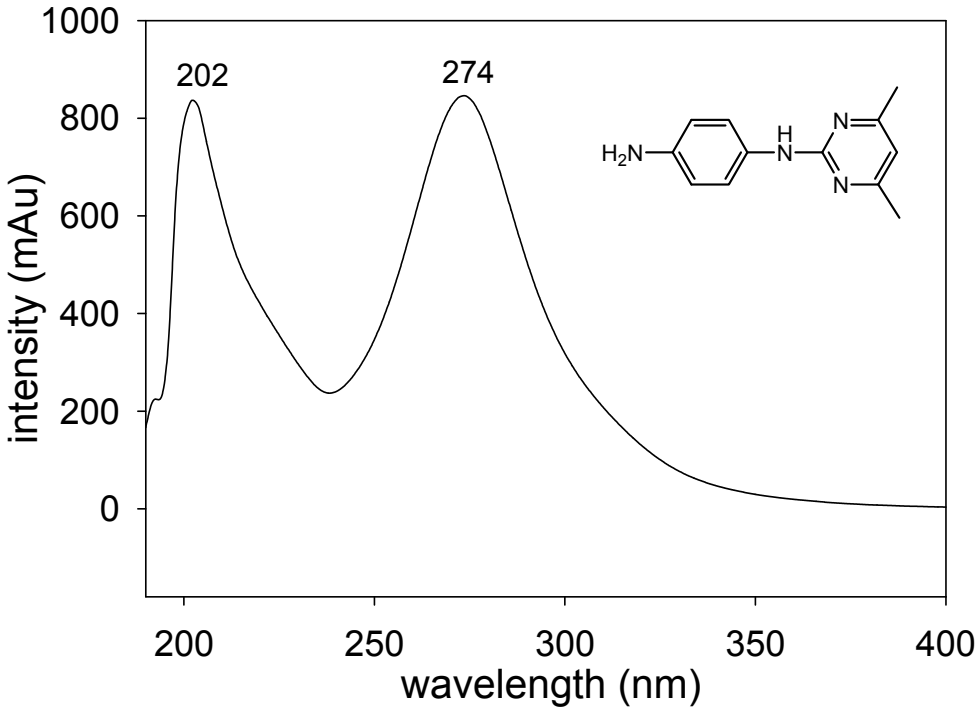

Figure S11. UV spectrum of *N*-(4,6-dimethylpyrimidin-2-yl)benzene-1,4-diamine.

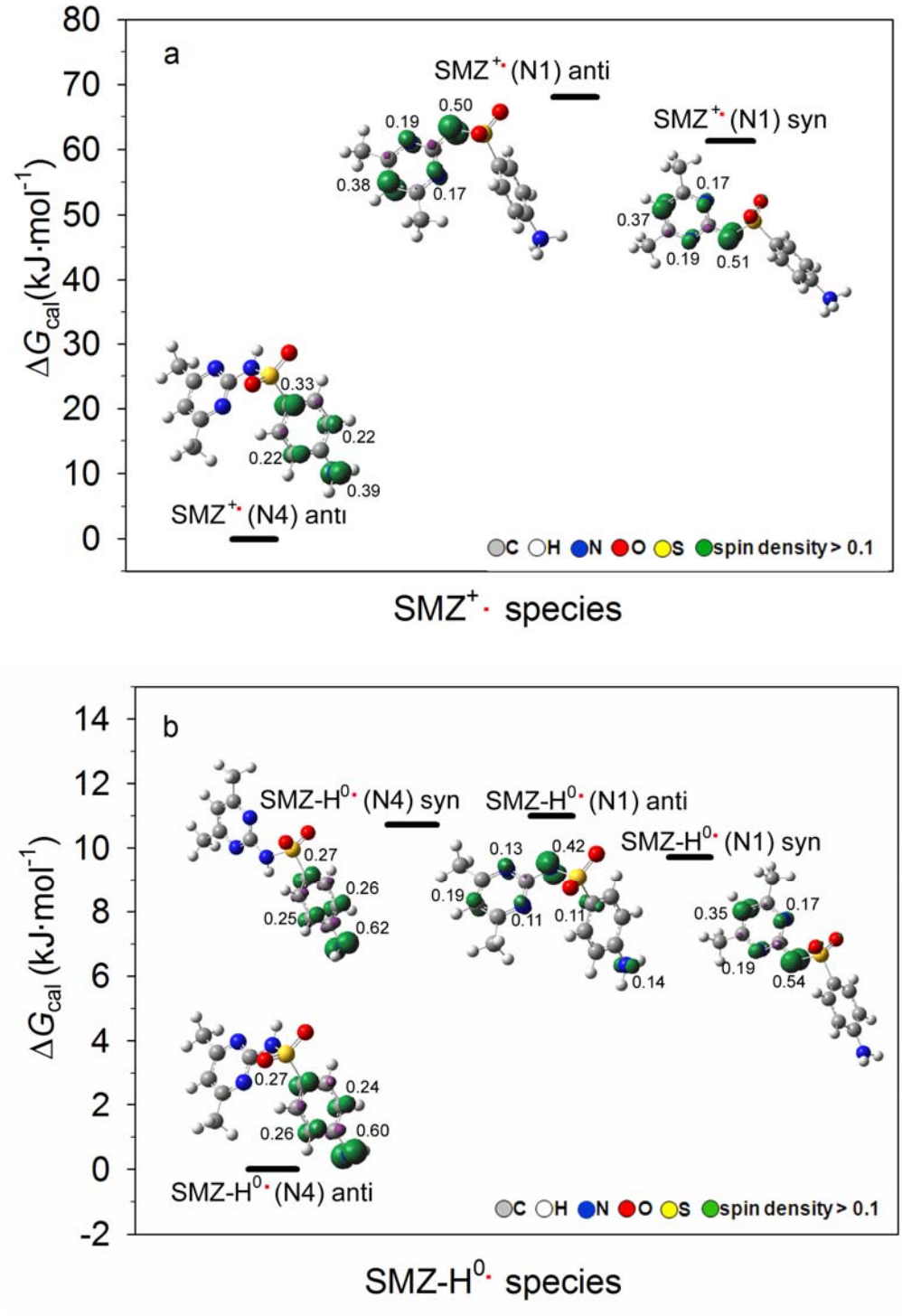

Figure S12. Relative free energies of formation in aqueous phase (calculated by PCM/DFT method) for (a) cationic radical ($SMZ^{+}\cdot$) and (b) neutral radical ($SMZ^{0}\cdot$) species. The structures represent ball-stick stereoisomers of $SMZ^{+}\cdot$ and $SMZ^{0}\cdot$ radical species with spin density isosurface at 0.0675 e $Å^{-3}$ plotted. Numbers are atomic spin densities calculated by NBO analysis.

Text S3. Literature Cited

1. Murray, J. W., Surface chemistry of hydrous manganese-dioxide. *J. Colloid Int. Sci.* **1974,** *46*, 357-371.
2. Villalobos, M.; Toner, B.; Bargar, J.; Sposito, G., Characterization of the manganese oxide produced by *Pseudomonas putida* strain Mnb1. *Geochim. Cosmochim. Acta* **2003,** *67*, 2649-2662.
3. Skoog, D. A.; West, D. M.; Holler, F. J., *Fundamentals of Analytical Chemistry*. Saunders College Publishing USA: TX, 1992.
4. Rubert, K. F.; Pedersen, J. A., Kinetics of oxytetracycline reaction with a hydrous manganese oxide. *Environ. Sci. Technol.* **2006,** *40*, 7216-7221.
5. Lin, C. E.; Chang, C. C.; Lin, W. C. Migration behavior and separation of sulfonamides in capillary zone electrophoresis. 2. Positively charged species at low pH. *J. Chromatogr. A* **1997**, *759*, 203-209.
6. Voorhies, J.D.; Adams, R.N. Voltammetry at solid electrodes. Anodic polarography of sulfa drugs. *Anal. Chem.* **1958**, *30*, 346-350.
7. Bricker, O.P. Some stability relations in the system MnO_2-H_2O at 25°C and one atmosphere total pressure. *Am. Mineral.* **1965**, *50*, 1296-1354.
8. McBride, M.B. 1994. *Environmental Chemistry of Soil*. Oxford University Press, New York.

Appendix C

C. Hedman Publication Relevant to Chapter 5 Discussion

A version of this chapter will be submitted for publication to the journal *Epidemiology* by Brian L. Sprague with the following co-authors: Amy Trentham-Dietz, Curtis J. Hedman, Jue Wang, Jocelyn C. Hemming, John M. Hampton, Diana S. M. Buist, Erin J. Aiello Bowles, Gale S. Sisney, and Elizabeth S. Burnside.

TITLE: **The association of serum xenoestrogens with mammographic breast density**

AUTHORS: Brian L. Sprague,[1] Amy Trentham-Dietz,[2,3] Curtis J. Hedman,[4] Jue Wang,[1] Jocelyn C. Hemming,[4] John M. Hampton,[3] Diana S. M. Buist,[5] Erin J. Aiello Bowles,[5] Gale S. Sisney,[6] Elizabeth S. Burnside,[3,6]

AFFILIATIONS: [1]Department of Surgery, University of Vermont, Burlington, VT 05401

[2]Department of Population Health Sciences, University of Wisconsin, Madison, WI 53726

[3]University of Wisconsin Carbone Cancer Center, Madison, WI 53726

[4]Environmental Health Division, Wisconsin State Laboratory of Hygiene, Madison, WI 53718

[5]Group Health Research Institute, Seattle, WA, 98101

[6]Department of Radiology, University of Wisconsin, Madison, WI 53726

CORRESPONDENCE: Brian L. Sprague, PhD

Office of Health Promotion Research, 1 S. Prospect St, Rm 4428B

University of Vermont, Burlington, VT 05401

(t) 802-656-4112; (f) 802-656-8826; Brian.Sprague@uvm.edu

SHORT TITLE: Xenoestrogen exposure and breast density

KEYWORDS: mammographic density, breast cancer, endocrine disruptors, epidemiology, phthalates, parabens

ACKNOWLEDGMENTS

This work was supported by the Department of Defense (BC062649), the Susan G. Komen Foundation (FAS0703857), and the National Cancer Institute (CA139548, CA014520). The authors would like to thank Kristi Klein and the staff of UW Health Clinics, Dr. Walter Peppler, Eva Baird, and Lori Wollett and staff of the UW OCT for their assistance in subject recruitment and data collection; Dr. Halcyon Skinner, Dr. Marty Kanarek, Dr. Ronald Gangnon, John Hampton, Tammy LeCaire, Tanya Watson, Matt Walsh, Jane Maney, and Cecilia Bellcross for study-related advice; Dr. Martin Yaffe and Chris Peressotti for assistance in breast density measurements; Dr. Karen Cruickshanks, Carla Schubert, and Scott Nash for assistance in sample storage; and Julie McGregor, Kathy Peck, and Dawn Fitzgibbons for study support.

CONFLICT OF INTEREST

The authors have no conflicts of interest to report.

ABBREVIATIONS

BPA, bisphenol A.

BMI, body mass index.

ABSTRACT

Background. Humans are exposed to many environmental chemicals which have estrogenic activity, raising concerns regarding potential effects on breast tissue and breast cancer risk. Phthalates, parabens, and phenols are estrogenically-active chemicals commonly found in consumer products, including shampoos, lotions, plastics, adhesives, detergents, and pharmaceuticals.

Objectives. We sought to evaluate the impact of these chemicals on breast tissue in humans. We examined the association of circulating serum levels of phthalates, parabens, and phenols with mammographic breast density.

Methods. A total of 264 postmenopausal women without breast cancer (ages 55-70, with no history of postmenopausal hormone use) were recruited from mammography clinics in Madison, Wisconsin. Subjects completed a questionnaire and provided a blood sample that was analyzed for mono-ethyl phthalate, mono-butyl phthalate, mono-benzyl phthalate, butyl paraben, propyl paraben, octylphenol, nonylphenol, and bisphenol A (BPA). Percent breast density was measured from subjects' mammograms using a computer-assisted thresholding method.

Results. After adjusting for age, body mass index, and other potentially confounding factors, serum levels of mono-ethyl phthalate and BPA were positively associated with percent breast density. Mean percent density was 12.9% among women with non-detectable mono-ethyl phthalate levels, 14.8% among women with detectable levels below the median (<6.6 ng/mL), and 18.2% among women with detectable levels above the median (P_{trend}=0.03). Similarly, mean percent density rose from 12.6% among women with non-detectable BPA levels to 13.2% among women with detectable levels below the median (<0.6 ng/mL) and 17.6% among women with

detectable levels above the median (P_{trend}=0.01). Serum levels of the other examined chemicals were not associated with breast density (P>0.10).

Conclusions. Women with higher serum levels of mono-ethyl phthalate and BPA have elevated breast density. Further investigation into the influence of these chemicals on breast tissue is warranted.

INTRODUCTION

Humans are widely exposed to xenoestrogens in the course of everyday life. Phthalates, parabens, and phenols are three of the most common classes of xenoestrogens found in foods and consumer products. Phthalates are used as a plasticizer in many consumer plastics, adhesives, detergents, and pharmaceuticals, and are also found in personal care products, such as shampoos, lotions, and shaving products (Committee on the Health Risks of Phthalates, 2008). Parabens are used a preservative in many of the same personal care products and pharmaceuticals, and are additionally used as antimicrobials in foods (Soni et al., 2005). Phenols are commonly used in the manufacture of consumer products made of polycarbonate plastics, the coatings of food containers, and as surfactants in detergents and personal care products (Vandenberg et al., 2007; Ying et al., 2002). Data from the National Health and Nutrition Examination Survey shows that the most common phthalates, parabens, and phenols are detectable in the urine of more than 90% of Americans (Calafat et al., 2010; Calafat et al., 2008; Silva et al., 2004).

Health concerns regarding exposure to xenoestrogens stem from their potential actions as endocrine disruptors. Laboratory studies have demonstrated that many phthalates, parabens, and phenols can bind to and activate the estrogen receptor, promote the proliferation of breast cancer cells, or increase uterine weight in immature mice (Byford et al., 2002; Harris et al., 1997; Jobling et al., 1995; Laws et al., 2000; Pugazhendhi et al., 2005; Routledge et al., 1998; Soto et al., 1995). Many of these chemicals have the ability to induce additional biological effects, including DNA damage, altered DNA methylation, altered sex hormone metabolism, and thyroid hormone antagonization (Anderson et al., 1999; Borch et al., 2004; Kang & Lee, 2005; Lovekamp-Swan & Davis, 2003; Moriyama et al., 2002).

Data on the health effects of these chemicals in humans is limited. Elevated BPA serum levels were associated with recurrent miscarriage in a small case-control study (Sugiura-Ogasawara et al., 2005) and cardiovascular disease in the National Health and Nutrition Examination Survey (Lang et al., 2008; Melzer et al., 2010). A variety of studies have reported links between urinary or serum phthalate levels and impaired sperm function in men (Duty et al., 2004; Hauser et al., 2007; Rozati et al., 2002), endometriosis in women (Cobellis et al., 2003; Reddy et al., 2006), early puberty (Wolff et al., 2010) and premature breast development (Colon et al., 2000). Most recently, a case-control study of women in Northern Mexico found that urinary levels of mono-ethyl phthalate were positively associated with breast cancer risk (Lopez-Carrillo et al., 2010). These findings raise important questions regarding the potential impacts of phthalates and other similar chemicals on breast tissue.

Mammographic breast density has emerged as one of the strongest risk factors for breast cancer, and a useful marker for the effects of various exposures on breast tissue (Boyd et al., 2005). Breast density refers to the appearance of breast tissue on a mammogram, reflecting the relative amounts of radiodense epithelial and stromal tissue versus radiolucent fat tissue (Boyd et al., 2010). A meta-analysis has estimated that women with density in 75% or more of the breast have a 4.6-fold increase in breast cancer risk compared to women density in less than five percent (McCormack & dos Santos Silva, 2006). Numerous breast cancer risk factors have been associated with breast density (Boyd et al., 2010), and breast density responds to changes in exposures including postmenopausal hormone use (Rutter et al., 2001) and chemoprevention with tamoxifen (Cuzick et al., 2004).

We hypothesized that circulating serum levels of phthalates, parabens, and phenols may be positively associated with mammographic breast density. We examined this relation in the

Wisconsin Breast Density Study, a cross-sectional study of postmenopausal women receiving a screening mammogram.

METHODS

Study population

The Wisconsin Breast Density Study is a cross sectional study of women receiving screening mammograms at the UW Health West Clinic or UW Health Breast Center in Madison, Wisconsin. The study was approved by the University of Wisconsin Health Sciences Institutional Review Board and all subjects provide written informed consent. Details on subject recruitment have previously been described (Sprague et al., 2011). Briefly, eligibility was limited to postmenopausal women between the ages of 55-70 who attended the mammography clinics for a screening mammogram between June 2008 and June 2009. Eligibility was further limited to women with no history of postmenopausal hormone use, breast implants, or a previous diagnosis of breast cancer. A total of 268 subjects were enrolled in the study.

Data collection

Each subject completed a study questionnaire and provided a blood sample immediately after completion of their screening mammogram. The questionnaire assessed established breast cancer risk factors and known correlates of mammographic breast density, including demographic and anthropometric factors, reproductive and menstrual history, family history of breast cancer, and lifestyle factors such as alcohol consumption, smoking, and physical activity.

A 30-mL blood sample was collected from each subject by venipuncture into uncoated glass Vacutainer tubes (Fisher Scientific, Pittsburgh, Pennsylvania). Immediately after spinning

down the sample, 4.5 mL of serum was transferred into borosilicate glass vials (Wheaton Science Products, Millville, New Jersey). The glass vials were prepared by baking at 450 degrees Celsius to burn off all organic carbon and the Teflon-coated caps were sonicated in methanol to remove any contaminants. The caps and vials were then assembled in a biosafety cabinet and remained sealed until the serum sample was collected. The serum samples were stored frozen at -70 degrees Celsius until thawed for analysis.

Phthalate, paraben, and phenol levels were quantified at the Wisconsin State Laboratory of Hygiene using methods based upon solid phase extraction (Strata-X, Phenomenex, Torrance, CA) (Phenomenex Application Note 14454) and isotope dilution high-performance liquid chromatography (Agilent 1100, Waldbronn, Germany) with tandem mass spectrometry (API4000, AB/SCIEX, Framingham, MA) with APCI negative ionization (Silva et al., 2003 and Ye et al., 2008). Analytical quality assurance (QA) parameters included reagent (all <LOD) and method blanks (all <LOD with exception of nonylphenol, of which had 5 of 9 were >LOD), calibration check standards (recovery = 98.7 % to 114.1 %, n=31 for phthalates and parabens and n=20 for phenols), and double charcoal treated human serum matrix control spikes at low (1ng/mL, recovery = 82.9 % to 114 %, n=12 for phthalates and parabens and n=14 for phenols) and mid (5 and 10ng/mL, recovery = 87.4 % to 112.9 %, n=12 for phthalates and parabens and n=19 for phenols) calibration curve levels. Lower limits of detection were based upon observed 3:1 signal to noise ratios, and are listed in **Table 2**.

As previously described (Sprague et al., 2011), endogenous sex hormone levels were measured at the Reproductive Endocrine Research Laboratory at the University of Southern California using a validated radioimmunoassay (Goebelsmann et al., 1979). Previous use of this assay by the laboratory has demonstrated a CV of 8.5% (Dorgan et al., 2010).

Breast density was assessed as previously been described (Sprague et al., 2012; Sprague et al., 2011). All subjects received a screening mammogram on a digital machine. Full resolution digital images of the craniocaudal view of the left breast were analyzed for breast density using a computer-aided thresholding technique via Cumulus software (Byng et al., 1994). Total breast area, dense area, and percent breast density were recorded by a single trained operator with high reliability (intraclass correlation coefficients > 0.92 for repeated measures).

Statistical analyses

All statistical analyses were performed using SAS Statistical Software (Version 9.2; SAS Institute, Inc., Cary, North Carolina). Insufficient serum was available for 4 study subjects, leaving a total of 264 samples for analysis. Serum propyl paraben level was missing for one additional woman and certain covariate data were missing for a small fraction of subjects (see Table 1). Multiple imputation was used to impute missing covariate data. Ten imputations were conducted using the Markov Chain Monte Carlo method (Schafer, 1997). The imputation model contained percent breast density and all variables listed in Tables 1 and 2. For statistical analyses, each model was fit separately to the ten imputed datasets and the results combined for statistical inferences using the methods of Rubin (Rubin, 1987).

Percent breast density was square root transformed to improve the normality of the data. Multivariable linear regression was used to assess the association between each xenoestrogen blood measure and the square root of percent breast density, while sequentially adjusting for (1) age; (2) body mass index; and (3) other variables which have previously been shown to be associated with density in this study population: parity, family history of breast cancer, vigorous physical activity, and pack-years of smoking (Sprague et al., 2011). To compare the difference in

breast density according to various xenoestrogen levels, separate models included each xenoestrogen serum level categorized as non-detectable, below the median of detectable values, and above the median of detectable values. Adjusted least-squares mean levels of square root percent density were calculated according to these categorized groups and reverse transformed for display purposes. Tests of trends across categorized groups were conducted by including the serum level category as an ordinal term in the regression models. Tests for effect modification of the relation between the serum chemicals and percent breast density by other circulating hormones and BMI were conducted by including continuous cross-product interaction terms in the regression models. Interactions were considered statistically significant if the P-values associated with the cross-product interaction terms were less than 0.05. All analyses were repeated using the square root of dense area (rather than percent density) as the outcome of interest.

RESULTS

Table 1 summarizes the characteristics of the study subjects. The mean age of participants was 60.6 (standard deviation, 4.4). About 31% of participants were overweight and 37% were obese. In general, the study population was highly educated (80.7% had attended at least some college), and reported low smoking rates (60.2% had never smoked).

The distributions of the measured serum phthalates, parabens and phenols are described in Table 2. Propyl paraben and butyl paraben were detected in more than half of the study samples. Mono-ethyl phthalate, octylphenol, nonylphenol, and bisphenol A were detected in 13-41% of samples. Mono-butylphthalate and mono-benzylphthalate were detected in very few samples (1.1% and 0.4%, respectively) and were excluded from further analyses. Table 3 presents the

spearman correlation coefficients between each of the xenoestrogens and age, BMI, serum estradiol, serum progesterone, and serum testosterone. There was a moderate positive correlation between nonylphenol and estradiol (r=0.2; p=0.001). No other significant correlations were observed.

The results of regression models including each xenoestrogen as a continuous variable are shown on the left hand side of Table 4. In the age-adjusted models there was a positive association between BPA and percent density that was of borderline statistical significance (P=0.07). Further adjustment for BMI and other variables attenuated the association between BPA and percent density, yet also revealed an association between mono-ethyl phthalate and percent breast density which was of borderline statistical significance (P=0.04 in the BMI-adjusted model and P=0.09 in the multivariable-adjusted model). Close examination revealed that two outlier values each of mono-ethyl phthalate and BPA substantially influenced these results. After excluding these outliers, mono-ethyl phthalate and BPA were both positively associated with percent density in the multivariable adjusted models (not shown in table; $\beta = 0.03$, $P = 0.01$ for mono-ethyl phthalate and $\beta = 0.19$, $P = 0.01$ for BPA). There was no evidence for an association between percent breast density and propyl paraben, butyl paraben, octylphenol or nonylphenol serum levels when treated as continuous variables.

Results from the regression models using categorized serum xenoestrogen levels are displayed in the right hand side of Table 4. In the multivariable-adjusted models there were statistically significant trends of increasing breast density with increasing mono-ethyl phthalate and BPA exposure categories. Mean percent density was 12.9% among women with non-detectable mono-ethyl phthalate levels, 14.8% among women with detectable levels below the median, and 18.2% among women with detectable levels above the median (P_{trend}=0.03).

Similarly, mean percent density rose from 12.6% among women with non-detectable BPA levels to 13.2% among women with detectable levels below the median and 17.6% among women with detectable levels above the median (P_{trend}=0.01). There was no evidence for a trend in breast density with increasing categories of propyl paraben, butyl paraben, octylphenol, or nonylphenol levels.

We assessed whether the associations of mono-ethyl phthalate and BPA with percent breast density varied according to measures of the endogenous hormone environment, including BMI, serum estradiol, serum progesterone, and serum testosterone. The association between mono-ethyl phthalate and percent breast density varied by progesterone level ($P_{interaction}$ = 0.04). Serum mono-ethyl phthalate levels were more strongly associated with percent breast density among women with higher progesterone levels (Figure 1). There was also a statistically significant interaction between mono-ethyl phthalate and estradiol ($P_{interaction}$ = 0.04). However, this interaction was strongly influenced by the two outlier values of mono-ethyl phthalate. Exclusion of these outliers eliminated the interaction ($P_{interaction}$ = 0.96). There were no statistically significant interactions between mono-ethyl phthalate and BMI or serum testosterone. The association between BPA and percent breast density varied according to BMI ($P_{interaction}$ = 0.03). BPA levels were positively associated with percent density only among women who were not obese (Figure 2). No statistically significant interactions were observed between BPA and the endogenous hormone measurements.

Similar results were obtained when evaluating the relation between each chemical and dense breast area (rather than percent density). Multivariable-adjusted regression revealed positive associations between dense area and mono-ethyl phthalate (P_{trend}=0.01) and BPA (P_{trend}=0.08).

DISCUSSION

This study provides the first evidence that mammographic breast density varies according to circulating serum levels of xenoestrogens in postmenopausal women. We found that serum levels of mono-ethyl phthalate and BPA were independently associated with elevated percent breast density. For both chemicals, percent breast density was elevated by about 5 percentage points among women with serum levels above the median detected value compared to women with undetectable levels.

Breast density is known to be one of the strongest risk factors for breast cancer (Boyd et al., 2010). Previous studies suggest that a 5 percentage point difference in percent density corresponds to an approximately 5-10% increase in breast cancer risk (Boyd et al., 1995; Maskarinec & Meng, 2000; Ursin et al., 2003). For comparison, an absolute difference of 5 percentage points in percent breast density is similar to the average increase in percent density observed after 1 year of estrogen plus progestin postmenopausal hormone use (Greendale et al., 2003; McTiernan et al., 2005), which is a known breast cancer risk factor (Rossouw et al., 2002).

To our knowledge, no previous studies have evaluated mammographic breast density in relation to biological measures of phthalate, paraben, or phenol exposures. We are aware of only one study examining the relation between these chemicals and breast cancer risk in humans. A case-control study examined breast cancer risk in relation to phthalates measured in urine samples from Mexican women (Lopez-Carrillo et al., 2010). Women with urinary mono-ethyl phthalate levels in the highest tertile were more than twice as likely to have breast cancer as women in the lowest tertile (OR=2.2; 95% CI: 1.33, 3.63). Our finding of elevated breast density among women with high circulating serum levels of mono-ethyl phthalate is consistent

with this finding. Interestingly, the same case-control study found that mono-butyl phthalate and mono-benzyl phthalate were inversely associated with breast cancer risk (Lopez-Carrillo et al., 2010). Since very few serum samples in our study had detectable levels of mono-butyl phthalate or mono-benzyl phthalate, we were unable to evaluate their association with mammographic breast density.

Humans are generally exposed to phthalates as diesters in consumer products. The metabolism of these diesters is rapid, with elimination half-lives generally less than 24 hours (Koch et al., 2006). Mono-ethyl phthalate is the primary metabolite of diethyl phthalate. Products that may contain diethyl phthalate include perfumes, deodorants, soaps, shampoos, cosmetics, and lotions (Committee on the Health Risks of Phthalates, 2008). A rise in serum mono-ethyl phthalate levels can be detected within 1 hour of dermal application of a cream containing diethyl phthalate (Janjua et al., 2007). Excretion of phthalate metabolites occurs primarily via urine (Committee on the Health Risks of Phthalates, 2008). In the case-control study described above, there was a positive linear trend between an index of personal care product use and urinary MEP levels (Romero-Franco et al., 2011).

BPA is widely used in plastics and cans for food packaging (Schecter et al., 2010). Exposure to BPA is considered to predominantly occur via food (National Toxicology Program, 2008). Intervention studies have revealed that the avoidance of foods packaged in plastic can lower BPA exposure levels substantially (Rudel et al., 2011). Following ingestion, BPA is metabolized via glucuronidation, with acute exposure studies suggesting an elimination half-life in the body of about 4-6 hours (Volkel et al., 2005; Volkel et al., 2002). However, a recent study of NHANES data suggested that there are either substantial non-food sources of exposure or that there is substantial accumulation of BPA in body compartments with long elimination times

(Stahlhut et al., 2009). Despite its short half-life in the body, BPA appears to be stored in adipose tissue in its lipophilic unconjugated forms (Fernandez et al., 2007). Release of free BPA from adipose tissue may represent a source of continuous exposure for target organs (Calafat et al., 2008).

The metabolism and excretion of phthalates, parabens, and phenols is efficient, and phthalate and BPA concentrations are about 20-100 times higher in urine than in blood (Hogberg et al., 2008; Teeguarden et al., 2011). Thus, urine is typically used as the biologic matrix for evaluating exposure levels in population studies. The National Health and Nutrition Examination Survey (NHANES) has evaluated urinary levels of these chemicals in a representative sample of the United States population (Centers for Disease Control and Prevention, 2009). Mono-ethyl phthalate and bisphenol A are detectable in over 90% of urine samples evaluated (Calafat et al., 2008; Silva et al., 2004). In the most recent study period (2007-2008), the geometric mean urinary levels of mono-ethyl phthalate and bisphenol A were 137 μg/L and 2.08 μg/L, respectively (Centers for Disease Control and Prevention, 2011). Higher creatinine-adjusted levels of both chemicals are observed among females than males, which may be attributable to differences in use of personal care products and/or differences in pharmacokinetic factors (Calafat et al., 2008; Silva et al., 2004).

While urine is most commonly used to assess exposure levels, previous studies have called for analyses of circulating blood levels, which may better represent the biologically relevant exposure of the target organs (Calafat et al., 2008). A number of studies have measured serum BPA levels in specific study populations (Vandenberg et al., 2010). The mean serum BPA in our sample was 0.4 ng/mL, which is quite similar to that observed in other studies of healthy adult female populations using a variety of detection methods (Inoue et al., 2000; Inoue

et al., 2001; Sugiura-Ogasawara et al., 2005; Takeuchi et al., 2004). Notably, this concentration is higher than that previously shown to stimulate responses in cell culture and animal experiments (Vandenberg et al., 2010). Previously, BPA levels in blood have been associated with polycystic ovarian syndrome, obesity, and recurrent miscarriage (Sugiura-Ogasawara et al., 2005; Takeuchi et al., 2004). Very few studies have assessed phthalate levels in serum samples. We observed a mean mono-ethyl phthalate concentration of 2.4 ng/mL, which is very similar to the mean of 1.2 ng/mL estimated in a study of recent mothers in Sweden (Hogberg et al., 2008).

The mechanisms by which mono-ethyl phthalate or BPA exposure could influence mammographic breast density are unclear. While in vitro assays indicate that phthalates and BPA have estrogenic activity (Harris et al., 1997; Matthews et al., 2001), their potency is believed to be 10,000-1 million times less than that of estradiol. In vitro experiments and human studies provide inconsistent evidence for mutagenicity (Hauser et al., 2007; Iso et al., 2006; Jonsson et al., 2005; Keri et al., 2007) and animal studies have revealed limited evidence for impacts on the mammary gland in adult animals (Committee on the Health Risks of Phthalates, 2008; National Toxicology Program, 2008). However, there is evidence that the offspring of rats exposed to BPA during pregnancy exhibit altered mammary gland architecture during puberty and adulthood, including an increased number of hyperplastic mammary ducts, increased stromal nuclear density, and increased terminal end bud density (Durando et al., 2007; Munoz-de-Toro et al., 2005). Additionally, a recent study reported that urinary BPA levels were associated with upregulated estrogen receptor and estrogen-related receptor expression among adult men (Melzer et al., 2011). Recent studies have also revealed that environmentally relevant doses of BPA can influence adiponectin production in human adipose tissue, which could influence insulin sensitivity and tissue inflammation (Hugo et al., 2008).

We explored potential interactions between the xenoestrogen exposures and the internal hormone environment. The association between mono-ethyl phthalate and breast density was somewhat stronger among women with higher progesterone levels. The association between BPA and breast density was limited to women who were not obese, but was not significantly modified by endogenous hormone levels. The interpretation of these findings is unclear. Given the limited statistical power to detect interactions, and the number of interactions tested, these findings require replication and should be interpreted with caution.

Due to the cross-sectional nature of the study, we were unable to investigate a temporal relationship between xenoestrogen exposures and mammographic breast density. While the pharmacokinetics of phthalate and BPA metabolism are not completely understood, a single blood measure is thought to primarily reflect exposure within the past 24 hours. It would seem improbable that low-level xenoestrogen exposure in the prior day could influence mammographic breast density. However, given the continuous low level nature of exposure and its correlation with lifestyle patterns that are often stable over long periods of time (e.g., diet, consumer product use), a single measure of xenoestrogen exposure may provide a reasonable surrogate for usual exposure levels. Data on repeated measures in individuals is limited, but there is some evidence for moderate correlation (intraclass correlation coefficient > 0.6) between urinary phthalate measures taken months apart (Hauser et al., 2004; Peck et al., 2010). It is also possible, however, that the associations between circulating levels of monoethyl phthalate and BPA and breast density may be due to confounding by a third factor that influences both xenoestrogen metabolism and breast density. Further investigation using longitudinal study designs will be necessary to confirm and further examine the associations observed in our study.

CONCLUSIONS

The results of this study indicate that serum levels of mono-ethyl phthalate and BPA are cross-sectionally associated with elevated mammographic breast density. Given the widespread exposure of the population to these chemicals and the strong association between breast density and breast cancer risk, these chemicals could significantly impact breast cancer risk. For mon-ethyl phthalate, the consistency between our findings and that of a previous case-control study of breast cancer risk are particularly striking. The results observed here need to be confirmed in larger study populations. Future studies evaluating these exposures in relation to breast density or breast cancer risk should seek to utilize longitudinal study designs, multiple exposure assessments, and a wide age range of subjects.

REFERENCES

Anderson, D., Yu, T. W., & Hincal, F. (1999). Effect of some phthalate esters in human cells in the comet assay. *Teratog Carcinog Mutagen, 19*(4), 275-280.

Borch, J., Ladefoged, O., Hass, U., & Vinggaard, A. M. (2004). Steroidogenesis in fetal male rats is reduced by DEHP and DINP, but endocrine effects of DEHP are not modulated by DEHA in fetal, prepubertal and adult male rats. *Reprod Toxicol, 18*(1), 53-61.

Boyd, N. F., Byng, J. W., Jong, R. A., Fishell, E. K., Little, L. E., Miller, A. B., Lockwood, G. A., Tritchler, D. L., & Yaffe, M. J. (1995). Quantitative classification of mammographic densities and breast cancer risk: results from the Canadian National Breast Screening Study. *J Natl Cancer Inst, 87*(9), 670-675.

Boyd, N. F., Martin, L. J., Bronskill, M., Yaffe, M. J., Duric, N., & Minkin, S. (2010). Breast tissue composition and susceptibility to breast cancer. *J Natl Cancer Inst, 102*(16), 1224-1237.

Boyd, N. F., Rommens, J. M., Vogt, K., Lee, V., Hopper, J. L., Yaffe, M. J., & Paterson, A. D. (2005). Mammographic breast density as an intermediate phenotype for breast cancer. *Lancet Oncol, 6*(10), 798-808.

Byford, J. R., Shaw, L. E., Drew, M. G., Pope, G. S., Sauer, M. J., & Darbre, P. D. (2002). Oestrogenic activity of parabens in MCF7 human breast cancer cells. *J Steroid Biochem Mol Biol, 80*(1), 49-60.

Byng, J. W., Boyd, N. F., Fishell, E., Jong, R. A., & Yaffe, M. J. (1994). The quantitative analysis of mammographic densities. *Phys Med Biol, 39*(10), 1629-1638.

Calafat, A. M., Ye, X., Wong, L. Y., Bishop, A. M., & Needham, L. L. (2010). Urinary concentrations of four parabens in the U.S. population: NHANES 2005-2006. *Environ Health Perspect, 118*(5), 679-685.

Calafat, A. M., Ye, X., Wong, L. Y., Reidy, J. A., & Needham, L. L. (2008). Exposure of the U.S. population to bisphenol A and 4-tertiary-octylphenol: 2003-2004. *Environ Health Perspect, 116*(1), 39-44.

Centers for Disease Control and Prevention. (2009). Fourth National Report on Human Exposure to Environmental Chemicals. Atlanta, GA: http://www.cdc.gov/exposurereport/.

Centers for Disease Control and Prevention. (2011). Fourth National Report on Human Exposure to Environmental Chemicals, Updated Tables, February 2011. Atlanta, GA: http://www.cdc.gov/exposurereport/.

Cobellis, L., Latini, G., De Felice, C., Razzi, S., Paris, I., Ruggieri, F., Mazzeo, P., & Petraglia, F. (2003). High plasma concentrations of di-(2-ethylhexyl)-phthalate in women with endometriosis. *Hum Reprod, 18*(7), 1512-1515.

Colon, I., Caro, D., Bourdony, C. J., & Rosario, O. (2000). Identification of phthalate esters in the serum of young Puerto Rican girls with premature breast development. *Environ Health Perspect, 108*(9), 895-900.

Committee on the Health Risks of Phthalates. (2008). Phthalates and Cumulative Risk Assessment: the Tasks Ahead. Washington, DC: National Research Council.

Cuzick, J., Warwick, J., Pinney, E., Warren, R. M., & Duffy, S. W. (2004). Tamoxifen and breast density in women at increased risk of breast cancer. *J Natl Cancer Inst, 96*(8), 621-628.

Dorgan, J. F., Stanczyk, F. Z., Kahle, L. L., & Brinton, L. A. (2010). Prospective case-control study of premenopausal serum estradiol and testosterone levels and breast cancer risk. *Breast Cancer Res, 12*(6), R98.

Durando, M., Kass, L., Piva, J., Sonnenschein, C., Soto, A. M., Luque, E. H., & Munoz-de-Toro, M. (2007). Prenatal bisphenol A exposure induces preneoplastic lesions in the mammary gland in Wistar rats. *Environ Health Perspect, 115*(1), 80-86.

Duty, S. M., Calafat, A. M., Silva, M. J., Brock, J. W., Ryan, L., Chen, Z., Overstreet, J., & Hauser, R. (2004). The relationship between environmental exposure to phthalates and computer-aided sperm analysis motion parameters. *J Androl, 25*(2), 293-302.

Fernandez, M. F., Arrebola, J. P., Taoufiki, J., Navalon, A., Ballesteros, O., Pulgar, R., Vilchez, J. L., & Olea, N. (2007). Bisphenol-A and chlorinated derivatives in adipose tissue of women. [Research Support, Non-U.S. Gov't]. *Reproductive toxicology, 24*(2), 259-264.

Goebelsmann, U., Bernstein, G. S., Gale, J. A., Kletzky, O. A., Nakamura, R. M., Coulson, A. H., & Korelitz, J. J. (1979). Serum gonadotropin, testosterone, estradiol and estrone levels prior to and following bilateral vasectomy. In I. H. Lepow & R. Crozier (Eds.), *Vasectomy: Immunologic and pathophysiologic effects in animals and man*. New York: Academic Press.

Greendale, G. A., Reboussin, B. A., Slone, S., Wasilauskas, C., Pike, M. C., & Ursin, G. (2003). Postmenopausal hormone therapy and change in mammographic density. *J Natl Cancer Inst, 95*(1), 30-37.

Harris, C. A., Henttu, P., Parker, M. G., & Sumpter, J. P. (1997). The estrogenic activity of phthalate esters in vitro. *Environ Health Perspect, 105*(8), 802-811.

Hauser, R., Meeker, J. D., Park, S., Silva, M. J., & Calafat, A. M. (2004). Temporal variability of urinary phthalate metabolite levels in men of reproductive age. *Environ Health Perspect, 112*(17), 1734-1740.

Hauser, R., Meeker, J. D., Singh, N. P., Silva, M. J., Ryan, L., Duty, S., & Calafat, A. M. (2007). DNA damage in human sperm is related to urinary levels of phthalate monoester and oxidative metabolites. *Hum Reprod, 22*(3), 688-695.

Hogberg, J., Hanberg, A., Berglund, M., Skerfving, S., Remberger, M., Calafat, A. M., Filipsson, A. F., Jansson, B., Johansson, N., Appelgren, M., & Hakansson, H. (2008). Phthalate diesters and their metabolites in human breast milk, blood or serum, and urine as biomarkers of exposure in vulnerable populations. *Environ Health Perspect, 116*(3), 334-339.

Hugo, E. R., Brandebourg, T. D., Woo, J. G., Loftus, J., Alexander, J. W., & Ben-Jonathan, N. (2008). Bisphenol A at environmentally relevant doses inhibits adiponectin release from human adipose tissue explants and adipocytes. *Environ Health Perspect, 116*(12), 1642-1647.

Inoue, K., Kato, K., Yoshimura, Y., Makino, T., & Nakazawa, H. (2000). Determination of bisphenol A in human serum by high-performance liquid chromatography with multi-electrode electrochemical detection. [Comparative Study

Research Support, Non-U.S. Gov't]. *Journal of chromatography. B, Biomedical sciences and applications, 749*(1), 17-23.

Inoue, K., Yamaguchi, A., Wada, M., Yoshimura, Y., Makino, T., & Nakazaw, H. (2001). Quantitative detection of bisphenol A and bisphenol A diglycidyl ether metabolites in human plasma by liquid chromatography-electrospray mass spectrometry. [Research

Support, Non-U.S. Gov't]. *Journal of chromatography. B, Biomedical sciences and applications, 765*(2), 121-126.

Iso, T., Watanabe, T., Iwamoto, T., Shimamoto, A., & Furuichi, Y. (2006). DNA damage caused by bisphenol A and estradiol through estrogenic activity. *Biol Pharm Bull, 29*(2), 206-210.

Janjua, N. R., Mortensen, G. K., Andersson, A. M., Kongshoj, B., Skakkebaek, N. E., & Wulf, H. C. (2007). Systemic uptake of diethyl phthalate, dibutyl phthalate, and butyl paraben following whole-body topical application and reproductive and thyroid hormone levels in humans. *Environ Sci Technol, 41*(15), 5564-5570.

Jobling, S., Reynolds, T., White, R., Parker, M. G., & Sumpter, J. P. (1995). A variety of environmentally persistent chemicals, including some phthalate plasticizers, are weakly estrogenic. *Environ Health Perspect, 103*(6), 582-587.

Jonsson, B. A., Richthoff, J., Rylander, L., Giwercman, A., & Hagmar, L. (2005). Urinary phthalate metabolites and biomarkers of reproductive function in young men. *Epidemiology, 16*(4), 487-493.

Kang, S. C., & Lee, B. M. (2005). DNA methylation of estrogen receptor alpha gene by phthalates. *J Toxicol Environ Health A, 68*(23-24), 1995-2003.

Keri, R. A., Ho, S. M., Hunt, P. A., Knudsen, K. E., Soto, A. M., & Prins, G. S. (2007). An evaluation of evidence for the carcinogenic activity of bisphenol A. *Reprod Toxicol, 24*(2), 240-252.

Koch, H. M., Preuss, R., & Angerer, J. (2006). Di(2-ethylhexyl)phthalate (DEHP): human metabolism and internal exposure-- an update and latest results. *Int J Androl, 29*(1), 155-165; discussion 181-155.

Lang, I. A., Galloway, T. S., Scarlett, A., Henley, W. E., Depledge, M., Wallace, R. B., & Melzer, D. (2008). Association of urinary bisphenol A concentration with medical disorders and laboratory abnormalities in adults. *JAMA, 300*(11), 1303-1310.

Laws, S. C., Carey, S. A., Ferrell, J. M., Bodman, G. J., & Cooper, R. L. (2000). Estrogenic activity of octylphenol, nonylphenol, bisphenol A and methoxychlor in rats. *Toxicol Sci, 54*(1), 154-167.

Lopez-Carrillo, L., Hernandez-Ramirez, R. U., Calafat, A. M., Torres-Sanchez, L., Galvan-Portillo, M., Needham, L. L., Ruiz-Ramos, R., & Cebrian, M. E. (2010). Exposure to phthalates and breast cancer risk in northern Mexico. *Environ Health Perspect, 118*(4), 539-544.

Lovekamp-Swan, T., & Davis, B. J. (2003). Mechanisms of phthalate ester toxicity in the female reproductive system. *Environ Health Perspect, 111*(2), 139-145.

Maskarinec, G., & Meng, L. (2000). A case-control study of mammographic densities in Hawaii. *Breast Cancer Res Treat, 63*(2), 153-161.

Matthews, J. B., Twomey, K., & Zacharewski, T. R. (2001). In vitro and in vivo interactions of bisphenol A and its metabolite, bisphenol A glucuronide, with estrogen receptors alpha and beta. *Chem Res Toxicol, 14*(2), 149-157.

McCormack, V. A., & dos Santos Silva, I. (2006). Breast density and parenchymal patterns as markers of breast cancer risk: a meta-analysis. *Cancer Epidemiol Biomarkers Prev, 15*(6), 1159-1169.

McTiernan, A., Martin, C. F., Peck, J. D., Aragaki, A. K., Chlebowski, R. T., Pisano, E. D., Wang, C. Y., Brunner, R. L., Johnson, K. C., Manson, J. E., Lewis, C. E., Kotchen, J. M., & Hulka, B. S. (2005). Estrogen-plus-progestin use and mammographic density in

postmenopausal women: Women's Health Initiative randomized trial. *J Natl Cancer Inst, 97*(18), 1366-1376.

Melzer, D., Harries, L., Cipelli, R., Henley, W., Money, C., McCormack, P., Young, A., Guralnik, J., Ferrucci, L., Bandinelli, S., Corsi, A. M., & Galloway, T. (2011). Bisphenol A exposure is associated with in vivo estrogenic gene expression in adults. *Environ Health Perspect, 119*(12), 1788-1793.

Melzer, D., Rice, N. E., Lewis, C., Henley, W. E., & Galloway, T. S. (2010). Association of urinary bisphenol a concentration with heart disease: evidence from NHANES 2003/06. *PLoS One, 5*(1), e8673.

Moriyama, K., Tagami, T., Akamizu, T., Usui, T., Saijo, M., Kanamoto, N., Hataya, Y., Shimatsu, A., Kuzuya, H., & Nakao, K. (2002). Thyroid hormone action is disrupted by bisphenol A as an antagonist. *J Clin Endocrinol Metab, 87*(11), 5185-5190.

Munoz-de-Toro, M., Markey, C. M., Wadia, P. R., Luque, E. H., Rubin, B. S., Sonnenschein, C., & Soto, A. M. (2005). Perinatal exposure to bisphenol-A alters peripubertal mammary gland development in mice. *Endocrinology, 146*(9), 4138-4147.

National Toxicology Program. (2008). NTP-CERHR Monograph on the Potential Human Reproductive and Development Effect of Bisphenol A. NIH Publication No. 08-5994. Research Triangle Park, NC.

Peck, J. D., Sweeney, A. M., Symanski, E., Gardiner, J., Silva, M. J., Calafat, A. M., & Schantz, S. L. (2010). Intra- and inter-individual variability of urinary phthalate metabolite concentrations in Hmong women of reproductive age. *J Expo Sci Environ Epidemiol, 20*(1), 90-100.

Phenomenex Strata-X SPE Application Note 14454. Accessed on 03/12/12 at http://www.phenomenex.com/Application/Detail/14454?alias=Strata .

Pugazhendhi, D., Pope, G. S., & Darbre, P. D. (2005). Oestrogenic activity of p-hydroxybenzoic acid (common metabolite of paraben esters) and methylparaben in human breast cancer cell lines. *J Appl Toxicol, 25*(4), 301-309.

Reddy, B. S., Rozati, R., Reddy, S., Kodampur, S., Reddy, P., & Reddy, R. (2006). High plasma concentrations of polychlorinated biphenyls and phthalate esters in women with endometriosis: a prospective case control study. *Fertil Steril, 85*(3), 775-779.

Romero-Franco, M., Hernandez-Ramirez, R. U., Calafat, A. M., Cebrian, M. E., Needham, L. L., Teitelbaum, S., Wolff, M. S., & Lopez-Carrillo, L. (2011). Personal care product use and urinary levels of phthalate metabolites in Mexican women. *Environ Int, 37*(5), 867-871.

Rossouw, J. E., Anderson, G. L., Prentice, R. L., LaCroix, A. Z., Kooperberg, C., Stefanick, M. L., Jackson, R. D., Beresford, S. A., Howard, B. V., Johnson, K. C., Kotchen, J. M., & Ockene, J. (2002). Risks and benefits of estrogen plus progestin in healthy postmenopausal women: principal results From the Women's Health Initiative randomized controlled trial. *JAMA, 288*(3), 321-333.

Routledge, E. J., Parker, J., Odum, J., Ashby, J., & Sumpter, J. P. (1998). Some alkyl hydroxy benzoate preservatives (parabens) are estrogenic. *Toxicol Appl Pharmacol, 153*(1), 12-19.

Rozati, R., Reddy, P. P., Reddanna, P., & Mujtaba, R. (2002). Role of environmental estrogens in the deterioration of male factor fertility. *Fertil Steril, 78*(6), 1187-1194.

Rubin, D. B. (1987). *Multiple imputation for nonresponse in surveys*. New York: John Wiley & Sons.

Rudel, R. A., Gray, J. M., Engel, C. L., Rawsthorne, T. W., Dodson, R. E., Ackerman, J. M., Rizzo, J., Nudelman, J. L., & Brody, J. G. (2011). Food packaging and bisphenol A and

bis(2-ethyhexyl) phthalate exposure: findings from a dietary intervention. *Environ Health Perspect, 119*(7), 914-920.

Rutter, C. M., Mandelson, M. T., Laya, M. B., Seger, D. J., & Taplin, S. (2001). Changes in breast density associated with initiation, discontinuation, and continuing use of hormone replacement therapy. *JAMA, 285*(2), 171-176.

Schafer, J. L. (1997). *Analysis of incomplete multivariate data*. London: Chapman and Hall.

Schecter, A., Malik, N., Haffner, D., Smith, S., Harris, T. R., Paepke, O., & Birnbaum, L. (2010). Bisphenol A (BPA) in U.S. food. *Environ Sci Technol, 44*(24), 9425-9430.

Silva, M. J., Barr, D. B., Reidy, J. A., Malek, N. A., Hodge, C. C., Caudill, S. P., Brock, J. W., Needham, L. L., & Calafat, A. M. (2004). Urinary levels of seven phthalate metabolites in the U.S. population from the National Health and Nutrition Examination Survey (NHANES) 1999-2000. *Environ Health Perspect, 112*(3), 331-338.

Silva, M.J., Melak, N.A., Hodge, C.C., Reidy, J.A., Kato, K., Barr, D.B., Needham, L.L., & Brock, J.W. (2003). Improved quantitative detection of 11 urinary phthalate metabolites in humans using liquid chromatography-atmospheric pressure chemical ionization tandem mass spectrometry. *J of Chrom B,* 789, 393-404.

Soni, M. G., Carabin, I. G., & Burdock, G. A. (2005). Safety assessment of esters of p-hydroxybenzoic acid (parabens). *Food Chem Toxicol, 43*(7), 985-1015.

Soto, A. M., Sonnenschein, C., Chung, K. L., Fernandez, M. F., Olea, N., & Serrano, F. O. (1995). The E-SCREEN assay as a tool to identify estrogens: an update on estrogenic environmental pollutants. *Environ Health Perspect, 103 Suppl 7*, 113-122.

Sprague, B. L., Trentham-Dietz, A., Gangnon, R. E., Buist, D. S., Burnside, E. S., Aiello Bowles, E. J., Stanczyk, F. Z., Sisney, G. S., & Skinner, H. G. (2012). The vitamin D pathway and mammographic breast density among postmenopausal women. *Breast Cancer Res Treat, 131*(1), 255-265.

Sprague, B. L., Trentham-Dietz, A., Gangnon, R. E., Buist, D. S., Burnside, E. S., Bowles, E. J., Stanczyk, F. Z., & Sisney, G. S. (2011). Circulating sex hormones and mammographic breast density among postmenopausal women. *Horm Cancer, 2*(1), 62-72.

Stahlhut, R. W., Welshons, W. V., & Swan, S. H. (2009). Bisphenol A data in NHANES suggest longer than expected half-life, substantial nonfood exposure, or both. *Environ Health Perspect, 117*(5), 784-789.

Sugiura-Ogasawara, M., Ozaki, Y., Sonta, S., Makino, T., & Suzumori, K. (2005). Exposure to bisphenol A is associated with recurrent miscarriage. *Hum Reprod, 20*(8), 2325-2329.

Takeuchi, T., Tsutsumi, O., Ikezuki, Y., Takai, Y., & Taketani, Y. (2004). Positive relationship between androgen and the endocrine disruptor, bisphenol A, in normal women and women with ovarian dysfunction. [Research Support, Non-U.S. Gov't]. *Endocrine journal, 51*(2), 165-169.

Teeguarden, J. G., Calafat, A. M., Ye, X., Doerge, D. R., Churchwell, M. I., Gunawan, R., & Graham, M. K. (2011). Twenty-four hour human urine and serum profiles of bisphenol a during high-dietary exposure. *Toxicol Sci, 123*(1), 48-57.

Ursin, G., Ma, H., Wu, A. H., Bernstein, L., Salane, M., Parisky, Y. R., Astrahan, M., Siozon, C. C., & Pike, M. C. (2003). Mammographic density and breast cancer in three ethnic groups. *Cancer Epidemiol Biomarkers Prev, 12*(4), 332-338.

Vandenberg, L. N., Chahoud, I., Heindel, J. J., Padmanabhan, V., Paumgartten, F. J., & Schoenfelder, G. (2010). Urinary, circulating, and tissue biomonitoring studies indicate widespread exposure to bisphenol A. *Environ Health Perspect, 118*(8), 1055-1070.

Vandenberg, L. N., Hauser, R., Marcus, M., Olea, N., & Welshons, W. V. (2007). Human exposure to bisphenol A (BPA). *Reprod Toxicol, 24*(2), 139-177.

Volkel, W., Bittner, N., & Dekant, W. (2005). Quantitation of bisphenol A and bisphenol A glucuronide in biological samples by high performance liquid chromatography-tandem mass spectrometry. *Drug Metab Dispos, 33*(11), 1748-1757.

Volkel, W., Colnot, T., Csanady, G. A., Filser, J. G., & Dekant, W. (2002). Metabolism and kinetics of bisphenol a in humans at low doses following oral administration. *Chem Res Toxicol, 15*(10), 1281-1287.

Wolff, M. S., Teitelbaum, S. L., Pinney, S. M., Windham, G., Liao, L., Biro, F., Kushi, L. H., Erdmann, C., Hiatt, R. A., Rybak, M. E., & Calafat, A. M. (2010). Investigation of relationships between urinary biomarkers of phytoestrogens, phthalates, and phenols and pubertal stages in girls. *Environ Health Perspect, 118*(7), 1039-1046.

Ye, X., Tao, L.J., Needham, L.L., Calafat, A.M. (2008). Automated on-line column-switching HPLC-MS/MS method for measuring environmental phenols and parabens in serum. *Talanta*, 76, 865-871.

Ying, G. G., Williams, B., & Kookana, R. (2002). Environmental fate of alkylphenols and alkylphenol ethoxylates--a review. *Environ Int, 28*(3), 215-226.

Table 1. Characteristics of study participants (N=264), Wisconsin Breast Density Study, 2008-2009.

	Mean±SD or n(%)
Age (years)	60.6±4.4
Body mass index (kg/m^2)[a]	28.9±6.6
First degree family history of breast cancer	63 (23.9)
Nulliparous	67 (25.4)
Smoking status	
Never	159 (60.2)
Former	91 (34.5)
Current	14 (13.3)
Vigorous physical activity (hours per week)[b]	4.2± 5.0
College degree[c]	153 (58.2)

SD, standard deviation.
[a]Body mass index data was missing for 2 subjects.
[b]Physically vigorous activities that cause large increases in heart rate or breathing, such as sports activities, climbing stairs, heavy gardening, or lifting/carrying heavy objects.
[c]Education data was missing for 1 subject.

Table 2. Distribution of serum phthalates, parabens and phenols in study participants (N=264), Wisconsin Breast Density Study, 2008-2009.

	Limit of Detection (3:1 S/N)	Mean	Median Detectable Value[b]	Range of Observed Values	No. (%) with detectable levels
Mono-ethyl phthalate (ng/mL)	0.11	2.43	6.59	<LOD - 132	36 (13.6)
Mono-butyl phthalate (ng/mL)	1.0	NA[c]	NA[c]	<LOD - 136	3 (1.1)
Mono-benzyl phthalate (ng/mL)	0.10	NA[c]	NA[c]	<LOD - 0.2	1 (0.4)
Propyl paraben (ng/mL)[a]	0.07	5.12	0.46	<LOD - 630.0	175 (66.5)
Butyl paraben (ng/mL)	0.02	0.10	0.13	<LOD - 2.26	143 (54.2)
Octylphenol (ng/mL)	0.25	0.48	1.78	<LOD - 58.2	35 (13.3)
Nonylphenol (ng/mL)	0.06	3.10	3.36	0.324 - 145.0	109 (41.3)
BPA (ng/mL)	0.24	0.44	0.56	<LOD - 14.5	71 (26.9)

[a]Data regarding serum propyl paraben was not available for 1 subject.
[b]Refers to the median of detected serum levels (i.e., excluding non-detectable samples).
[c]Not available; summary statistics were not calculated due to insufficient numbers of subjects with detectable levels.

Table 3. Spearman correlation coefficients between serum xenoestrogens and other subject characteristics, Wisconsin Breast Density Study, 2008-2009.

	Age (P value)	BMI (P value)	Estradiol (P value)	Progesterone (P value)	Testosterone (P value)
Mono-ethyl phthalate	0.06 (0.37)	0.04 (0.57)	-0.04 (0.48)	-0.02 (0.76)	0.01 (0.88)
Propyl paraben	-0.04 (0.52)	-0.08 (0.20)	0.002 (0.97)	0.09 (0.14)	0.07 (0.29)
Butyl paraben	-0.10 (0.10)	-0.05 (0.43)	0.09 (0.16)	0.08 (0.18)	0.11 (0.07)
Octylphenol	-0.11 (0.07)	-0.02 (0.70)	0.04 (0.55)	0.05 (0.44)	0.03 (0.66)
Nonylphenol	-0.05 (0.38)	0.05 (0.38)	0.20 (0.001)	0.06 (0.31)	0.08 (0.21)
BPA	0.03 (0.63)	-0.08 (0.18)	-0.03 (0.62)	0.11 (0.07)	0.09 (0.14)

[a]Data regarding serum propyl paraben was not available for 1 subject.

Table 4. The association of serum phthalates, parabens and phenols with mammographic breast density (N=264), Wisconsin Breast Density Study, 2008-2009.

Chemical	Linear regression of square root percent breast density on chemical levels			Mean percent density (95% Confidence Interval)[c]			
	β coefficient	SE (β)	P[d]	Non-detect	Below Median[e]	Above Median[e]	P_{trend}[d]
Mono-ethyl phthalate (pg/mL)							
Age-adjusted	0.004	0.008	0.57	12.8 (11.5, 14.3)	16.4 (11.1, 22.6)	16.9 (11.5, 23.2)	0.09
Age- and BMI-adjusted	0.014	0.007	0.04	12.8 (11.6, 14.1)	14.9 (10.5, 20.1)	18.9 (13.9, 24.6)	0.01
Multivariable-adjusted[a]	0.011	0.007	0.09	12.9 (11.7, 14.1)	14.8 (10.5, 19.9)	18.2 (13.4, 23.8)	0.03
Propyl paraben (pg/mL)[b]							
Age-adjusted	-0.0014	0.0020	0.48	12.5 (10.3, 14.8)	13.4 (11.1, 15.8)	14.2 (11.9, 16.8)	0.30
Age- and BMI-adjusted	-0.0006	0.0018	0.72	12.9 (10.9, 15.0)	13.3 (11.3, 15.4)	13.8 (11.8, 16.0)	0.52
Multivariable-adjusted[a]	-0.0004	0.0017	0.80	12.8 (10.9, 14.8)	13.3 (11.4, 15.4)	13.9 (12.0, 16.1)	0.42
Butyl paraben (pg/mL)							
Age-adjusted	0.23	0.45	0.61	13.9 (11.9, 16.1)	12.8 (10.3, 15.4)	12.9 (10.4, 15.6)	0.50
Age- and BMI-adjusted	-0.51	0.39	0.20	14.5 (12.7, 16.3)	12.2 (10.1, 14.4)	12.6 (10.5, 14.9)	0.17
Multivariable-adjusted[a]	-0.57	0.38	0.13	14.4 (12.7, 16.3)	12.4 (10.4, 14.7)	12.4 (10.4, 14.7)	0.13
Octylphenol							
Age-adjusted	-0.0160	0.0257	0.54	13.3 (11.8, 14.8)	13.6 (8.9, 19.2)	14.0 (8.9, 20.2)	0.80
Age- and BMI-adjusted	-0.0056	0.0225	0.80	13.4 (12.1, 14.7)	11.2 (7.5, 15.6)	15.5 (10.8, 21.2)	0.76
Multivariable-adjusted[a]	-0.0104	0.0219	0.64	13.4 (12.2, 14.7)	11.2 (7.6, 15.5)	14.5 (9.9, 19.9)	0.94
Nonylphenol							
Age-adjusted	-0.0077	0.0086	0.37	14.0 (12.2, 15.8)	12.6 (9.9, 15.7)	12.2 (9.5, 15.3)	0.28
Age- and BMI-adjusted	-0.0108	0.0075	0.15	13.8 (12.3, 15.5)	12.5 (10.1, 15.1)	12.7 (10.3, 15.4)	0.39
Multivariable-adjusted[a]	-0.0100	0.0073	0.17	14.1 (12.6, 15.7)	12.1 (9.8, 14.6)	12.5 (10.1, 15.1)	0.20
BPA							
Age-adjusted	0.1115	0.0615	0.07	12.4 (11.0, 14.0)	12.3 (9.1, 16.0)	20.1 (15.9, 16.0)	0.002
Age- and BMI-adjusted	0.0751	0.0540	0.16	12.6 (11.3, 14.0)	13.3 (10.3, 16.7)	17.8 (14.2, 21.7)	0.01
Multivariable-adjusted[a]	0.0645	0.0527	0.22	12.6 (11.4, 14.0)	13.2 (10.3, 16.5)	17.6 (14.2, 21.5)	0.01

SE, standard error; BMI, body mass index.

[a]Adjusted for age, body mass index, parity, family history of breast cancer, vigorous physical activity, and smoking.

[b]Data regarding serum propyl paraben was not available for 1 subject.

[c]Mean percent density displayed is reverse transformed from model of square root density.

[d]P refers to the statistical test of the continuous chemical variable; P_{trend} refers to the test for the ordinal variable representing non-detect, below median detected value, and above median detected value in a separate model.

[e]Refers to the median of detected serum levels (i.e., excluding non-detectable samples).

FIGURE LEGENDS

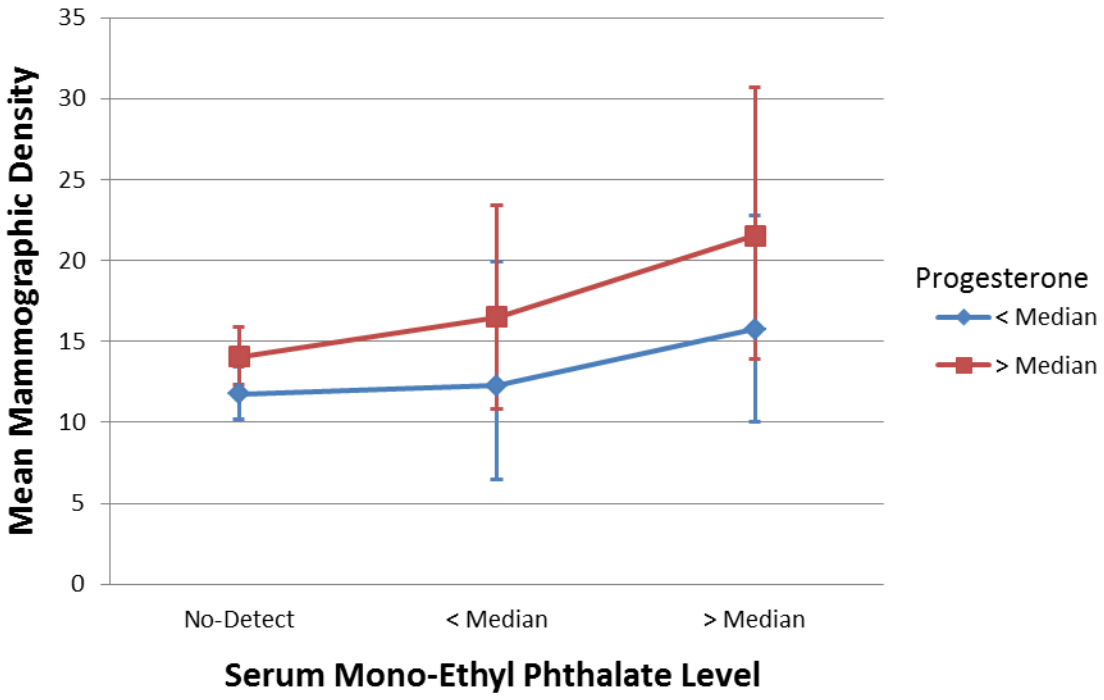

Figure 1. Interaction plot between serum mono-ethyl phthalate and progesterone levels (N=264), Wisconsin Breast Density Study, 2008-2009. Percent density shown is reverse transformed from regression model of square root percent density and adjusted for age, body mass index, parity, family history of breast cancer, vigorous physical activity, and smoking; error bars indicate 95% confidence limits.

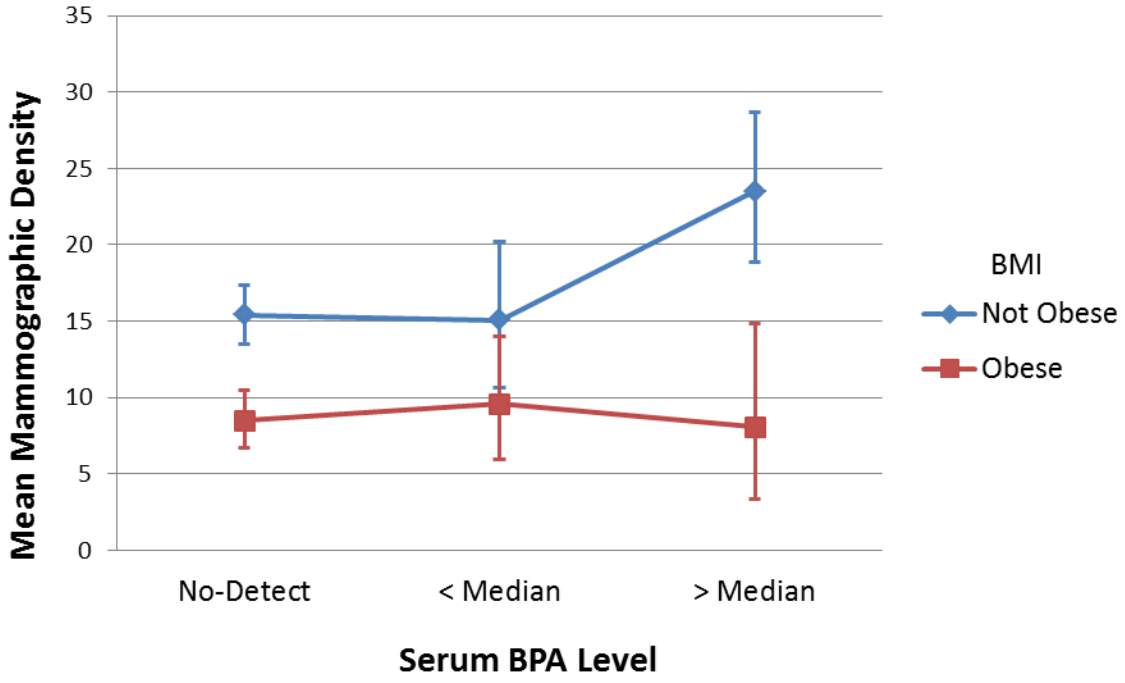

Figure 2. Interaction plot between serum BPA and BMI levels (N=264), Wisconsin Breast Density Study, 2008-2009. Percent density shown is reverse transformed from regression model of square root percent density and adjusted for age, parity, family history of breast cancer, vigorous physical activity, and smoking; error bars indicate 95% confidence limits.